

Preparation and evaluation of polymer microspheres for enhanced lateral flow immunoassay: the case study for malaria.

By

**Henriëtte Renée Hobbs
HBBHEN001**

Dissertation submitted for the degree
Doctor of Philosophy (PhD) in the

Institute of Infectious Disease and Molecular Medicine
Faculty of Health Sciences
University of Cape Town

November 2015

Supervisor: Prof. Jonathan Blackburn (University of Cape Town)
Co-supervisor: Dr. Justin Jordaan (Rhodes University)

The copyright of this thesis vests in the author. No quotation from it or information derived from it is to be published without full acknowledgement of the source. The thesis is to be used for private study or non-commercial research purposes only.

Published by the University of Cape Town (UCT) in terms of the non-exclusive license granted to UCT by the author.

PLAGIARISM DECLARATION:

**UNIVERSITY OF CAPE TOWN
FACULTY OF HEALTH SCIENCES
INSTITUTE OF INFECTIOUS DISEASE AND MOLECULAR MEDICINE**

Full name:	Henriëtte Renée Hobbs	Student number:	HBBHEN001
Title of the work:	Preparation and evaluation of polymer microspheres for enhanced lateral flow immunoassay: the case study for malaria.		

Declaration:

I, ...**Henriëtte Reneé Hobbs**..., , hereby declare that the work on which this thesis is based is my original work (except where acknowledgements indicate otherwise) and that neither the whole work nor any part of it has been, is being, or is to be submitted for another degree in this or any other university. I authorise the University to reproduce for the purpose of research either the whole or any portion of the contents in any manner whatsoever.

Signature: _____

Signed by candidate

Date:12 November 2015.....

DECLARATION OF FREE LICENSE

I, **Henriëtte Renée Hobbs**, hereby:

- (a) Grant the University free license to reproduce the above thesis in whole or in part, for the purpose of research;
- (b) Declare that:
 - (i) The above thesis is my own unaided work, both in conception and execution, and that apart from the normal guidance from my supervisor(s), I have received no assistance except as stated below
 - (ii) Neither the substance nor any part of the thesis has been submitted in the past, or is being, or is to be submitted for a degree at this University or at any other University, except as stated below.

I am now presenting the thesis/dissertation for examination for the Degree of PhD.

Signature:

Signed by candidate

Date: 12 November 2015

ACKNOWLEDGEMENTS

With the deepest gratitude I would like to acknowledge and thank those who have helped make this thesis possible.

First and foremost, I would like to extend my sincerest gratitude to my supervisor and co-supervisor for their continuous guidance, support and invaluable advice:

To Professor Jonathan Blackburn, I am forever grateful for your assistance, guidance and suggestions which you kindly provided and for making yourself available to discussions, despite your busy schedule.

To Dr. Justin Jordaan, thank you for your invaluable expertise on the research topic, your passion towards the science and your generous guidance throughout this PhD.

To my fellow colleagues, who shared in the frustrations, successes and celebrations, thank you for always being there to put a smile on my face.

A personal thank you goes to my parents, for your unconditional love and support, your encouragement and for always believing in me. A heartfelt thank you to my husband Brett, for your love, your words of encouragement when I needed them most and the endless support you gave me throughout my PhD and continue to give me every day.

Finally, thank you to the Council of Scientific and Industrial Research for blessing me with the bursary to pursue my PhD and for funding this research.

TABLE OF CONTENTS

Acknowledgements.....	i
Table of Contents	ii
Abbreviations	vi
List of Tables	x
List of Figures	x
Abstract	1

CHAPTER 1

LITERATURE REVIEW

1.1. Introduction.....	2
1.2. Point-of-care diagnosis of infectious diseases	2
1.3. Point-of-care diagnostic tests	3
1.4. RDT detection agents	5
1.5. Malaria diseases	10
1.6. Prevention and treatment of malaria	14
1.7. Malaria biomarkers	15
1.8. Diagnosis of malaria	18
1.8.1. Microscopy	18
1.8.2. Molecular diagnosis	20
1.8.3. Hemozoin detection	21
1.8.4. Immunoassay	21
1.8.5. Emerging diagnostic technologies	22
1.8.6. Point-of-care technologies: Rapid diagnostic tests.....	24

CHAPTER 2

MICROSPHERE ENGINEERING FOR LATERAL FLOW

2.1. INTRODUCTION	27
2.2. MATERIALS AND METHODS.....	29
2.2.1. Materials.....	29
2.2.2. Synthesis of functional polymer microspheres	29
2.2.3. Protein binding capacity of microspheres.....	31
2.2.4. Dry weight determination	32

2.2.5.	Dye binding to epoxide microspheres	32
2.2.5.1.	<i>Dye screening</i>	32
2.2.5.2.	<i>Maximum dye binding capacity of preferred dyes</i>	33
2.2.6.	Particle size distribution	33
2.3.	RESULTS AND DISCUSSION	34
2.3.1.	Synthesis of functional polymer microspheres	34
2.3.2.	Protein binding capacity of microspheres.....	34
2.3.3.	Dye binding to epoxide microspheres.....	35
2.3.4.	Particle size distribution (PSD) of epoxide microspheres	38
2.4.	CONCLUSIONS	39

CHAPTER 3

EVALUATION OF ANTIBODY CONJUGATION

3.1.	INTRODUCTION	40
3.2.	MATERIALS AND METHODS.....	45
3.2.1.	Materials.....	45
3.2.2.	Antibody conjugation to magnetic microspheres	46
3.2.3.	Protein Quantification: BCA Assay.....	47
3.2.4.	Bead-based sandwich ELISA	47
3.2.5.	Sandwich ELISA substrate selection	49
3.2.6.	Sandwich ELISA dynamic range.....	49
3.3.	RESULTS AND DISCUSSION	49
3.3.1.	Quantification of antibody conjugation	49
3.3.2.	Sandwich ELISA buffer screening.....	50
3.3.3.	Sandwich ELISA substrate evaluation	53
3.3.4.	ELISA dynamic range	55
3.3.5.	Random versus oriented antibody immobilisation	56
3.4.	CONCLUSIONS	57

CHAPTER 4

LATERAL FLOW IMMUNOASSAY DEVELOPMENT: PROOF-OF-CONCEPT ON HUMAN CHORIONIC GONADOTROPIN (hCG)

4.1. INTRODUCTION	60
4.2. MATERIALS AND METHODS.....	63
4.2.1. Materials.....	63
4.2.2. Epoxide microsphere preparation and antibody conjugation	64
4.2.3. Assembly of lateral flow assay	65
4.2.4. Lateral flow component optimisation	66
4.2.5. Microsphere optimisation for lateral flow	67
4.2.6. Anti-hCG-conjugated-colloidal gold: “Gold” Standard.....	68
4.2.7. Microsphere and colloidal gold comparison	68
4.3. RESULTS AND DISCUSSION	69
4.3.1. Epoxide microsphere preparation and antibody conjugation	69
4.3.2. Lateral flow component optimisation	70
4.3.2.1. Flow formulation	70
4.3.2.2. Dye loading.....	72
4.3.2.3. Antibody loading	74
4.3.3. Volumetric loading of microspheres	75
4.3.4. Lateral flow detection sensitivity	76
4.3.5. Antibody stability.....	78
4.3.6. Colloidal gold comparison.....	79
4.4. CONCLUSIONS	83

CHAPTER 5

LATERAL FLOW IMMUNOASSAY: MALARIA

5.1. INTRODUCTION	85
5.2. MATERIALS AND METHODS.....	87
5.2.1. Materials.....	87
5.2.2. Antibody striping to nitrocellulose membrane.....	87

5.2.3. Antibody conjugation to microspheres (HRP2 and pLDH).....	88
5.2.4. Lateral flow reagents	88
5.2.5. Multiplex lateral flow assay	88
5.2.6. Anti-HRP2-conjugated-colloidal gold: “Gold” standard	89
5.2.7. Microspheres and colloidal gold comparison	89
5.3. RESULTS AND DISCUSSION	89
5.3.1. Antibody conjugation to microspheres	89
5.3.2. Lateral flow buffers	90
5.3.3. Lateral flow detection sensitivity	92
5.3.4. Antibody stability.....	95
5.3.5. Multiplex lateral flow	98
5.3.6. Colloidal gold comparison.....	100
5.4. CONCLUSIONS	104

CHAPTER 6

CONCLUSIONS AND FUTURE PERSPECTIVES

6.1 CONCLUDING CHAPTER.....	107
LIST OF REFERENCES	112
APPENDIX.....	129

Abbreviations:

°C	Degree Celsius
µg	Microgram
µl	microliter
µm	Micrometer
<i>A. funestus</i>	<i>Anopheles funestus</i>
<i>A. gambiae</i>	<i>Anopheles gambiae</i>
Ab-Ag-Ab	Antibody - antigen – antibody
Abs	Absorbance
ABTS	2,2'-azino-bis-(3-ethylbenzthiazoline-6-sulfonic acid
ACT	Artemisinin-based combination therapy
AO	Acridine Orange
AP	Alkaline phosphatase
APAD	3-acetaylpyridine adenine dinucleotide
ATP	Adenosine triphosphate
AuNP	Gold nanoparticle
BBi	British Biocell International
BCA	Bicinchoninic acid assay
BCP	Benzothiocarboxypurine
BSA	Bovine Serum Albumin
C. diff	Clostridium difficile
CdTe	Cadmium telluride
cm	Centimeter
DNA	Deoxyribonucleic acid
DTT	Dichlorodiphenyltrichloroethane
EDA	Ethylenediamine
EDTA	Ethylenediaminetetraacetic acid
EIA	Enzyme immunoassay
ELISA	Enzyme linked immunosorbent assay
EtOH	Ethanol
Fab	Fragment, antigen-binding (antibody)

Fc	Fragment, crystallisable (antibody)
FCM	Flow cytometry
Guaiacol	2-methoxyphenol
H ₂ O ₂	Hydrogen peroxide
HBV	Hepatitis B virus
hCG	Human chorionic gonadotropin
HCl	Hydrochloric acid
HCV	Hepatitis C virus
HIV	Human immunodeficiency virus
HRP	Horseradish peroxidase
HRP2	Histidine rich protein 2
IFA	Immunofluorescence antibody testing
IgA	Immunoglobulin A
IgD	Immunoglobulin D
IgE	Immunoglobulin E
IgG	Immunoglobulin G
IgM	Immunoglobulin M
K _d	Dissociation constant
kDa	Kilo-Dalton
L	Litre
LAMP	Loop-mediated isothermal amplification
M	Molar
mg	Milligram
mIU	Milli international units
ml	millilitre
mM	Millimolar
mm	Millimeter
mRNA	Messenger ribonucleic acid
MRSA	Methicillin-resistant staphylococcus aureus
MS	Mass spectrometry
Na ₂ HPO ₄	Sodium phosphate dibasic

NaCl	Sodium Chloride
NADH	Nicotinamide adenine dinucleotide
NaH ₂ PO ₄	Sodium phosphate monobasic
NaHCO ₃	Sodium bicarbonate
NaN ₃	Sodium azide
ng	Nanogram
NHS-LC-biotin	N-hydroxysuccinimide ester long chain biotin
nm	Nanometer
NP4	Nonoxynol-4
O/W	Oil- in-water
OPD	o-phenylenediamine, 1,2-diaminobenzene
<i>P. falciparum</i>	<i>Plasmodium falciparum</i>
<i>P. knowlesi</i>	<i>Plasmodium knowlesi</i>
<i>P. malariae</i>	<i>Plasmodium malariae</i>
<i>P. ovale</i>	<i>Plasmodium ovale</i>
<i>P. vivax</i>	<i>Plasmodium vivax</i>
PBS	Phosphate buffered saline
PCR	Polymerase chain reaction
PEG	Polyethylene glycol
PEI	Polyethyleneimine
<i>Pf</i> HRP1	<i>Plasmodium falciparum</i> Histidine rich protein 1
<i>Pf</i> HRP2	<i>Plasmodium falciparum</i> Histidine rich protein 2
<i>Pf</i> HRP3	<i>Plasmodium falciparum</i> Histidine rich protein 3
pLDH	<i>Plasmodium</i> lactate dehydrogenase
PS	Polystyrene
PSD	Particle size distribution
RDT	Rapid Diagnostic Test
RNA	Ribonucleic acid
rpm	Rotations per minute
rRNA	Ribosomal ribonucleic acid
Strep A	Group A streptococcus
TBS	Tris buffered saline
TPP	Target product profiles

TRAP	Thrombospondin-related anonymous protein
UTI	Urinary tract infection
UV	Ultraviolet
UCPs	Up-converting phosphors
W/O	Water-in-oil
WHO	World Health Organisation

List of Tables:

Table 1.1:	Summary of Rapid Diagnostic Tests conducted by the WHO	26
------------	--	----

List of Figures:

Figure 1.1:	Target product profiles (TPP), users and settings within the point-of-care spectrum.....	4
Figure 1.2:	A world map, illustrating the global distribution of common <i>Plasmodium</i> species in red	10
Figure 1.3:	Lifecycle development stages of the malaria parasite in the human and mosquito host.....	11
Figure 1.4:	Global distribution of dominant malaria vector species	13
Figure 1.5:	The current and predicted global distribution of malaria.....	14
Figure 1.6:	Examples of Giemsa stained thick (top) and thin (bottom) blood smear of artefacts that may result in incorrect diagnosis	19
Figure 1.7:	Fluorescent microscopy for the detection of malaria	20
Figure 1.8:	Schematic representation of the MOT diagnostic device principle	23
Figure 1.9:	Schematic representation of positive and negative results obtained with a lateral flow assay and agglutination assay.....	25
Figure 2.1:	Chemical structure of reactive azo dyes	29
Figure 2.2:	Sequential chemical reactions during microsphere synthesis protocol.....	31
Figure 2.3:	Light microscope image of initial polymer microsphere suspensions.....	34
Figure 2.4:	BSA binding capacity of polymer microspheres.....	35
Figure 2.5:	Macro view of dyed microsphere suspensions.....	35
Figure 2.6:	Light microscope image of dyed microsphere suspensions	36
Figure 2.7:	Spectrum scan between 420nm – 700 nm to determine maximum absorbance wavelength of azo dyes.....	37
Figure 2.8:	Percentage of dye bound to epoxide microspheres before and after removal of non-specific binding	37
Figure 2.9:	Percentage of Chicago Sky Blue and Congo Red dye bound to epoxide functional polymer microspheres with varying dye loads.....	38
Figure 2.10:	Particle size distribution of the synthesised polymer microspheres.....	39
Figure 3.1:	Structure of an antibody.....	40
Figure 3.2:	Illustration of a bead-based sandwich ELISA.....	43
Figure 3.3:	Illustration of a bead-based sandwich ELISA experimentation	48
Figure 3.4:	Experimental outline of bead-based sandwich ELISA.....	48
Figure 3.5:	Antibody conjugation efficiency to different batches of MagReSyn®	

Epoxide and MagReSyn® Streptavidin microspheres	50
Figure 3.6: Bead-based ELISA of microsphere negative controls (MagReSyn® Epoxide and MagReSyn® Streptavidin) without primary antibody in PBS, Tween20 and TBS, Tween20	51
Figure 3.7: Bead-based ELISA of microsphere negative controls (MagReSyn® Epoxide and MagReSyn® Streptavidin) without primary antibody in PBS, Tween20, and PBS, Tween20, casein.....	51
Figure 3.8: Bead-based ELISA of control MagReSyn® Epoxide and MagReSyn® Streptavidin in PBS Tween20 and PBS, Tween20, Casein, with primary antibody conjugated microspheres, and only HRP-conjugated secondary antibody.....	52
Figure 3.9: Illustration of possible challenges for using detergent to remove non-specific binding during ELISA.	52
Figure 3.10: Bead-based sandwich ELISA of antibody conjugated microspheres, MagReSyn® Epoxide-IgG-conjugated and MagReSyn® Streptavidin-IgG-conjugated, with PBS, Tween20 and PBS, Tween20, casein	53
Figure 3.11: Relative absorbance of OPD, Guaiacol and ABTS in a bead-based sandwich ELISA of MagReSyn® Epoxide-IgG-conjugated and MagReSyn® Streptavidin-IgG-conjugated microspheres over a set time interval	54
Figure 3.12: Dynamic curve with ABTS as the substrate and varying amounts of antigen.....	55
Figure 3.13: Bead-based sandwich ELISA of random (MagReSyn® Epoxide-IgG-conjugated) and oriented (MagReSyn® Streptavidin-IgG-conjugated) immobilised antibodies..	57
Figure 4.1: Lateral flow diagnostic assay	61
Figure 4.2: Illustration for lateral flow component assembly onto a backing card	65
Figure 4.3: Illustration of lateral flow assay in a microwell plate	65
Figure 4.4: Illustration of the lateral flow parameters explored	67
Figure 4.5: Light microscope images of microspheres suitable for lateral flow	69
Figure 4.6: Lateral flow of BSA and casein finished Chicago Sky Blue dyed microspheres without conjugated antibody (control) and hCG- conjugated-microspheres (hCG) in BSA-based running buffer	70
Figure 4.7: Lateral flow of BSA and casein finished negative control and positive (hCG) Chicago Sky Blue dyed microspheres in casein-based running buffer	71
Figure 4.8: Lateral flow of negative control and positive (hCG) microspheres.....	72

Figure 4.9:	Lateral flow of anti-hCG-conjugated-microsphere samples containing either 2, 15 or 50 mg Congo Red dye.ml ⁻¹ microsphere suspension.....	73
Figure 4.10:	Lateral flow of anti-hCG-conjugated-microspheres with varying amounts of anti-hCG antibody, in running buffer (control) and sample buffer.	74
Figure 4.11:	Lateral flow with varying volumes of anti-hCG-conjugated-microspheres, in sample buffer.	76
Figure 4.12:	Lateral flow assay to determine the lowest limit of antigen detection of anti-hCG-conjugated-microspheres	77
Figure 4.13:	Stability of anti-hCG-conjugated-microspheres incubated from 1 to 6 hours at 50°C, 60°C and 70°C	78
Figure 4.14:	Lateral flow of negative control and positive (hCG) colloidal gold nanoparticles in running and sample buffer.	80
Figure 4.15:	Lateral flow assay to determine the lowest limit of antigen detection of anti-hCG-conjugated colloidal gold nanoparticles..	81
Figure 4.16:	Stability of anti-hCG-conjugated-colloidal gold incubated from 1 to 6 hours at 50°C, 60°C and 70°C.....	82
Figure 5.1:	Schematic of the multiplex antibody striping on nitrocellulose membrane for lateral flow	88
Figure 5.2:	Lateral flow of control and positive (anti-HRP2-conjugated and anti-pLDH-conjugated) microspheres in running buffer.	90
Figure 5.3:	Specificity of anti-HRP2-conjugated-microspheres in running buffer (R) and running buffer supplemented with HRP2 antigen (S1) or pLDH antigen (S2) ...	91
Figure 5.4:	Specificity of anti-pLDH-conjugated-microspheres in running buffer (R), and running buffer supplemented with HRP2 antigen (S1) or pLDH antigen (S2).. .	92
Figure 5.5:	Lateral flow to determine the lowest limit of detection of HRP2 using a lateral flow assay in microwell format.....	93
Figure 5.6:	Lateral flow to determine the lowest limit of detection of pLDH using a lateral flow assay in microwell format.....	94
Figure 5.7:	Stability of anti-HRP2-conjugated-microspheres incubated from 1 to 6 hours at 50°C, 60°C and 70°C.....	96
Figure 5.8:	Stability of anti-pLDH-conjugated-microspheres incubated from 1 to 6 hours at 50°C, 60°C and 70°C.....	97
Figure 5.9:	Multiplex lateral flow with both anti-HRP2-conjugated-microspheres and anti-pLDH-conjugated-microspheres in running (R) and sample (S) buffer	99
Figure 5.10:	Lateral flow of negative control and positive (HRP2) colloidal gold nanoparticles in running (R) and sample (S) buffer.	100

Figure 5.11: Specificity of anti-HRP2-conjugated-colloidal gold nanoparticles in running buffer (R) and running buffer supplemented with HRP2 antigen (S1) or pLDH antigen (S2).....	101
Figure 5.12: Lateral flow to determine the limit of antigen detection of HRP2-colloidal gold nanoparticles (standard)	102
Figure 5.13: Stability of anti-HRP2-conjugated colloidal gold nanoparticles incubated from 1 to 6 hours at 50°C, 60°C and 70°C	103

ABSTRACT

We proposed that the development of a new high capacity polymer microsphere technology, termed ReSyn, could be developed as viable detection reagents for lateral flow technology. This body of work outlines the development of this new high capacity polymer microsphere technology for suitability to flow on lateral flow membranes, and highly specific biomarker detection for immunoassay development. Proof-of-concept was achieved using hCG (pregnancy biomarker) and validated for detection of pLDH and HRP2 as biomarkers of malaria. The sensitivity, stability and multiplex capability of these microspheres were further explored and compared against the current 'gold' standard detection agent for lateral flow, colloidal gold.

Malaria was selected as a suitable target for evaluation of the microsphere technology since it is considered to be a global epidemic that can benefit greatly from improved point-of-care diagnostics. Malaria affects almost half of the world's population and is responsible for causing approximately 655 000 deaths per annum in 2010, with 90% of these deaths occurring in Africa and 85% of these deaths occurring in children under 5 years of age (del Prado *et al.*, 2014; Kokwaro, 2009; White *et al.*, 2014; WHO, 2009). Febrile disease diagnosis at point-of-care is often based on symptomatic diagnosis rather than on the use of validated diagnostic technologies, and is considered one of the major contributing factors for the high morbidity and mortality rate of malaria (Chandler *et al.*, 2008; Kain *et al.*, 1998; Kokwaro, 2009). Improved diagnostic technologies, allowing for sensitive and accurate diagnosis at the point-of-care, could assist alleviating these problems through the improved management of disease (Bell *et al.*, 2006). Lateral flow rapid diagnostic tests are the preferred method for point-of-care diagnostics in resource constrained areas but have several limitations including sensitivity and stability in resource constrained settings (Bell *et al.*, 2006). Improvements in detection agents are seen as a viable approach to improving these features of diagnostic assays.

The results of this study show that the polymer microspheres provide improved stability to immobilised antibodies, with potential for translation into improved stability for diagnostic assays in tropical malaria endemic regions. The polymer microspheres offered high specificity and comparable visual sensitivity to the market leader colloidal gold and is therefore considered as alternate detector agents in lateral flow assays. Additionally, the microspheres can be dyed various colours (red and blue in this study), allowing for specific and sensitive multiplex detection of multiple analytes in a single sample. This increases the versatility of the microspheres for lateral flow diagnostic application, and improves the interpretation of lateral flow diagnostic technology at the point-of-care.

CHAPTER 1

LITERATURE REVIEW

1.1. Introduction

Diagnosis of infectious diseases in rural settings, at point-of-care, remains challenging due to various limitations including the lack of resources (e.g. clean water and electricity), availability of trained/skilled staff, labour intensive and time consuming techniques (microscopy) and the requirement for specialised equipment (Moody, 2002). The only true point-of-care technologies for infectious diseases, such as malaria detection, are rapid diagnostic tests (RDT's), also known as first generation point-of-care diagnostic tests (Pai *et al.*, 2012). However, several challenges to RDT's hinder the effective management of infectious diseases, including a general lack of sensitivity and low stability. We believe that these shortfalls may in part be alleviated by the development of new polymer microsphere diagnostic detection agents for lateral flow diagnostic assays. Improved point-of-care diagnostics (RDT technology) potentially provides for improved disease management, reducing the emergence of drug resistance, reducing healthcare expenditure, and reducing morbidity related to the disease (Gubbins *et al.*, 2014).

1.2. Point-of-care diagnosis of infectious diseases

Infectious diseases are known to cause millions of deaths annually, with majority of the incidences occurring in developing countries, with the largest burden on Africa (Peeling *et al.*, 2010; Yager *et al.*, 2008). In addition to the three main global infectious diseases (human immunodeficiency virus (HIV), tuberculosis (TB) and malaria), pneumonia, acute respiratory infection, sexually transmitted diseases, Human African trypanosomiasis, visceral leishmaniasis and the common flu (*Haemophilus influenza*) are also considered key players in contributing to the rate of mortality in the developing world (Mabey *et al.*, 2004; Peeling *et al.*, 2010). It has been estimated that there are approximately 2 billion people currently infected with TB, 39.5 million people living with HIV, approximately 500 million cases of malaria annually and over 500 000 new infections of Gonorrhoea, syphilis and chlamydia daily (Gerbase *et al.*, 1998; WHO, 2007; WHO/UNAIDS, 2006; Yager *et al.*, 2008).

Of the diseases above, many currently rely on complicated diagnostic techniques, such as sputum microscopy and culture incubation for the diagnosis of TB, and agglutination tests for the diagnosis of trypanosomiasis (Mabey *et al.*, 2004; Peeling *et al.*, 2010). Syndromic diagnosis (based on symptoms) is also often used by healthcare providers, and although they

may be effective, inaccurate diagnosis and treatment often results in overtreatment, wasted resources and potentially increased drug resistance (Yager *et al.*, 2008).

Various strategies for reducing the burden of disease have been initiated, including vaccination programmes, healthcare education, sanitation and the promotion of hand washing, safe sex practice, the use of insecticides and insecticide treated bed-nets, mass drug administration, and improved availability of medication (Mabey *et al.*, 2004; Peeling *et al.*, 2010). With these strategies in place, has unfortunately not significantly reduced the disease burden, thus appropriate clinical management of disease continues to be of importance and remains a major global health challenge (Peeling *et al.*, 2010). The majority of these patients in rural areas of developing countries may have to walk for hours before reaching a clinic, and are treated at facilities that often lack the required infrastructure to accurately and rapidly diagnose disease (Peeling *et al.*, 2010).

Infectious disease management consists of identifying the cause of infection, initiating treatment and controlling host reactions to infection (Bissonnette *et al.*, 2012). The time required to complete the diagnostic cycle (clinical sampling, transport, microbiology testing, confirmation of results, quality control and validation, interpretation of result) often remains challenging (≥ 24 hours) while point-of-care diagnostic tests are anticipated to provide specific and sensitive answers at the bedside with minimal delay, making rapid diagnostic tests (RDT's) arguably the best solution for management of diseases in resource constrained settings (≤ 2 hours) (Bissonnette *et al.*, 2012).

1.3. Point-of-care diagnostic tests

Point-of-care testing is defined as “patient specimens assayed at or near the patient with the assumption that test results will be available instantly to assist caregivers with immediate diagnosis and/or clinical intervention and to make a decision or take appropriate action, which will lead to an improved health outcome”, and therefore need to meet the “ASSURED” criteria of being affordable, sensitive, specific, user friendly, rapid and robust, equipment free and delivered (Pai *et al.*, 2012). Point-of-care tests play an important role in disease prevention and management since caregivers can initiate appropriate treatment, reducing disease transmission, further reducing the need for patient follow-up visits (Loubiere *et al.*, 2010; Pai *et al.*, 2012). In addition, point-of-care tests could reduce the workload for rural clinics/laboratories, streamline care where large numbers of patients are treated daily and can potentially empower patients to self-test in the privacy of their own homes (Loubiere *et al.*, 2010; Pai *et al.*, 2012).

Point-of-care tests are often based on microbial particle-based or antibody-based detection (Gubbins *et al.*, 2014). Point-of-care tests are generally more affordable, and equipment free, however newer possibly more sensitive second generation point-of-care technologies that require equipment have been developed, including cartridge-based nucleic acid amplification tests. A third generation of point-of-care tests involving hand-held devices and mobile phone-based devices are an active area of development (Pai *et al.*, 2012). Point-of-care tests are classified into five distinct types, based on the setting in which they are used (Figure 1.1.).

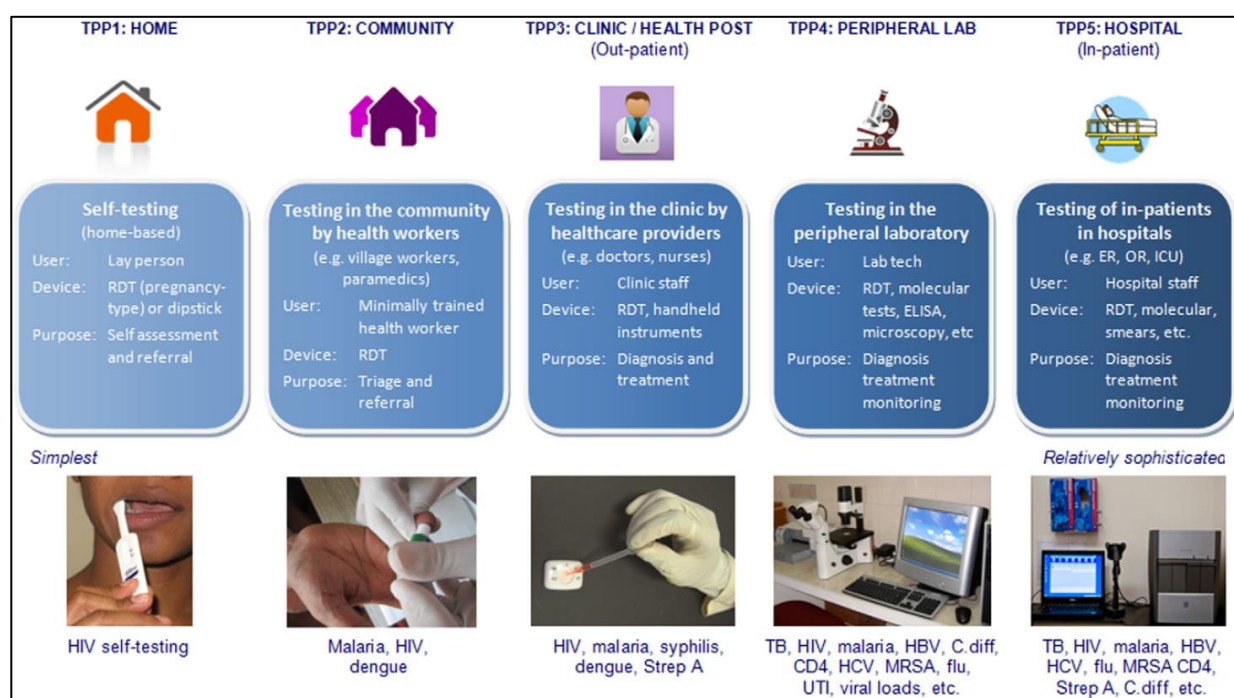


Figure 1.1: Target product profiles (TPP), users and settings within the point-of-care spectrum. HBV: Hepatitis B virus, HCV: Hepatitis C virus, UTI: Urinary tract infection, MRSA: methicillin-resistant staphylococcus aureus, C. diff: clostridium difficile, Strep A: group A streptococcus. Reproduced from (Pai *et al.*, 2012).

As illustrated in Figure 1.1, the point-of-care test can range from a simple dipstick assay to an automated molecular test, or portable analyser, while a single test (e.g. lateral flow assay) may be used across all five TPP settings, with certain devices being limited to certain users and TTP (e.g. ELISA, microscopy) (Pai *et al.*, 2012).

Although point-of-care tests are available for a variety of diseases (e.g. HIV, malaria, dengue, syphilis, hepatitis), are inexpensive and often meet the ASSURED criteria, these tests will not have any impact unless they are widely used and followed with an appropriate treatment regime (Cobelens *et al.*, 2012). In high transmission areas where adequate resources and healthcare infrastructures are limited, effective diagnosis, prevention and treatment of disease (e.g. malaria) is challenging. In these resource constrained settings, lateral flow diagnostic devices and dipstick assays are considered the preferred solution for true point-of-care

diagnostics as they do not require electricity, clean water, or cold storage, and are easy to use and interpret by individuals with minimal training (Urdea *et al.*, 2006).

1.4. RDT detection agents

Lateral flow assays are the most suitable diagnostic technology for use at true point-of-care, they are unfortunately the least sensitive (Goryacheva *et al.*, 2013; Sajid *et al.*, 2014). Two main approaches are potentially suitable to target the limitations of current lateral flow diagnostic assays: improve the materials and detection methods of the assay; develop new labels or label systems which would improve the analytical signal generated (Goryacheva *et al.*, 2013).

An alternate avenue of improving sensitivity is to improve the immobilisation of the capture antibody onto the nitrocellulose membrane (Fribe *et al.*, 2009). Currently, capture antibodies are immobilised onto the nitrocellulose *via* adsorption which results in a monolayer of randomly immobilised antibodies of approximately $0.4 \mu\text{g}\cdot\text{cm}^{-2}$ (Fribe *et al.*, 2009). Oriented immobilisation of the capture antibody to the nitrocellulose membrane surface is an area which has been investigated to improve the functional activity and stability of the immobilised antibodies in lateral flow assays (Rejeb *et al.*, 1998). The surface of the nitrocellulose membrane can be functionalised to amine groups which allow for covalent oriented immobilisation of oxidised antibody and subsequently result in maximum paratope (antigen recognition site) availability (Rejeb *et al.*, 1998). The study by Rejeb *et al.*, 1998 illustrated that the functionalised membrane had reduced non-specific binding and that the functionalisation process did not affect the porous state of the membrane (Rejeb *et al.*, 1998). Oriented immobilisation of the capture antibody may have its advantages; however, as only the top layer (10 μm) of the three-dimensional nitrocellulose membrane is capable of being visualised, any detection agents captured below this top layer (oriented or randomly immobilised) will remain undetected (Puertas *et al.*, 2010; Wang *et al.*, 2009b).

The choice of a detector particle is driven by several key factors such as the necessity for stability (covalent attachment versus passive adsorption), qualitative versus quantitative results, level of sensitivity, need for multiplex detection, and the cost of manufacturing (Wong *et al.*, 2009). The most common detector labels used in lateral flow assays are colloidal gold and latex (Wong *et al.*, 2009).

The first account of a diagnostic immunoassay utilising an antibody-conjugated colloidal gold nanoparticle (AuNP) as a detector reagent was reported in 1981 (Leuvering *et al.*, 1981). Colloidal gold is currently the most widely used label available in lateral flow diagnostic

immunoassay due to its stability and sensitivity, in addition to well established and reproducible manufacturing (Wang *et al.*, 2009a). A colloidal gold particle consists of an elemental gold core surrounded by a double ionic layer of negative charges and often 20 – 40 nm in diameter for lateral flow application (Wong *et al.*, 2009). Colloidal gold (conjugated and unconjugated) is readily available from commercial sources, is nontoxic, has an intense colour which is easily detected and remains stable in both liquid and dried forms (Wong *et al.*, 2009). The advantage of colloidal gold over alternate particles is its mobility in the porous nitrocellulose membrane and being less susceptible to aggregation (Shyu *et al.*, 2002). The drawbacks include leaching of the antibody (not covalently attached), as well as only providing for single colour detection, where the colour intensity is related to the size of the colloidal gold particle (Chenggang *et al.*, 2008). The range of disadvantages have led to an active field in the research and development of new detection agents due to the potential benefit of improved sensitivity for point-of-care diagnosis.

Various new particle preparations have been explored in the development of lateral flow assays with the aim of improving sensitivity, while retaining the specificity of current commercially available detector particles, namely colloidal gold nanoparticles and latex (Sajid *et al.*, 2014). Detector particles that have been considered are magnetic particles, colloidal carbon, colloidal selenium, silver nanoparticles (including enhancement of detection through signal amplification), quantum dots, up-converting phosphor, organic fluorophores, colloidal “dyes”, liposomes and enzymes (Gao *et al.*, 2014; Goryacheva *et al.*, 2013; Sajid *et al.*, 2014; Wong *et al.*, 2009).

The approaches to enhancing the signal of colloidal gold are to either modify the colloidal gold nanoparticles without affecting the assay procedure, or to incorporate additional steps (enhancements) to the procedure, resulting in a multi-step assay format (Goryacheva *et al.*, 2013). The use of silver and gold conjugated nanoparticles is an example of modifying the colloidal gold nanoparticle, where the core of the nanoparticle consists of silver and the shell consists of gold nanoparticles, which resulted in enhanced sensitivity with stability comparable to the conventional colloidal gold nanoparticles (Liao *et al.*, 2010). Several techniques have been developed to enhance the signal at the test-line of lateral flow assays after assay development, including silver nanoparticles and conjugated enzymes (Goryacheva *et al.*, 2013). Silver enhancement involves submerging the gold nanoparticle labelled membrane into a silver solution containing a reducing agent (Goryacheva *et al.*, 2013; Horton *et al.*, 1991; Linares *et al.*, 2012). The transfer of electrons from the reducing agent in the solution to the silver ions results in the deposition of metallic silver at the site where colloidal gold is present and has been shown to increase sensitivity of the assay 100-fold (Horton *et al.*, 1991). This technique is however restricted by the requirement of additional assay steps and the preceding

wash steps are crucial in removing interfering ions (Goryacheva *et al.*, 2013). Enzyme enhancement involves the incorporation of an enzyme label (e.g. horseradish peroxidase, alkaline phosphatase) into the conjugated antibody on the detector particle (Gao *et al.*, 2014; Goryacheva *et al.*, 2013; Sajid *et al.*, 2014). In this technique the developed membrane is read with a strip reader after being submerged into a substrate solution (Goryacheva *et al.*, 2013). The chromogenic substrate results in a darker colour at the capture lines when compared to the unmodified gold nanoparticles with claimed enhanced sensitivity of one order of magnitude (Parolo *et al.*, 2012).

Colloidal carbon (carbon black), colloidal iron oxide (magnetic nanoparticles) and colloidal dyes have also been explored for their use in enhancing lateral flow detection (Goryacheva *et al.*, 2013). The black colour of colloidal carbon nanoparticles allows for easy visual detection and was first used as a label in rapid immunochromatographic tests in 1993 with claimed sensitivities close to that of an ELISA (Van Amerongen *et al.*, 1993). Colloidal carbon can be functionalised with various biological molecules and is further considered an inexpensive detection agent (Sajid *et al.*, 2014). The performance of carbon black was compared to silver enhanced gold, colloidal gold and latex nanoparticles, and was found to be 100 times more sensitive than the standard colloidal gold, with a lower detection limit of $0.01 \mu\text{g}.\text{ml}^{-1}$ compared to $0.1 \mu\text{g}.\text{ml}^{-1}$, $1 \mu\text{g}.\text{ml}^{-1}$ and $1 \text{mg}.\text{ml}^{-1}$ for silver enhanced gold, colloidal gold and latex respectively (Linares *et al.*, 2012). Carbon black particles range between $150 \pm 50 \text{ nm}$ in size and may form aggregates ($0.5 - 2 \mu\text{m}$), although the low density of the particles allow for larger particles to be used in lateral flow, subject to the membranes having suitable pore sizes of 8 – 12 times the diameter of the aggregates (Linares *et al.*, 2012). However, this label has not achieved wide adoption possibly due to the presence aggregates and irregular shaped particles (Sajid *et al.*, 2014). Colloidal iron oxide labels have been used for enhanced detection due to their magnetic properties and the ability to read the signals at the capture lines with a simple magnetic particle detector (Goryacheva *et al.*, 2013; Handali *et al.*, 2010; Nor *et al.*, 2012; Sajid *et al.*, 2014; Wang *et al.*, 2009b). Advantages of using magnetic nanoparticles is the stability of the signal since the signal does not degrade over time and where only the top $10 \mu\text{m}$ of the nitrocellulose membrane is available for visual detection, the use of magnetic nanoparticles allows for measurement of the magnetic signal throughout the depth of the membrane, resulting in claimed enhancement in sensitivities from 10 – 1000-fold (Wang *et al.*, 2009b). Colloidal dyes make use of organic nanoparticles which are loaded with a colourless indigo dye precursor (5-bromo-4-chloro-3-indolyl acetate) and coupled to antibodies. The dyed particles are activated through hydrolysis to produce a blue compound (5-bromo-4-chloro-3-hydroxyindole), which in turn oxidises to become an insoluble precipitate (5,5'-dibromo-4,4'-dichloro-indigo) (Mak *et al.*, 2011). The advantage of this approach is that the visibly

detectable signal is both quantitative and qualitative with a signal to noise ratio 2 times higher than that of conventional colloidal gold (Mak *et al.*, 2011).

Fluorescent labels (e.g. rhodamine, cyanine, fluorescein) are widely used in diagnostic detection due to their high sensitivity and potential for simultaneous detection of multiple analytes (multiplexing) which can be quantified (Wang *et al.*, 2006). The use of single fluorescent labels in membrane based assays are limited due to the high light scattering caused by the membrane support and the interference of internal fluorescence caused by the assay proteins and analytes (Goryacheva *et al.*, 2013). They are therefore incorporated in microspheres (polystyrene) or by doping of silica nanoparticles (Choi *et al.*, 2004; Goryacheva *et al.*, 2013; Nooney *et al.*, 2012; Oh *et al.*, 2009). Quantum dots are inorganic luminescent semiconducting nanocrystals that are water dispersible and can easily be combined with biomolecules for use in diagnostic assays with a claimed enhanced sensitivity of 10-fold when compared to colloidal gold (by UV light analysis) (Goryacheva *et al.*, 2013; Sajid *et al.*, 2014). Quantum dots are however toxic and their disposal is currently of concern for point-of-care application (Sajid *et al.*, 2014). The toxicity of quantum dots can be overcome by incorporation into silica nanoshells (Bruchez *et al.*, 1998). The limit of detection using CdTe quantum dot test strips decreased by 10-fold when compared to colloidal gold test strips (Yang *et al.*, 2010). Up-converting phosphors (UCPs) have received much attention in lateral flow assay development (Sajid *et al.*, 2014). UCPs are photo-luminescent inorganic crystals consisting of rare earth metals, capable of photon up-conversion upon photon absorption (Riuttamaki *et al.*, 2014). These UCPs combine absorber and emitter ions in sub-micron sized crystals of 200 – 400 nm in diameter, to up-convert low-energy (infra-red) radiation to high-energy (visible) light, by making use of a multiphoton absorption process and phosphorescence emission (Hampl *et al.*, 2001). Detection of UCPs remains unaffected by the environment (e.g. buffer composition, assay temperature) with minimal background signal and no photo-bleaching (Hampl *et al.*, 2001). UCPs enable multiplex detection, while the brightness of the crystals and the absence of auto-fluorescence support quantification over a wide range of analyte concentrations (Hampl *et al.*, 2001). The use of UCPs in diagnostics such as lateral flow assays, result in enhanced sensitivity of 10 – 100-fold when compared to colloidal gold and coloured latex beads under the same experimental conditions (Corstjens *et al.*, 2001; Hampl *et al.*, 2001). Disadvantages of using UCPs include the complex preparation and labelling processes, the non-specific binding of untreated phosphor particles with biomolecules and the requirement for surface modification to enable bio-conjugation (Goryacheva *et al.*, 2013).

Latex particles have also been incorporated into lateral flow immunoassays with several claimed advantages over colloidal gold as a detector agent. The surface of latex particles can be functionalised (carboxylation, amidation, hydroxylation, amination) to facilitate antibody

attachment and increase stability of attached capture agents through covalent coupling chemistries (Gella *et al.*, 1991; Wong *et al.*, 2009). A requirement for quantitative lateral flow diagnostic devices is the reproducible attachment of the antibodies (Wong *et al.*, 2009). Latex particles can also incorporate a variety of colour dyes, allowing multiple ligands to be conjugated covalently to different coloured particles for multiplexing, with simple interpretation of diagnostic results (Wong *et al.*, 2009). The disadvantage of latex however is its tendency to aggregate and the modified latex particles often require an optical instrument to measure the signal (reflectance, contrast, colour change or fluorescence), increasing the potential cost of diagnosis, but providing for quantitation for e.g. monitoring of treatment (Shyu *et al.*, 2002; Wong *et al.*, 2009). The aggregation of latex is a major concern in a lateral flow diagnostic device since, unlike colloidal gold aggregation which is visible, there is no distinct colour change with latex aggregation and it remains undetected in the assay, leading to reduction in assay sensitivity (Wong *et al.*, 2009). Colloidal gold remains more sensitive than standard coloured latex beads due to the smaller size of colloidal gold allowing higher packing density of the nanoparticles at the capture lines on the nitrocellulose membrane and the higher colour intensity of colloidal gold allows for better discrimination of low positive signals in an assay (O' Farrell, 2013). The sensitivity limitations of latex are however overcome with the use of alternate (fluorescent) labels.

The current commercial standards, colloidal gold and latex, unfortunately do not provide a universal solution to the key lateral flow assay requirements. Should an assay require covalent attachment of antibodies then only latex can be considered since colloidal gold utilises adsorption *via* hydrophobic and electrostatic interaction (Wong *et al.*, 2009). If sensitivity is required colloidal gold would be the preferred detector due to its small size and its ability to give a higher packing density on the capture (control and test) lines of lateral flow devices, while multiplex detection would favour the use of latex beads (Wong *et al.*, 2009). Both particles would potentially benefit from the use of a reader while latex particles labelled with fluorescent labels could result in enhanced sensitivity (with reader) while the cost for both colloidal gold and latex based assays are comparable from colloidal gold suppliers such as British BioCell International, Diagnostic Consulting Network and latex bead suppliers such as Bangs Lab, Dynal and Merck (Wong *et al.*, 2009).

A new high capacity polymer microsphere technology (termed ReSyn) has several features which could alleviate the limitations of current RDT lateral flow detection particles. The polymer microspheres have a comparatively higher functional group density, potentially providing for enhanced stability of immobilised biologicals through multipoint covalent attachment (Brady *et al.*, 2009; Twala *et al.*, 2012). The microspheres may be coloured to provide for multiplex and quantitative detection in lateral flow, while the high capacity of the microspheres and high

functional group density may potentially provide for a high chromophore capacity, increasing the contrast against the nitrocellulose membrane, further improving assay sensitivity for visual detection. Considering this is a polymer microsphere technology, it may be suitable for multiplex detection, and further provide for quantitative detection of biomarkers.

1.5. Malaria

Malaria is an infectious disease which affects approximately 40% of the world's population and has become widespread through tropical and sub-tropical regions, including America, Asia and Africa (Bell *et al.*, 2006). Malaria is a disease which is often associated with poverty, causing febrile illness and contributing to the high mortality and morbidity rates found in the tropics (Bell *et al.*, 2006). Out of the 109 countries reported to be endemic for malaria, 45 are located in Africa (WHO, 2009). It has been estimated that approximately 216 million clinical cases occur annually around the world, with 85% in sub-Saharan Africa and an approximate mortality of 655 000 deaths in 2010 (del Prado *et al.*, 2014; White *et al.*, 2014; WHO, 2009). The majority of the countries affected by malaria simply do not have the health infrastructure or resources to effectively combat the disease and this eventually leads to poor economic growth and persistence of the disease (Bosman *et al.*, 1999). The global distributions of the *Plasmodium* species that are associated with malaria incidence in humans (*Plasmodium falciparum*, *Plasmodium vivax*, *Plasmodium ovale* and *Plasmodium malariae*) are illustrated in Figure 1.2 (Talman *et al.*, 2007). The fifth species, known as *Plasmodium knowlesi*, primarily affecting monkeys (with potential cross-species infection to humans) is not included due to its comparatively low incidence (White *et al.*, 2014).

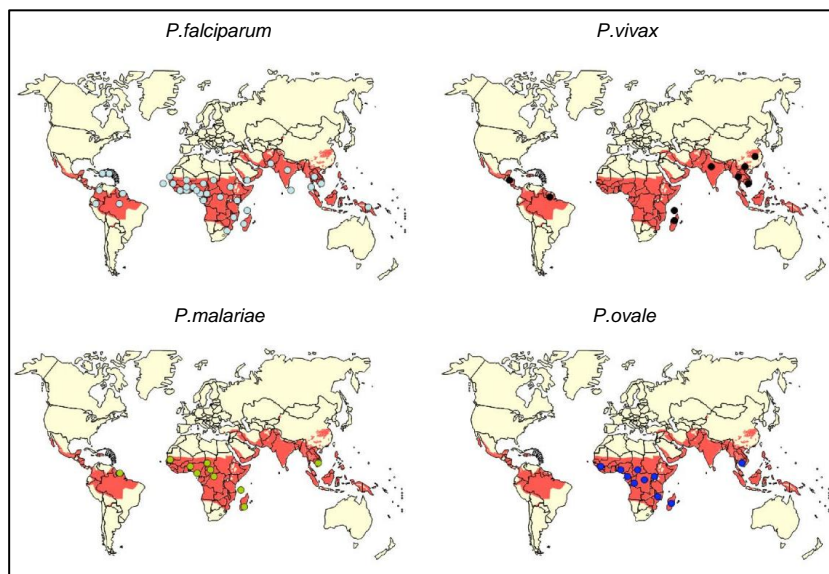


Figure 1.2: A world map, illustrating the global distribution of common *Plasmodium* species in red (reproduced from Talman *et al.*, 2007). Dots represent locations where the various *Plasmodium* species have been reported.

The effect of malaria on economic growth, human health and longevity is of major concern for developing countries (Makler *et al.*, 1998; Sachs *et al.*, 2002). Malaria is a poverty related disease and the economic burden of malaria has been estimated to cost African countries more than \$12 billion per annum, with approximately 40% of the African health expenditure on malaria alone (Kokwaro, 2009). In 2005 the World Health Organisation (WHO) estimated that a larger quantity of anti-malarial drugs were distributed/administered compared to the quantity of rapid diagnostic tests purchased, suggesting the possibility that anti-malarial drugs are potentially wasted on patients with non-malarial disease (Bell *et al.*, 2006). Research aimed at improved malaria diagnostics receives less than 1% of the overall annual research and development expenditure on malaria, compared to 37% for drug discovery and development research, even though the ultimate impact of improved diagnosis for the management of the disease potentially has a greater effect on morbidity of the disease (Bell *et al.*, 2006).

All five identified *Plasmodium* species exhibit a similar life cycle consisting of an insect vector and a vertebrate host, with minor variations in the time taken to complete a full lifecycle (White *et al.*, 2014). The sexual stage of the parasite lifecycle occurs in the female *Anopheles* mosquito while the asexual stage occurs within the human host (Figure 1.3) (White *et al.*, 2014).

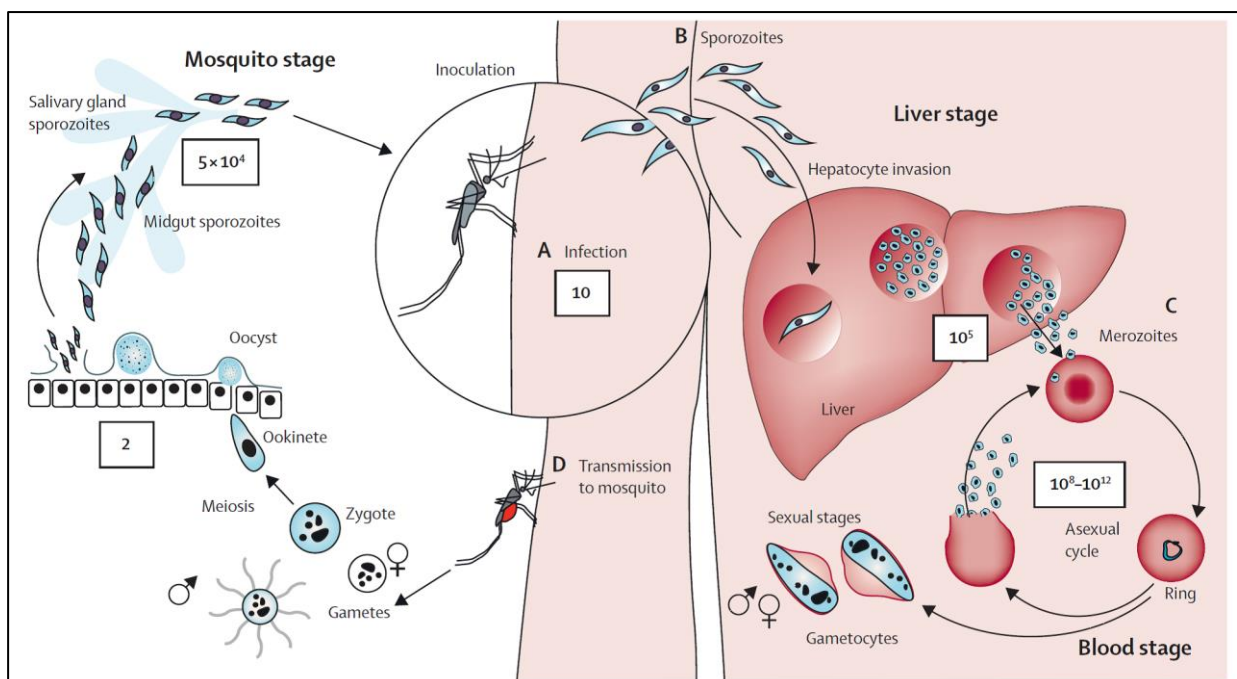


Figure 1.3: Lifecycle development stages of the malaria parasite in the human and mosquito host (reproduced from White *et al.*, 2014).

The female mosquito requires a blood meal to facilitate egg production and during the feeding process, thousands of haploid sporozoites from an infected mosquito are injected into a human host where they travel *via* the blood stream to the hepatocytes (White *et al.*, 2014; Winzeler, 2006). Once the sporozoites have invaded the hepatocytes they asexually reproduce to

merozoites which, once released into the blood stream, proceed to invade new erythrocytes (White *et al.*, 2014; Winzeler, 2006). Each sporozoite produces between 10 000 and 30 000 new merozoites within 1 week after hepatocyte invasion, with an asexual blood-stage cycle of 72 hours for *P. malariae*, 48 hours for *P. falciparum*, *P. vivax* and *P. ovale*, and 24 hours for *P. knowlesi* (White *et al.*, 2014). Within the erythrocytes the parasite consumes the red blood cell's contents, alters the cell membrane to facilitate nutrient exchange and matures from the ring stage to the trophozoite stage, producing a mature schizont (White *et al.*, 2014). Rupturing of the mature schizont releases approximately 30 new merozoites into the blood stream to infect/invade new erythrocytes (White *et al.*, 2014; Winzeler, 2006). A small subset of the parasites undergo gametocytogenesis in the human host to produce mature male and female gametocytes (White *et al.*, 2014; Winzeler, 2006). If these sexual forms of the parasite are transferred to a mosquito during a blood meal, they undergo sexual reproduction in the mosquito's midgut to produce new sporozoites (through oocyst formation) which migrate to the mosquito salivary glands and facilitate parasite transmission to the next host, completing the malarial parasite life-cycle (Winzeler, 2006).

P. falciparum and *P. vivax* are considered the most important infectious human *Plasmodium* species (Bosch *et al.*, 2007; White *et al.*, 2014). *P. vivax* is the most widespread malaria parasite likely due to its potential for a dormant liver stage, where not all of the injected sporozoites mature into schizonts but instead a proportion remain as hypnozoites and can result in dormancy for up to 30 years (Hulden *et al.*, 2011). *P. falciparum* has the highest mortality rate and can rapidly progress to cause coma and death, while *P. vivax*, *P. ovale* and *P. malariae* cause acute illness, but are rarely fatal (Bell *et al.*, 2006).

There are over 400 different *Anopheles* mosquito species; 25 of these are regarded as important malaria vectors, with *A. gambiae* and *A. funestus* the primary malaria vectors of *P. falciparum* in Africa during the wet and dry season respectively (Gullan *et al.*, 2010; Kelly-Hope *et al.*, 2009; Kiszewski *et al.*, 2004; White *et al.*, 2014). While most other species of mosquito feed on animals, these malaria vectors preferably feed on humans, classifying them as anthropophilic (Kiszewski *et al.*, 2004; Sachs *et al.*, 2002; Sinka *et al.*, 2012). Figure 1.4 illustrates the global distribution of *Anopheles* mosquitos, clearly illustrating the dominance of *A. gambiae* and *A. funestus* in central Africa (Sinka *et al.*, 2012).

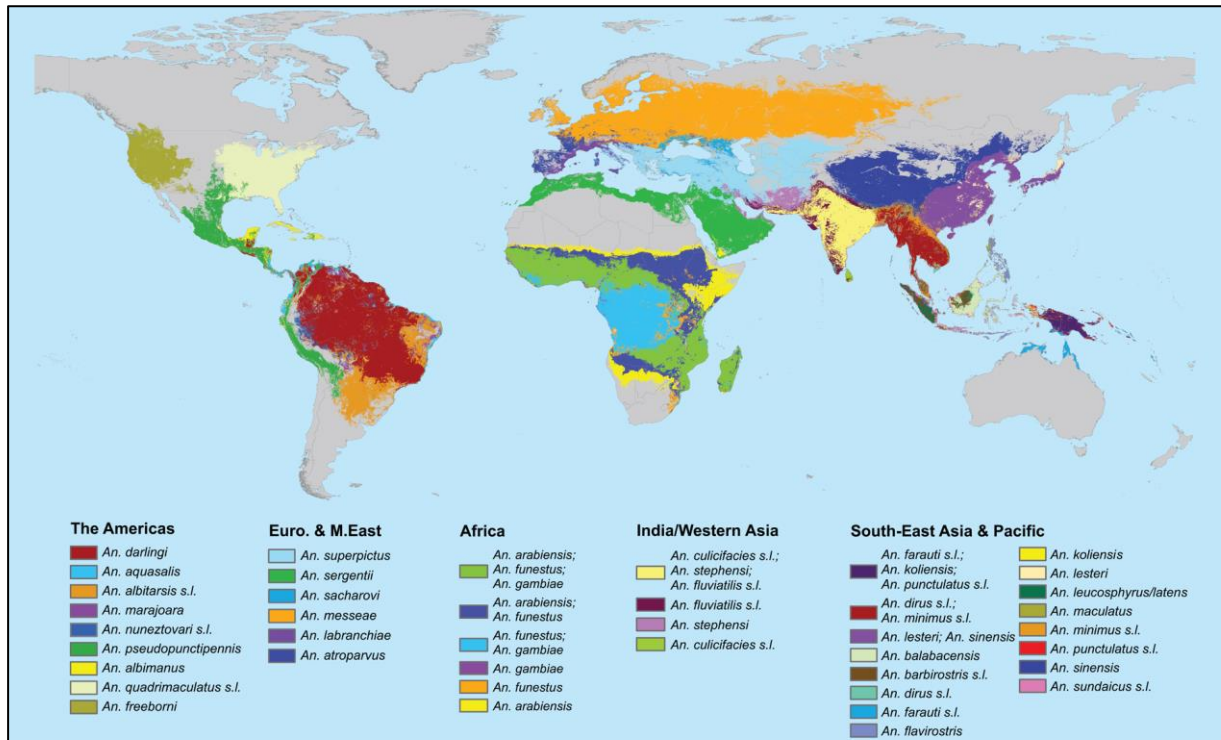


Figure 1.4: Global distribution of dominant malaria vector species (reproduced from Sinka *et al.*, 2012).

The future impact of global warming and climate change on malaria has become a public health concern due to the possible spread of malaria and its vectors (Gething *et al.*, 2010; Siraj *et al.*, 2014). The *Plasmodium* parasite undergoes an essential life-cycle change within the mosquito prior to it becoming infectious to other hosts, which is highly dependent on temperature (Sachs *et al.*, 2002). Parasite transmission becomes less likely at temperatures below 18 °C while parasite development ceases at temperatures below 16°C (Sachs *et al.*, 2002; Siraj *et al.*, 2014). Furthermore, at lower temperatures, feeding declines and the rate and stability of parasite transmission therefore decreases in temperate climates (Sachs *et al.*, 2002). Additional climatic features that affect parasite transmission include humidity and rainfall, the effect of which are the topic of a study by Sachs *et al.* in 2002. It was suggested that these changes may facilitate the spread and persistence of malaria into regions currently unaffected and that the distribution range of *Anopheles* will shift outwards rather than jump into different locations (Rogers *et al.*, 2000; Tonnang *et al.*, 2010). Of further concern for the spread of malaria vectors and parasites that are introduced into unaffected areas through travellers or trading activities, is the possibility of increased survival in these regions as a result of climate change (Rogers *et al.*, 2000; Tonnang *et al.*, 2010).

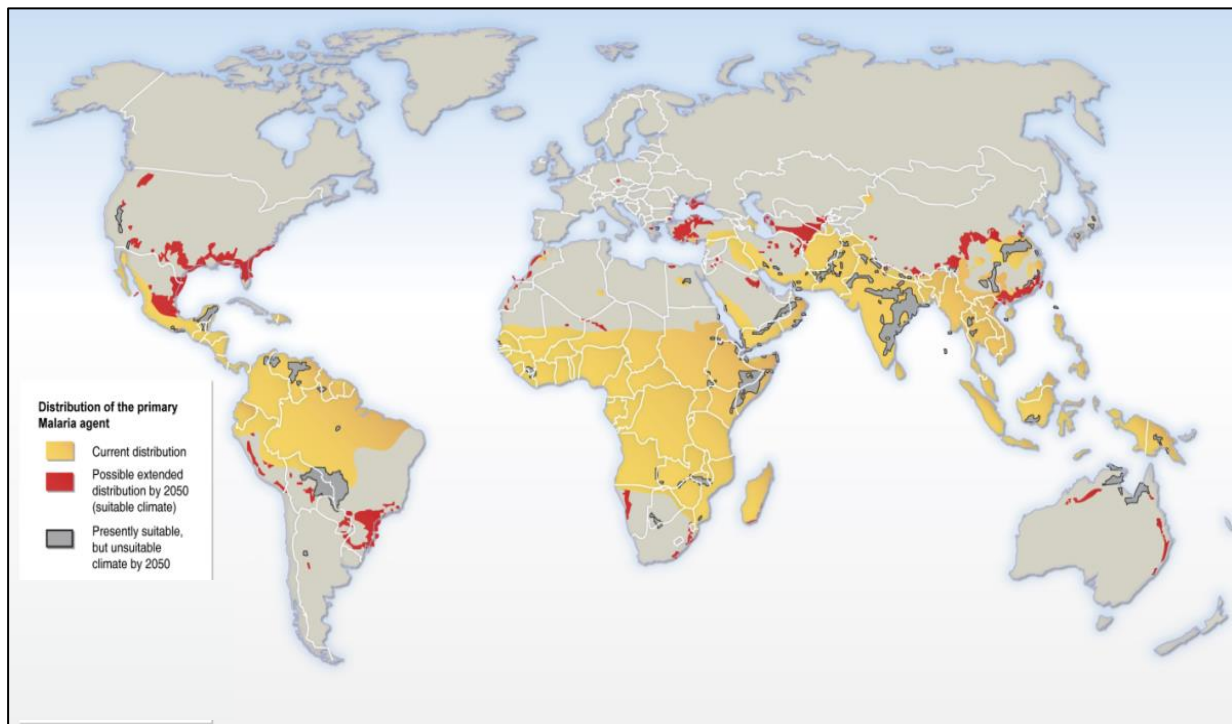


Figure 1.5: The current and predicted global distribution of malaria (reproduced from Rogers *et al.*, 2000).

1.6. Prevention and treatment of malaria

Preventative measures such as the use of insecticide treated bed nets (e.g. Pyrethroid) and indoor spraying of DDT (dichlorodiphenyltrichloroethane) are effective control measures in areas with moderate to high transmission rates, as both strategies kill the anopheles mosquito vector (del Prado *et al.*, 2014; White *et al.*, 2014). Access to anti-malarial drugs is currently a problem and would allow for successful treatment and reduced transmission rates (del Prado *et al.*, 2014; White *et al.*, 2014). The extensive use of chloroquine and sulphadoxine-pyrimethamine, as effective and low cost treatments for suspected malaria infection, contributed to the rise of drug resistant parasites which has led to the introduction of more expensive first line anti-malarial drugs such as artemisinin-combination therapies since 2007 (Kokwaro, 2009; Loubiere *et al.*, 2010; Murray *et al.*, 2008; Urdea *et al.*, 2006).

In tropical and sub-tropical regions symptomatic diagnosis of malaria is problematic, especially considering the range of disease with similar symptoms (headache, fever, diarrhoea) that may result in incorrect diagnosis and thereby contribute to malaria mortality (Bell *et al.*, 2006; Ly *et al.*, 2010; Murray *et al.*, 2008; Tangpukdee *et al.*, 2009). In addition, incorrect initial diagnosis leads to late diagnosis, which contributes to the rise of drug resistant parasites due to incorrect initial drug administration (Kokwaro, 2009; White *et al.*, 2014).

Anti-malarial drugs differ in their mode of action and the rate of parasite clearance: artemisinin-based therapy has been shown to reduce the parasite burden in the body by a factor of 10^4 with every treatment cycle; while previous front-line treatments including quinine, sulphadoxine-pyrimethamine and mefloquine have shown to reduce the parasite burden by a factor of $10^2 - 10^3$; and antibiotics only reduce the parasite burden by a factor of 10 (Nosten *et al.*, 2004). The main objective for the treatment of uncomplicated malaria (non-specific symptoms such as headache and fever are present, but there are no signs of vital organ dysfunction/failure) is to effectively reduce the parasite burden, with the aim of ultimately clearing the parasite biomass, further reducing the possibility of transmission (Bell *et al.*, 2004; Nosten *et al.*, 2004; White, 2014). It has previously been shown that initiating treatment within 48 hours of fever onset allows maximum reduction in gametocyte burden, which prevents the switch to gametocytogenesis (Nosten *et al.*, 2004). Earlier detection could therefore effectively decrease the rate of transmission, reduce drug expenditure and ultimately reduce mortality. More recently, a possible vaccine targeted against the circumsporozoite protein of *P. falciparum*, has been developed (White *et al.*, 2014). A large clinical trial is currently underway where this vaccine is evaluated in seven African countries and thus far it has shown good safety, but only moderate efficiency (del Prado *et al.*, 2014; White *et al.*, 2014).

1.7. Malaria biomarkers

During the life cycle of the *Plasmodium* (malaria) parasite, several species specific antigens are expressed at different stages, and these antigens may be used as biological markers for disease detection and diagnosis (Bell *et al.*, 2006; Drakeley *et al.*, 2009; White *et al.*, 2014). The parasite specific antigens (biomarkers) most often used for malaria detection are histidine rich protein 2 (HRP2), *Plasmodium* lactate dehydrogenase (pLDH) and aldolase, which are secreted into the blood throughout the asexual lifecycle stages of the parasite (Bell *et al.*, 2006). HRP2 is a heat-stable, water soluble antigen specific for detection of *P. falciparum*, while pLDH and aldolase are conserved key enzymes of the malaria parasite's glycolytic pathway, which are suitable as biomarkers for detection of all *Plasmodium* species that infect humans, and are thus classified as pan-species reactive (Bell *et al.*, 2006).

Infection with *Plasmodium falciparum* mediates parasite dependent alterations of the erythrocyte membrane, resulting in the development of surface protrusions (knobs) which enable erythrocyte sequestration (adherence of red blood cells containing late stage malaria parasites to the capillaries and therefore are not available in the blood (Leech *et al.*, 1984). Erythrocytes containing early stage malaria parasites (rings) do not express the surface protrusions (knob negative) and circulate in the blood stream, while erythrocytes containing late stage malaria parasites (trophozoites and schizonts) express the surface protrusions

(knob positive) and sequester to the endothelium of capillaries (Howard *et al.*, 1986; Leech *et al.*, 1984). HRP1, HRP2 and HRP3 are proteins synthesised by *Plasmodium falciparum*, with HRP1 solely expressed by knob positive infected erythrocytes, HRP2 expressed in both knob positive and knob negative erythrocytes and thus found in high abundance, with HRP3 structurally similar to HRP2 but found in the lowest abundance (Howard *et al.*, 1986; Rock *et al.*, 1987).

HRP2 is a 60 – 105 kDa protein produced by the asexual and early sexual stages of the parasite and is composed of 10% aspartic acid residues, 34% histidine residues, and 37% alanine amino acid residues (Baker *et al.*, 2010). The protein is exported through the erythrocyte cytoplasm, accumulates in the extracellular plasma and may be detected in serum, plasma and urine (Desakorn *et al.*, 2005; Kifude *et al.*, 2008). Theories have suggested the possible roles of HRP2 to be detoxification of free haem by polymerisation of haem into hemozoin; however, the protein has further been implicated in remodelling of the erythrocyte cytoskeleton, modulating the host immune response, and inhibiting neutrophil-mediated immune response required to kill the asexual form of *P. falciparum* (Baker *et al.*, 2010; Desakorn *et al.*, 2005; Howard *et al.*, 1986). The localised concentration of HRP2 increases throughout the intra-erythrocytic developmental cycle of the parasite and most of the antigen is released during rupturing of the schizont and has been detected in synchronised *in vitro* cultures as early as 2-8 hours after ring development, thus being the ideal biomarker for *Plasmodium falciparum* detection (Kifude *et al.*, 2008). Quantification studies have revealed that each parasite excretes an average of 5.2 femtogram HRP2, with a mean plasma elimination half-life of 3.67 days (Desakorn *et al.*, 2005; Fogg *et al.*, 2008).

Tests based on HRP2 have been shown to provide sensitivities and specificities in excess of 90% when there are between 60 – 100 parasites. μl^{-1} of blood (Makler *et al.*, 1998). HRP2 expression is limited to *P. falciparum* and assays are indicative of infection with this *species* only, while infection with the remaining three species can remain undetected and may be misdiagnosed as malaria-negative (Makler *et al.*, 1998). Previous studies have found that HRP2 antigen remains in the blood for several weeks after the parasites have been cleared from the host and therefore, these assays are not suitable for monitoring parasite clearance during malaria treatment (Makler *et al.*, 1998). False-positive results have also occurred as a result of cross reactivity with a rheumatoid factor (Wongsrichanalai *et al.*, 2007). However, replacement of IgG antibodies with IgM has been shown to eliminate this problem (Wongsrichanalai *et al.*, 2007). Recent episodes of fever have also been found to affect the sensitivity of the assay as fever often produces high levels of circulating non-specific heterophilic antibodies, that can result in false positives (Bell *et al.*, 2006).

Malaria parasites lack the citric acid cycle and depend on anaerobic glycolysis for energy production, where the infected red blood cell utilises glucose at a much higher rate than normal red blood cells, resulting in parasitized red blood cells consuming 30 – 50 times more glucose than the human host (Brown *et al.*, 2004; Choi *et al.*, 2007). pLDH is one of the most abundant *Plasmodium* enzymes and is involved in this anaerobic metabolism, catalysing the reduction of pyruvate to lactate using nicotinamide adenine dinucleotide (NADH) and 3-acetylpyridine adenine dinucleotide (APAD) as co-factors (Choi *et al.*, 2007; Talman *et al.*, 2007). Parasite pLDH is a 316 amino acid protein found in the cytosol and it has been proposed that parasite pLDH is present at higher levels in trophozoites than in the ring stage due to the increased metabolic requirements (Gomez *et al.*, 1997; Wiwanitkit, 2007). This antigen is produced solely by viable parasites and pLDH-based assays are capable of detecting all malaria causing species, allowing for the monitoring of anti-malarial therapy (Makler *et al.*, 1998). Various assay formats have been explored for pLDH using immunocapture, dipstick and immunodot techniques for diagnosis (Kakkilaya, 2003).

Aldolase is a key enzyme in the glycolytic cycle of the parasite, ultimately assisting in the generation of adenosine triphosphate (ATP) (Moody, 2002). Higher vertebrates have three tissue specific aldolase isoenzymes while *P. falciparum* and *P. vivax* only possess one aldolase isoenzyme, which is 396 amino acids in length and is relatively conserved with a molecular weight of 41kDa (Dzakah *et al.*, 2013; Lee *et al.*, 2006; Tritten *et al.*, 2009). Aldolase is believed to interact with actin and thrombospondin-related anonymous protein (TRAP) which are associated with the invasion machinery of the parasite (Bosch *et al.*, 2007; Jewett *et al.*, 2003). Aldolase is considered a pan-specific antigen, is localised to the cytoplasm of the parasite, and is often used in combination with HRP2, providing sensitivity of 75 – 95% at >500 parasites μl^{-1} blood (Dzakah *et al.*, 2013; Moody, 2002). The genetic diversity of this antigen in *P. falciparum* and *P. vivax* is highly conserved, preventing detection failure which may be seen with other antigens (Tritten *et al.*, 2009).

Performance of rapid diagnostic tests are influenced by intra-species diversity of the biomarkers, stage-specific expression of the antigens, and *in vivo* stability of the antigen (Bell *et al.*, 2006). HRP2 is highly variable and significant sequence variation has been observed between PfHRP2 and PfHRP3 isolated within the same country (Baker *et al.*, 2010). HRP2 protein diversity was shown to adversely affect the sensitivities of HRP2-based tests as certain isolates in the Amazon region of Peru have been found to lack either HRP2, HRP3, or both, which results in positive microscopic tests, but negative rapid diagnostic tests (Gamboa *et al.*, 2010; Tritten *et al.*, 2009). In Peru, the overall frequency of parasites lacking HRP2 and HRP3 were 41% and 70% respectively, while 21.6% of the parasites lacked both genes (Gamboa *et al.*, 2010). The strains with deleted HRP2 genes however still remained positive for pLDH,

supporting the need for multiplex rapid diagnostic assays (the simultaneous measurement of more than one correlated analyte in a single sample) applicable for certain regions of the world where these gene deletions are (or may become) common (Gamboa *et al.*, 2010; Tozzoli, 2007).

1.8. Diagnosis of malaria

In 2004 the Bill and Melinda Gates Foundation selected malaria as one of the six priority global diseases in the developing world with regards to diagnostics (Urdea *et al.*, 2006). In high transmission areas where adequate resources and healthcare infrastructures are limited, effective diagnosis, prevention and treatment of malaria become extremely challenging due to various factors such as parasite sequestration, life cycle development changes of the different malaria species (time to complete a full life cycle differs), persisting viable and non-viable parasitemia (active versus previous malaria infection), drug resistance, immunity and population movement (David *et al.*, 1983; Tangpukdee *et al.*, 2009). The Global Malaria Control strategy and the Roll Back Malaria initiative places emphasis on applying current diagnostic tools effectively and developing new tools for improving the management of the disease (WHO, 2000). Currently, various limitations exist for accurate, rapid, inexpensive and sensitive diagnosis of malaria, and the “gold standard” for malaria diagnosis remains microscopy (Wongsrichanalai *et al.*, 2007). Although there are several diagnostic technologies suitable for detection of malaria, true point-of-care diagnostics and disease management of malaria still remains challenging.

1.8.1. Microscopy

Light microscopic examination of thick and thin blood smears stained with either Giemsa, Wrights or Field’s stain, can provide information on the species, the stage, and the density of parasitemia with a sensitivity of 5 to 10 parasites. μl^{-1} of blood for well trained staff (Kakkilaya, 2003; Makler *et al.*, 1998; Moody, 2002; Murray *et al.*, 2008). The different stages of the parasite (ring, trophozoite and schizont) are morphologically different, with the ring stage having a characteristic “ring” with a large chromatin dot, the trophozoite stage having a denser pigment and larger chromatin dot and the mature schizont stage having a large nuclei containing merozoites clustered around a dark coarse mass (White, 2014). For quantification purposes, thick blood smears are preferred since they can provide improved sensitivity at low parasitemia, while a major disadvantage of this procedure is the potential lysis of erythrocytes during the staining procedure, that can result in irregularities and difficulties in interpretation (Moody, 2002). Thin blood smears, stained with Giemsa or Wright’s stain, provide a monolayer

of erythrocytes and can allow for morphological identification of the infecting *Plasmodium* species with greater specificity (Makler *et al.*, 1998; Moody, 2002).

The detection threshold for Giemsa stained thick blood smears is estimated to be 4 – 20 parasites. μl^{-1} blood. However, under field conditions this threshold is considered closer to 50 – 100 parasites. μl^{-1} (Tangpukdee *et al.*, 2009; Wongsrichanalai *et al.*, 2007). Unfortunately, microscopy is prone to human error, and accuracy is dependent on several factors including level of staff training, condition of the microscope, workload of the staff, and quality of the laboratory reagents and supplies (Wongsrichanalai *et al.*, 2007). Blood film preparations may generate artefacts formed from stain precipitation, dirt and cell debris resulting in false-positives while false-negative results often occur at low parasite densities (Figure 1.6; Wongsrichanalai *et al.*, 2007). Although microscopy is still considered the gold standard for malaria diagnosis, it is evident in Figure 1.6 that microscopy in the hands of an inexperienced microscopy analyst could result in incorrect diagnosis.

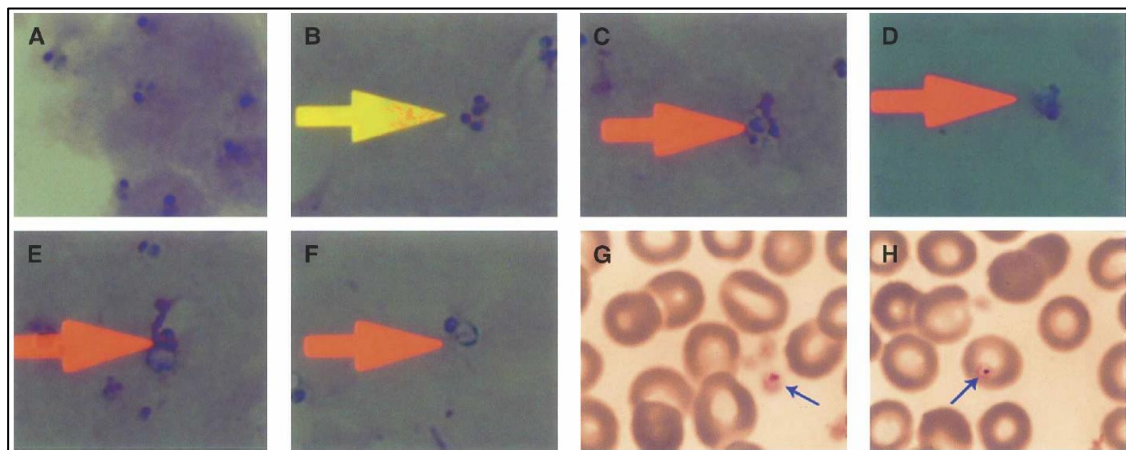


Figure 1.6: Examples of Giemsa stained thick (top) and thin (bottom) blood smear of artefacts that may result in incorrect diagnosis, reproduced from Wongsrichanalai *et al.*, 2007. **A:** Early trophozoite of *P. falciparum*; **B:** Two ring forms that look like artefacts; **C – H:** Artefacts that resemble *P. falciparum* trophozoites on thin film **C – F** and thin film **G – H**.

Fluorescent microscopy has also been considered useful as an enhanced detection method in the diagnosis of malaria since DNA-binding fluorescent dyes are used to identify infected red blood cells containing parasite deoxyribonucleic acids (DNA) present in the parasite nucleus and fluoresce strongly when excited by UV light (Makler *et al.*, 1998; Moody, 2002). Acridine orange (AO) and benzothiocarboxypurine (BCP) are two commonly used fluorochromes for malaria staining. A diagnostic technique called the buffy coat method uses AO to stain parasites in a specialised capillary tube, followed by differential centrifugation and visualisation (Mattia *et al.*, 1993). Rhodamine-123 may be used for assessing parasite viability, since this dye is only taken up if the parasite membrane is functional, potentially allowing for monitoring of parasite clearance during treatment (Moody, 2002). Methods utilising AO as a stain provide sensitivity and specificity values of 41 – 93% and >93% respectively, at ~100 parasites. μl^{-1}

(Moody, 2002). BCP stains the nucleic acids of viable parasites intensely while leaving the erythrocyte inclusions and leukocytes poorly stained, which allows for the rapid and accurate examination of lysed blood, either in suspension or on the unfixed thick blood film with sensitivity and specificity values of >95% (Moody, 2002). The use of AO and BCP however has its limitations, since fluorescent methods require specialised training, equipment (fluorescent microscope) and reagents (toxicity requires special disposal) (Makler *et al.*, 1998). Furthermore, these techniques fail to differentiate among *Plasmodium* species (Makler *et al.*, 1998).

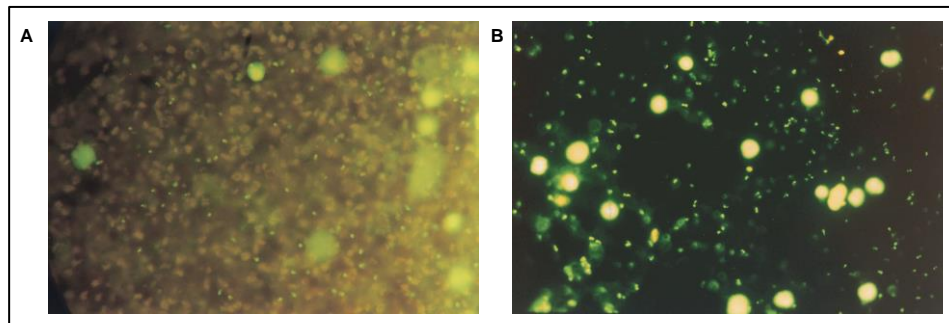


Figure 1.7: Fluorescent microscopy for the detection of malaria. **A:** Acridine Orange in the Quantitative Buffy Coat method and **B:** Benzoethiocarboxypurine method. Reproduced from Moody *et al.*, 2002.

1.8.2. Molecular diagnosis

Various molecular DNA based techniques have been employed for use in malaria diagnostics and include polymerase chain reaction (PCR), microarray, loop-mediated isothermal amplification (LAMP), mass spectrometry (MS) and flow cytometry (FCM) (Tangpukdee *et al.*, 2009).

PCR has been successfully used in malaria diagnostics to provide high sensitivity (parasitemia of 5 parasites. μl^{-1}) and 100% specificity for all 4 human infective species (Kakkilaya, 2003; Makler *et al.*, 1998; Moody, 2002). Nested and multiplex PCR have been used to amplify various genes of *Plasmodium*, such as the small sub-unit 18S rRNA, the large sub-unit RNA and circumsporozoite genes (Moody, 2002). PCR technology is reported to be 10-times more sensitive than microscopy and thus, amplified parasite DNA can be detected in other non-invasive samples such as urine or saliva with sensitivity and specificity of 73% and 97% respectively (saliva) (Sutherland *et al.*, 2009).

The LAMP technique for malaria diagnosis uses isothermal amplification (does not require temperature cycling) and is considered simple and inexpensive, involving the detection of the 18s rRNA gene of *Plasmodium* (conserved in each species), which allow the various species to be distinguished in a mixed infection (Tangpukdee *et al.*, 2009). LAMP is considered potentially more affordable than PCR and has potential for use in rural clinical settings, as it

requires minimal equipment (a water-bath or heat block) but the reagents for this technique are expensive and require cold storage. Although LAMP has a detection limit of > 5 parasites. μl^{-1} blood, each LAMP assay can only detect a single *Plasmodium* species and thus mixed infections will require more than one LAMP assay to be used (Pöschl *et al.*, 2010; Sirichaisinthop *et al.*, 2011; Tangpukdee *et al.*, 2009). In addition LAMP is highly susceptible to false positives if the sample is contaminated with small amounts of DNA (Hsiang *et al.*, June 2014). Microarray technology enables the detection/probing of multiple targets in a single sample and would be ideal for point-of-care diagnostics if the technique could potentially be miniaturised and automated (Tangpukdee *et al.*, 2009).

1.8.3. Hemozoin detection

Flow cytometry has been evaluated as a diagnostic tool and is based on detecting hemozoin, a parasitic crystallised pigment in the parasite food vacuole which is formed when the parasite digests host haemoglobin (Gascoyne *et al.*, 2004; Tangpukdee *et al.*, 2009). The presence of hemozoin is detected by the depolarisation of the laser light when the cells pass through the detection channel, and potentially provides sensitivity and specificity values of 49 – 98% and 82 – 97% respectively (Tangpukdee *et al.*, 2009).

Mass spectrometry is potentially a rapid, robust, automatable and high throughput technique for malaria diagnostics with sensitivities of 10 parasites. μl^{-1} of blood (Tangpukdee *et al.*, 2009). This technique comprises of cleaning up the whole blood sample which is then subsequently analysed through a direct UV laser desorption mass spectrometer, and identifies heme from hemozoin (Tangpukdee *et al.*, 2009). Both flow cytometry and mass spectrometry do however suffer from the same drawbacks, including the requirement for expensive equipment and facilities, and highly trained and skilled staff (Tangpukdee *et al.*, 2009).

1.8.4. Immunoassay

Enzyme immunoassays (EIA) and Enzyme linked immunosorbent assay (ELISA) (refer to section 3.1 and Figure 3.2) utilise enzyme-labelled antibodies to detect biological molecules (antigens, proteins) in samples and is a technique widely used as a diagnostic tool (Lequin, 2005; Noedl *et al.*, 2006). The most commonly used enzymes for enzyme-based immunoassays are alkaline phosphatase (AP) and horseradish peroxidase (HRP) since their substrates are non-toxic and inexpensive, and provide a colour change that is easily observed with the naked eye and measured spectrophotometrically (Voller *et al.*, 1976). Radioactive isotopes and fluorescent dyes may also be attached to the antibodies or antigens, referred to as Radioimmunoassay's (RIA) or immunofluorescence respectively (Voller *et al.*, 1976). These

techniques suffer the same drawbacks including the requirement for a detection instrument and trained staff, limiting their application to point-of-care. Reducing these techniques to point-of-care has necessitated the development of new, miniaturised readers, and the automation of sample processing through e.g. microfluidic technologies (Gascoyne *et al.*, 2004).

Nucleic acid lateral flow immunoassays (NALFIA) incorporate a PCR amplification step followed by the lateral flow immunoassay, where the labelled amplicon products are captured by specific antibodies present at the test and control lines (Matson, 2013). The performance of NALFIA to detect all four human *Plasmodium* species have been evaluated with direct comparison to PCR (combined with gel electrophoresis) and microscopy (Mens *et al.*, 2008). This technique was 10 fold more sensitive than gel analysis with a limit of detection in the range of 0.3 – 3 parasites. μl^{-1} (Mens *et al.*, 2008). The performance of NALFIA was considered good in both laboratory and field settings, with claimed specificity and sensitivity values of 94.8% and 97.4% respectively (Mens *et al.*, 2012). This molecular tool, although labour intensive, may potentially be advantageous in a point-of-care setting if inexpensive and portable thermal-cyclers could be used with stabilised PCR reagents (Matson, 2013; Mens *et al.*, 2012).

Isothermal recombinase polymerase amplification (RPA) in combination with lateral flow, also known as LF-RPA, amplifies DNA using oligonucleotide primers at temperatures just above room temperature in less than 30 minutes, after which the amplicons are run on a lateral flow assay (Kersting *et al.*, 2014; Piepenburg *et al.*, 2006). This diagnostic tool, requiring reduced temperatures, may potentially overcome the limitations of NALFIA. This technique reduce the requirement for instrumentation, and provides sensitivity and specificity comparable to conventional PCR (Kersting *et al.*, 2014). The performance of this diagnostic tool however still needs to be evaluated in a resource limited field-setting to determine its suitability for point-of-care diagnosis (Kersting *et al.*, 2014).

Gel diffusion assays are also commonly used in clinical laboratories and are based on the passive diffusion of antigens towards specific antibodies which result in precipitation lines in an agar gel and allows for easy diagnosis of disease (Riley *et al.*, 2002). This technique however lacks sensitivity and is often prone to interpretation errors (Riley *et al.*, 2002).

1.8.5. Emerging diagnostic technologies

Microfluidics and nanotechnology potentially provide solutions to sample processing (reducing training requirements and potential for human error), improving disease detection and assay performance (Yager *et al.*, 2008). Microfluidic technology has been introduced to study disease

pathogenesis with the hope of being used in the field for both diagnosis and prognosis of diseases such as malaria (Antia *et al.*, 2008). Microfluidics is a technology based on manipulating microliter volumes of fluids/samples in micron-sized channels with claimed advantages of being inexpensive, versatile and portable (Antia *et al.*, 2008). The detection reagents used in these emerging diagnostics include fluorescent and magnetic beads (Yager *et al.*, 2008). Microfluidics and nanoparticles are considered the next generation of diagnostic technologies, with claimed advantages of improved sensitivity. However, several challenges to their implementation as diagnostics remain, including toxicity of reagents and cost, currently preventing their application for point-of-care diagnosis in rural communities (Yager *et al.*, 2008).

The Magneto Optical Test (MOT) has been evaluated as a fast and easy method of detecting malaria parasites in resource poor settings since it does not require a stable source of electricity (solar battery) or cold storage (Mens *et al.*, 2010; Orbán *et al.*, 2014). The fundamental principle behind the test is that the *Plasmodium* parasite digests globin from haemoglobin, resulting in deposition of the toxic heme component in a rod-shaped, crystalline hemozoin (Butykai *et al.*, 2013; Mens *et al.*, 2010; Orbán *et al.*, 2014). The MOT principle is similar to flow cytometry and is based on detecting hemozoin (Mens *et al.*, 2010). Hemozoin is paramagnetic, allowing it to become temporarily magnetic when an external magnetic field is applied. Therefore, any hemozoin crystals present in an infected sample will align within the field of an externally applied magnetic force, a phenomenon known as the Cotton-Mouton effect (Figure 1.8) (Mens *et al.*, 2010).

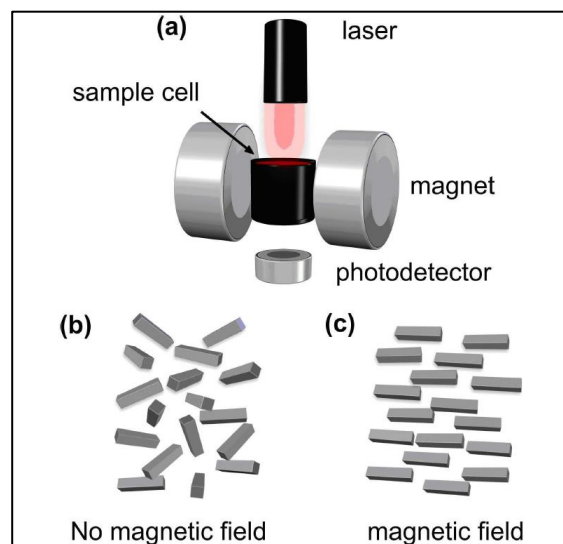


Figure 1.8: Schematic representation of the MOT diagnostic device principle reproduced from Mens *et al.*, 2010. (a) Lysed blood samples are placed between two poles of magnet and a laser beam passed through sample before and during application of the magnetic field. The transmitted intensity is recorded - if hemozoin is present the intensity of the transmitted magnetic signal increases. (b) No magnetic field, crystals are randomly oriented and a baseline signal is obtained. (c) Application of magnetic field results in crystals aligning, resulting in a measurable increase in intensity.

The MOT method is considered a potentially high-throughput and affordable point-of-care technology to rapidly screen patients for malaria, with an analytical sensitivity of 50 – 100 parasites. μl^{-1} (Mens *et al.*, 2010). Studies using the rotating-crystal magneto-optical (MO) diagnostic method on artificial (synthetic) hemozoin crystals (500 – 900 nm in length) resulted in a detection threshold of 15 picogram hemozoin per μl of blood which is equivalent to ≤ 30 parasites. μl^{-1} , but still requires validation in clinical testing (Butykai *et al.*, 2013). The study was repeated on synchronised *in vitro* *P. falciparum* cultures with resulting detection limits of 40 parasites. μl^{-1} for ring stage parasites, which are below the current threshold for RDT's (100 parasites. μl^{-1} blood) and within the detection range of expert microscopy (Orbán *et al.*, 2014). These studies were further performed on frozen blood samples and would need to be repeated on freshly lysed blood in order to support diagnosis at true point-of-care (Orbán *et al.*, 2014). The limitations of this technique also include the possibility of false positives, due to the presence of hemozoin in blood after parasite clearance, and false negatives which could result from infections containing early ring stage parasites with low levels of hemozoin (Orbán *et al.*, 2014).

1.8.6. Point-of-care technologies: Rapid diagnostic tests

The technologies with potentially the most impact on the management of malaria, are RDT's that are expected to be stable, sensitive, accurate and simple to use and interpret (Bell *et al.*, 2006). They are characterised as having little to no requirement for trained staff and a simple readout that is visually detectable (or at the least requires a simple reader for e.g. quantification purposes). Unfortunately these tests are currently considered the least sensitive and accurate for malaria diagnosis detecting between 100 – 500 parasites. μl^{-1} of blood (Hatta *et al.*, 2008; Moody, 2002; Wongsrichanalai *et al.*, 2007). The most prominent point-of-care test formats include agglutination, dip-stick, and lateral flow assays.

The latex agglutination test, which is a rapid, simple and portable diagnostic test suitable for biomedical field application, involves aggregation of antigen or antibody coated latex particles in the presence of a specific biomarker (Polpanich *et al.*, 2007). However, due to non-specific proteins adsorbing to the latex particles, non-specific agglutination can occur, resulting in false positives (Polpanich *et al.*, 2007). Agglutination testing has been shown to have a lower sensitivity and specificity when compared to lateral flow RDT's. This was illustrated in a study using hCG, where the agglutination assay resulted in sensitivity and specificity values of 82% and 43% respectively, while the lateral flow assay resulted in comparative sensitivity and specificity values of 99% and 100% respectively (Hassan *et al.*, 2009). The principle of lateral flow assays and agglutination assays is illustrated in Figure 1.9.

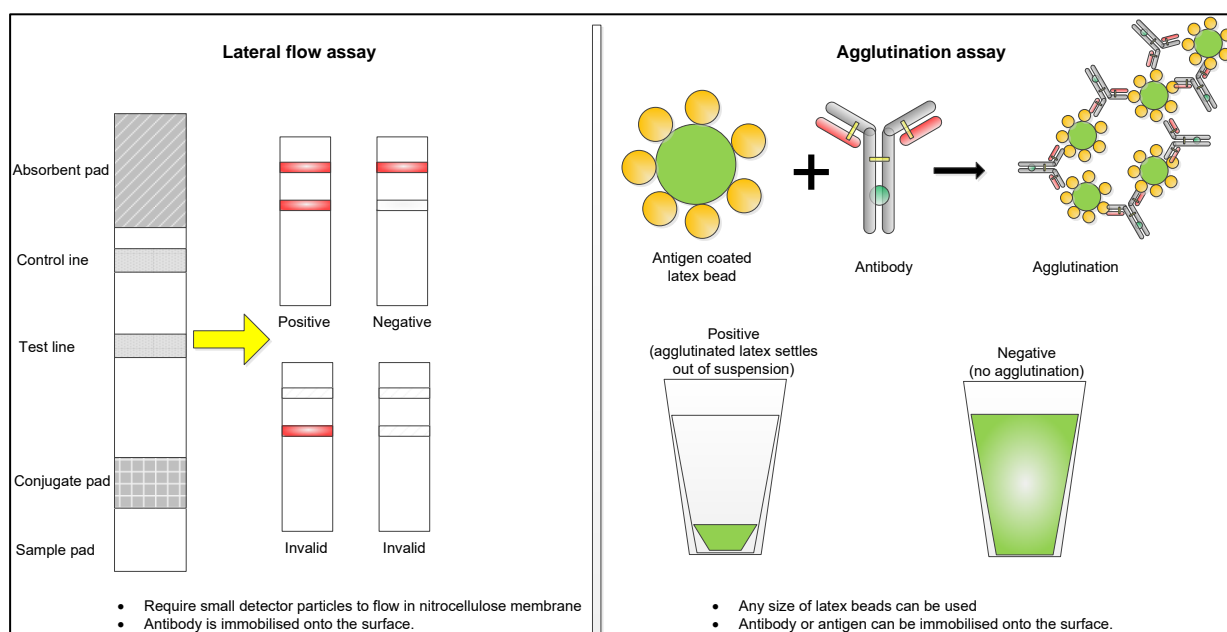


Figure 1.9: Schematic representation of positive and negative results obtained with a lateral flow assay and agglutination assay (adapted from Sajid *et al.*, 2014).

The stability of RDT's in tropical and sub-tropical areas is questionable, where high temperature and humid storage conditions may lead to deterioration of components and deformation of antigen-binding sites on the antibodies within these assays (Bell *et al.*, 2006). There are several factors that influence the suitability of these rapid diagnostic tests for malaria including the antigen being detected. As an example, the accuracy of rapid diagnostic tests may be adversely affected during treatment of malaria as certain antigens, such as HRP2, have a tendency to persist in the blood for several weeks after treatment while other antigens such as pLDH are rapidly cleared, and may thereby be used to monitor parasite clearance during treatment (Bell *et al.*, 2006).

Despite the numerous published lateral flow diagnostic test trial reports, it is difficult to accurately compare their efficiency since these tests are not performed under equivalent conditions, on the same epidemiological population, or under conditions prevalent in malaria infected territories (Murray *et al.*, 2008; Wongsrichanalai *et al.*, 2007). This led to an independent evaluation of the performance of selected commercially available lateral flow malaria tests under standard conditions by the World Health Organisation in 2009 (WHO, 2009). The results from these studies revealed numerous limitations regarding the sensitivity and specificity of these lateral flow diagnostic devices and are briefly summarised in Table 1.1 below.

Table 1.1: Summary of Rapid Diagnostic Tests conducted by the WHO (WHO, 2009)

Rapid Diagnostic Test	Antigen detected	Sensitivity 100-500 par.µl ⁻¹	Specificity 100-500 par.µl ⁻¹	Reference
ParaSight-F	HRP-2	>95%	97-99%	(Kilian <i>et al.</i> , 1997)
ICT Malaria Pf	HRP-2	92.5-100%	96.2-98.3%	(Garcia <i>et al.</i> , 1996; Gaye <i>et al.</i> , 1998; Jelinek <i>et al.</i> , 2000; Kilian <i>et al.</i> , 1997)
ParaCheck	HRP-2	~94%	~87.3%	(Fogg <i>et al.</i> , 2008)
PATH Pf Malaria IC	HRP-2	96%	99%	(Gaye <i>et al.</i> , 1998)
ICT Malaria Pf/Pv	HRP-2 Aldolase	95.5% (Pf) 75-95% (Pv)	89.8% (Pf) 94.8% (Pv)	(Tjitra <i>et al.</i> , 1999)
OptiMal	pLDH	88.5% (Pf) 61.5% (Pv)	99.4 (Pf) 100% (Pv)	(Jelinek <i>et al.</i> , 2000)
ICpLDH	pLDH	92%	100%	(Piper <i>et al.</i> , 1999)
ParaBank	pLDH	84.7%	94.6%	(Fogg <i>et al.</i> , 2008)
CareStart	pLDH	95.6%	91.5%	(Fogg <i>et al.</i> , 2008)
VstaPan	pLDH	91.1%	89.6%	(Fogg <i>et al.</i> , 2008)

* For a more detailed review on current rapid diagnostic tests refer to WHO report entitled: “Malaria rapid diagnostic test performance”

The current malaria rapid diagnostic tests are limited to blood based detection, which is problematic in countries where drawing of blood is frowned upon, and there is potential for accidental infection by the use of contaminated needles (Wilson *et al.*, 2008). HRP2 antigen has been detected in urine and saliva, albeit it at lower concentrations of the antigen in these non-invasive body fluids (Wilson *et al.*, 2008). Increasing the sensitivity of rapid diagnostic tests may therefore allow for detection of malaria in these non-invasive samples and assist in malaria management.

Rapid diagnostic tests are currently used by primary healthcare workers, but in conjunction with other methods to confirm the results and monitor treatment (Tangpukdee *et al.*, 2009). It is thereby evident that new RDT's for malaria offering improved sensitivity or stability could potentially offer significant advantages to management of malaria in remote prevalent areas.

We therefore propose that the development of the ReSyn polymer microsphere technology as lateral flow detection particles can address all the key requirements, possibly making it suitable for all RDT applications. Due to the potential benefit of improved detection agents for the management of malaria, we use this as a model disease for evaluation of the new detection microspheres (ReSyn). This thesis aims to address the first step in the development of a new platform for lateral flow detection agents, engineering of the ReSyn microspheres such that they are suitable for flow on lateral flow membranes with sensitivities and specificities in the range of the current commercial standard, colloidal gold.

CHAPTER 2

MICROSPHERE ENGINEERING FOR LATERAL FLOW

2.1. INTRODUCTION

Emulsions comprise of two immiscible liquids, with one liquid (the dispersed phase) being dispersed in the second liquid (the continuous phase), resulting in either an oil-in-water (o/w), water-in-oil (w/o) or anhydrous emulsion (Malick *et al.*, 1996). For emulsions to be made, the liquids are often subjected to mechanical shear forces, such as vigorous stirring, in the presence of an emulsifier (often a detergent), resulting in the otherwise insoluble substances remaining dispersed in an aqueous phase (Malick *et al.*, 1996). Microspheres that have been formed by emulsion polymerisation have found application in for instance the development of drug delivery systems, agglutination assays, nucleic acid hybridization assays and diagnostic assays (Malick *et al.*, 1996).

The physical and optical properties of microspheres are carefully considered in the context of detection, handling and final application, and small spheres (with diameters in the range of 0.1 – 0.4 μm) are ideal for lateral flow assays while larger microspheres ($\sim 4 - 10 \mu\text{m}$) are ideal for e.g. bead-based cytometric assays (Holmes *et al.*, 2007; Meza, 2000). Membrane manufacturers offer a range of nitrocellulose membranes with varying pore sizes, to accommodate particle size variations (e.g. colloidal gold vs latex) and vary lateral flow parameters such as speed of capillary flow (Wong *et al.*, 2009). Synthetic polymer microspheres, as opposed to silica or biopolymers, generally have higher protein binding capacity due to higher functional group densities, while the routine and simple incorporation of functional groups allows for covalent coupling, which may subsequently result in increased stability of immobilised biologicals (Ahmad *et al.*, 2014; Malick *et al.*, 1996). Various strategies are available to immobilise biological ligands onto polymer microspheres including adsorption, covalent coupling to surface functionalised microspheres, and affinity binding of ligand to microspheres pre-coated with a binding protein such as Streptavidin or Protein A/G, or chemical ligand such as chelated metal ions (Di Marco *et al.*, 2010; Tan *et al.*, 2012).

The polymer microspheres synthesised in this study for application as lateral flow detection agents, were produced using a modified water-in-oil emulsion technique (Jordaan *et al.*, 2009). The synthesis process was carefully considered as the particle size distribution and properties of the microspheres may be readily manipulated by adjusting both the quantity of the detergent during the emulsion process and the speed of mixing (energy input) (Jordaan *et al.*, 2009). Larger particle preparations are favoured with lower quantities of detergent and/or slower

mixing, while smaller particles are favoured with increased detergent and faster mixing speeds. The standard preparation of the microspheres, described by Jordaan *et al.*, (2009) produce aldehyde-functional microspheres, which may subsequently be converted to primary amine, epoxide or carboxyl functionality through reaction with various chemicals. The use of epoxide microspheres were considered the preferred functionality for use in lateral flow immunoassays due the potential stabilisation (covalent immobilisation) of the antibodies, which potentially addresses the lack of stability of current lateral flow devices to point-of-care (Mateo *et al.*, 2007).

One advantage of using polymer microspheres, in particular ReSyn with its high functional group density, in RDT diagnostic assays is the possibility of incorporating a high concentration of reactive dye, resulting in intensely coloured microspheres, thus potentially increasing the sensitivity of the assay over latex microspheres, as well as further allowing for the use of multiple colours in multiplexing assays (a claimed benefit of latex beads), allowing for the detection of various biomarkers in a single assay (Malick *et al.*, 1996).

Textile dyes, also commonly known as reactive dyes, are synthetic, inexpensive, commercially available and easily immobilised on surfaces bearing various functional groups (Denizli *et al.*, 2001). The chemical structure of dyes consists of conjugated systems of aromatic rings and double bonds, resulting in dye classes having anthroquinoid, indigoid and azo structures; all of which have strong transitions in the UV-visible spectrum (Chacko *et al.*, 2011). Azo dyes (characterized by having N=N bonds) are the most common and inexpensive dye class and were therefore considered for incorporation into the diagnostic microspheres.

A variety of dyes were considered in the evaluation of coupling to the microspheres, and for the potential of multiplexing. The initial selection was based on the tinctorial strength (ability to impart colour to materials) of the dye (Lambourne *et al.*, 1999). The higher the tinctorial strength of a dye, the less dye is required to achieve a certain depth of shade. The measure of tinctorial strength is related to the dye extinction coefficient, which is a measure of the optical density of a dye in relation to its concentration measured at the dye's maximum absorbance wavelength (Bailey *et al.*, 1989; Jung *et al.*, 2014). The higher the extinction coefficient of a dye the greater contribution each dye molecule makes to achieve a desired colour (Bailey *et al.*, 1989; Jung *et al.*, 2014). The chemical structures of the selected azo dyes used for this study are illustrated in Figure 2.1.

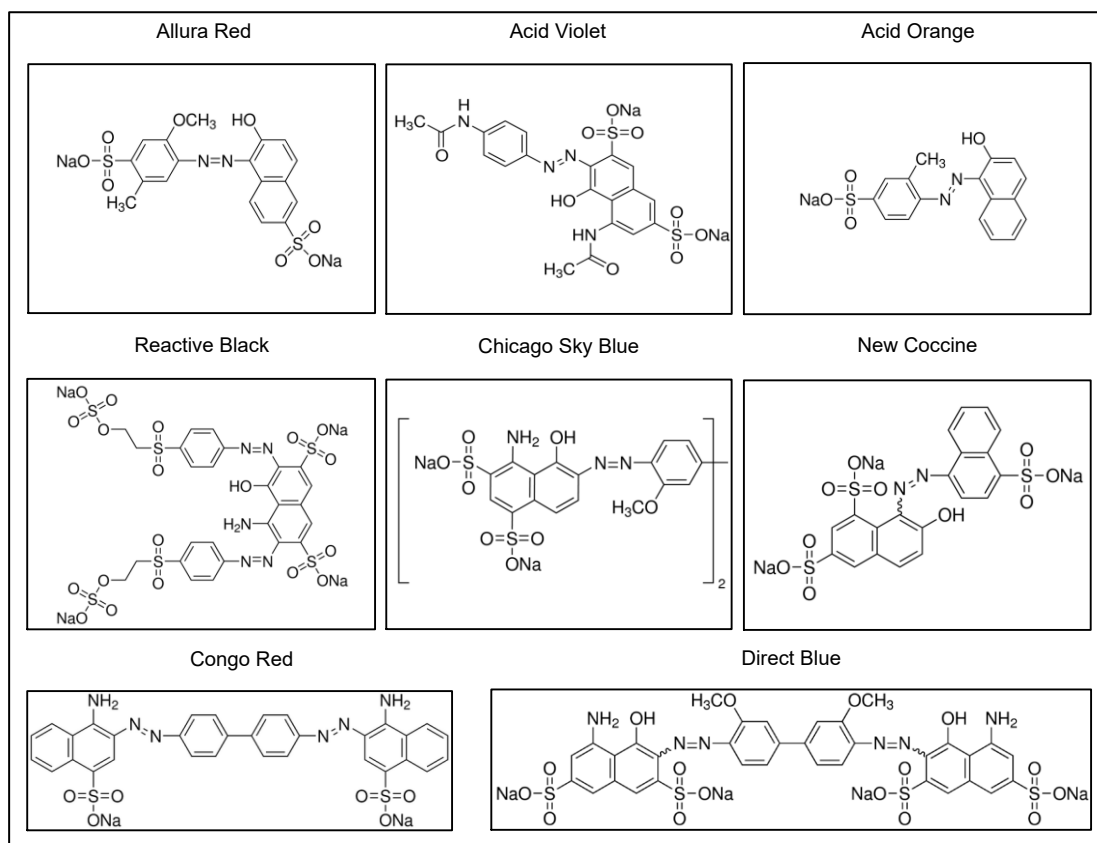


Figure 2.1: Chemical structure of reactive azo dyes, available online: www.sigmaaldrich.com, accessed 6 November 2014.

2.2. MATERIALS AND METHODS

2.2.1. Materials

All reagents used were supplied by Sigma Aldrich (Germany) unless otherwise stated. Ultra-pure water from a MilliQ system (Millipore) was autoclaved and used for all experiments. Centrifugation was performed using a Beckman-Coulter Allegra X-22 centrifuge at room temperature (25°C) at 2000 x g for 5 minutes. The continuous end-over-end mixing/incubation steps were performed at room temperature (25°C) on an ELMI Intelli-mixer RM-2 at 25 rpm (180° rotation). Absorbance readings were obtained with a spectrophotometer (Powerwave HT, Biotek Instruments)

2.2.2. Synthesis of functional polymer microspheres

For the preparation of a 10 ml batch of aldehyde functional polymer microspheres, 5 ml mineral oil and 100 µl Nonoxynol-4 (NP4) (Dow Chemical company) was dispensed into two separate 15 ml conical tubes and mixed until dissolved using vortexing (Vortex Genius 3, IKA). A 200 µl volume of 20% glutaraldehyde aqueous solution and 200 µl of 10%

Polyethyleneimine (PEI, adjusted to pH 10 with HCl) were added to each of the respective tubes and vortexed for 30 seconds. The two suspensions were mixed and vortexed briefly at maximum speed. The polymerisation proceeded for 1 hour on a vortex mixing platform (Vortex Genius 3, IKA, setting 6). The tube was centrifuged, the supernatant decanted and the pellet washed with 10 ml of sodium phosphate buffer (0.1M, pH 4.5). The oily supernatant was decanted and the pellet was washed a further two times by resuspension in 10 ml of sodium phosphate buffer with recovery between each wash by centrifugation as above. The pellet was washed a further three times with 10 ml of 20% ethanol (centrifugal recovery as above) and the pellet resuspended to a final volume of 10 ml in water and stored at 4°C for further experimentation.

Amine functionalised polymer microspheres were produced by resuspending the pellet in 5 ml of ethylenediamine (EDA, 0.5 M, adjusted to pH 7.5 with HCl) and incubating at 4°C with end-over-end mixing for 18 hours. The microspheres were recovered from the suspension by centrifugation, the supernatant discarded and the pellet subsequently washed with 5 ml of water, vortexed for 1 minute and recovered by centrifugation. The pellet was washed an additional 3 times with ultra-pure water. The washed microsphere pellet was resuspended in water to a final volume of 5 ml and chemically reduced by the addition of 200 µl of sodium borohydride (0.5 M in 1 M NaOH). The reduction was allowed to continue for 30 minutes and mixed by gentle inversion every 5 minutes. The microspheres were recovered from this reaction by centrifugation, the supernatant discarded and the pellet washed a further four times with water (with recovery by centrifugation). The reduced, amine functional, polymer microspheres were functionalised to epoxide by resuspending the pellet in 5 ml of freshly prepared 1,4-butanediol diglycidyl ether (1.5 M), followed by vortexing for 20 seconds and incubation with end-over-end mixing for 48 hours. After recovery of the microspheres by centrifugation, the supernatant was discarded and the pellet washed six times with water as described above. The final epoxide activated microsphere pellet was resuspended in 10 ml water and possible aggregates from centrifugal recovery were allowed to settle. After 3 minutes the supernatant (9 ml) was transferred to a clean tube and stored at 4°C. These microspheres were used in subsequent experimentation.

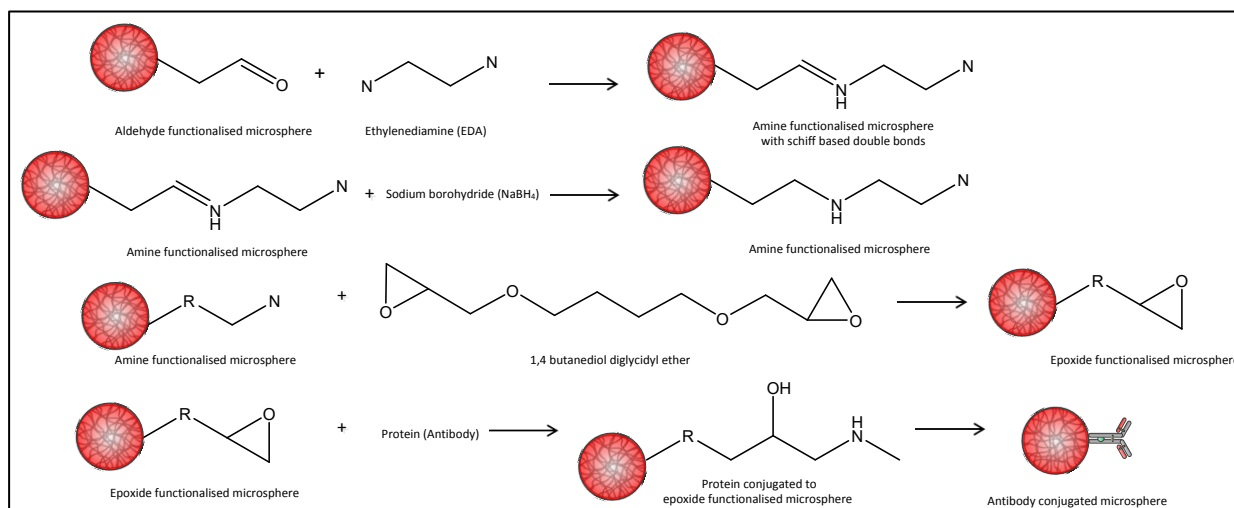


Figure 2.2: Sequential chemical reactions during microsphere synthesis protocol

2.2.3. Protein binding capacity of microspheres

Bovine Serum Albumin Fraction 5 (BSA) (Roth) was used as the standard protein to determine the binding capacity of the synthesised microspheres (Fahmy *et al.*, 2012; Puertas *et al.*, 2010; Sondhi *et al.*, 2014). The capacity was determined for all microsphere preparations in triplicate, and functional chemistries using the same technique. Non-covalently attached protein was removed for quantification by elution with 4 M NaCl (Bates, 2005; Engstrand *et al.*, 2008). For amine functional microspheres it was expected that all protein would elute due to the non-covalent ionic nature of the binding. The total protein binding capacity of the microspheres was determined by quantifying the difference in the total protein added to the microspheres, corrected for the quantity left in solution and eluted during the salt-washing to remove ionically bound protein.

Briefly, 250 μl of the respective functionalised microsphere suspension (aldehyde/amine/epoxide) was aliquoted in triplicate into separate Eppendorf tubes, centrifuged as above, and the supernatant discarded. The pellets were resuspended in 1 ml of BSA (10 mg.ml^{-1}), vortexed for 5 seconds and subsequently allowed to incubate at 4°C with end-over-end mixing for 18 hours. The microspheres were recovered by centrifugation and the supernatant transferred to a clean tube.

The aldehyde and epoxide microsphere pellets were each washed three times with 1 ml of NaCl (4 M), recovered by centrifugation, and the supernatants pooled together to a final volume of 4 ml. The amine microsphere pellets were washed three times with 1 ml of Tris (50 mM, pH 8), followed by centrifugation as above and the supernatants pooled together to a final volume of 4 ml. Subsequently, the bound protein was eluted from the amine microspheres by

washing the pellets 4 times with 500 μl of NaCl (4 M) and the supernatants pooled to a final volume of 2 ml.

The unbound BSA in the supernatant was measured spectrophotometrically by aliquoting 200 μl of the pooled supernatant in triplicate into a Ultra-violet (UV)-96 well plate and reading the absorbance at 280 nm. Water was used as blank and the 10 $\text{mg}\cdot\text{ml}^{-1}$ BSA standard was diluted 10X and read for quantification of the results.

2.2.4. Dry weight determination

In order to normalise the protein binding capacity of the microspheres, the dry weight of the synthesised microsphere batches was determined using lyophilisation. A total of 500 μl of microsphere suspension was transferred to pre-weighed microcentrifuge tubes in duplicate (per batch). Microsphere samples were pre-frozen at -80°C for 1 hour, and subsequently lyophilised in a freeze-drier (Labconco Triad), for 24 hours at a shelf-temperature of 0°C .

2.2.5. Dye binding to epoxide microspheres

2.2.5.1. Dye Screening

Dye binding and leaching studies were performed on epoxide functionalised polymer microspheres prepared as described in section 2.2.2 and using a selection of 8 azo reactive dyes, namely Chicago Sky Blue, Direct Blue, Acid Violet, Congo Red, Reactive Black, Acid Orange, New Coccine and Allura Red.

The maximum absorbance wavelength of each dye was determined by wavelength scanning (420 to 700 nm) of 200 μl aliquots of each dye (5 $\mu\text{g}\cdot\text{ml}^{-1}$) into a UV-transparent 96 well flat bottomed microwell plate using a spectrophotometer. Subsequently, the extinction coefficient of each dye (at optimal wavelength) was determined by the preparation of a standard curve from a serial dilution of the dye.

The binding capacity for each dye to the microspheres was determined as follows: for each of the dyes (8 total) 800 μl (2.16 mg) of polymer microsphere suspension was aliquoted into an Eppendorf tube followed by the addition of 200 μg (1 $\mu\text{g}\cdot\mu\text{l}^{-1}$) of dye. The tubes were vortexed for 10 seconds and incubated with end-over-end mixing for 1 hour. The microspheres were recovered by centrifugation, the supernatant transferred to a clean tube and the pellets washed once with 1 ml of water (centrifugal recovery as above). The supernatants were pooled and residual dye content determined by spectrophotometric measurement at the

respective peak wavelengths. The amount of dye bound to the microspheres was calculated as the difference between the original solution and the final supernatant.

The dyed microsphere pellets were resuspended into 600 μ l water, vortexed for 10 seconds and subsequently split into two Eppendorf tubes. To evaluate potential non-specific binding, 1 ml of either NaCl (4 M) or EtOH (100%) was added to the aliquots for each dye, the reactions vortexed for 10 seconds and allowed to incubate with end-over-end mixing for 1 hour. The microspheres were recovered by centrifugation, the supernatant transferred to a clean tube after which 200 μ l of each supernatant was aliquoted in triplicate into a UV-96 well plate and the absorbance read at each dye's respective optimum wavelength using a spectrophotometer. The quantity of dye that leached from the microspheres into the supernatant was determined using the extinction coefficient of each dye.

2.2.5.2. *Maximum dye binding capacity of preferred dyes*

Two dyes were selected based on performance in section 2.2.5.1, namely Congo Red and Chicago Sky Blue. The maximum dye binding capacity of each of the two dyes were explored by adding varying amounts of dye (200 μ g, 400 μ g, 600 μ g, 800 μ g) to 400 μ l (1.08 mg) epoxide functional microspheres.

Stock solutions (1 mg.ml⁻¹) of Chicago Sky Blue and Congo Red were prepared and varying volumes were added to 400 μ l aliquots of microspheres and made up to 1 ml using ultra-pure water. The suspensions were vortexed for 10 seconds and incubated with end-over-end mixing for 1 hour after which the microspheres were recovered by centrifugation and the supernatant transferred to a clean tube. The pellets were repeatedly washed with 1 ml of water until the supernatants cleared. All supernatants were pooled together and the dye quantified by absorbance spectroscopy (correcting for dilution of the washes).

To each pellet, 1 ml NaCl (4 M) was added and the reactions incubated with end-over-end mixing for 1 hour after which the microspheres were centrifuged and the supernatants transferred to a clean tube for quantification of leached dye by absorbance spectroscopy.

2.2.6. Particle size distribution

The particle size distribution (PSD) of the Chicago Sky Blue dyed epoxide functionalised microspheres was determined using light microscope analysis of microsphere preparations (Olympus BX53, fitted with Olympus DP72 eyepiece, 100X magnification) with CellSens software measuring tools and histogram plotted using SigmaPlot (Systat Software). Briefly, the

diameters of each of the 2192 microspheres were measured using CellSens software and the values were incorporated into SigmaPlot for plotting as a histogram for PSD determination.

2.3. RESULTS AND DISCUSSION

2.3.1. Synthesis of functional polymer microspheres

Considering the possible adverse flow properties of microsphere aggregates, the polymer microspheres were visualised using light microscopy at each step of the preparation and dyeing (Figure 2.3).

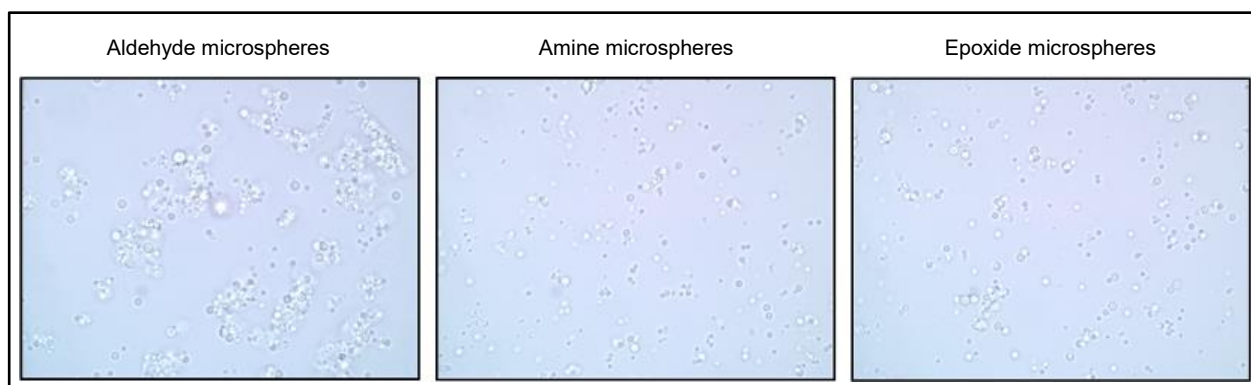


Figure 2.3: Light microscope image of initial polymer microsphere suspensions.

The initial aldehyde microspheres appeared to have a high degree of aggregation which appeared to reduce through functionalisation to amine and epoxide microspheres. Sodium borohydride is a mild reducing agent which reduces potentially unstable Schiff bases to stable secondary amines, in the preparation of amine microspheres (Hermanson, 2008).

2.3.2. Protein binding capacity of microspheres

The protein binding capacity of the aldehyde, amine and epoxide functional microspheres were determined using BSA as the model protein. Aldehyde, amine and epoxide functionalised microspheres had protein binding capacities of 1.8 ± 0.08 , 2.1 ± 0.03 and 2.3 ± 0.12 mg BSA per mg microspheres respectively (Figure 2.4). The dry weight of the microspheres (1 ml) were 3.06 ± 0.16 , 2.51 ± 0.10 and 2.70 ± 0.11 for aldehyde, amine and epoxide microspheres respectively.

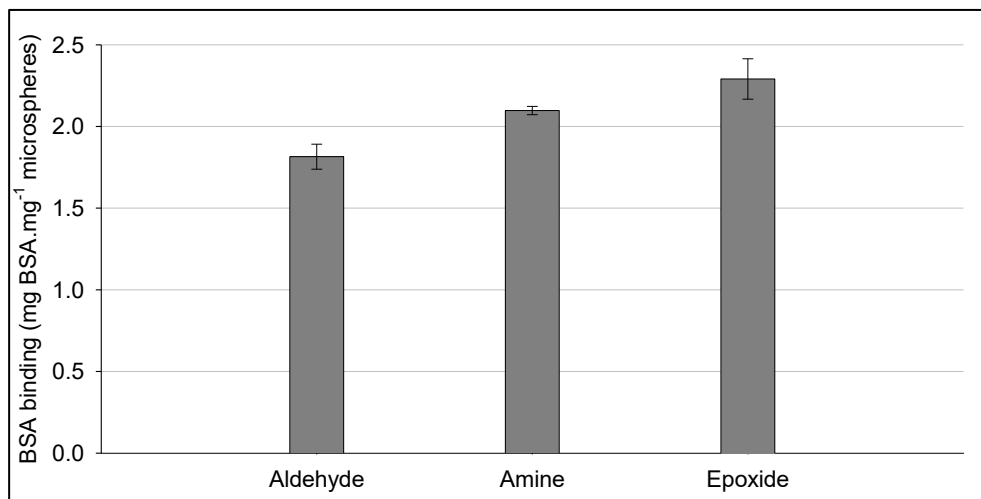


Figure 2.4: BSA binding capacity of polymer microspheres. Error bars represent standard deviation of triplicate experimental sets.

It was observed in Figure 2.3 that aldehyde microspheres have a higher degree of aggregation when compared to the amine and epoxide microspheres, which may have resulted in the slightly reduced protein binding capacity.

2.3.3. Dye binding to epoxide microsphere

The synthesised polymer microspheres remain translucent under light microscopy indicating the dye was indeed binding and not aggregating. The comparative visual intensities of the dyes are illustrated in Figure 2.5.

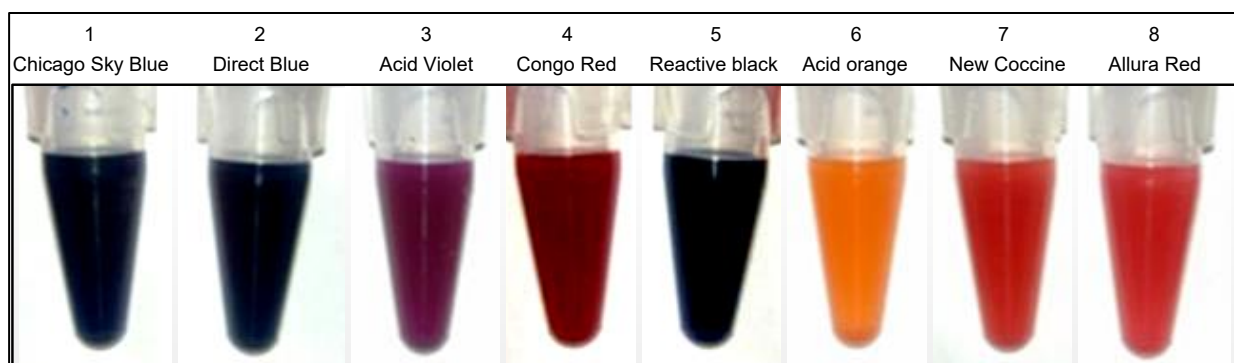


Figure 2.5: Macro view of dyed microsphere suspensions.

Microscopic images of the dyed microsphere preparations are illustrated in Figure 2.6. The reactive dyes resulted in varying degrees of aggregation of the microspheres, and were further considered when selecting the dyes for further development.

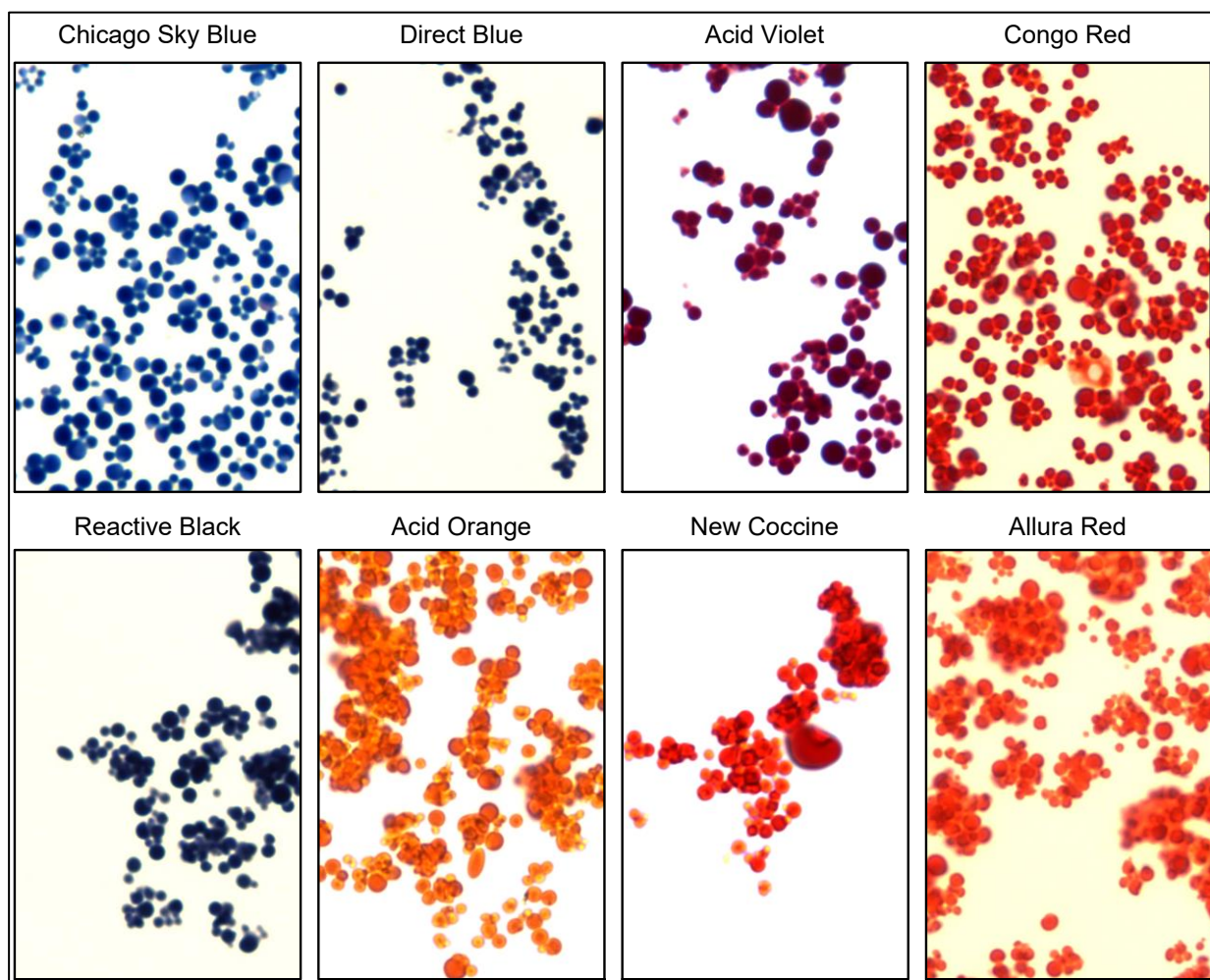


Figure 2.6: Light microscope image of dyed microsphere suspensions.

Of the eight dyes evaluated, Chicago Sky Blue, Direct Blue and Congo Red resulted in the least amount of microsphere aggregation. It was later determined that aggregation may partially be overcome experimentally by buffer formulation (varying pH, detergent and salt concentrations), and the dyes may be revisited as necessary.

The maximum absorbance wavelength of each dye was determined with a spectrum scan of a standard concentration of each dye (Figure 2.7), and the optimal wavelength was subsequently used for preparation of a standard curve for each dye for determination of the extinction coefficient.

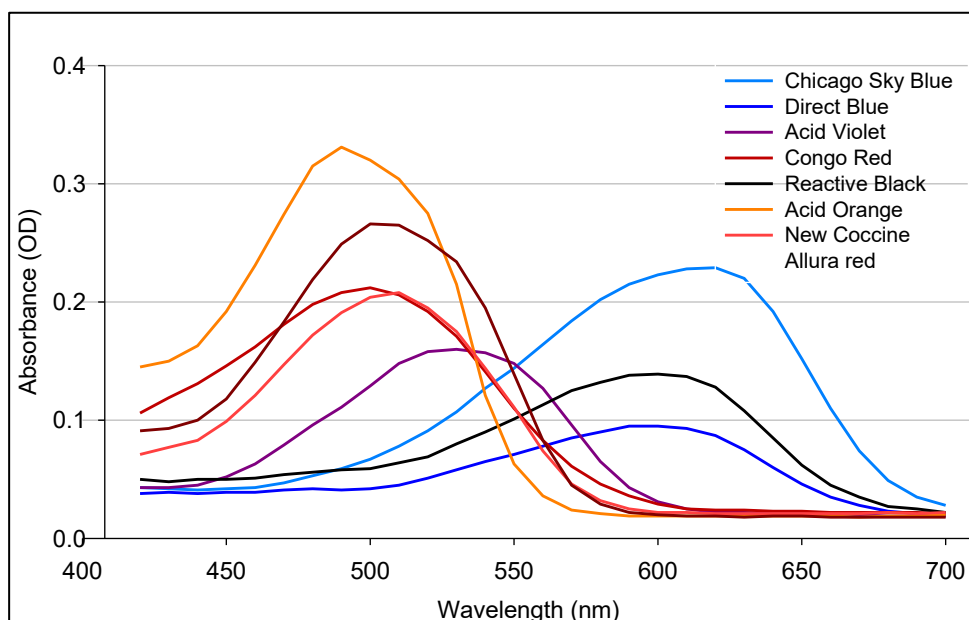


Figure 2.7: Spectrum scan between 420 – 700 nm to determine maximum absorbance wavelength of azo dyes.

The maximum absorbance wavelengths of the dyes were 610 nm (Chicago Sky Blue), 600 nm (Direct Blue and Reactive Black), 520 nm (Acid Violet), 500 nm (Congo Red and Allura Red), 490 nm (Acid Orange) and 510 nm (New Coccine).

Possible leaching of dyes from the microspheres was determined using two washing agents, EtOH (for potential non-specific hydrophobic interaction) and NaCl (elution of non-specific ionic interaction). The results are indicated in Figure 2.8 below. NaCl appeared to cause leaching of the dyes from several of the microsphere preparations, indicating a high degree of ionic binding of the dyes to the microspheres.

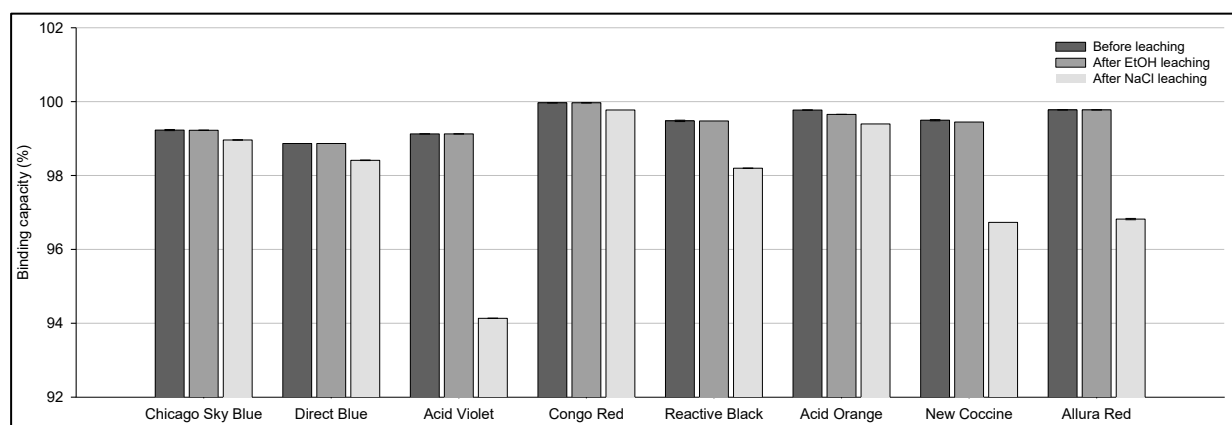


Figure 2.8: Percentage of dye bound to epoxide microspheres before and after removal of non-specific binding. Error bars represent standard deviation of triplicate experimental sets using a single batch of microspheres.

Of the eight dyes analysed, three dyes (Chicago Sky Blue, Congo Red and Acid Orange) performed well regarding binding efficiency and resistance to leaching. Congo Red performed

the best followed by Acid Orange and Chicago Sky Blue. Acid Violet showed the highest degree of ionic interaction. Due to the similarity in colour and appearance of Acid Orange and Congo Red, Congo Red was selected for further evaluation due to its lower cost (reducing eventual cost of the microspheres for diagnostic application), and reduced particle aggregation. Chicago Sky Blue was superior in all aspects under consideration and was selected for further experimentation.

To determine the maximum dye load, increasing amounts of each dye were added to a constant volume of the microspheres (400 μl , 1.08 mg) with suitable elution procedures to evaluate non-specific binding (Figure 2.9).

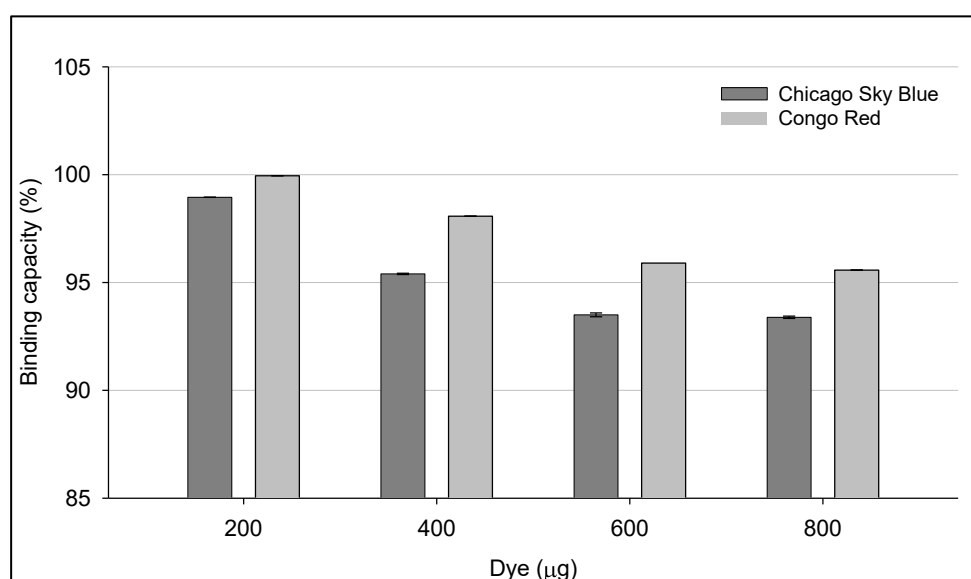


Figure 2.9: Percentage of Chicago Sky Blue and Congo Red dye bound to epoxide functional polymer microspheres with varying dye loads. Error bars represent standard deviation of triplicate experimental sets on a single batch of microspheres.

The preliminary experiments indicate that the particles are not to be saturated at 800 μg of dye (2 $\text{mg}\cdot\text{ml}^{-1}$). Dye content is further evaluated in Chapter 4 in relation to lateral flow assay sensitivity.

2.3.4. Particle size distribution (PSD) of epoxide microspheres

Particle size determinations were performed using microscopic examination of the epoxide microspheres. Diameter measurements of 2192 individual Chicago Sky Blue dyed microspheres were plotted as a histogram (SigmaPlot). The subsequent size distribution graph (SigmaPlot) illustrated that 46.9% of the microspheres in the suspension are below 1.0 μm in size with 34.4% of the microsphere suspension being in the range of 0.5 – 0.7 μm in size (Figure 2.10). There are also a few larger microspheres (1.5 – 4 μm) present in the suspension, with 35.1% of the suspension being larger than 1.5 μm .

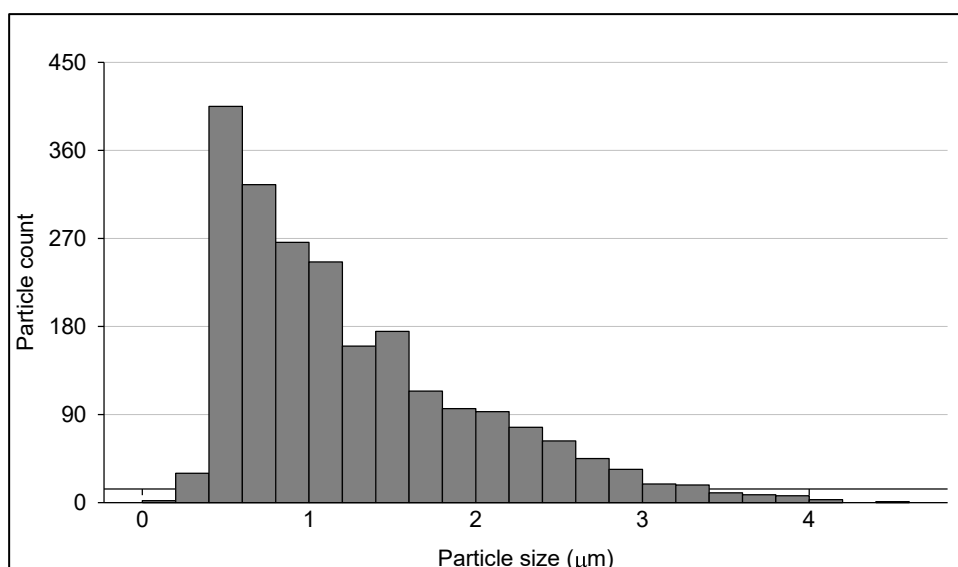


Figure 2.10: Particle size distribution of the synthesised polymer microspheres.

The results suggest the microsphere distribution is not uniform in size, however 46.9% of the suspension are potentially suitable as lateral flow detection agents ($<1\ \mu\text{m}$).

2.4. CONCLUSIONS

Epoxide functionalised microspheres of suitable PSD and colour have been synthesised for evaluation as lateral flow detection agents. Due to the preferred requirement of small particles for lateral flow, a high degree of energy was used for emulsion preparation, while the detergent was varied (since detergent had a more pronounced effect on particle size). The microsphere suspension resulted in a PSD with 46.9% of the particles having a size below $1\ \mu\text{m}$ in diameter, and therefore suitable for lateral flow on a nitrocellulose membrane (Meza, 2000).

The protein binding capacity of the epoxide functionalised polymer microspheres was considered sufficient for their application in a lateral flow diagnostic device considering the capacity is higher than that of colloidal gold and latex, and further that only a surface coating of the microspheres is required for lateral flow application. The microspheres readily adsorbed and bound the reactive azo dyes and it was determined that 1 mg dye per ml (2.7 mg) epoxide microsphere would be sufficient to produce an intensely coloured and visually detectable microsphere, although further dye load optimisation may be required as the particles were not yet saturated under these experimental conditions. Of the eight dyes evaluated, Chicago Sky Blue and Congo Red performed the best for the criteria and possible application in lateral flow devices and were selected for further evaluation and development.

CHAPTER 3

EVALUATION OF ANTIBODY CONJUGATION

3.1. INTRODUCTION

Immunoglobulins (IgG's), or antibodies, are glycoproteins with molecular weight of approximately 150 000 Da (Subramanian *et al.*, 1996). There are five isotypes of immunoglobulins in placental mammals, namely IgM, IgE, IgG, IgD and IgA, each with a distinct functionality and IgG being the most commonly used for the plurality of applications of antibodies (Arruebo *et al.*, 2009). IgG class is further classified into four isotypes (IgG1, IgG2, IgG3 and IgG4), with IgG3 isotype the least favourable therapeutic candidate due its shorter half-life and susceptibility to proteolysis (Correia, 2010). The basic structure of an antibody is illustrated in Figure 3.1 (adapted from Lu *et al.*, 1996). The Fc fragment of the antibody contains a carbohydrate moiety and has no antigen binding activity while the F(ab')₂ domain consists of two identical Fab' fragments with antigen binding sites, at the amino terminal of each fragment and are held together by disulphide bridges which provides stability to the molecule (Lu *et al.*, 1996).

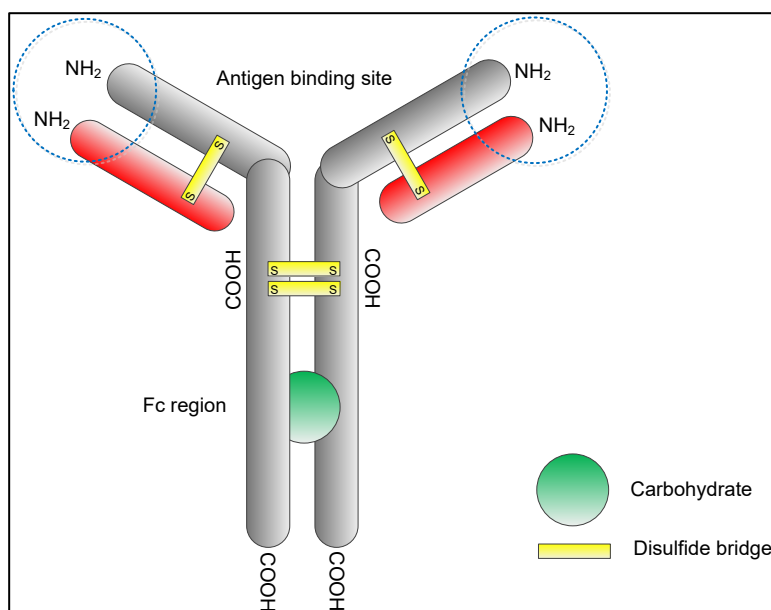


Figure 3.1: Structure of an antibody (adapted from Lu *et al.*, 1996) .

The strategy used to immobilise antibodies to a surface is dependent on the nature of the assay, as some assays require maximum sensitivity while others require maximum stability (Jung *et al.*, 2008). Immobilisation of proteins inevitably results in loss of biological activity and it has been shown that soluble antibodies have up to 1000 fold stronger binding affinities to antigens than when immobilised, with immobilised and soluble antibodies having dissociation constants (K_d) in the range of $10^{-7} - 10^{-5} \text{ mol.L}^{-1}$ and $10^{-10} - 10^{-9} \text{ mol.L}^{-1}$ respectively (Lu *et al.*,

1996; Tajima *et al.*, 2011). The loss of activity is assumed to be as a result of either protein denaturation, random orientation or steric hindrance of the antigen binding sites (Lu *et al.*, 1996; Tajima *et al.*, 2011). Antibody immobilisation strategies have gained much interest as several studies suggest that oriented antibodies are more stable, and further retain more functionality than randomly immobilised antibodies, resulting in enhanced immunoassay sensitivity (Jung *et al.*, 2008; Puertas *et al.*, 2010; Rejeb *et al.*, 1998; Tajima *et al.*, 2011; Yuan *et al.*, 2008).

It is important that the antibody immobilisation technique maintain the conformation and structural integrity of the protein in order to allow for antigen binding and detection (Tajima *et al.*, 2011). The simplest method for antibody immobilisation is physical adsorption, which is the non-specific interaction of an antibody with a solid support *via* ionic, hydrogen, hydrophobic and Van Der Waals interactions, and results in randomly orientated antibodies (Jung *et al.*, 2008; Nisnevitch *et al.*, 2001; Peluso *et al.*, 2003). The extent of these interactions are dependent on the chemical properties and surface characteristics of the antibody and immobilisation surface, which may in turn be affected by the solvent (Nisnevitch *et al.*, 2001).

Covalent immobilisation is a common method of antibody immobilisation and involves coupling through the side chains of amino-acid residues on antibodies to various reactive groups such as aldehyde, epoxide, and thiol functional groups on a chemically activated solid surface (Jung *et al.*, 2008). This chemical immobilisation results in very stable covalent linkages but usually results in random orientation (Mateo *et al.*, 2002).

Several strategies for site-specific (also known as directed) immobilisation suggest the use of the carbohydrate chain or disulfide bridges of the antibodies (Guzov *et al.*, 1988; Nisnevitch *et al.*, 2001). This however requires chemical treatments and antibody modification, such as carbohydrate oxidation or disulfide bond reduction of the antibody prior to immobilisation, which are more expensive and can result in antibody denaturation (Kang *et al.*, 2007). Alternate site-specific oriented attachment can be achieved using bacterial antibody binding proteins, Protein A and Protein G, or linkers such as polyethylene glycol (PEG) (Lu *et al.*, 1996). Protein A and G are proteins extracted from the membrane of *Staphylococcus aureus* and have extremely high affinities for the Fc portion of the antibody and attach *via* electrostatic and hydrophobic interactions, allowing orientation of the immobilised antibody, without chemical modification (Jung *et al.*, 2008; Turkova, 1999). Although the use of Fc binding proteins (such as Protein A or G) results in a potentially higher quantity of active antibodies, as a result of two immobilisation steps the surface density is potentially reduced (Peluso *et al.*, 2003). This antibody-Protein A interaction can further be stabilised using crosslinkers such as carbodiimide and glutaraldehyde after the coupling of the two proteins resulting in a more

stable antibody interaction (Turkova, 1999). Previous studies utilising flexible linkers such as PEG have demonstrated that target antigens are captured more efficiently (2 fold) than antibodies linked directly to the solid surface (Jung *et al.*, 2008).

An alternate strategy for directed immobilisation utilises biotinylated antibodies for immobilisation on streptavidin-functional surfaces (Jung *et al.*, 2008). Biotin is a water-soluble vitamin which has a strong binding affinity for the bacterial protein streptavidin, in a near irreversible interaction with a dissociation constant of 10^{-15} M (Jung *et al.*, 2008). Each streptavidin can bind up to four biotin molecules (Nisnevitch *et al.*, 2001). The amino groups of the antibodies can also be used as possible biotinylation sites, but this has been shown to result in random immobilisation (Jung *et al.*, 2008). Site-specific biotinylation of the antibodies through modification of the thiol groups of the cysteine residues results in directed immobilisation (Jung *et al.*, 2008). Antibody orientation studies comparing passive adsorption, covalent immobilisation and affinity binding (streptavidin-biotin) suggest that all three antibody immobilisation methods have comparable sensitivities; however affinity binding resulted in the highest specificity (Thiramanas *et al.*, 2013). The enhanced sensitivity that may be provided through biotinylated antibodies have led to the development of various assay designs (Hermanson, 2008). Although streptavidin-biotin immobilisation is not considered strictly “oriented”, it may present the antibodies in a more favourable orientation and provide improved antigen detection (sensitivity) (Hermanson, 2008).

An ELISA is a powerful, sensitive and rapid tool for quantifying proteins (antibodies and antigens) in complex biological samples and is widely used for a variety of research and diagnostic applications since it does not require sophisticated equipment and both magnetic and non-magnetic microspheres can be used (Kuang *et al.*, 2013; Osmekhina *et al.*, 2010; Steinitz, 2000; Vogt *et al.*, 1987). The highly quantitative and reproducible nature of ELISA's allow for them to accurately measure inflammatory biomarkers (Cox *et al.*, 2012; Leng *et al.*, 2008). A limitation of ELISA is the narrow dynamic range of the assay, which is defined as the range over the linear relationship between the antigen concentration and the absorbance at a certain wavelength (Leng *et al.*, 2008). The dynamic range of the assay indicates the quantification limits of the assay, while the lowest limit of detection determines the sensitivity of the assay (Cox *et al.*, 2012).

The principle is based on detecting hybridisation events between a capture antibody, a detector antibody and the target protein, as illustrated in a bead-based ELISA Figure 3.2 (adapted from Osmekhina *et al.*, 2010).

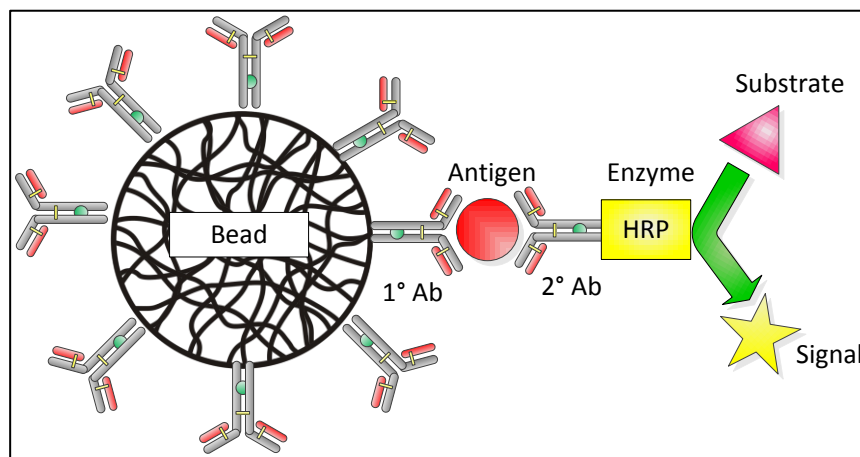


Figure 3.2: Illustration of a bead-based sandwich ELISA (adapted from Osmekhina *et al.*, 2010).

In potentially the simplest form of bead-based ELISA, the capture antibody is immobilised onto a microsphere surface, and the detection antibody (secondary antibody) is linked to an enzyme, often horseradish peroxidase (HRP; refer Figure 3.2). The enzyme catalyses the conversion of a substrate to a chromophoric product, resulting in an easily detectable signal (such as colour formation) which can be measured using a suitable reader, such as a spectrophotometer (Osmekhina *et al.*, 2010; Steinitz, 2000). The magnitude of the signal which is a direct result of the enzyme activity is directly proportional to the quantity of the antigen. The use of an enzyme allows for signal amplification, enabling detection of low antigen concentrations (Steinitz, 2000).

Peroxidases are preferred for applications such as diagnostics since they are heat stable, and catalyse a variety of substrates producing a stable chromophoric product, and are optimally active at pH's that do not disrupt antibody-antigen interactions (Chaurasia *et al.*, 2013; Fahmy *et al.*, 2012; Jeyachandran *et al.*, 2010; Mohamed *et al.*, 2011; Veitch, 2004). Horseradish (*Armoracia rusticana*) is a perennial herb found in temperate regions and are often used in ELISA diagnostics (Hamilton *et al.*, 1999; Veitch, 2004).

A variety of substrates have been used for HRP based ELISA including Guaiacol, ABTS (2,2'-azino-bis-(3-ethylbenzthiazoline-6-sulfonic acid), and OPD (o-phenylenediamine). Guaiacol (2-methoxyphenol) is a methoxy-substituted monophenol which in the presence of peroxidase is oxidised from the colourless Guaiacol to a phenoxy radical, which subsequently undergoes polymerisation to form the Guaiacol-derived chromophore tetraguaiacol (orange to brown colouration) and may be measured at 470 nm (Bonini *et al.*, 2007; Chaurasia *et al.*, 2013; Johannes *et al.*, 2006; Li *et al.*, 2008). ABTS is a non-phenolic heterocyclic colourless compound which is oxidised by peroxidase to a di-cation (ABTS^{2+}) and cation radicals ($\text{ABTS}^{\bullet+}$) which are blue-green in appearance and absorbs in the visible spectrum at 420 nm (Li *et al.*, 2008). OPD is a colourless, non-fluorescent chemical, that may be oxidised by

peroxidase to form DAP (2,3-diaminophenazine) which can be measured spectrophotometrically at 450 nm (Fornera *et al.*, 2010; Tarcha *et al.*, 1987; Zhang *et al.*, 2000). The ability of peroxidase to catalyse the range of substrates is known to vary, as different types and subclasses of peroxidases have different affinities for the substrates (Chaurasia *et al.*, 2013; Mika *et al.*, 2013). The suitability of OPD, Guaiacol and ABTS as substrates with horseradish peroxidase was thus evaluated for ELISA development.

The biggest challenge to the development of quantitative ELISA is considered non-specific binding, as the microwell plates, or microspheres used in the process can exhibit non-specific binding for proteins and other molecules, resulting in undesirable interactions between the reagents in the assay (Steinitz, 2000). Several blocking agents and detergents have been proposed to assist in blocking the available binding sites of both the microwell and the unoccupied binding sites on the microspheres after immobilisation of the primary antibody (refer figure 3.2). Proteins such as BSA, casein, gelatin or fish serum may be used to saturate the microwells and beads while detergents such as Tween20 are common additives in the wash buffer to reduce non-specific binding during the assay procedure (Jeyachandran *et al.*, 2010; Kuang *et al.*, 2013; Mika *et al.*, 2013; Ramos-Vara, 2005; Steinitz, 2000). Non-specific binding and off-target interactions may also be reduced with higher salt concentrations in the wash buffers (Güven *et al.*, 2014).

Blocking proteins can be categorised according to the mechanism by which the proteins inhibit non-specific binding (Vogt *et al.*, 1987). BSA, the most commonly used blocking protein, may adopt different conformations on hydrophilic and hydrophobic surfaces, resulting in different blocking capabilities, with a higher blocking capacity on hydrophobic surfaces such as polystyrene (Jeyachandran *et al.*, 2010). BSA and Tween20 concentrations as low as 5 $\mu\text{g}.\text{ml}^{-1}$ and 0.0002% respectively, have been sufficient to completely block microwell surfaces (Steinitz, 2000). Recent studies have shown that BSA at high concentrations (10 $\text{mg}.\text{ml}^{-1}$), with up to 12 hours incubation time, results in a conformational adsorption more favourable to blocking non-specific binding than that obtained with low concentrations and shorter incubation times (Jeyachandran *et al.*, 2010). Casein is an amphipathic protein and has been shown to be effective in preventing non-specific binding at low concentrations, and may in some cases be more effective at blocking certain sites than BSA (Esser, 2010; Vogt *et al.*, 1987).

Many factors may affect the sensitivity and reproducibility of an ELISA and these include: buffer composition, hybridisation time, blocking agent, pH and temperature (Osmekhina *et al.*, 2010; Vogt *et al.*, 1987). Due to the proprietary and comparatively new polymer technology being developed as lateral flow agents, a bead-based ELISA system was established to evaluate the composition of the buffer systems and ingredients on non-specific interactions of

the microspheres, which may result in non-specific binding in lateral flow. The use of magnetic beads, allowed for rapid evaluation of the multitude of parameters compared to lateral flow evaluation using non-magnetic beads. MagReSyn magnetic microspheres are highly porous polymer particles with diameters in the range of 7 – 10 μm . The high binding capacity and functional group density of the microspheres make these ideal for use in bead-based ELISA where various protein (antibody) immobilisation chemistries may be evaluated. The magnetic core of the microspheres potentially allow for reduced assay time and simpler reagent handling during the numerous wash steps, as the microspheres can be easily collected/pelleted by a magnet and time consuming centrifugation steps are avoided. The magnetic microspheres are prepared from the same polymer material and are therefore chemically similar to the non-magnetic microspheres discussed for lateral flow assays (Chapter 4 and 5), and was thus considered the ideal platform for evaluation of immobilisation chemistries.

3.2. MATERIALS AND METHODS

3.2.1. Materials

MagReSyn[®] Epoxide microspheres, and MagReSyn[®] Streptavidin microspheres were supplied by ReSyn Biosciences (South Africa). The binding capacity for MagReSyn[®] Epoxide and MagReSyn[®] Streptavidin were claimed as >0.8 and >1.0 mg protein per mg microsphere respectively. The microspheres were supplied as a 10 mg.ml⁻¹ suspension in acetone (epoxide) and phosphate storage buffer (streptavidin, 80 mM NaH₂PO₄ pH 7.5, 150 mM NaCl, 1.5 mM EDTA, 0.05% Tween20, 0.02% NaN₃). The antibodies (rabbit anti-mouse IgG, rabbit biotinylated anti-mouse IgG, rabbit horseradish peroxidase conjugated anti-mouse IgG and mouse anti-NF2 IgG) were purchased from Sigma Aldrich. Ultra-pure water was purified using a MilliQ system (Millipore – autoclaved) and used for all experimentation. The end-over-end incubation steps were performed at room temperature (25°C) using an ELMI Intelli-mixer set on full rotational mixing at 15 rpm, unless otherwise stated. Incubations on the vortex platform mixer were performed at room temperature (25°C) on an IKA Vortex Genius 3, setting 1, to ensure the beads remained in suspension during the experimentation. The composition of the phosphate buffered saline (PBS) buffer was 0.1 M sodium phosphate, 150 mM NaCl, pH 7.2, and that of the Tris buffered saline (TBS) was 0.05 M Tris-Cl, 150 mM NaCl, pH 8. Bicinchoninic acid (BCA) assay reagent was purchased from Pierce (USA). Absorbance readings were obtained with a spectrophotometer (Powerwave HT, Biotek Instruments). A magnetic separator was used to collect/pellet the magnetic microspheres throughout the ELISA experimental steps.

3.2.2. Antibody conjugation to magnetic microspheres

In a Lo-Bind Eppendorf tube, 1 ml (10 mg) MagReSyn[®] Epoxide microspheres were washed three times with water, followed by two equilibrations in conjugation buffer (0.1 M NaHCO₃, pH 9). The pellet was resuspended in 500 µl of conjugation buffer, to which 500 µl rabbit anti-mouse IgG solution (0.2 µg.µl⁻¹ in 0.1 M NaHCO₃, pH 9) was added to the suspension and vortexed immediately for 10 seconds. The immobilisation reaction was allowed to incubate with end-over-end mixing for 48 hours. The reaction was placed on a magnetic separator and the supernatant transferred to a clean Eppendorf tube. The pellet was washed once with 1 ml of water, the supernatants pooled (final volume 2 ml) and kept aside for protein quantification using the BCA assay (section 3.2.3).

The antibody conjugated MagReSyn[®] Epoxide pellet was washed an additional three times with 1 ml of water after which it was blocked with 1 ml of casein solution (10 mg.ml⁻¹ in 50 mM NaHCO₃, pH 9) with end-over-end mixing for 12 hours. The microspheres were recovered using a magnetic separator, the supernatant discarded, and the magnetic bead pellet washed three times with 1 ml of water with resuspension of the pellet between each wash. The blocked microsphere pellet, containing covalently immobilised IgG was resuspended in 1 ml water and stored at 4°C for a maximum of 5 days, for subsequent experimentation. The MagReSyn[®] Epoxide-IgG conjugated microsphere suspension was subsequently shown to be stable over a 5 day period under these conditions (ELISA quantification).

Antibody conjugation using streptavidin-biotin affinity was evaluated to determine the potential benefit of providing oriented immobilisation of the antibody. The microsphere suspension (1 ml of MagReSyn[®] Streptavidin), was washed three times with water and equilibrated twice with streptavidin-biotin conjugation buffer (PBS, 0.05% Tween20). The pellet (recovered by a magnetic separator) was subsequently resuspended in 500 µl conjugation buffer, to which 500 µl of biotinylated rabbit anti-mouse IgG solution (0.2 µg.µl⁻¹ in PBS, 0.05% Tween20) was added to the suspension with immediate vortex mixing for 10 seconds. This immobilisation reaction was incubated with end-over-end mixing for 1 hour at room temperature (25°C). The reaction was placed on a magnetic separator and the supernatant transferred to a new Lo-Bind Eppendorf tube. The pellet was washed once with 1 ml of conjugation buffer, the supernatants pooled together (final volume 2 ml) and kept aside for quantification of binding capacity using a BCA assay. The antibody conjugated MagReSyn[®] Streptavidin pellet was washed an additional three times with 1 ml wash buffer (PBS, 0.05% Tween20, 0.35 M NaCl), and equilibrated once in storage buffer (PBS, 0.05% Tween20). The conjugated microspheres were resuspended in the storage buffer and kept at 4°C for up to 5 days for subsequent experimentation. The

suitability of the buffer for storage of the MagReSyn[®] Streptavidin-IgG conjugate was evaluated using bead-based ELISA (section 3.2.4).

Negative control reactions (500 μ l, 5 mg) for MagReSyn[®] Epoxide and MagReSyn[®] Streptavidin were prepared using the steps described above, excluding the addition of primary antibody to either reaction.

3.2.3. Protein quantification: BCA assay

The unbound antibodies in the supernatants were quantified using a BCA quantification kit (Pierce) following the protocol as described by the manufacturer. Briefly, BCA reagents were prepared fresh by mixing calculated volumes of kit reagent A, B and C in a 15 ml tube. In a polystyrene (PS)-96 well flat bottomed microwell plate, 150 μ l of the pooled antibody supernatant was aliquoted in triplicate, followed by the addition of 150 μ l freshly prepared BCA reagent. The plate was sealed, wrapped in foil and incubated at 37°C for 2 hours. Water was used in the reagent blank and was treated in parallel to the antibody samples. Absorbance was read at 562 nm using a spectrophotometer. A standard curve for each antibody was prepared using a dilution series of the antibodies and the BCA assay. The linear regression equation from each standard curve was used to quantify the protein concentrations in the supernatants. The quantity of bound protein was calculated as the difference between the original protein concentration and the quantity left in the supernatant after antibody conjugation.

3.2.4. Bead-based sandwich ELISA

A bead-based sandwich ELISA was set up with all relevant controls, including reactions with no microspheres, negative controls without primary antibody, negative controls without the addition of antigen, or secondary antibody. The experimental reactions are illustrated in Figure 3.3. The same experimental procedure was used for evaluating the various components of ELISA including buffer composition and blocking agents. For the experimental set, incubation time was set at 2 hours for antibody-antigen binding steps, and conducted at 25°C in 50 μ l reaction volumes. The wells were blocked with 300 μ l of BSA (10 mg.ml⁻¹) containing buffer. Two buffers were evaluated for ELISA, namely PBS (pH 7.4) and TBS (pH 8.0), with and without the addition of Tween20 (0.05%). The inclusion of casein in the buffers was further evaluated. The bead-based sandwich ELISA as illustrated below was further used to evaluate the effectiveness of the blotting agents BSA and Casein on non-specific binding on the plate and microsphere surface respectively.

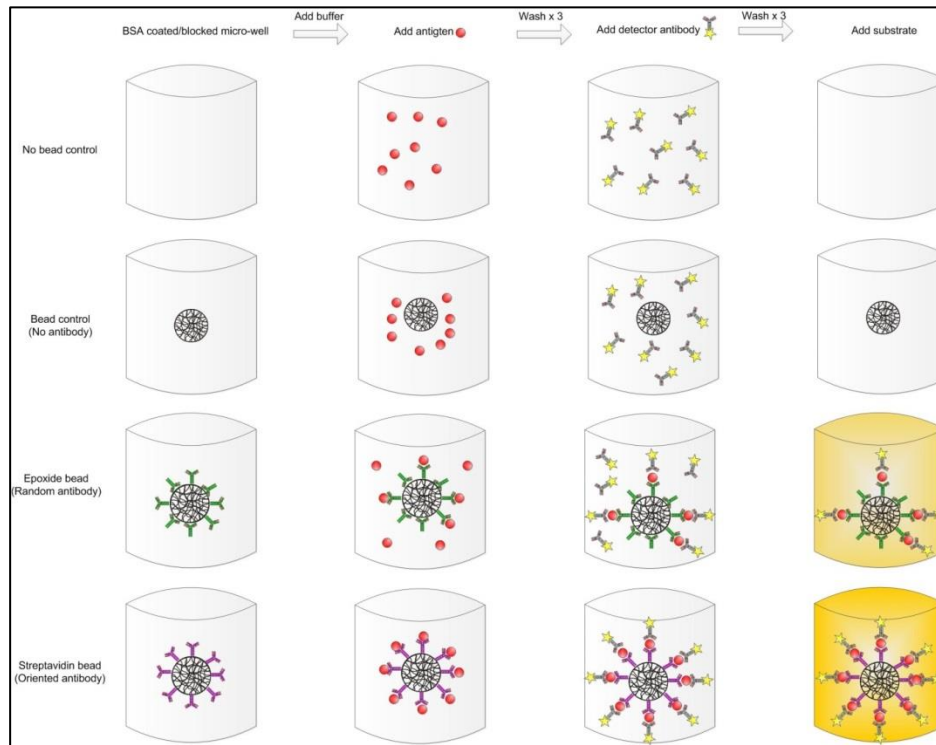


Figure 3.3: Illustration of a bead-based sandwich ELISA experimentation. Controls included antibody conjugated beads excluding antigen and secondary antibody (not illustrated). Rabbit anti-mouse IgG (green) and biotinylated rabbit anti-mouse IgG (purple) were used for random and orientated immobilisation respectively, as illustrated.

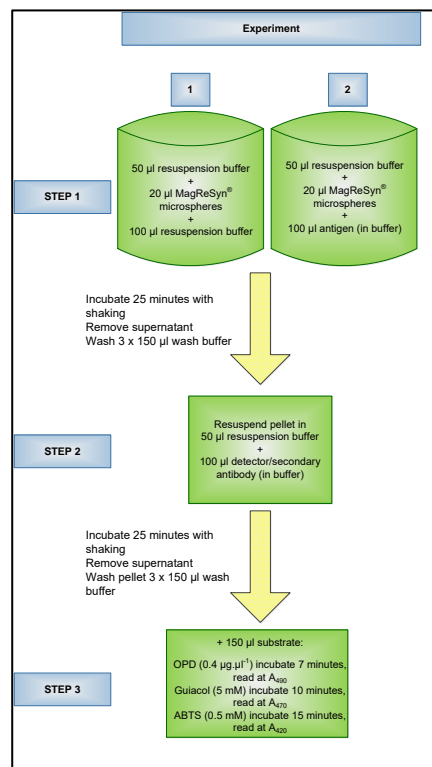


Figure 3.4: Experimental outline of bead-based sandwich ELISA. Resuspension buffer (PBS, pH 7.4), antigen ($1 \text{ ng} \cdot \mu\text{l}^{-1}$ mouse anti-human NF2 IgG), wash buffer (PBS, pH 7.4, 0.05% Tween20) secondary antibody ($1 \text{ ng} \cdot \mu\text{l}^{-1}$ HRP conjugated rabbit anti-mouse IgG).

The experimental set up as depicted in Figure 3.4 was the standard bead-based ELISA protocol used, unless otherwise stated. Antibody controls, antigen controls and bead controls were included to ascertain any non-specific interaction of the ELISA reagents with the microspheres.

3.2.5. Sandwich ELISA substrate selection

Three common ELISA substrates, having varying reaction kinetics with horseradish peroxidase, were evaluated for suitability to quantify the antigen. The substrates selected for evaluation were OPD (0.4 mg.ml⁻¹, SIGMAFAST™ OPD, Sigma-Aldrich), Guaiacol (5 mM, Fluka, (Morawski *et al.*, 2001)), and ABTS (0.5 mM, Roche, (Gunne *et al.*, 2012)) all prepared in SIGMAFAST™ buffer (0.4 mg.ml⁻¹ urea-hydrogen peroxide, 0.05 M phosphate-citrate pH5) and evaluated in a bead-based sandwich ELISA as described in Figure 3.4 in triplicate with PBS, 0.05% Tween20 as wash buffer and using OPD, Guaiacol or ABTS as substrates respectively. As the reaction rates of the substrates with peroxidase differed, the incubation time of the substrates in the ELISA varied and a time-course study was performed to determine the ideal incubation times based spectrophotometric tracking of stopped reactions.

3.2.6. Sandwich ELISA dynamic range

The dynamic range for ELISA quantification was explored with ABTS as a substrate. A bead-based sandwich ELISA as described in Figure 3.4 was set up with the exception that the antigen concentration was varied from 0.05 ng.µl⁻¹ – 2.25 ng.µl⁻¹ in the experimental reactions.

3.3. RESULTS AND DISCUSSION

3.3.1. Quantification of antibody conjugation

Quantification of bound antibody to MagReSyn® Epoxide and MagReSyn® Streptavidin microspheres was determined by quantifying the antibody containing solutions before and after addition of the microspheres. Standard curves of the antibodies were used to transform the absorbance values to protein quantities, resulting in an R² value of 0.9962 for the anti-mouse IgG antibody (equation: $y = 0.0285x + 0.0037$) and an R² value of 0.9972 for the biotinylated anti-mouse IgG antibody (equation: $y = 0.0279x + 0.0175$).

It was shown that MagReSyn® Epoxide and MagReSyn® Streptavidin microspheres bound almost all antibody in solution with binding efficiencies of 86.4% ± 7.3 and 91.2% ± 7.2

respectively (Figure 3.5). This may potentially be improved by increasing the incubation time for coupling, or by improving the microsphere antibody interaction through mixing.

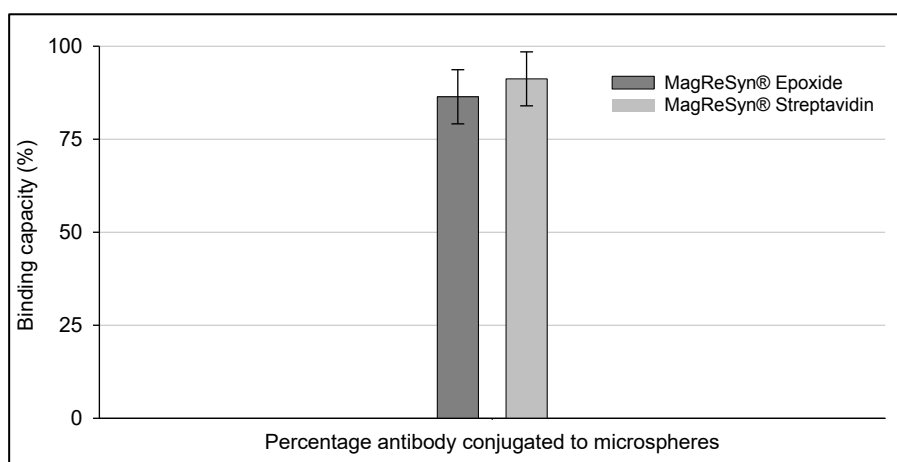


Figure 3.5: Antibody conjugation efficiency to different batches of MagReSyn® Epoxide and MagReSyn® Streptavidin microspheres. Error bars represent standard deviation of conjugation efficiency among 4 microsphere batches.

Low background signal in ELISA is often best achieved with low concentrations of primary antibody, since increased primary antibody concentrations often result in background signal and noise, potentially reducing assay sensitivity (Osmekhina *et al.*, 2010).

3.3.2. Sandwich ELISA buffer screening

The aim of these experiments was to determine potential non-specific and off-target interactions of the reagents used in the ELISA with the microspheres. Negative control MagReSyn® microspheres (MagReSyn® Epoxide and MagReSyn® Streptavidin) were finished with casein due to the preferred compatibility of casein as a finishing agent for lateral flow (refer Chapter 4), and initially evaluated with OPD as a substrate to determine the effect of various buffer components on non-specific interaction with the microspheres. Two common ELISA buffers, namely PBS and TBS were evaluated (Figure 3.6) as well as the inclusion of blocking protein in the assay buffer (Figure 3.7). Primary antibodies were initially excluded in the negative control MagReSyn® microspheres to determine any non-specific interaction with the microspheres alone. Any non-specific interaction from this control reaction was therefore as a direct result of interaction between the microspheres and antigen or secondary antibody in the reaction. Controls, without microspheres, were further included to determine the extent of non-specific protein interaction with the microwell plate.

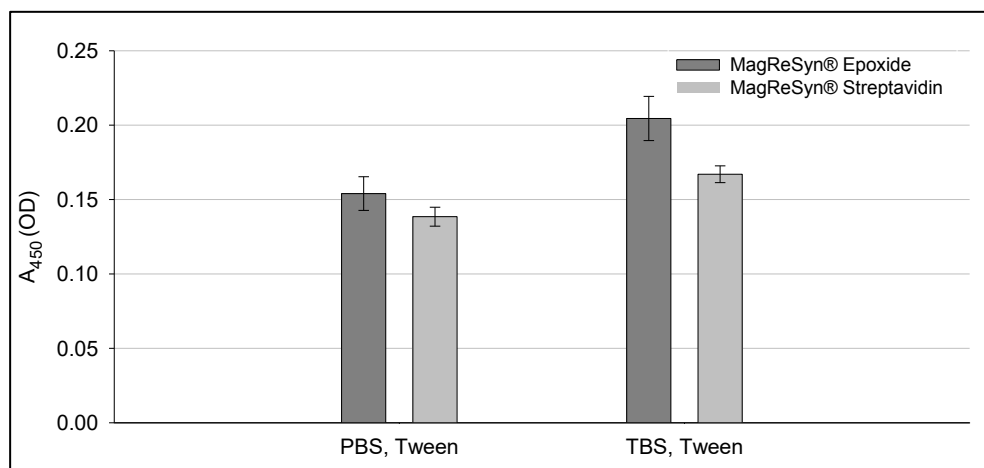


Figure 3.6: Bead-based ELISA of microsphere negative controls (MagReSyn® Epoxide and MagReSyn® Streptavidin) without primary antibody in PBS, Tween20 (pH 7.4, 0.05% Tween20) and TBS, Tween20 (pH 8, 0.05% Tween20). Error bars represent standard deviation of triplicate experimental sets.

A comparatively high degree of non-specific interaction was observed with MagReSyn® microspheres, in both PBS and TBS (Figure 3.6) as compared to the no-bead control which resulted in an average signal of 0.05 Abs. For plate blocking, the previously reported ideal BSA concentration of 10 mg.ml⁻¹ for polystyrene was used (Jeyachandran *et al.*, 2010). Polystyrene is hydrophobic and BSA layer was shown to have a 95% blocking efficiency against non-specific IgG binding (Jeyachandran *et al.*, 2010). The non-specific signals observed with both microsphere preparations was lower in PBS than TBS, and PBS was therefore selected for further evaluation. Inclusion of a blocking protein has been shown to prevent non-specific interaction in ELISA, and the inclusion of casein was selected for evaluation with control microspheres (no antibody) due to its compatibility with lateral flow buffer formulation (refer Chapter 4) (Esser, 2010; Vogt *et al.*, 1987).

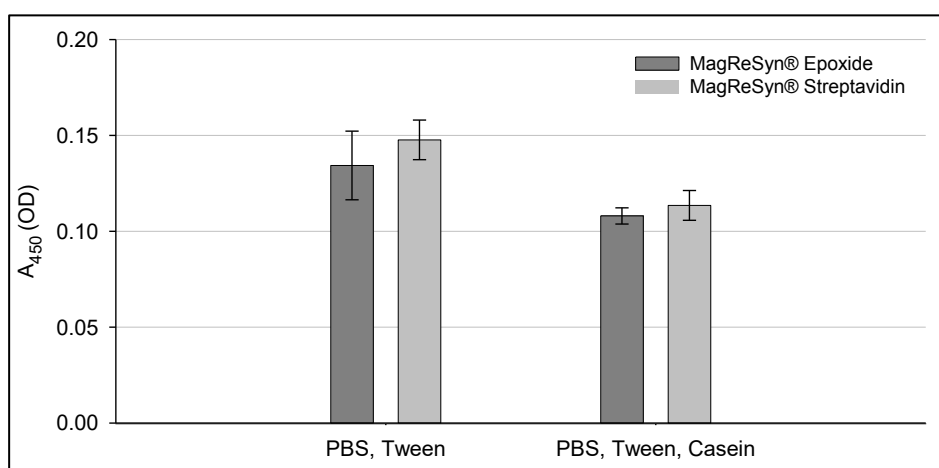


Figure 3.7: Bead-based ELISA of microsphere negative controls (MagReSyn® Epoxide and MagReSyn® Streptavidin) without primary antibody in PBS, Tween20 (pH 7.4, 0.05% Tween20), and PBS, Tween20, Casein (pH 7.4, 0.05% Tween20, 1% casein). Error bars represent standard deviation of triplicate experimental sets.

The inclusion of casein as a blocking agent had a minimal effect on reducing non-specific binding. This control experiment was repeated with microsphere controls containing immobilised primary antibodies to determine the possible non-specific interaction between the primary and secondary antibodies (figure 3.8).

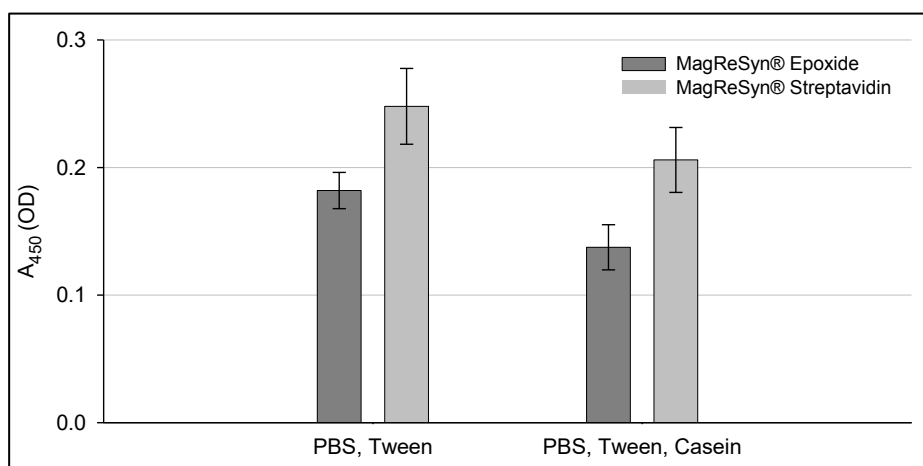


Figure 3.8: Bead-based ELISA of control MagReSyn® Epoxide and MagReSyn® Streptavidin in PBS, Tween20 (pH 7.4, 0.05% Tween20) and PBS, Tween20, Casein (pH 7.4, 0.05% Tween20, 1% casein) with primary antibody conjugated microspheres, and only HRP-conjugated secondary antibody, with no antigen present in the assay reaction. Error bars represent standard deviation of triplicate experimental sets.

MagReSyn® Epoxide-IgG-conjugated and MagReSyn® Streptavidin-IgG conjugated microspheres were finished with casein after antibody immobilisation, followed by wash steps with water (no detergent). Previous studies have suggested that this may allow some loosely bound antibodies to remain on the surface of the microsphere, resulting in non-specific interaction, and further causing the subsequent blocking agent (casein) to not be able to access and block certain areas of the microsphere (Esser, 2010). Incorporating detergent (e.g. Tween20) in the subsequent ELISA wash steps, after microsphere finishing, has been shown to remove loosely attached antibodies, exposing binding sites for non-specific attachment (Esser, 2010). This may explain the reduction in binding with casein in the buffer (which may subsequently fill the exposed binding pockets). This principle is illustrated in Figure 3.9.

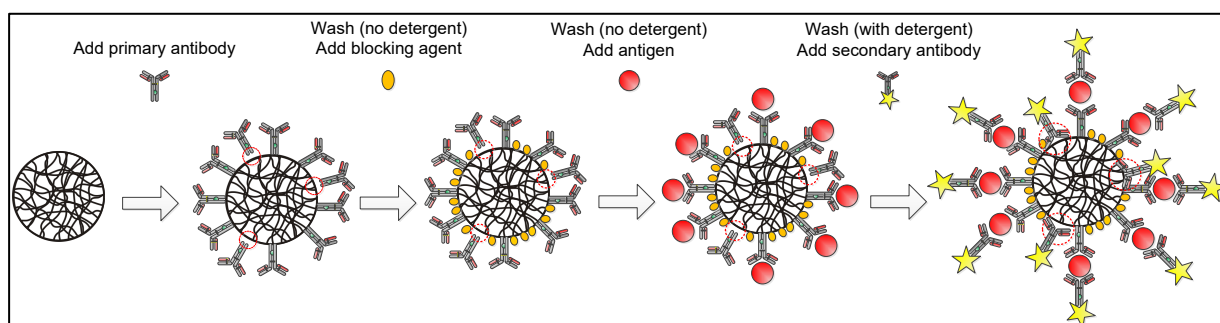


Figure 3.9: Illustration of possible challenges for using detergent to remove non-specific binding during ELISA (adapted from Esser *et al.*, 2010).

Studies have shown that detergent in the wash buffer could remove loosely attached antibody, and/or cause labile blocking to be removed resulting in some non-specific attachment of the conjugate to the microspheres (Esser, 2010). This principle could potentially have resulted in the increase in background between experimental sets illustrated in Figure 3.7 and 3.8.

From the results obtained above, the buffers were compared in positive control ELISA for Streptavidin-antibody and epoxide antibody using standard antigen concentration to determine any possible effect on antibody-antigen interaction (Figure 3.10)

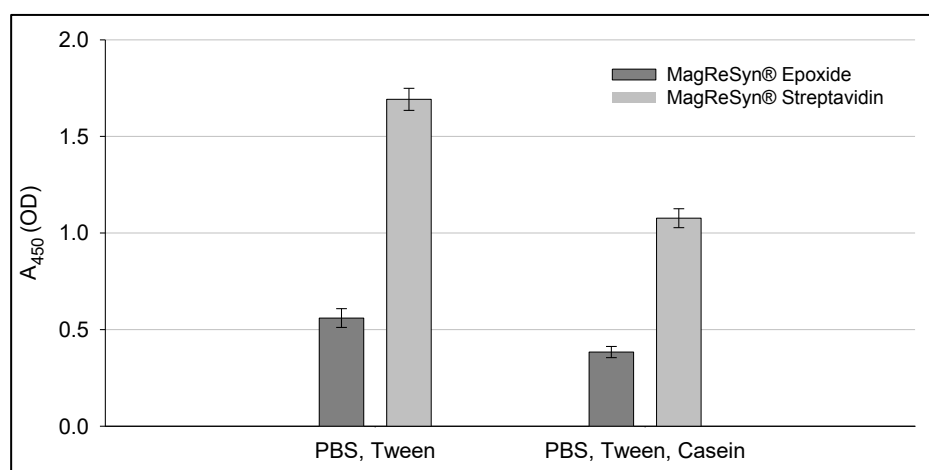


Figure 3.10: Bead-based sandwich ELISA of antibody conjugated microspheres, MagReSyn® Epoxide-IgG-conjugated and MagReSyn® Streptavidin-IgG-conjugated, with PBS, Tween20 (PBS, pH 7.4, 0.05% Tween20) and PBS, Tween20, Casein (PBS, pH 7.4, 0.05% Tween20, 1% casein). Error bars represent standard deviation of triplicate experimental sets.

The inclusion of casein in the standard ELISA buffer appeared to reduce the observed enzymatic signal suggesting that it may inhibit the enzymatic reaction of OPD with the HRP-conjugated secondary antibody, possibly due to increased viscosity of the solution containing the protein (casein), thus potentially preventing efficient mixing and reducing the sensitivity of the assay, or direct inhibition of the enzymatic reaction due to interaction between HRP and casein. Casein was therefore not included in further experimentation.

3.3.3. Sandwich ELISA substrate evaluation

OPD, Guaiacol and ABTS are common enzyme substrates for horseradish peroxidase and were explored for their use in the development of the bead-based sandwich ELISA and to ultimately aid in confirming the effect of antibody orientation on assay sensitivity by comparing random vs oriented antibodies. Relative absorbance of the various substrates over a set time interval is illustrated in Figure 3.11. As was expected, the reaction kinetics for the substrates

varied and their suitability in the ELISA using MagReSyn[®] microspheres is illustrated in Figure 3.11.

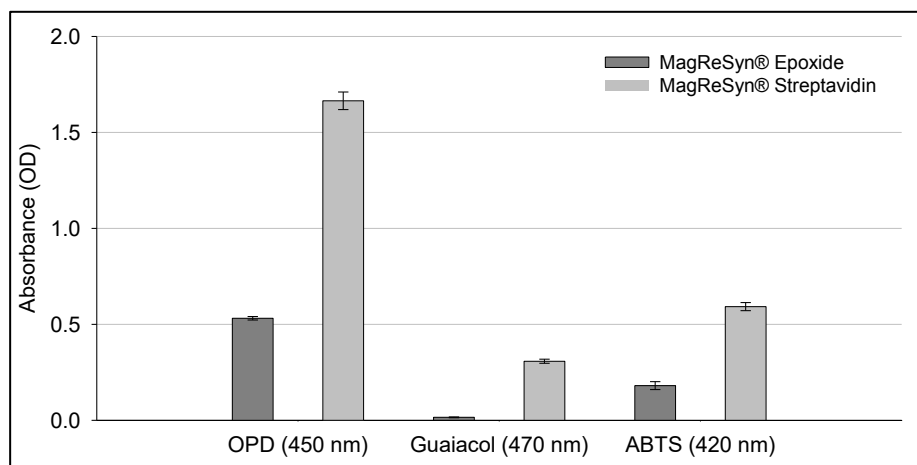


Figure 3.11: Relative absorbance of OPD, Guaiacol and ABTS in a bead-based sandwich ELISA of MagReSyn[®] Epoxide-IgG-conjugated and MagReSyn[®] Streptavidin-IgG-conjugated microspheres over a set time interval. Error bars represent standard deviation of triplicate experimental sets.

For assays using Guaiacol as a substrate, a slight visual colour change was observed after 10 minutes incubation, with an increased colour change in the streptavidin microsphere ELISA (MagReSyn[®] Streptavidin-IgG-conjugated), with a streptavidin to epoxide (oriented versus random) antibody ratio for this substrate of 21.4 : 1. The low enzymatic reaction with the sample may be due to interaction of the polymeric enzyme product with the microspheres.

OPD and ABTS resulted in visible colour changes after 5 and 15 minutes incubation respectively with a similar oriented to random antibody ratios of 3.13 : 1 and 3.27 : 1 for these substrates respectively. The reaction rates for the three substrates differed significantly with OPD resulting in a very high background signal compared to ABTS and Guaiacol.

The ideal pH for horseradish peroxidase with OPD as chromogenic substrate is considered pH 5 (Bovaird *et al.*, 1982). Previous studies have shown that horseradish peroxidase is 1.5 fold more active with OPD as the substrate in low (20 mM) phosphate concentrations than at high (100 mM) phosphate concentrations (Bovaird *et al.*, 1982). In this ELISA, the buffer pH was therefore selected as pH 5, and the wash buffer consisted of PBS which had a low (10 mM) phosphate concentration. According to Fornera *et al.*, 2010, these parameters favour high enzyme activity for OPD as a substrate, thus resulting in increased rate of the 2, 3-diaminophenazine (DAP) product formation. The high background absorbance observed with OPD could also be as a result of the non-enzymatic oxidation in the presence of H₂O₂ (Fornera *et al.*, 2010).

ABTS has previously been reported to be more sensitive in certain assay procedures. This has been attributed to the formation of the stable ABTS radical cation which is directly related to the oxidation of ABTS by horseradish peroxidase (Fornera *et al.*, 2010).

The difference in the oxidation rates of the various substrates by horseradish peroxidase could be due to the different redox potential between the substrate and the enzyme as well as different enzyme affinities (Li *et al.*, 2008; Mohamed *et al.*, 2011). The activity against various substrates can be affected by manipulating the pH, temperature, incubation time and concentration of phosphate and H₂O₂. For reliable, reproducible and simple spectrophotometric quantification of horseradish peroxidase with OPD, it has been suggested that the reaction conditions be such that only DAP is formed as the oxidation product and that non-enzymatic oxidation of OPD be kept to a minimum. OPD showed a high background for the ELISA while ABTS provided a wide dynamic range for the evaluation of enzyme orientation. ABTS was therefore selected as the preferred substrate.

3.3.4. ELISA dynamic range

The quantification capability of the microspheres in the ELISA is determined by the dynamic range of the assay which gives an indication of the quantification limits, while the lower limit of detection indicates the sensitivity of the assay. The dynamic range of the assay was investigated to determine any effect of the antibody orientation on diagnostic limitations of the antigen binding capability of the oriented versus random enzyme immobilization. This was determined by varying the antigen concentrations with ABTS as the preferred substrate (Figure 3.12). The curves were constructed and only the linear portion of each curve was included to construct the trend line equation and linear regression fit.

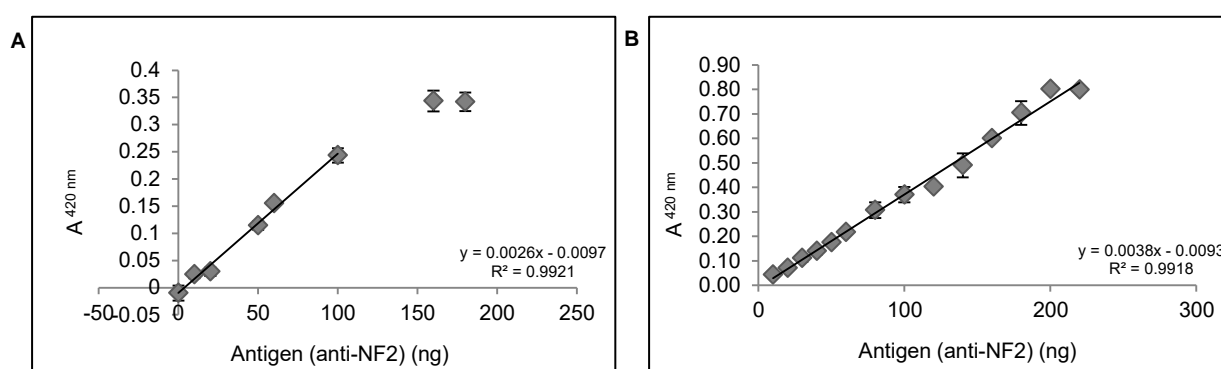


Figure 3.12: Dynamic curve with ABTS as the substrate and varying amounts of antigen. **A:** MagReSyn® Epoxide-IgG-conjugated microspheres and **B:** MagReSyn® Streptavidin-IgG-conjugated microspheres. Error bars represent standard deviation of triplicate experimental sets.

The dynamic range for MagReSyn® Epoxide-IgG-conjugated and MagReSyn® Streptavidin-IgG-conjugated microspheres were obtained with ABTS as the substrate. Due to the difference

in orientation of the antibodies on the microspheres, different maximal reaction kinetics was observed with the ABTS substrate. The antibodies that were immobilised in a random orientation had slower reaction kinetics to ABTS than the oriented antibodies with consequently lower kinetic readings. The streptavidin immobilised antibodies provided for a higher dynamic range likely due to the orientation of the antibodies.

The results in Figure 3.12 suggest the maximum limit of detection of randomly immobilised antibodies, at the current primary antibody content on MagReSyn® Epoxide microspheres, using ABTS as the substrate, was in the range of 100 ng. The maximum limit of detection of oriented immobilised antibodies on MagReSyn® Streptavidin microspheres, using ABTS, was in excess of 200 ng. The use of orientated antibodies therefore provides for a more efficient utilisation of primary antibody for ELISA development, and clearly illustrates that oriented immobilisation results in improved antibody accessibility.

3.3.5. Random versus oriented antibody immobilisation

To illustrate the availability of the random and oriented immobilised antibodies, a bead-based ELISA was set up using two different substrate concentrations of both ABTS and OPD as substrates for comparative purposes and to confirm the oriented to random antibody efficiency (Figure 3.13).

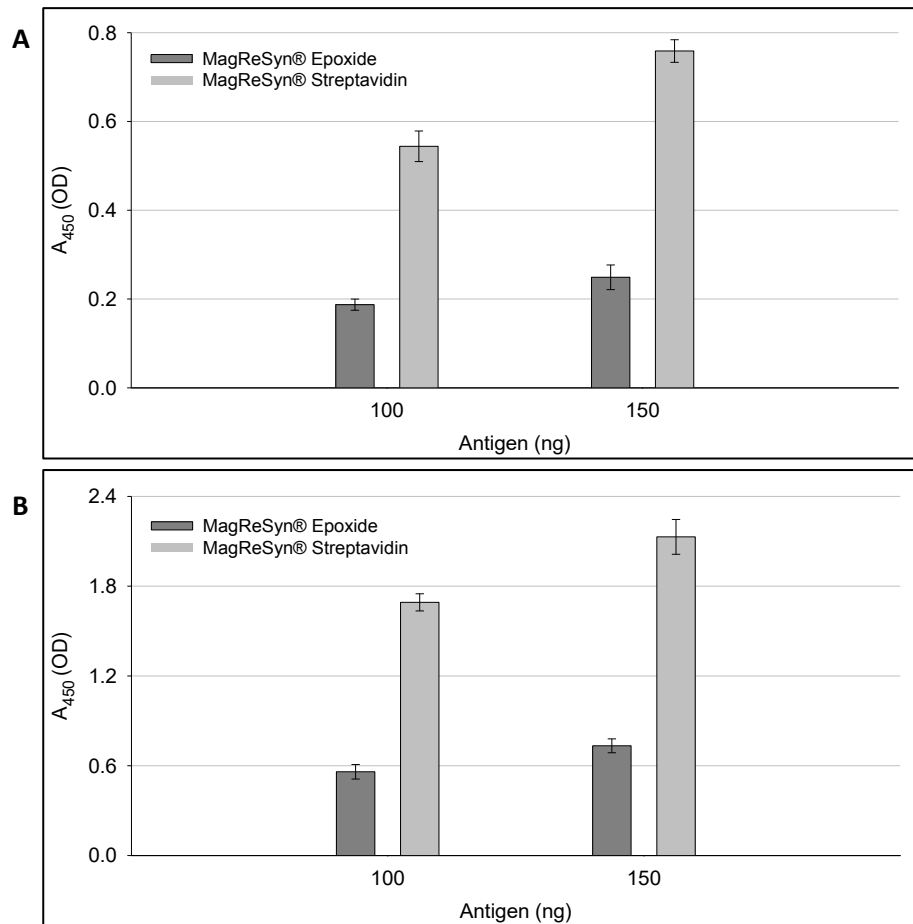


Figure 3.13: Bead-based sandwich ELISA of random (MagReSyn® Epoxide-IgG-conjugated) and oriented (MagReSyn® Streptavidin-IgG-conjugated) immobilised antibodies with **A:** ABTS and **B:** OPD as substrate. Error bars represent standard deviation of triplicate experimental sets.

The reaction containing 100 ng antigen and secondary antibody respectively resulted in a random to oriented ratio of near 3 (2.91 and 3.02 with ABTS and OPD respectively) while the reaction with 150 ng antigen and secondary antibody respectively, resulted in a similar random to oriented ratio of 3 (3.03 and 2.90 for ABTS and OPD respectively). This indicates that 2/3 of the antibody function is lost through random immobilisation of antibodies, as previously reported in literature (Jung *et al.*, 2008; Kausaite-Minkstimiene *et al.*, 2010).

3.4. CONCLUSIONS

Antibody immobilisation strategies such as covalent attachment through epoxide functional group modification or the use of biotin-streptavidin techniques remain challenging in ELISA's due to non-specific binding. Although various blocking agents exist, their use in the ELISA system should be carefully considered. BSA was an ideal blocking agent of the microwell plate used in these experiments, while the presence of casein in the wash buffer appeared to have minimal effect on the reduction of non-specific binding on the microspheres. The results

presented here confirm that oriented antibody immobilisation results in a 3 fold increase in antigen detection when compared to random immobilised antibody while the application of oriented immobilisation however remains challenging for lateral flow application.

Increased sensitivity, and availability of antibodies, is ideal for certain applications such as for inclusion in diagnostic devices (Wong *et al.*, 2009). The increased orientation of antibodies in lateral flow diagnostic devices could therefore potentially result in improved detection of antigens at lower concentrations and present them in a format suitable for capture at the detection zone, and possibly improve assay sensitivity where antigens are present in low abundance in samples such as urine. The sensitivity of lateral flow diagnostic devices are greatly affected by non-specificity and thus strategies to reduce non-specific interactions are critical in improving overall lateral flow sensitivity (Jung *et al.*, 2008). Important factors to consider when reducing non-specificity are the surface chemistries of the immobilisation surface, as well as the blocking methods used (Wong *et al.*, 2009). The proper selection of the linker molecule and the coupling chemistry to be used are also important factors to consider for avoiding non-specific interactions during immobilisation (Jung *et al.*, 2008).

The ideal antibody immobilisation strategy results in uniform antibody orientation, and requires minimal surface modification and gentle incubation conditions to prevent denaturation of the antibody (Jung *et al.*, 2008). Consistent immobilisation of proteins is considered to be one of the key elements to ensure the production of reproducible and sensitive diagnostic assays (Wong *et al.*, 2009). Although several mechanisms of antibody immobilisation exist and have been explored, the immobilisations on microspheres for lateral flow are more challenging.

Adsorption of antibodies on immobilised Protein A/G surfaces may be a favourable solution for directed immobilisation, however this may not always be suitable for all lateral flow assay formats, potentially depending on whether the antigen or the antibody is to be detected in the assay, as well as the source of the immobilised antibody, since this may result in non-specific interaction due to the affinity of Protein A/G for antibodies. The lateral flow assay under development involved the immobilisation of antibodies on the nitrocellulose membrane and aimed to detect antigen in the sample, using standard commercially available antibodies used in lateral flow assays. For this reason, having Protein A/G immobilisation on the detector particle is not ideal, due to the difficulty in blocking the unbound Protein A sites, which would inevitably recognise and bind to the antibodies immobilised on the nitrocellulose strip at the test and control lines, potentially resulting in false positives. Protein A/G however are often used in lateral flow assays where the antigen is immobilised onto the membrane and the antibody is detected in the sample (E.g. HIV 1/2 rapid tests) (Setty *et al.*, 2014; WHO, 2004).

Most IgG's have a carbohydrate moiety (glycan), oxidation of this oligosaccharide domain would result in aldehyde groups that can be covalently coupled to aminated surfaces (Kang *et al.*, 2007). However, this immobilisation would not be ideal for lateral flow assays as antigen binding sites of the antibody contain amine (NH₂) residues which would potentially also be affected by any blocking strategy of the microsphere. Although reversible protection of the antibody Fab site is an option to overcome this, the procedure is complex and potentially expensive for lateral flow development.

Biotinylation reagents may contain either aliphatic spacers (e.g. NHS-LC-Biotin) or hydrophilic spacers (e.g. PEG, also known as polyethylene oxide or PEO), with the greatest potential for assay sensitivity being achieved with the use of long spacer arms (Hermanson, 2008). Biotinylation of proteins using aliphatic spacers often result in protein aggregation, non-specific binding and precipitation, due to the increased hydrophobicity of the reaction and it is therefore suggested that aliphatic biotinylation be kept to a minimum to prevent these adverse effects (Hermanson, 2008). However, biotinylation using hydrophilic PEG-based spacers result in water-soluble complexes that do not aggregate or precipitate (Hermanson, 2008). Biotinylation of antibodies may provide a solution for lateral flow assay development. However, an aliphatic NHS-spacer is the most common biotinylation agent for antibody modification and therefore may potentially adversely affect the lateral flow assay. Of further consideration for this application is potentially the increased cost of biotinylation compared to alternative orientation methods, the potential loss in activity of the antibody due to biotinylation and the potential decreased stability of the antibody due to the attachment with fewer binding sites.

Of the immobilisation strategies explored, oriented immobilisation was therefore considered potentially less feasible for lateral flow development and initial proof-of-concept for lateral flow was performed using random immobilisation. The oriented immobilisation on microspheres should however be evaluated due to the potential for improved sensitivity. Various factors affecting the binding of antibody to polymer microspheres have been explored and their compatibility with a lateral flow assay has been determined. The compatibility of blotting agents, e.g. BSA and Casein, and detergent concentrations (Tween20) in lateral flow assays is the topic of the next chapter.

The results provide a viable system for evaluating mechanisms of immobilisation and orientations of antibodies as well as the potential of various agents for reducing non-specific binding in lateral flow and ELISA applications. Although potentially a mechanism of enhancing sensitivity, the presentation of antibodies was not evaluated in this study, but will be the subject of future work on expanding the diagnostic sensitivity of the lateral flow agents.

CHAPTER 4

LATERAL FLOW IMMUNOASSAY DEVELOPMENT: PROOF-OF-CONCEPT ON HUMAN CHORIONIC GONADOTROPIN (hCG)

4.1. INTRODUCTION

Immunochromatographic strip tests, also referred to as lateral flow assays, may either be competitive or non-competitive (sandwich assay) and the type of assay used often depends on the type of analyte being detected, as non-competitive assays are suitable for high molecular mass analytes with more than one epitope (e.g. protein) while competitive assays are preferred for small molecular mass analytes (e.g. hapten) (Posthuma-Trumpie *et al.*, 2009; Verheijen *et al.*, 1998; Wang *et al.*, 2009a). The format of a competitive immunochromatographic assay involves antibodies conjugated to a detector particle while the capture line consists of analytes conjugated to an immobilised protein on the membrane (Verheijen *et al.*, 1998; Wang *et al.*, 2009a). Higher concentration of analytes present in the sample will more efficiently block the capture of the detector particle, resulting in a decreased signal and thus the signal at the readout zone is indirectly proportional to the amount of analyte in the sample (Verheijen *et al.*, 1998; Wang *et al.*, 2009a). In a non-competitive immunochromatographic assay the antibody conjugated detector particle binds to the analyte present in the sample and the complex then uses the free epitope of the analyte to bind to the immobilised antibody on the membrane, forming an antibody-antigen-antibody sandwich (Posthuma-Trumpie *et al.*, 2009). In this assay, the signal is directly proportional to the concentration of analyte in the sample (Posthuma-Trumpie *et al.*, 2009).

Lateral flow immunochromatographic assays embody an amalgamation of technologies that provide a relatively low cost and accurate means of diagnosing diseases at the true point-of-care (Bell *et al.*, 2006). Lateral flow diagnostic devices are thus the preferred method of disease detection in resource poor settings. For the purpose of this study; a non-competitive (sandwich) lateral flow immunoassay was considered the ideal format since it is suitable for detection of antigens. The principle of lateral flow is based on the migration of a liquid along the surface of a membrane as illustrated in (Figure 4.1)

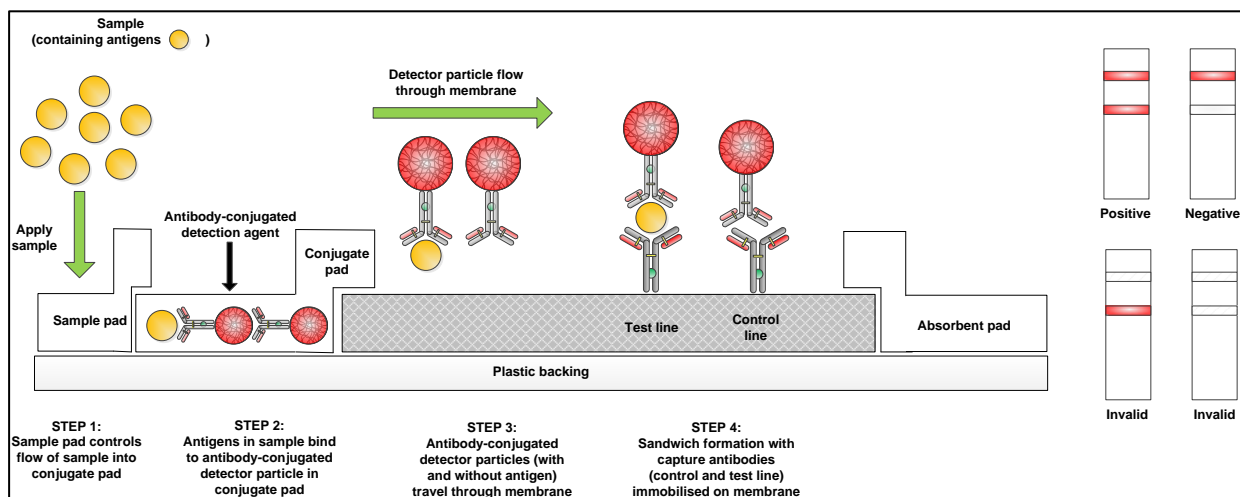


Figure 4.1: Lateral flow diagnostic assay (adapted from Posthuma-Trumpie *et al.*, 2009).

The general methodology of a lateral flow immunoassay requires a sample (blood/urine/saliva) to be applied to the sample pad of the test strip. The liquid sample then migrates by capillary action through the various assay components as follows: first the sample comes into contact with the conjugate pad containing a multitude of antibody-conjugated detector particles. Any biomarker antigens present in the sample bind to the antibodies on the detector particles and these antigen-bound detector particles migrate along the nitrocellulose membrane under capillary action. The exposed surface of the antigen (if present) is captured by pre-immobilised antibody on the test line of the nitrocellulose membrane, resulting in a detectable signal (visible colour change) while antigen-free detector particles accumulate at a control line with pre-immobilised antibody against the antibody immobilised on the detector particles, revealing the reliability of the test/assay (Kakkilaya, 2003). To maintain the flow, an absorbent pad is placed at the distal side of the strip to which the sample is applied, drawing the liquid through the strip (Posthuma-Trumpie *et al.*, 2009).

The ideal material to be used for the membrane depends on the ease of immobilising proteins as well as the capillary forces, and size of the pores, which determines the ease and speed at which the sample and the antibody complexes travel through the membrane (Henderson *et al.*, 2002; Posthuma-Trumpie *et al.*, 2009). The most common membrane material used is nitrocellulose, with pore sizes ranging between 0.05 – 15 μm (Bandla *et al.*, 2011; Wong *et al.*, 2009). However, other polymeric materials such as nylon, polyethersulfone, polyethylene and fused silica have also been used (Leung *et al.*, 2003; Posthuma-Trumpie *et al.*, 2009). The membrane is thin and fragile and is therefore often supplied attached to a thin plastic backing to allow easy handling and cutting (Posthuma-Trumpie *et al.*, 2009). The pores of the membrane are not evenly distributed and thus the capillary flow rate (seconds.cm^{-1}) of the membrane is a more valuable criterion in the selection process for a particular lateral flow

application. The sensitivity of the assay is inversely proportional to the speed at which the assay develops (Wong *et al.*, 2009).

Once the capture antibodies have been immobilised on the membrane, the remaining membrane needs to be blocked to avoid non-specific protein binding (Verheijen *et al.*, 1998). There are two options for blocking; one requires blocking the membrane in a blocking buffer, rinsing the excess buffer off and drying the membrane in a convection oven at 37°C (Fribe *et al.*, 2009). The second option is known as “blocking-on-the-fly” where the membrane is not blocked, instead the release buffer and sample buffers are specially formulated with blocking agent to block the membrane as the assay develops (“on-the-fly”) (Fribe *et al.*, 2009). Pre-blocking of membrane, although occasionally used, is not advisable since it may affect the hydrophobicity and wetting properties of the membrane, while blocking-on-the-fly is often preferred as it has less risk of incorporating air bubbles or artefacts in the membrane which could obstruct the flow of the liquid (Fribe *et al.*, 2009; Posthuma-Trumpie *et al.*, 2009).

The sample pad is usually made of either cellulose, cross-linked silica or glass fibre and its function is to ensure an even distribution of the sample to the conjugate pad (Leung *et al.*, 2003; Sajid *et al.*, 2014). The distribution of the sample pad pores can be readily manipulated during manufacturing to be symmetrical or asymmetrical, which could allow the sample pad to act as a filter to remove coarse/large materials if required as a potential sample processing step (Fribe *et al.*, 2009; Posthuma-Trumpie *et al.*, 2009).

The ideal conjugate pad should wet with ease, readily absorb fluid, should evenly distribute the antibody-detector particle upon addition to the pad and should easily release the detector particle upon sample addition (Verheijen *et al.*, 1998). The conjugate pad is preferably first treated with a release buffer containing blocking agent (BSA), detergent (e.g. Triton) and additives (e.g. PVP), after which the membrane is dried in a convection oven at 37°C for 1 hour (Kestrel, 2013). The antibody conjugated detector particles are then applied to the pre-treated conjugate pad and dried at 37°C for a further 2 hours (Verheijen *et al.*, 1998).

The absorbent pad consists of cellulose fibres and its function is to wick the fluid of the assay through the membrane (Leung *et al.*, 2003; Posthuma-Trumpie *et al.*, 2009). The volumetric capacity of the absorbent pad allows for large volumes of fluid (sample) to be applied to the sample pad which in turn can improve the sensitivity of the assay (Leung *et al.*, 2003; Posthuma-Trumpie *et al.*, 2009).

The principle of a lateral flow diagnostic device relies on the detection (visual or reader assisted) of a signal at the control and test line, with the signal being directly proportional to the

concentration of analyte in the sample (Posthuma-Trumpie *et al.*, 2009; Sajid *et al.*, 2014). Electronic readers provide the advantage for more sensitive analysis and quantification of the response, with significant enhancements having been made to reduce the cost of these devices (Wong *et al.*, 2009). The main limitation of current lateral flow diagnostic devices is their lack of sensitivity and thus various avenues to improve assay sensitivity have been explored (WHO, 2009), and are discussed in Chapter 1.

The detector particles used in the current diagnostic devices (colloidal gold and latex) have limitations which include leaching and aggregation (Chenggang *et al.*, 2008; Wong *et al.*, 2009). Although not currently a lateral flow detection agent, the ReSyn polymer microsphere technology used in this study were considered a potentially viable alternative to existing lateral flow detection agents, and could potentially alleviate several of the stated drawbacks of current lateral flow detection agents. The previously demonstrated high binding capacity, chromophoric properties, increased stability of antibodies (through multipoint covalent attachment) and low cost technology base, potentially make this technology suitable for enhanced lateral flow. It is the aim of this chapter to evaluate the suitability of the microspheres for inclusion in lateral flow tests. To increase throughput this was evaluated using a lateral flow assay in microwell format .

The human pregnancy test, detecting human chorionic gonadotropin (hCG) as the biomarker, was selected as a model system due to the availability of reagents, and the various other studies that have used hCG as a model analyte providing for potential comparison of results (Fu *et al.*, 2011).

4.2. MATERIALS AND METHODS

4.2.1. Materials

All chemicals and reagents were supplied by Sigma Aldrich (Germany) unless otherwise stated, and were of analytical grade or better. Antibodies, including those for the control line (polyclonal goat anti-mouse IgG) and test line (polyclonal goat anti-hCG alpha) as well as the monoclonal mouse anti-hCG beta clone 7 IgG, and anti-hCG-conjugated colloidal gold (anti-hCG beta clone 7 standard) were purchased from Arista Biologicals (United States). Colloidal gold (40 nm) was purchased from British BioCell International (BBI - UK). The hCG antigen was kindly supplied by Kestrel Biosciences. Plastic backed nitrocellulose membranes were purchased from the following suppliers: HF-75 (Millipore), FF-60 (GE Healthcare), FF-85 (GE Healthcare), CN-95 (Unisant) and CN-145 (Unisant) as well as an unbacked membrane AE-100 (GE healthcare). BSA was purchased from Roth and ultra-pure MilliQ water (Millipore) was

autoclaved and used for all experiments. Centrifugation was performed using a Beckman-Coulter microfuge 18 at room temperature (25°C) at 2000 x g for 5 minutes. The end-over-end mixing/incubation steps were performed at 4°C on an ELMi Intelli-mixer set on program F1 and 15 rpm (180° rotation). Unless otherwise stated, the running buffer for microsphere lateral flow contained PBS, 0.1% Tween20, 1% casein, while sample buffer contained the same components but was supplemented with hCG antigen as described below. The colloidal gold lateral flow buffers were similarly defined as running buffer (0.1 M Tris, pH 8, 0.1% Tween20, 0.1% BSA) or sample buffer (colloidal gold running buffer supplemented with hCG antigen). All lateral flow assay experiments were set-up in a microwell format, where buffer (100 µl) and detector reagent (10 µl) were pre-mixed in a well of a microwell plate, and the membrane subsequently placed within the solution (Figure 4.3). The standard protocols for colloidal gold conjugation, as stipulated by the Diagnostics Consulting Network, were followed where colloidal gold was used as a label.

4.2.2. Epoxide microsphere preparation and antibody conjugation

Epoxide functional polymer microspheres of ~1 µm in diameter were prepared as described in Chapter 2 (2.2.2). For initial experimentation two separate preparations of polymer microspheres were dyed with Chicago Sky Blue and Congo Red dye using 1 mg dye.ml⁻¹ microsphere suspension, as described in Chapter 2 (2.2.5.1). The final dyed microsphere pellet was resuspended in water and stored at 4°C for a maximum of 5 days.

The dyed microsphere suspension was vortexed for 30 seconds after which 500 µl (1.35 mg) was aliquoted into a LoBind Eppendorf tube, centrifuged and the supernatant discarded. The pellet was equilibrated for antibody conjugation with 2 x 500 µl of conjugation buffer (0.1 M Borate-Cl, pH 8.2). The microspheres were recovered by centrifugation and the final pellet resuspended in 500 µl conjugation buffer followed by the addition of 500 µl anti-hCG antibody (0.2 µg.µl⁻¹ in conjugation buffer). The suspension was immediately vortexed for 10 seconds and incubated with end-over-end mixing for 48 hours with subsequent recovery by centrifugation. The supernatant was transferred to a clean Eppendorf tube and the pellet washed once with 1 ml conjugation buffer and the supernatant pooled to a final volume of 2 ml to quantify unbound antibody using a BCA assay as described in Chapter 3 (3.2.5). The anti-hCG-conjugated-microsphere pellet was resuspended to 500 µl in conjugation buffer and divided into two equal 250 µl aliquots followed by the addition of either 1 ml blocking buffer 1 (10 mg.ml⁻¹ BSA) or blocking buffer 2 (10 mg.ml⁻¹ casein) to respective microsphere preparations. The reactions were vortexed for 30 seconds and incubated with end-over-end mixing overnight at 4°C, after which the anti-hCG-conjugated-microspheres were recovered by centrifugation, the supernatants discarded, and the pellets subsequently washed twice with

lateral flow buffer (10 mM Phosphate buffer, pH 8). The final pellet was resuspended in 250 μ l of either storage buffer 1 (10 mM Phosphate buffer, pH 8, 0.1% Tween20, 0.5% BSA) or storage buffer 2 (10 mM Phosphate buffer, pH 8, 0.1% Tween20, 0.5% Casein) respectively. The resuspended pellets were sonicated (Bandelin Sonoplus sonicator, SH70G probe, 10 pulses at 0.5 second intervals) to reduce aggregation. Reduction of aggregation was confirmed with microscope analysis (Olympus BX53, fitted with Olympus DP72 eyepiece, 100X magnification) of the suspensions before and after sonication. The resuspended pellets were stored at 4°C for up to 5 days with no adverse effect on antibody stability/reactivity during storage.

4.2.3. Assembly of lateral flow assay

Preparation of lateral flow devices involved assembly of the nitrocellulose membrane and absorbent pad. The nitrocellulose membrane was cut to a desired size (~3 cm) and the back of the membrane fixed onto a backing card making use of the adhesive on the backing card. The assembly of a typical lateral flow assay is illustrated in Figure 4.2. For proof-of-concept, the lateral flow assay for the polymer microsphere experiments consisted only of the nitrocellulose membrane and the absorbent pad, and tested in a microwell assay format, excluding the variance of the sample and conjugate pads (Figure 4.3).

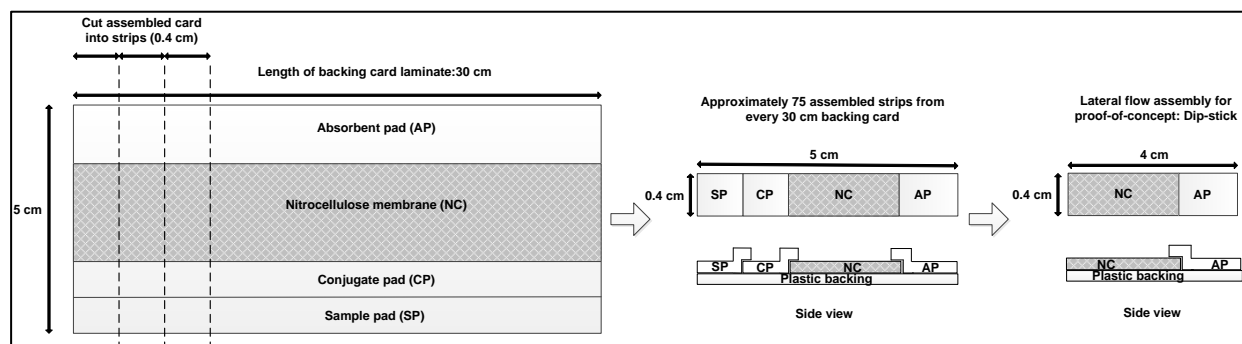


Figure 4.2: Illustration for lateral flow component assembly onto a backing card.

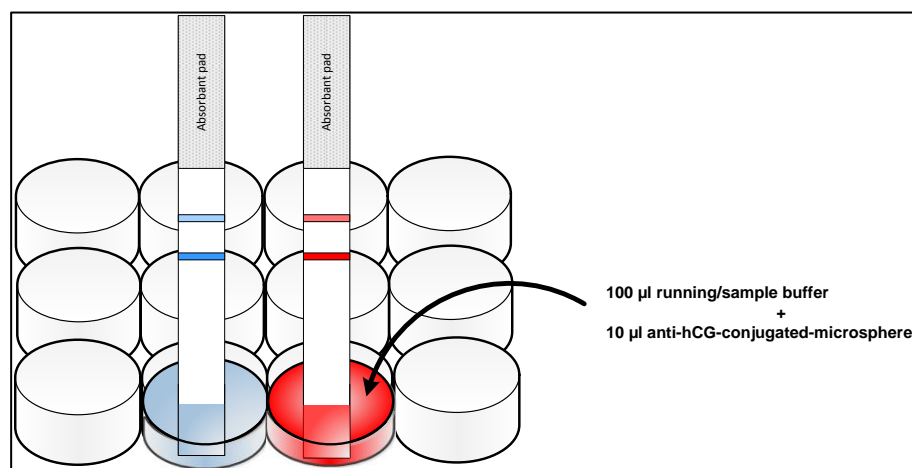


Figure 4.3: Illustration of lateral flow assay in a microwell plate.

The lateral flow membrane, fitted with an absorbent pad, was placed in the wells of a microwell plate, containing the pre-mixed buffer components. Control line and test line antibody solutions were prepared to a final concentration of 1 mg.ml^{-1} in buffer (PBS, 1% sucrose) and subsequently striped on the membrane using a BioDot Inc. ZX1000 dispenser (operating parameters: $1 \text{ } \mu\text{l.cm}^{-1}$ dispensing rate, non-contact striping). As per standard lateral flow, the control line was striped at the top and the test line(s) were striped below the control line. The striped membranes were analysed by visual inspection for striping errors, and errors were excluded for lateral flow development. The striped membranes were placed on a drying rack and allowed to dry in a convection oven at 37°C for 1 hour.

4.2.4 Lateral flow component optimisation

The performance of several nitrocellulose membranes with different pore sizes, protein binding capacities and wicking rates were tested for application in lateral flow of the synthesised polymer microspheres. Of the membranes evaluated, CN-95 provided the most promising results with respect to wicking rate and flow performance of the polymer microspheres, and was selected for further development.

The lateral flow assay was optimised using both the blue and red dyed anti-hCG-conjugated-microspheres and the corresponding negative controls (without conjugated antibody) on pre-striped nitrocellulose membranes fitted with an absorbent pad. After identification of the ideal lateral flow buffer formulation, the dye load and antibody load on red conjugated microsphere preparations were optimised to achieve the lowest possible detection limit for the polymer microspheres.

The suitability of the two blocking buffers for preventing non-specific interaction in lateral flow were assessed by using a lateral flow assay in wells of a 96 well round-bottomed microwell plate containing $100 \text{ } \mu\text{l}$ of running buffer (PBS, 0.1% Tween20) supplemented with either BSA or casein (1%), followed by the addition of $10 \text{ } \mu\text{l}$ BSA or casein finished blue anti-hCG-conjugated-microspheres. The pre-striped nitrocellulose strip was placed in the respective wells and allowed to develop for 10 minutes after which the strips were removed from the reaction and visually inspected for colour accumulation at the capture lines in both positive and negative controls. The colour formation at the capture lines were quantified using a gel documentation system (Syngene G.Box, using indirect illumination, upper white - without filter). Positive controls containing $0.5 \text{ mIU hCG antigen.}\mu\text{l}^{-1}$ were run to ensure compatibility.

4.2.5. Microsphere optimisation for lateral flow

Several microsphere parameters that could potentially impact the sensitivity of the lateral flow assay were identified and further explored using red anti-hCG-conjugated-microspheres in running buffer excluding the antigen and sample buffer (running buffer supplemented with antigen), as described in 4.2.4.

The parameters that were identified for optimisation were dye content, primary antibody content and microsphere content. The experimental layout is illustrated in Figure 4.4.

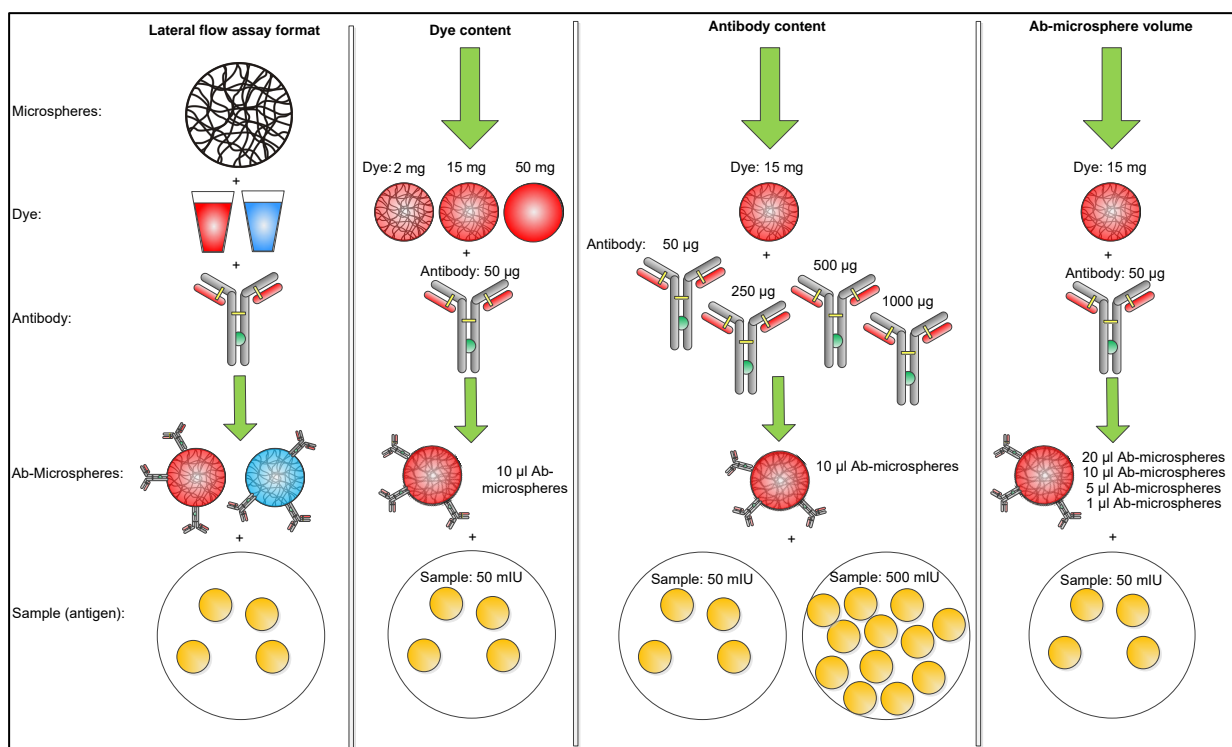


Figure 4.4: Illustration of the lateral flow parameters explored.

The dye content of the microspheres was explored to determine the effect of dye load on visual intensity of the microspheres at the test line. Epoxide functional polymer microspheres (1 ml, ~1 µm PSD) were dyed with either 2 mg, 15 mg or 50 mg Congo Red dye respectively, after which 50 µg anti-hCG antibody was conjugated to 250 µl (0.68 mg) dyed microsphere suspension, the beads finished with casein, washed and equilibrated in running buffer, and sonicated as described in 4.2.2. The lateral flow reactions/tests were set up with sample buffer containing 50 mIU hCG antigen per well, per reaction.

The quantity of primary antibody conjugated to the microspheres was explored to determine the effect of antibody load on sensitivity. A lateral flow assay was set up using epoxide functional polymer microspheres (15 mg dye.ml⁻¹) with varying amounts of anti-hCG antibody (200 µg, 1000 µg, 2000 µg and 4000 µg) conjugated per 1 ml (2.7 mg) dyed microsphere

suspension. The beads were finished with casein, sonicated and run in sample buffer containing either 50 mIU or 500 mIU antigen per reaction.

The volume of anti-hCG-conjugated-microspheres loaded onto the nitrocellulose membrane was varied to determine the effect of volumetric load on test sensitivity. A lateral flow assay was set up using epoxide-functional anti-hCG-conjugated-microspheres (15 mg dye.ml⁻¹, 200 µg anti-hCG.ml⁻¹, casein finished) and varying volumes of the microsphere suspension (20 µl, 10 µl, 5 µl and 1 µl) loaded in the sample buffer containing 50 mIU hCG antigen per reaction.

4.2.6. Anti-hCG-conjugated-colloidal gold: “Gold” Standard

Colloidal gold (BBI) was prepared as a negative control for lateral flow by blocking 1 ml of gold suspension with 500 µl BSA (10 mg.ml⁻¹; (Kestrel, 2013)). The reaction was incubated with end-over-end mixing for 1 hour at room temperature (25°C) after which the colloidal gold was recovered by centrifugation at 16 000 x g for 45 minutes, the supernatant discarded and the pellet resuspended to OD 10 in storage buffer (0.05 mM Na₂HPO₄, pH 7.4, 1% BSA, 0.1% sodium azide) and stored at 4°C. Commercially available anti-hCG-conjugated-colloidal gold (Arista Biologicals) was used as the positive control.

Colloidal gold running buffer (0.1 M Tris, pH 8, 0.1% Tween20, 0.1% BSA), and sample buffer (running buffer supplemented with 0.5 mIU hCG antigen.µl⁻¹ buffer) were prepared fresh and 100 µl of each were aliquoted into respective wells of a 96 well round bottomed plate followed by the addition of 10 µl each negative and positive control microspheres. A pre-stripped nitrocellulose membrane was inserted into the wells, incubated and analysed as described in section 4.2.4.

4.2.7. Microsphere and colloidal gold comparison

The conjugated microspheres were evaluated against standard colloidal gold with respect to sensitivity and stability.

The optimised conditions for microsphere lateral flow as determined in this chapter (15 mg dye.ml⁻¹, 200 µg anti-hCG.ml⁻¹, casein finished, and 10 µl microspheres per assay) were used in this evaluation in a lateral flow assay microwell format. The sensitivity was evaluated by decreasing the concentration of hCG antigen in sample buffer from 50 mIU to 0.5 mIU per reaction.

The stability was evaluated by analysing the efficiency of antigen detection after incubation of the anti-hCG-conjugated particle preparations at elevated temperatures (accelerated denaturation). Briefly, Eppendorf tubes containing either 100 µl of anti-hCG-conjugated-microspheres or hCG-conjugated-colloidal gold beads were incubated at 50, 60 and 70°C for 1, 3 and 6 hours. After each incubation time interval, 10 µl of each suspension was removed and run on a lateral flow assay containing 100 µl sample buffer (50 mIU hCG antigen per reaction).

4.3. RESULTS AND DISCUSSION

4.3.1. Epoxide microsphere preparation and antibody conjugation

The epoxide polymer microspheres were dyed for use in a lateral flow assay to be visible on a lateral flow device and against the white background of the nitrocellulose membrane. The dyes were selected based on previous performance and contrast (Chapter 2, 2.2.5). The microspheres readily took up the dyes without significant aggregation or leaching (Figure 4.5).

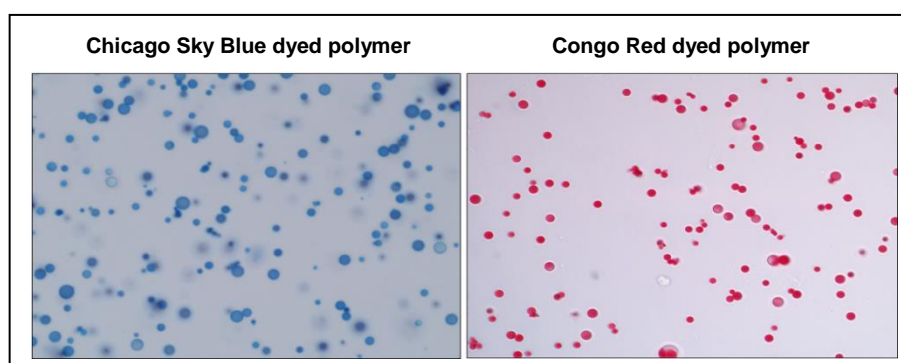


Figure 4.5: Light microscope images of microspheres suitable for lateral flow. Images are representative of a microsphere batch dyed with Chicago Sky Blue (left) and Congo Red (right).

Quantification of anti-hCG antibody conjugation to epoxide functional polymer microspheres was determined using the BCA assay as described previously (refer Chapter 3, section 3.2.3) and quantified against an anti-hCG antibody standard curve ($y = 0.0187x + 0.0129$, R^2 value of 0.9970).

The maximal antibody binding capacity of Chicago Sky Blue dyed microspheres and Congo Red dyed microspheres were both in the region of 30 µg antibody per 250 µl (0.68 mg) bead suspension (29.22 ± 0.25 , and 32.88 ± 0.19 respectively) as determined by the antibody conjugation experiment containing 50 µg anti-hCG antibody.

4.3.2. Lateral flow component optimisation

4.3.2.1. Flow formulation

BSA and casein are the most utilised proteins used to block non-specific interactions in various immunoassay formats (Jeyachandran *et al.*, 2010; Steinitz, 2000). This has been achieved through blocking of the microspheres and inclusion of the proteins in the running buffer. The effect of these two agents was evaluated on blue microspheres with and without conjugated anti-hCG antibody, subsequently referred to as “hCG” and “control” respectively. For initial specificity determination, control microspheres (unconjugated) and anti-hCG-conjugated-microspheres, were run in buffer excluding the target antigen, hCG. The lateral flow results were quantified by densitometry (Syngene Gene Tools) (Fernández-Sánchez *et al.*, 2005). The results for BSA based running buffer (PBS, 0.1% Tween20, 1% BSA) are presented in Figure 4.6 A and B below, while casein running buffer (PBS, 0.1% Tween20, 1% casein) results are presented in Figure 4.7 A and B below.

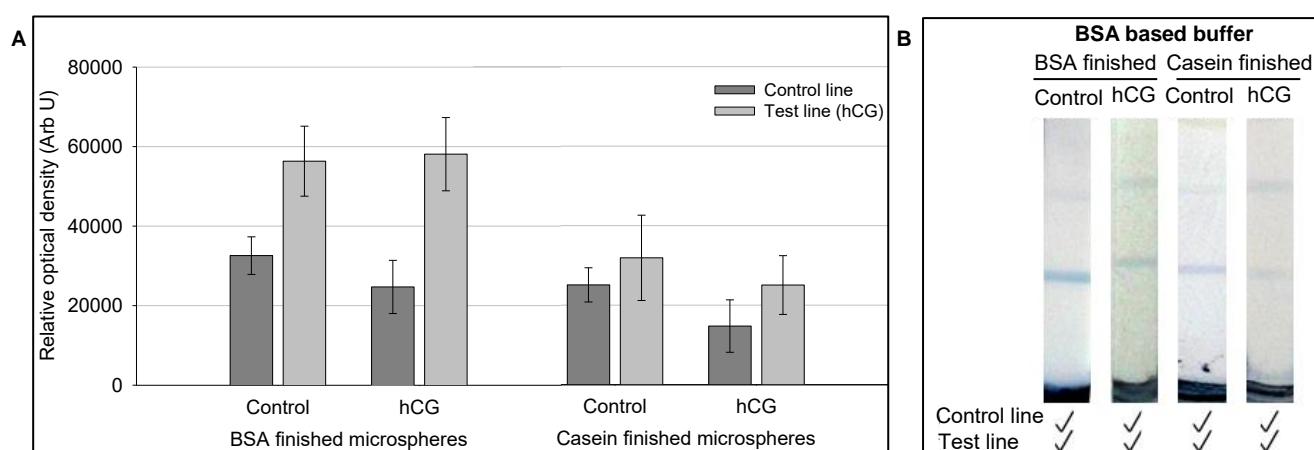


Figure 4.6: Lateral flow of BSA and casein finished Chicago Sky Blue dyed microspheres without conjugated antibody (control) and hCG-conjugated-microspheres (hCG) in BSA-based running buffer. **A:** Quantified results, **B:** Representative lateral flow image with control line above the test line. Error bars represent standard deviation of triplicate lateral flow experimental sets.

It is expected that the negative control microspheres would not result in binding at the test or control line while the anti-hCG-conjugated-microspheres would only bind to the control line. However, some non-specific binding is clearly evident at the test line for all buffers and conditions.

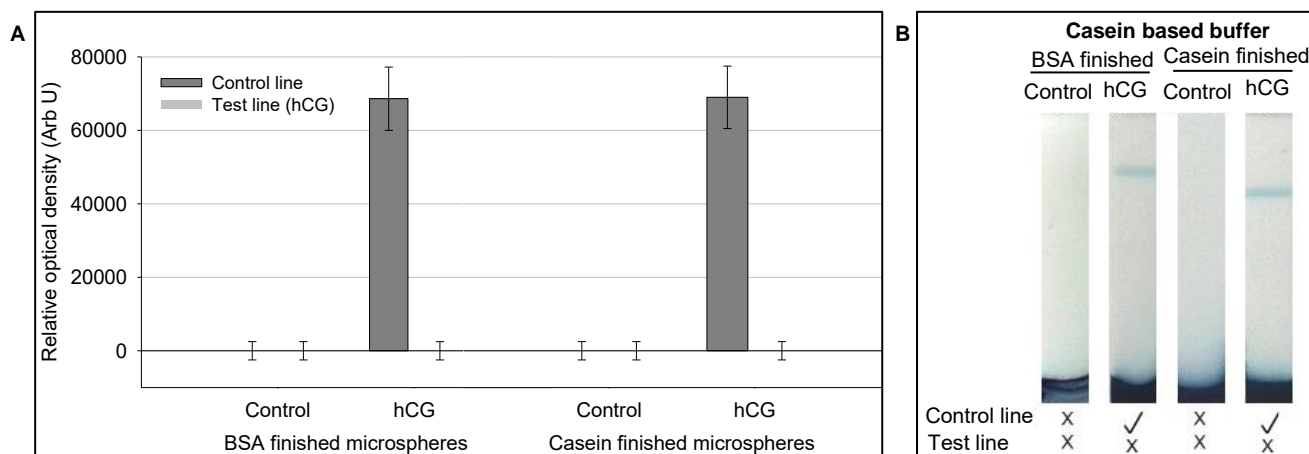


Figure 4.7: Lateral flow of BSA and casein finished negative control and positive (hCG) Chicago Sky Blue dyed microspheres in casein-based running buffer. **A:** Quantified results, **B:** Representative lateral flow image with control line above the test line. Error bars represent standard deviation of triplicate lateral flow experimental sets.

The casein-based running buffer performed well with both BSA and casein finished microspheres. No binding was observed with the negative controls at either the control or the test line. Expected binding was observed at the control line with the anti-hCG-conjugated-microspheres, with the control line of the BSA and casein finished anti-hCG-conjugated-microspheres having similar intensities (densitometry analysis). The results reveal the importance of buffer formulation on lateral flow assay development and the presence of casein appears to not only remove non-specific binding, but also increase the particle density at the control lines. The suitability of the running buffer containing casein was subsequently evaluated for both negative and positive controls for blue and red microspheres (Figure 4.8).

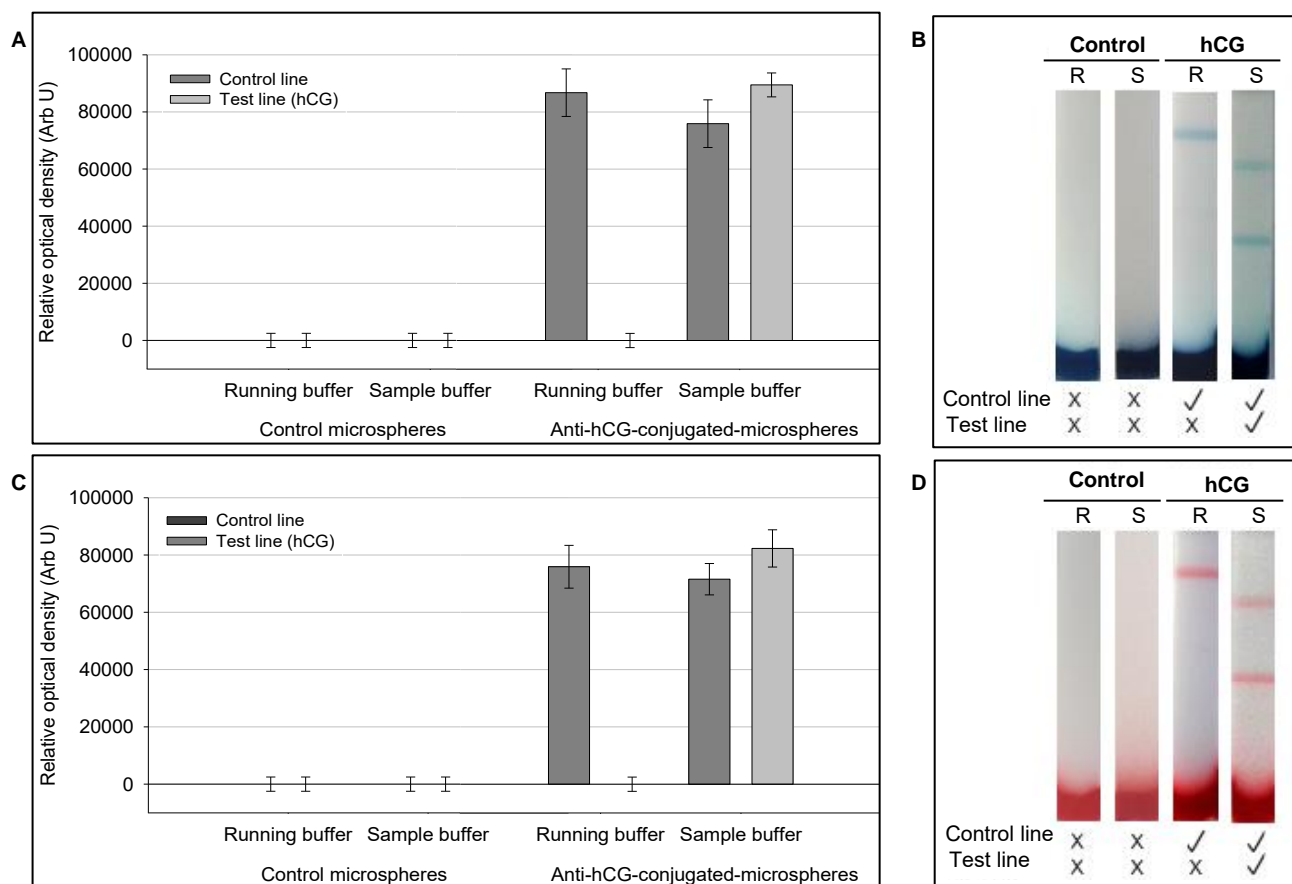


Figure 4.8: Lateral flow of negative control and positive (hCG) microspheres. **A:** Quantified results and **B**, representative lateral flow image of blue microspheres with control line above test line, **C:** Quantified results and **D**, representative lateral flow image of red microspheres with control line above the test line. Running buffer (R) and sample buffer (S). Error bars represent standard deviation of triplicate lateral flow experimental sets.

The blue and red dyed microspheres performed as expected in both the running and sample buffer. The negative control (unconjugated, casein finished) microspheres resulted in no binding at the test or the control lines, in either the running or sample buffer and was dye independent. The anti-hCG-conjugated-microspheres in the running buffer resulted in development of an intense control line with no non-specific binding observed on the test line. The anti-hCG-conjugated-microspheres in the sample buffer resulted in the development of both the test and control lines, for both the blue and red microsphere detection agents. These results confirm the suitability of the buffers for the two coloured lateral flow detection reagents.

4.3.2.2. Dye loading

The dye content of the microspheres was further explored to determine the effect on both bead performance and detection sensitivity (Figure 4.9). The amount of antibody conjugated to the microspheres remained constant while the dye content of the microspheres was varied (2 mg, 15 mg, 50 mg).

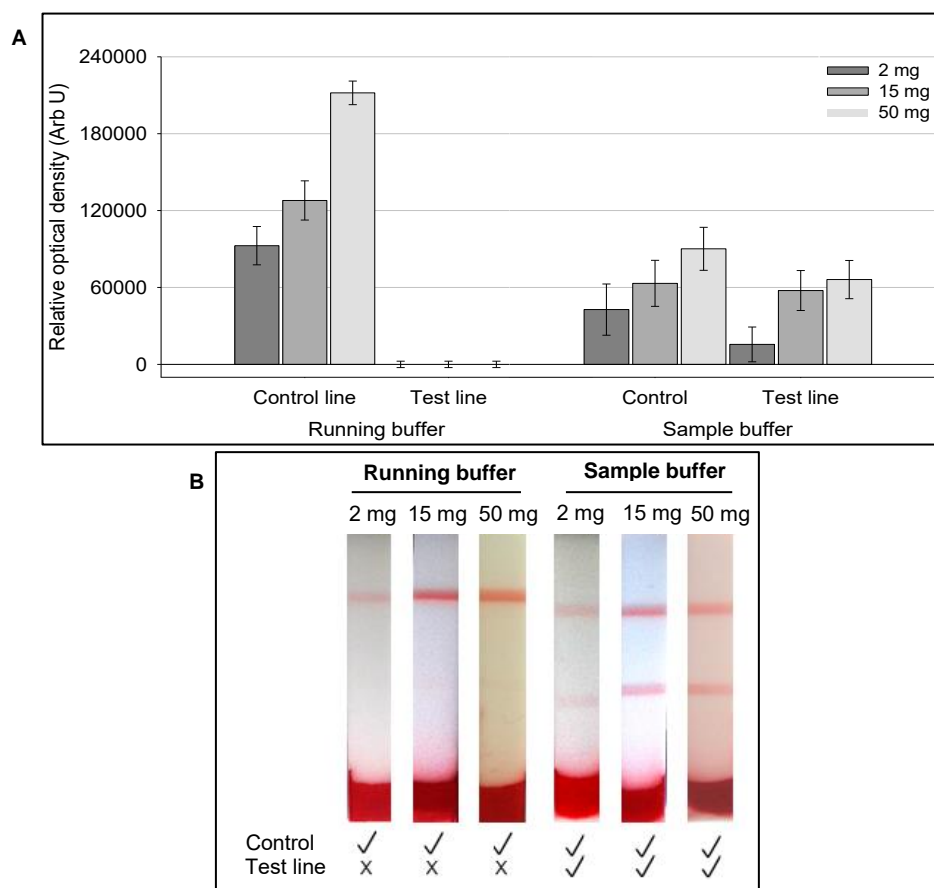


Figure 4.9: Lateral flow of anti-hCG-conjugated-microsphere samples containing either 2, 15 or 50 mg Congo Red dye.ml⁻¹ microsphere suspension. **A:** Quantified results, **B:** Representative lateral flow image with control line above the test line. Error bars represent standard deviation of triplicate lateral flow experimental sets.

The performance of the anti-hCG-conjugated-microspheres in the running buffer was similar with regards to time of control line development (it was thought that the increased density may potentially negatively influence the particle flow and thereby the time required for resolution but this appeared to have little effect), and absence of non-specific binding at the test line in all cases. As the dye content increased, there was a quantifiable increase in signal intensity on the control line.

In the sample buffer (positive for hCG), the test and control line intensity of the microspheres containing 2 mg dye were comparatively low when compared to the signal intensity observed with the microspheres containing 15 and 50 mg dye respectively (Figure 4.9). According to the quantified data analysis, the anti-hCG-conjugated-microspheres dyed with 50 mg dye resulted in a higher signal on both the test and control lines compared to the anti-hCG-conjugated-microspheres dyed with 15 mg dye (Figure 4.9 A). However, visually, the test and control lines of the anti-hCG-conjugated-microspheres dyed with 15 mg and 50 mg dye, appeared similar in intensity (Figure 4.9 B). During assay development, it was observed that the nitrocellulose membrane itself became pink-red when 50 mg dye was used, indicating potential dye leaching

during running. The results suggest that an increased dye load on the microspheres could result in higher signal intensities, but more than a three-fold increase in dye (from 15 to 50 mg) only resulted in an increase in intensity between 10 and 30% (which was not discernible by visual inspection). These results suggest that dye in excess of 15 mg dye.ml⁻¹ microspheres would not significantly increase the performance of the lateral flow assay, and could be problematic for lateral flow application due to dye leaching.

4.3.2.3. Antibody loading

After the suitable dye content for the detection microspheres was determined (15 mg. ml⁻¹ microspheres), this was kept constant and the effect of the concentration of conjugated anti-hCG antibody on the sensitivity for lateral flow was evaluated for two different concentrations of antigen (50 mIU and 500 mIU hCG per reaction) (Figure 4.10). Two control reactions (microspheres conjugated with either 200 µg or 4000 µg anti-hCG antibody) in running buffer only (no hCG antigen), were included in these experiments to ascertain any potential non-specific binding that may occur at the test line due to variation in antibody loading.

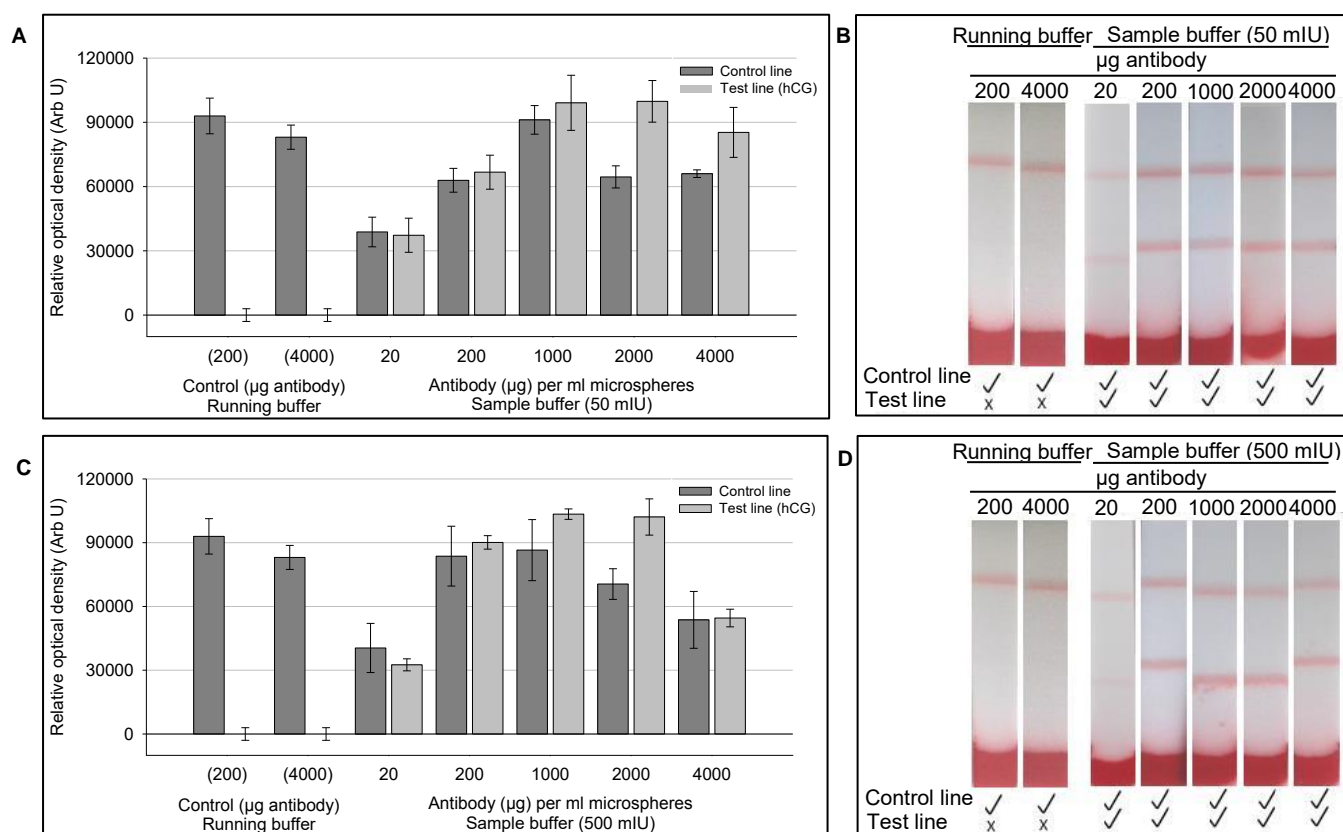


Figure 4.10: Lateral flow of anti-hCG-conjugated-microspheres with varying amounts of anti-hCG antibody, in running buffer (control) and sample buffer containing **A:** 50 mIU and **C:** 500 mIU hCG antigen per reaction. B and D are representative lateral flow images of A and C respectively with control line above the test line. Error bars represent standard deviation of triplicate lateral flow experimental sets.

The anti-hCG-conjugated-microspheres in running buffer (control, no antigen) resulted in strong visible signals at the control line and no non-specific binding was observed at the test line, with similar results irrespective of the amount of anti-hCG antibody immobilised. According to densitometry analysis, the anti-hCG-conjugated-microspheres in running buffer containing the antigen resulted in a gradual increase in the control and test line signal (up to 1000 µg anti-hCG) after which the control line signal decreased with more antibody conjugated to the microspheres while the test line signal remained stable up to 2000 µg of antibody. Visually, higher concentrations of anti-hCG antibody conjugated to the microspheres resulted in minimal difference in both the test and control line intensity values. However, the lowest concentration of 20 µg resulted in weak signals with both visual and densitometry analysis.

Higher antibody concentrations on the microspheres did not necessarily result in increased signal intensity. There is a range of plausible explanations, including steric hindrance as the control and test lines can only bind a certain quantity of microspheres (Posthuma-Trumpie *et al.*, 2009). A further explanation could be that the microspheres are potentially porous and overloading with antibody could result in the antibody immobilising to the interior of the microspheres, which could potentially bind the antigen in the sample and not be accessible to the capture antibody on the test line. In addition, only a fraction of the immobilised antibodies may remain active (random orientation) and able to capture antigen in solution, whereas previous studies have found that the fraction of immobilized antibodies able to capture antigen eventually decreases with higher antibody surface coverage, as a result of monolayer saturation and crowding (Saha *et al.*, 2014).

4.3.3. Volumetric loading of microspheres

The volume of anti-hCG-conjugated-microspheres (200 µg anti-hCG per 1 ml (2.7 mg) microsphere suspension) that were loaded in each lateral flow reaction was explored as a parameter that could affect sensitivity and to determine the ideal microsphere content required for a lateral flow device. The standard running buffer containing 50 mIU hCG antigen per reaction was used for evaluation of this parameter. The volume of anti-hCG-conjugated-microspheres that were loaded into each reaction was varied from 1 to 20 µl and the signal intensity evaluated. The results are illustrated in Figure 4.11.

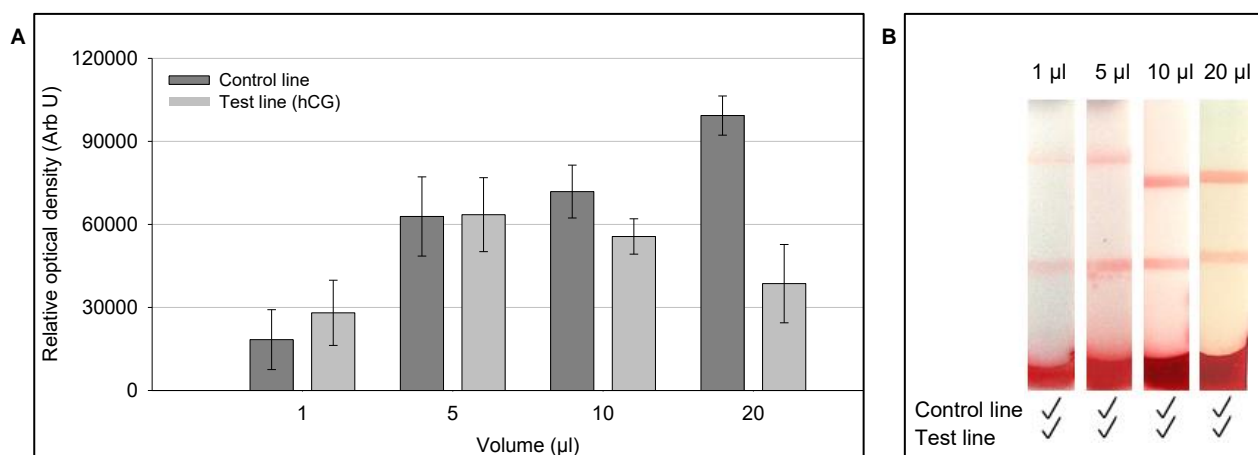


Figure 4.11: Lateral flow with varying volumes of anti-hCG-conjugated-microspheres, in sample buffer. **A:** Quantified results, **B:** Representative lateral flow image with control line above the test line. Error bars represent standard deviation of triplicate lateral flow experimental sets.

It is evident from the data that the control line increases in intensity with increased microsphere content; however the intensity of the test line is affected by the increased volume. Perhaps the simplest explanation for this is ‘boulders in a stream’ as described by Wong *et al* 2009. As the concentration of microspheres collects at the control line this impedes capillary flow of the liquid and microspheres, negatively impacting the colour development at higher microsphere loadings. This may possibly be overcome by increasing the time of lateral flow development and the size of the absorbent pad used (to prevent saturation), or decreasing the particle size. The ideal microsphere load for lateral flow is proposed as 5 to 10 µl since this provides easily visible positive and negative control lines.

4.3.4. Lateral flow detection sensitivity

For the proof-of-concept study, these preliminary parameters were selected for evaluation of sensitivity. The lowest limit of detection, i.e. the lowest possible concentration of antigen, detectable by the lateral flow assay, was explored using the ideal parameters determined in the aforementioned experiments (15 mg dye, and 200 µg anti-hCG per ml microspheres, casein finished, and 10 µl microsphere volume) and varying the concentration of the antigen in the running buffer. The results are presented in Figure 4.12 below.

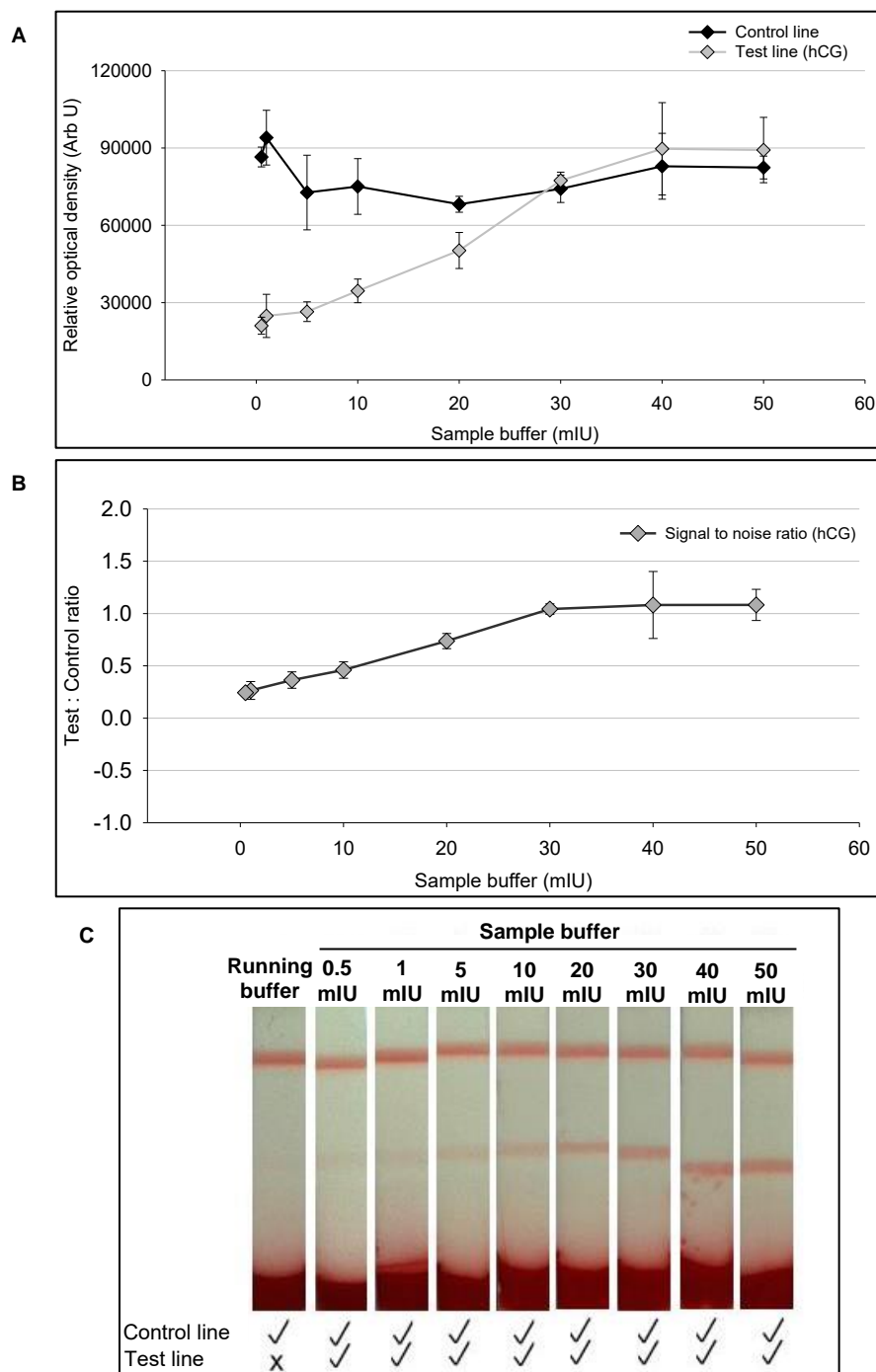


Figure 4.12: Lateral flow assay to determine the lowest limit of antigen detection of anti-hCG-conjugated-microspheres. **A:** Quantified results, **B:** signal to noise ratio depicting lower limit of detection, **C:** Representative lateral flow image with control line above the test line. Error bars represent standard deviation of triplicate lateral flow experimental sets.

According to densitometry, the control line intensity remained fairly constant and clearly visually detectable. The consistency observed with the control line intensity of ~80 000 arbitrary units across the lateral flow strips indicate good experimental reproducibility. There was a gradual decrease in the test line intensity with a distinct reduction below 20 mIU although capture lines were visible at 5 mIU and this was considered the limit of detection for

visual detection. However, a concentration of 0.5 mIU could potentially be detectable by densitometry.

4.3.5. Antibody stability

Stability studies evaluate the effect environmental factors have on the quality of the product which are then used to compare predictive shelf life and determine storage conditions (Bajaj *et al.*, 2012; Kommanaboyina *et al.*, 1999; Leung *et al.*, 2003). The accelerated denaturation results are presented in Figure 4.13 below.

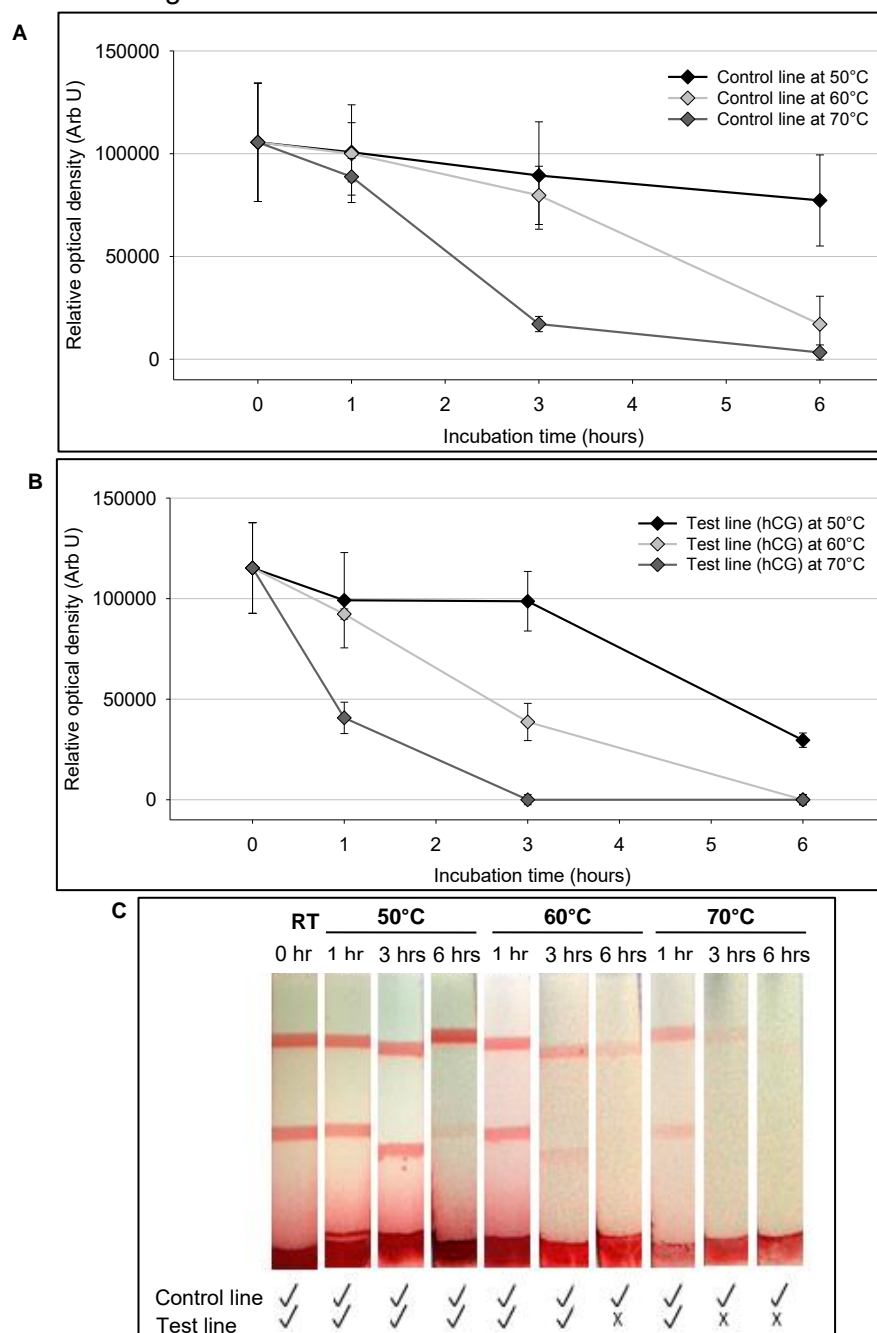


Figure 4.13: Stability of anti-hCG-conjugated-microspheres incubated from 1 to 6 hours at 50°C, 60°C and 70°C. **A** and **B**: Quantified results, **C**: Representative lateral flow image with control line above the test line. Error bars represent standard deviation of triplicate lateral flow experimental sets.

According to densitometry and visual analysis, the control line at 50°C remained relatively stable for up to 6 hours of incubation, while the test line signal remained stable for up to 3 hours. Incubation at 60°C resulted in strong control line signals for up to 3 hours incubation and strong test line signals for 1 hour incubation, while longer incubation (6 hours) resulted in a reduced control line signal and no detectable test line signal. Incubation of the anti-hCG-conjugated-microspheres at 70°C for 1 hour resulted in visible control and test lines, while longer incubation times (3 and 6 hours) were detrimental to control and test line development.

Stability studies at temperature extremes have previously been performed on commercially available lateral flow assays (pLDH and HRP2 based diagnostic tests) using real world blood samples and it was found that at certain temperatures and exposure times, a control line appeared while the assay failed to produce a test line (Chiodini *et al.*, 2007). A similar result was observed in this study (e.g. 60°C for 6 hours, 70°C for 3 hours), likely due to the denaturation of the antigen binding site of the hCG antibody conjugated to the microsphere and thus reduced antigen detection sensitivity, resulting in fewer anti-hCG-conjugated-microspheres immobilising onto the test line. Heat denatured antibodies will however still display linear epitopes and will still bind to the control line antibody, even though the antigen binding domain may be denatured, thereby not binding at the test line, as observed in Figure 4.13. However, the strips were not incubated at elevated temperatures, in real world applications, the control line antibodies would denature at elevated temperatures potentially resulting in comparative decreases in signal at the control line. Improved stability at the test line was not the purpose of this study, however several strategies to improve stability at the control line have been proposed, including immobilisation on a microsphere matrix (Wong *et al.*, 2009).

4.3.6. Colloidal gold comparison

Colloidal gold is the most frequently used particle for lateral flow assays (Linares *et al.*, 2012). The performance of the anti-hCG-conjugated-microspheres was compared to the performance of standard anti-hCG-conjugated-colloidal gold nanoparticles. A lateral flow assay with negative control colloidal gold (BSA finished) and anti-hCG-conjugated-colloidal gold was set up in colloidal gold based running and sample buffers (Figure 4.14).

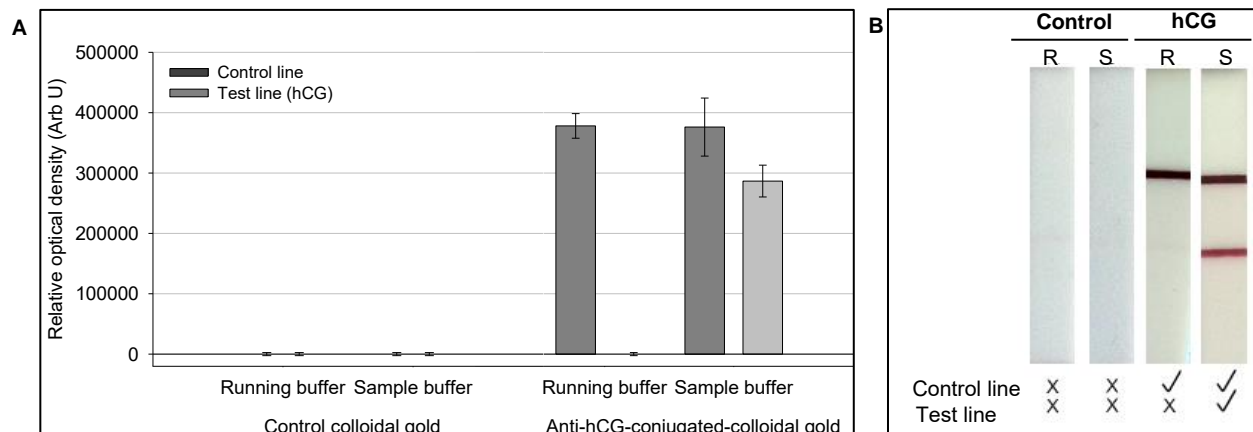


Figure 4.14: Lateral flow of negative control and positive (hCG) colloidal gold nanoparticles in running and sample buffer. **A:** Quantified results, **B:** Representative lateral flow image with control line above the test line. Running buffer (R) and sample buffer (S). Error bars represent standard deviation of triplicate lateral flow experimental sets.

Densitometry and visual analysis of the nitrocellulose membranes resulted in no signal at either the test or control line for the negative control colloidal gold nanoparticles, in either the running or sample buffer. The anti-hCG-conjugated-colloidal gold nanoparticles resulted in a signal at only the control line in running buffer while the gold nanoparticles in sample buffer resulted in both a control and a test line signal as expected. The lowest limit of detection of the lateral flow assay using anti-hCG-conjugated-colloidal gold nanoparticles was explored to compare to the data generated for the polymer microspheres (Figure 4.15).

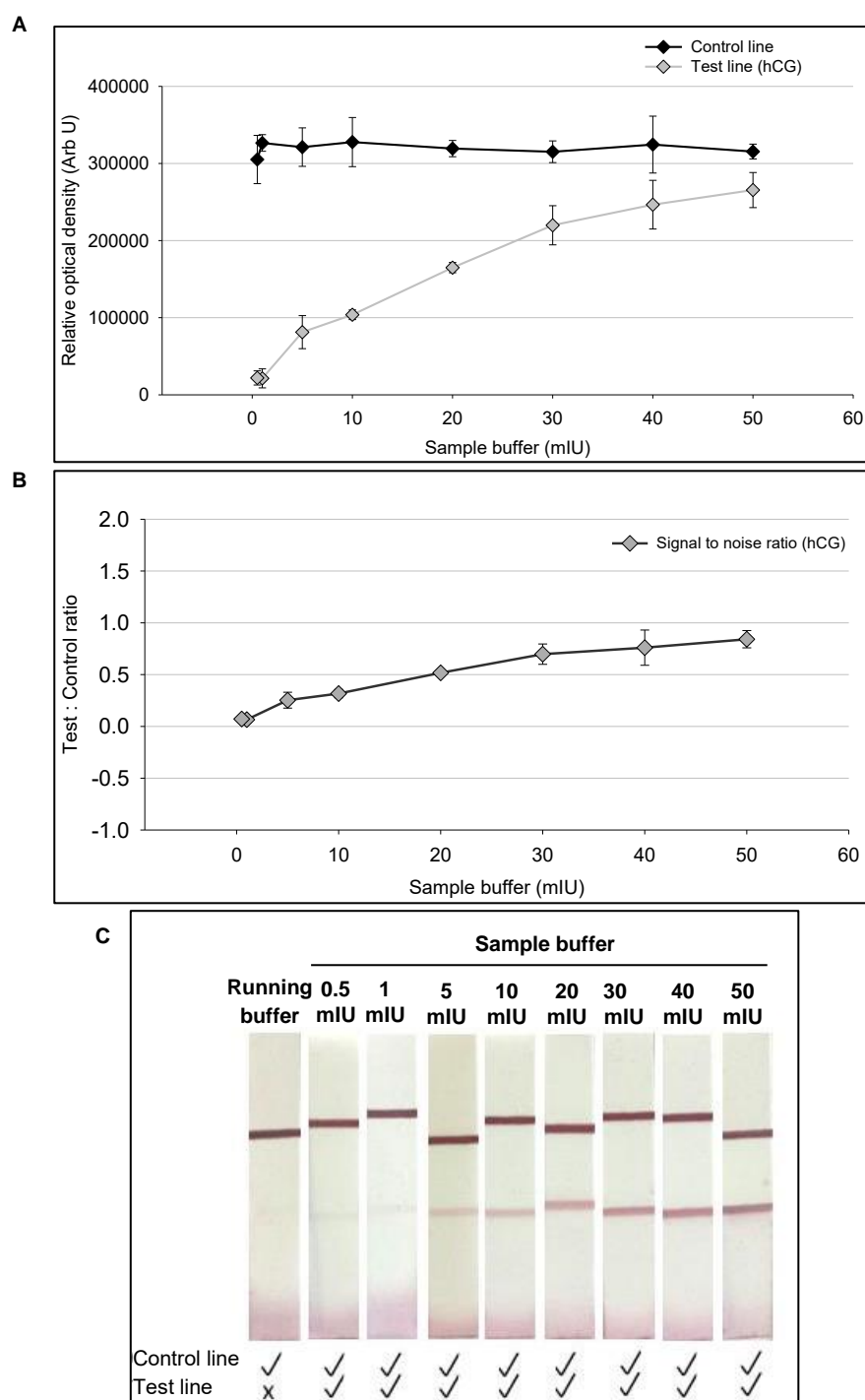


Figure 4.15: Lateral flow assay to determine the lowest limit of antigen detection of anti-hCG-conjugated colloidal gold nanoparticles. **A:** Quantified results, **B:** signal to noise ratio depicting lower limit of detection, **C:** Representative lateral flow image with control line above the test line. Error bars represent standard deviation of triplicate lateral flow experimental sets.

Densitometry and visual analysis revealed that the control line of the anti-hCG-conjugated-colloidal gold nanoparticles remained relatively constant while the test line intensity gradually reduced with decreasing antigen concentrations.

The results suggest the limit of antigen detection, for a definitive positive result using anti-hCG-conjugated-colloidal gold nanoparticles in this lateral flow assay is in the range of 5 mIU per

reaction, as the test line signal with antigen concentrations below 5 mIU were barely visible on the membrane and could be considered by the reader as a false negative.

Accelerated decay at elevated temperatures was utilised to determine the stability of the anti-hCG-conjugated-colloidal gold nanoparticles (Figure 4.16).

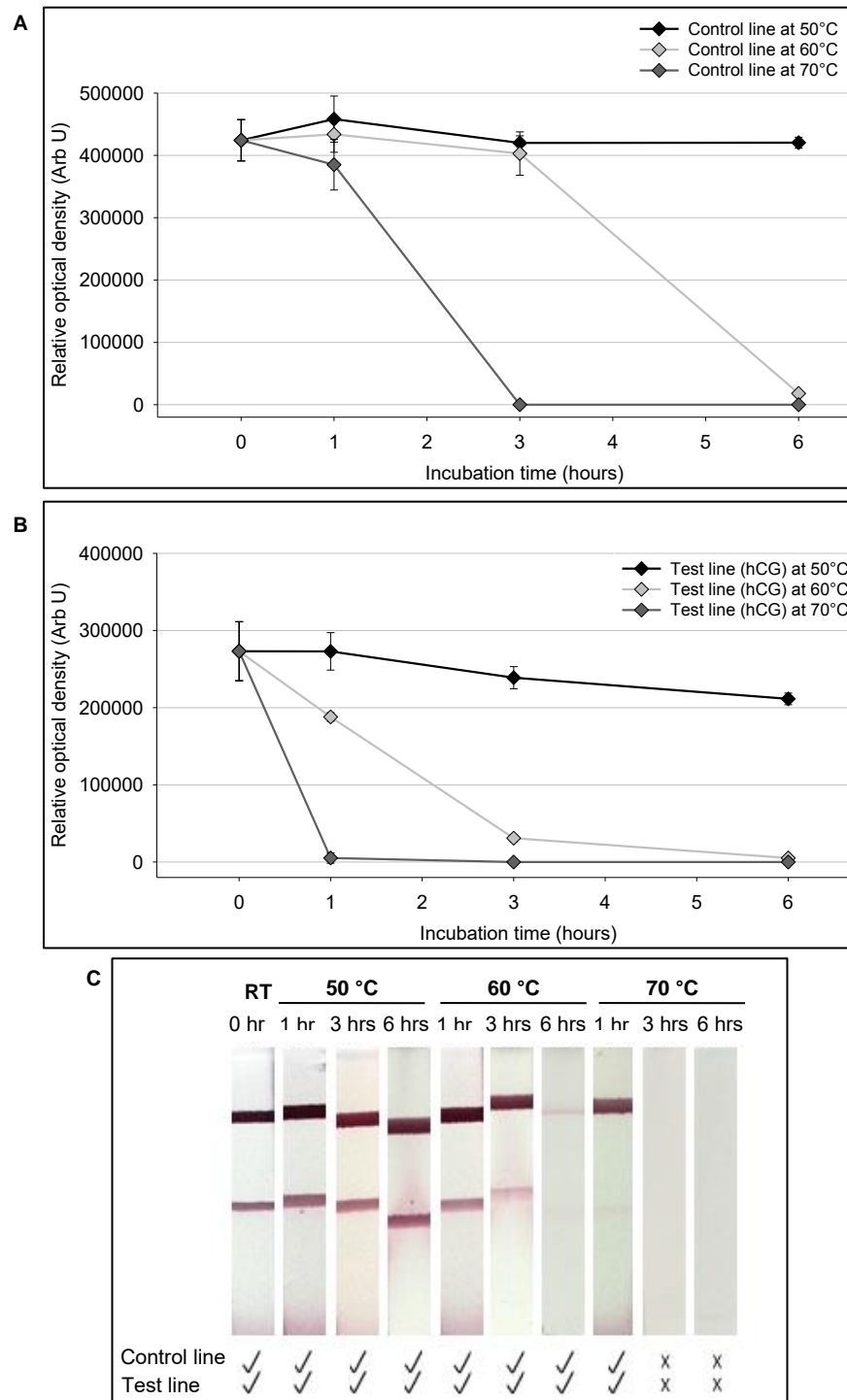


Figure 4.16: Stability of anti-hCG-conjugated-colloidal gold incubated from 1 to 6 hours at 50°C, 60°C and 70°C. **A** and **B**: Quantified results, **C**: Representative lateral flow image with control line above the test line. Error bars represent standard deviation of triplicate lateral flow experimental sets.

The densitometry and visual analysis of the anti-hCG-conjugated-colloidal gold nanoparticles at 50°C resulted in stable control and test line intensities irrespective of the incubation time (1, 3, 6 hours). Incubation of the nanoparticles at 60°C resulted in a strong control and test line signal for up to 1 hour incubation while longer incubation (3 hours) resulted in a strong control line and weak test line with 6 hours incubation being detrimental to both control and test line development. Incubation at 70°C for 1 hour resulted in a visible and detectable control line while the test line was weak and barely detectable. Longer incubation times (3 and 6 hours) at 70°C were detrimental to control and test line development.

4.4. CONCLUSIONS

The suitability of the polymer microspheres as detector particles in lateral flow assays were explored and the preliminary ideal parameters for 1 ml of microsphere suspension was determined as 15 mg dye and 200 µg antibody loading. Further evaluation of the interplay between antibody content and dye content however is required to determine the perfect antibody and dye ratio for this application for future commercial use. The recommended volume of the microspheres for application to lateral flow assays is 10 µl. The ideal parameters determined in this study, provides a limit of sensitivity arguably within the same range as the market leader colloidal gold, at 5 mIU per reaction (or 50 mIU.ml⁻¹) for visual detection. For quantifiable detection with a reader, this is potentially reduced to 0.5 mIU per reaction (5 mIU.ml⁻¹), or potentially even lower, resulting in a similar range of detection as reported in previous studies by Fu *et al.* 2011 and Choi *et al.* 2005, who used hCG as the model protein. Their studies revealed limits of detection for standard anti-hCG-colloidal gold of 1.5 mIU.ml⁻¹ (Choi *et al.*, 2005; Fu *et al.*, 2011).

The covalent conjugation of antibody to microspheres appeared to provide improved stability as illustrated by incubation at high temperatures. The control line development potentially indicates the availability and stability of linear epitopes, being captured at the control line. The development of a test line is indicative of the stability of the antibody Fab region, where the microspheres produced a positive result after 1 hour at 70°C while the colloidal gold did not display a signal. Further evidence of increased stability can be seen in the test line at 60°C for 3 hours, where the microspheres provide a strong positive result as compared to that of colloidal gold. The increase in stability could be a result of the multipoint antibody attachment within the microsphere; however, additional stability tests (humidity and light) would have to be explored next to determine the comprehensive improvement in stability of the microspheres for lateral flow application. The stability benefit of covalent immobilisation of antibodies may be extended to the antibodies at the test and control line by potentially adsorbing antibody-

conjugated microspheres to the membranes, rather than just adsorbing detection antibody, but was not considered within the scope of this study.

What was evident is that the lateral flow assay using the microspheres resulted in many of the microspheres getting trapped at the bottom of the nitrocellulose membrane. This was less pronounced with the colloidal gold beads and thus suggests possible aggregation, initial binding (before the buffer can block the membrane), or particle size with a proportion of the particles potentially not currently suitable for lateral flow ($>3\ \mu\text{m}$) and possibly hindering the particle flow of the smaller microspheres. The signal to noise ratio of colloidal gold, as well as the intensity and sharpness of the test and control lines were visibly better than that observed with the polymer microspheres. The polymer microspheres themselves did not leach in the buffer during storage and thus, the reduced contrast observed with the polymer microspheres may not necessarily be as a result of leaching, but rather be attributed to the larger particles flowing on the strip. Further microsphere engineering aimed at reducing particle size and aggregation may overcome the identified limitations. However, further evaluation of alternate blocking techniques, and the use of alternate membranes may also potentially provide improvement and will be explored. Particle aggregation could potentially lead to loss of sensitivity, loss of reproducibility and robustness and remains a definite area for further investigation.

Of potential interest is the quantifiability provided by the microspheres, which may provide opportunities in diagnostics where quantification is important, such as monitoring clearance of disease (companion diagnostics).

The results obtained from this study illustrate the suitability of the polymer microspheres as detector particles in lateral flow assays. Further microspheres engineering is required to improve the performance of the assay, however promising results were obtained regarding stability which could potentially benefit current lateral flow assays. Proof-of-concept has been established and can potentially be extended to a multitude of lateral flow diagnostics. Lateral flow immuno-chromatographic assays provide a relatively low cost and accurate means of diagnosing disease at point-of-care, where the high mortality of malaria and the possible benefit of improved and multiplex diagnosis can have a positive impact on malaria management.

CHAPTER 5

LATERAL FLOW IMMUNOASSAY: MALARIA

5.1. INTRODUCTION

The early symptoms of malaria include headache, fever, weakness, chills, abdominal pain, diarrhoea, nausea, vomiting and anorexia (Tangpukdee *et al.*, 2009). In tropical and sub-tropical regions, several diseases exist with symptoms that resemble malaria and this often leads to incorrect diagnosis, which is a major contributor to malaria mortality (Bell *et al.*, 2006; Ly *et al.*, 2010; Murray *et al.*, 2008). In addition to late diagnosis of malaria, a major drawback of incorrect diagnosis is the subsequent rise of drug resistant parasites (Kokwaro, 2009).

The World Health Organisation has provided strict stipulations for rapid diagnostic tests and include the capability to: 1) detect and distinguish between all *Plasmodium* species with a sensitivity of at least 100 parasites. μl^{-1} of blood; 2) to distinguish between viable (active) and non-viable (previous infection) parasites; 3) provide very few false-positives; 4) provide no false-negatives; 5) be rapid (<20 minutes), equipment free, portable, robust, simple to operate and affordable to acquire and maintain (Gascoyne *et al.*, 2004; Moody, 2002; Urdea *et al.*, 2006; WHO, 2000). Additional ideal diagnostic capabilities include quantitative/semi-quantitative information measurements to allow drug therapy to be monitored, the identification and incorporation of target putative markers that can detect complications such as resistance, and detect multiple diseases, as well as a colour strip on the packaging to monitor heat exposure and thus indicate the reliability of the test (WHO, 2009).

It is evident from the literature review that, of the numerous diagnostic techniques available, few are suited for true point-of-care diagnostics for field use in developing countries. Microscopy is considered the “gold standard” for malaria diagnosis, however this technique is labour-intensive, time consuming and highly dependent on the interpretation skill and experience of the staff examining the slide (Bell *et al.*, 2006; Makler *et al.*, 1998; Moody, 2002; Murray *et al.*, 2008; Wongsrichanalai *et al.*, 2007). In resource-poor areas where financial constraints may prevent the purchasing of even regular microscopes, the use of more expensive fluorescent microscopes in these areas is less feasible (Makler *et al.*, 1998). Although PCR-based molecular diagnostics, microarrays, flow cytometry, mass spectrometry and enzyme immunoassays have various advantages for diagnostics, including the ability to process high sample volumes, these techniques are impractical in developing countries given that they are labour intensive, expensive, involve multiple sample processing steps and require

a “clean room”, specialised equipment, electricity and trained personnel (Makler *et al.*, 1998; Tangpukdee *et al.*, 2009).

Antigen-based tests have been developed that allow for the rapid and accurate detection of various malaria species, including *P. falciparum*, *P. ovale*, *P. malariae*, *P. vivax* and *P. knowlesi*, by capturing parasite specific antigens present in blood (Kakkilaya, 2003; Ly *et al.*, 2010; Tangpukdee *et al.*, 2009). These rapid diagnostic tests are available in different formats, from dipsticks and cards to cassettes, pads, wells and strips (Kakkilaya, 2003). Lateral flow immunochromatographic assays arguably provide the most suitable format for point-of-care application and embody an amalgamation of different technologies that provide a relatively low cost and accurate means of diagnosing diseases (Bell *et al.*, 2006). However, this technology has several limitations including lack of sensitivity and stability which needs to be addressed (refer to section 1.8.6, table 1.1).

In 2009, the World Health Organisation evaluated the performance of several commercially available malaria lateral flow diagnostic devices, revealing numerous limitations regarding the sensitivity and specificity of these lateral flow diagnostic assays (Murray *et al.*, 2008; WHO, 2009; Wongsrichanalai *et al.*, 2007) highlighting the need for more sensitive diagnostic devices. Malaria lateral flow diagnostic tests currently have a lower detection limit of 100 *Plasmodium spp* parasites. μl^{-1} of blood, which translates to a parasitemia of 0.002%, approximating to 500 million parasites per infected individual (Vigário *et al.*, 2001). Consequently, lateral flow diagnostic tests for malaria are currently only relevant for febrile detection, at which point clinical symptoms and illness have already set in, reducing the productivity of the infected individual as well as the efficacy of anti-malarial treatment (Bahk *et al.*, 2010).

The development of rapid diagnostic tests for use in areas with little or no infrastructure have several technical challenges to overcome (highlighted in Chapter 1), including lack of clean water, electricity and cold storage facilities (Urdea *et al.*, 2006). These challenges make e.g. lateral flow diagnostic tests, the preferred solution for diagnostics in resource constrained settings (Makler *et al.*, 1998). The management of malaria in developing countries is set to improve substantially if the disease can be diagnosed accurately and treated accordingly. For this to become reality, the point-of-care diagnostic techniques need to be critically reviewed, improved, and efficiently deployed. The development of improved point-of-care diagnostic devices, suitable for early malaria detection, while remaining cost effective and simple to use, is of high priority for disease management in malaria endemic countries. This chapter aims to evaluate the prototype polymer microspheres for detection of malaria antigens, illustrating

suitability for multiplex detection and compatibility of the diagnostic detection reagents for the highly specific detection of a range of antigens.

5.2. MATERIALS AND METHODS

5.2.1. Materials

All reagents were supplied by Sigma Aldrich (Germany) unless otherwise stated. Antibodies for the control line (polyclonal goat anti-mouse IgG), test line 1 (monoclonal mouse anti-HRP2 IgM, clone 5) and test line 2 (monoclonal anti-pLDH IgG2b, clone 21), as well as the monoclonal antibodies (monoclonal mouse anti-HRP2 IgG, clone 4 and monoclonal mouse anti-pLDH IgG, clone 23) required for conjugation to the microspheres were purchased from Arista Biologicals (United States). Anti-HRP2-conjugated colloidal gold was further purchased from Arista Biologicals. Colloidal gold (40 nm) was purchased from British BioCell International (BBI, UK). HRP2 antigen ($0.33 \mu\text{g}.\mu\text{l}^{-1}$) was supplied by the National Bioproducts Institute (NBI, South Africa) and pLDH antigen ($0.42 \mu\text{g}.\mu\text{l}^{-1}$) was supplied by the University of Cape Town. Ultra-pure water from the MilliQ system (Millipore) was autoclaved and used for all experiments. Centrifugation was performed using a Beckman-Coulter microfuge 18 at room temperature (25°C) at $2000 \times g$ for 5 minutes. The end-over-end mixing/incubation steps were performed at 4°C on an ELMI Intellimixer set on program F1 and 15 rpm, 180° rotation. All lateral flow assay experiments were set-up in a microwell format, where buffer (100 μl) and detector reagent (10 μl) were pre-mixed in a well of a microwell plate, unless otherwise stated, and the membrane subsequently placed within the solution (Figure 4.3). The standard protocols for colloidal gold, as stipulated by the Diagnostics Consulting Network, have been followed where colloidal gold was used as a label.

5.2.2. Antibody striping to nitrocellulose membrane

Control and test line antibodies ($1 \text{ mg}.\text{ml}^{-1}$ in PBS, 1% sucrose) were striped onto CN-95 nitrocellulose membranes (Unisart) as described in Chapter 4 (4.2.3). Three sets of nitrocellulose membranes were striped, each containing the anti-mouse IgG antibody at the control line, and either anti-HRP2 IgM or anti-pLDH IgG at the test line, subsequently referred to as HRP-striped or pLDH-striped. The multiplex-striped nitrocellulose membranes contained anti-mouse IgG at the control line, anti-HRP2 IgM at test line 1 and anti-pLDH IgG at the test line 2 (Figure 5.1).

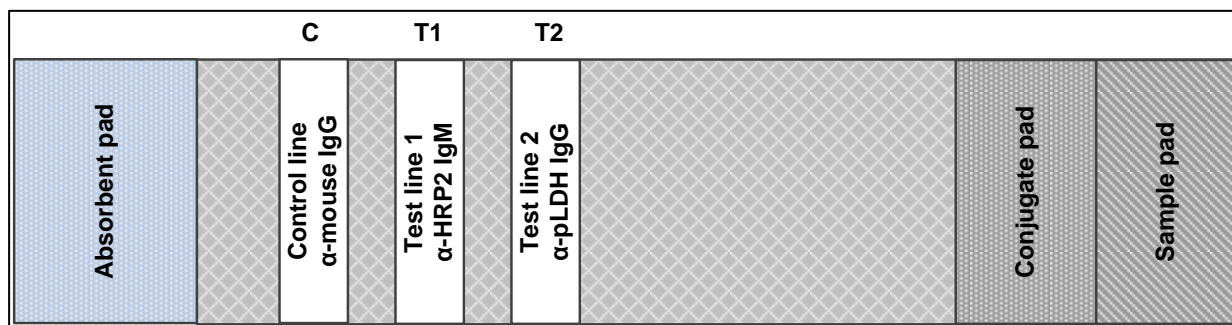


Figure 5.1: Schematic of the multiplex antibody striping on nitrocellulose membrane for lateral flow.

5.2.3. Antibody conjugation to microspheres (HRP2 and pLDH)

Epoxide-functionalised polymer microspheres were synthesised and dyed as described in Chapter 4 (4.2.2) after which 200 µg anti-HRP2 and anti-pLDH antibodies were conjugated to 1 ml (2.7 mg) red microspheres (anti-HRP2-conjugated-microspheres) and blue microspheres (anti-pLDH-conjugated-microspheres) respectively, the microspheres were finished with casein and sonicated as described in Chapter 4 (4.2.2). The quantity of antibodies bound to the microspheres was determined using the BCA method as described in Chapter 3 (3.2.3).

5.2.4. Lateral flow reagents

The compatibility of the lateral flow running buffer (PBS, 0.1% Tween20, 1% casein) identified in Chapter 4 was evaluated with red anti-HRP2-conjugated-microspheres and blue anti-pLDH-conjugated-microspheres respectively. A lateral flow assay was set up using 100 µl running buffer and 10 µl casein-finished negative control microspheres (no antibody) and experimental microspheres (anti-HRP2-conjugated and anti-pLDH-conjugated) on HRP2-striped or pLDH-striped nitrocellulose lateral flow membranes.

The assay specificity was evaluated for the lateral flow using both red anti-HRP2-conjugated-microspheres and blue anti-pLDH-conjugated-microspheres in running buffer (PBS, 0.1% Tween20, 1% casein), running buffer supplemented with HRP2 antigen (10 ng.µl⁻¹) and pLDH antigen (10 ng.µl⁻¹).

5.2.5. Multiplex lateral flow assay

The preparation of a multiplex lateral flow assay was explored using the multiplex-striped nitrocellulose membrane and mixing the red anti-HRP2-conjugated-microspheres and the blue anti-pLDH-conjugated-microspheres in a single lateral flow reaction using buffer (PBS, 0.1% Tween20, 1% casein) with and without antigens (10 ng.µl⁻¹).

5.2.6. Anti-HRP2-conjugated-colloidal gold: “Gold” standard

BSA-finished colloidal gold (negative control) was prepared as described in Chapter 4 (4.2.6) and anti-HRP2-conjugated-colloidal gold was used as supplied. The lateral flow assay control was set up using 10 μl of negative control colloidal gold nanoparticles and anti-HRP2-conjugated-colloidal gold nanoparticles in colloidal gold running buffer (0.1 M Tris, pH 8, 0.1% Tween20, 0.1% BSA) and sample buffer (running buffer supplemented with HRP2 antigen, 10 $\text{ng}\cdot\mu\text{l}^{-1}$). The specificity was evaluated by running 10 μl anti-HRP2-conjugated-colloidal gold in 100 μl running buffer supplemented with the correct and incorrect antigen (10 $\text{ng}\cdot\mu\text{l}^{-1}$) of HRP2 and pLDH respectively.

5.2.7. Microspheres and colloidal gold comparison

The anti-HRP2-conjugated-microspheres were evaluated against the standard anti-HRP2-colloidal gold nanoparticles with respect to sensitivity and stability. Anti-pLDH conjugated microspheres were evaluated alongside the anti-HRP2-conjugated-microspheres.

The sensitivity of the anti-HRP2-conjugated-microspheres, anti-HRP2-conjugated-colloidal gold nanoparticles and anti-pLDH-conjugated-microspheres was evaluated by decreasing the concentration of antigen (HRP2 or pLDH) in the sample buffers as described in Chapter 4 (4.2.7).

The stability of the microspheres and nanoparticles was evaluated by analysing the lateral flow efficiency of detection after incubation of the antibody conjugated particle suspensions at elevated temperatures from 50 to 70°C for 1, 3 and 6 hours, as described in Chapter 4 (4.2.7).

5.3. RESULTS AND DISCUSSION

5.3.1. Antibody conjugation to microspheres

The quantity of anti-HRP2 and anti-pLDH antibody conjugated to red and blue microspheres was quantified using the BCA method with standard curves calculated using the equation of each respective antibody (anti-HRP2: R^2 value of 0.9992, equation $y = 0.0178x - 0.0154$; anti-pLDH: R^2 value of 0.9985 equation, $y = 0.0206x - 0.0056$). The red and blue polymer microspheres bound almost all measurable protein content (95.04 % and 94.43 % for anti-HRP2 and anti-pLDH antibodies respectively).

5.3.2. Lateral flow buffers

The compatibility and specificity of the lateral flow running buffer was explored with negative control (unconjugated, casein finished) and experimental (anti-HRP2-conjugated and anti-pLDH-conjugated) microspheres (Figure 5.2).

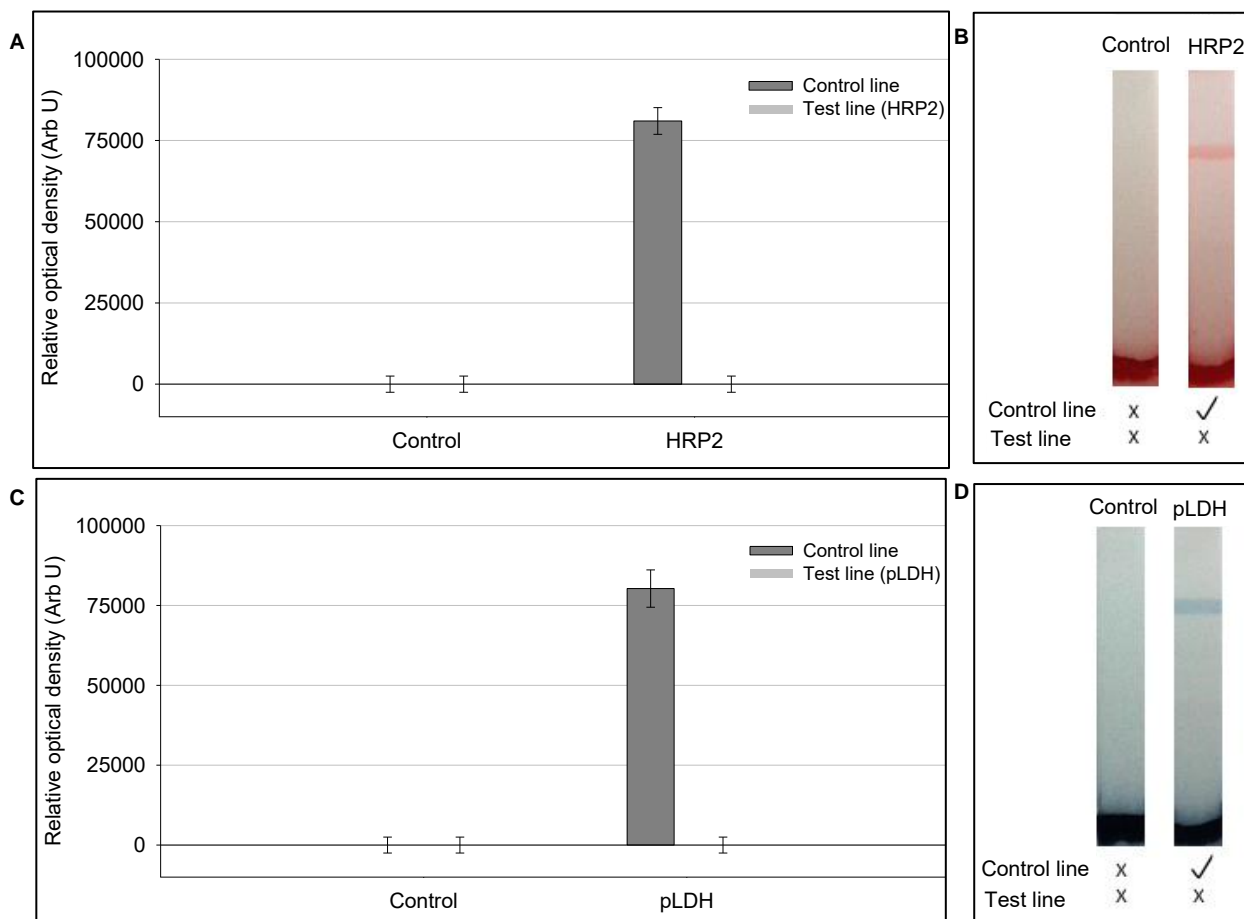


Figure 5.2: Lateral flow of control and positive (anti-HRP2-conjugated and anti-pLDH-conjugated) microspheres in running buffer. **A:** Quantified results and **B,** representative lateral flow image for HRP2-microspheres with control line above the test line and **C:** Quantified results and **D,** lateral flow image for pLDH-microspheres with control line above the test line. Error bars represent standard deviation of triplicate lateral flow experimental sets.

No signal was detected at either the test or control line with the negative control microspheres in running buffer while a visible signal was observed at the control line for both anti-HRP2- and anti-pLDH conjugated microspheres. The control line signal of ~ 80 000 remains consistent across lateral flow test strips indicating good experimental reproducibility. No non-specific binding was observed, indicating compatibility of the running buffer for both antibodies and microsphere preparations.

The specificity of the lateral flow assay was determined individually for running buffer (no antigen) and sample buffer (containing the corresponding antigen) on both the anti-pLDH and anti-HRP2 striped membranes (Figure 5.3 – HRP2 and Figure 5.4 - pLDH).

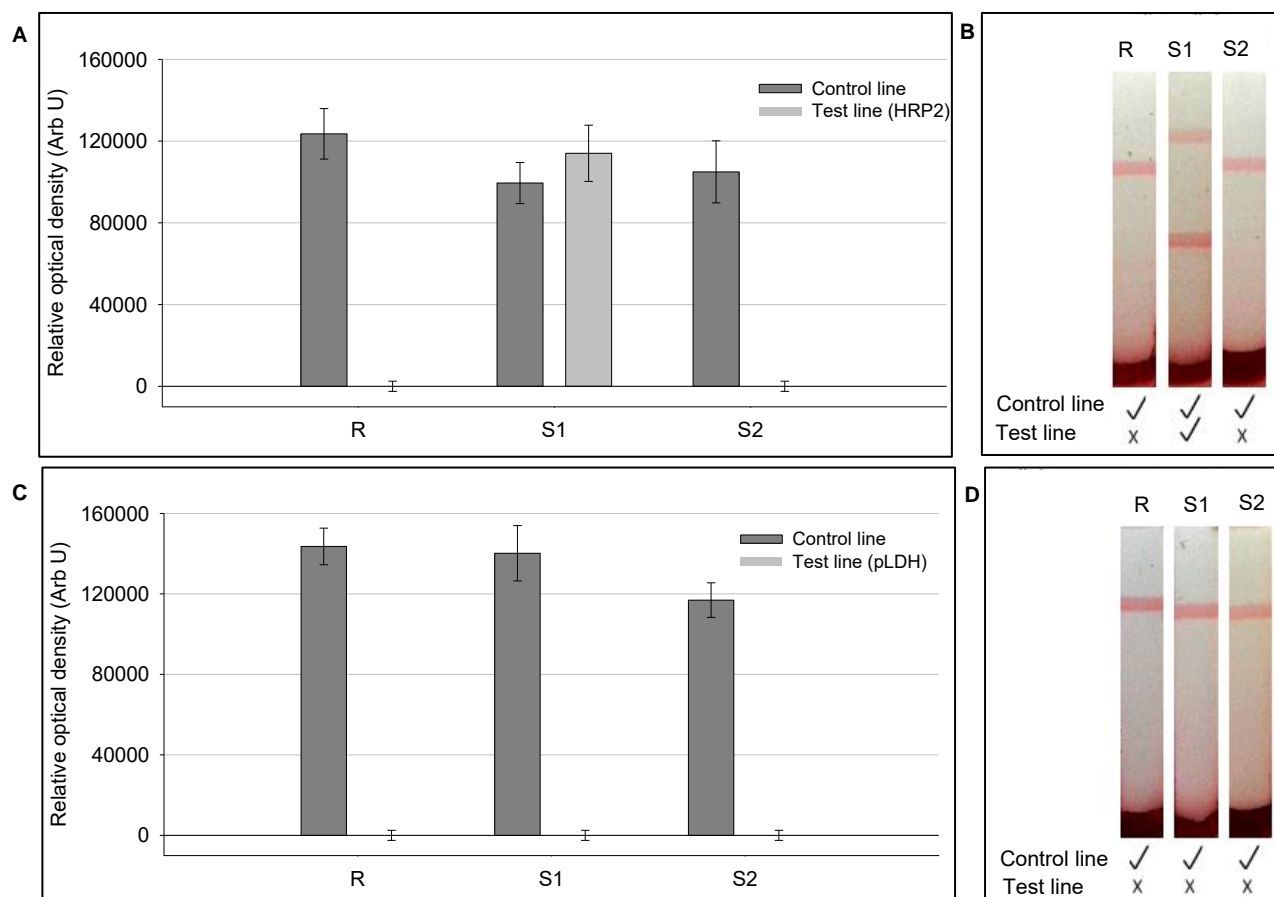


Figure 5.3: Specificity of anti-HRP2-conjugated-microspheres in running buffer (R) and running buffer supplemented with HRP2 antigen (S1) or pLDH antigen (S2). **A:** Quantified results and **B,** representative lateral flow image on anti-HRP2-stripped membrane with control line above the test line, **C:** Quantified results and **D,** representative lateral flow image on anti-pLDH striped membrane with control line above the test line. Error bars represent standard deviation of triplicate lateral flow experimental sets.

The results indicated no antibody cross-reactivity. Briefly, for the anti-HRP2-stripped membranes a signal was observed at the control line with the antigen free running buffer with no non-specific binding observed at the test line; whereas in the sample buffer containing the HRP2 antigen (S1) a signal was observed at both the control and test line indicating a positive result as anticipated. The controls with sample buffer containing pLDH antigen (S2) on the anti-pLDH-stripped membranes indicated no antibody cross-reactivity. Similar results were obtained for the anti-pLDH microspheres (Figure 5.4), indicating no non-specific interaction and alluding to their potential application in a multiplex lateral flow format.

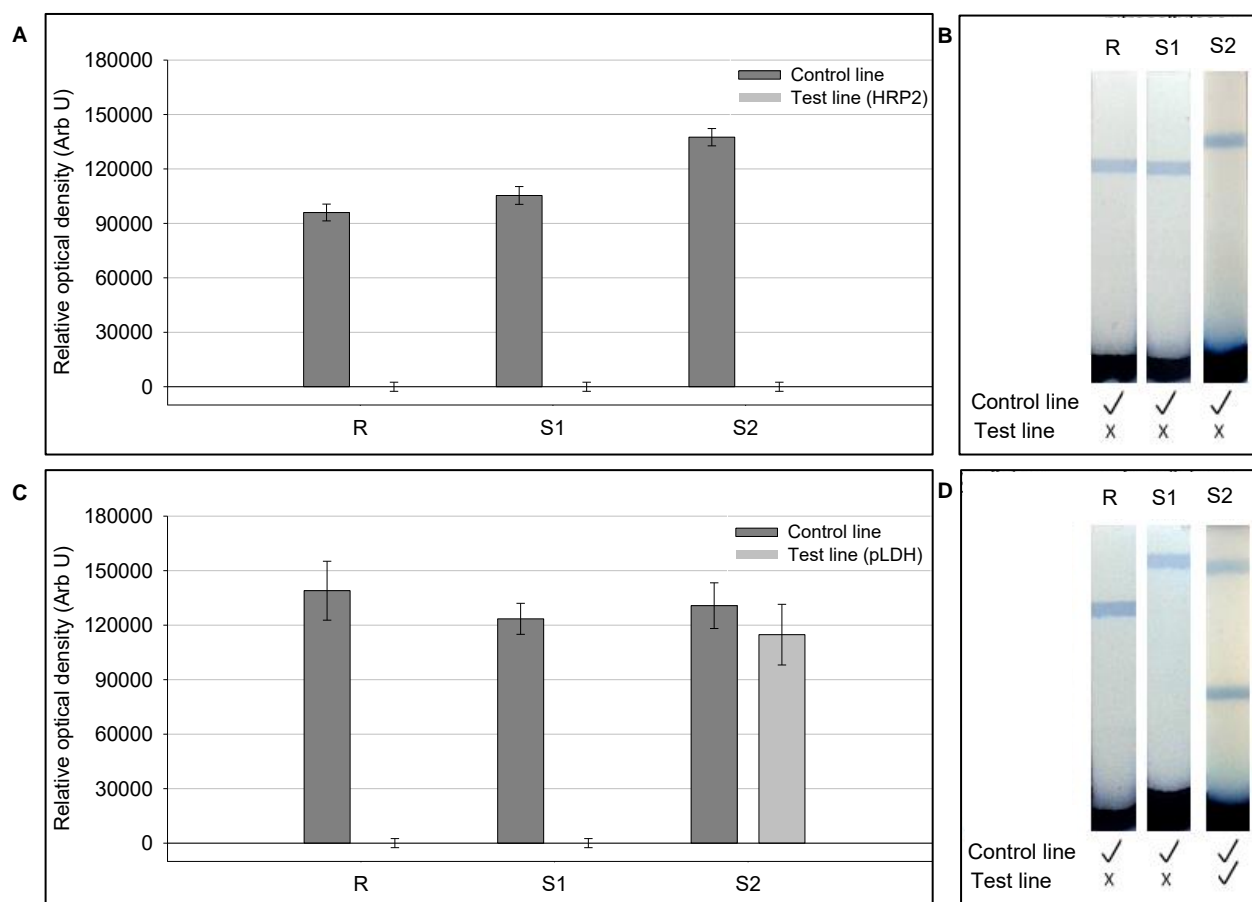


Figure 5.4: Specificity of anti-pLDH-conjugated-microspheres in running buffer (R), and running buffer supplemented with HRP2 antigen (S1) or pLDH antigen (S2). **A:** Quantified results and **B,** representative lateral flow image on anti-HRP-stripped membrane with control line above the test line, **C:** Quantified results and **D,** representative lateral flow image on anti-pLDH striped membrane with control line above the test line. Error bars represent standard deviation of triplicate lateral flow experimental sets.

5.3.3. Lateral flow detection sensitivity

The lowest limit of antigen detection (sensitivity) for anti-HRP2-conjugated-microspheres and anti-pLDH-conjugated-microspheres was explored using a lateral flow assay in microwell format with decreasing quantities of antigen in sample buffer (Figure 5.5 – HRP2 and Figure 5.6 - pLDH).

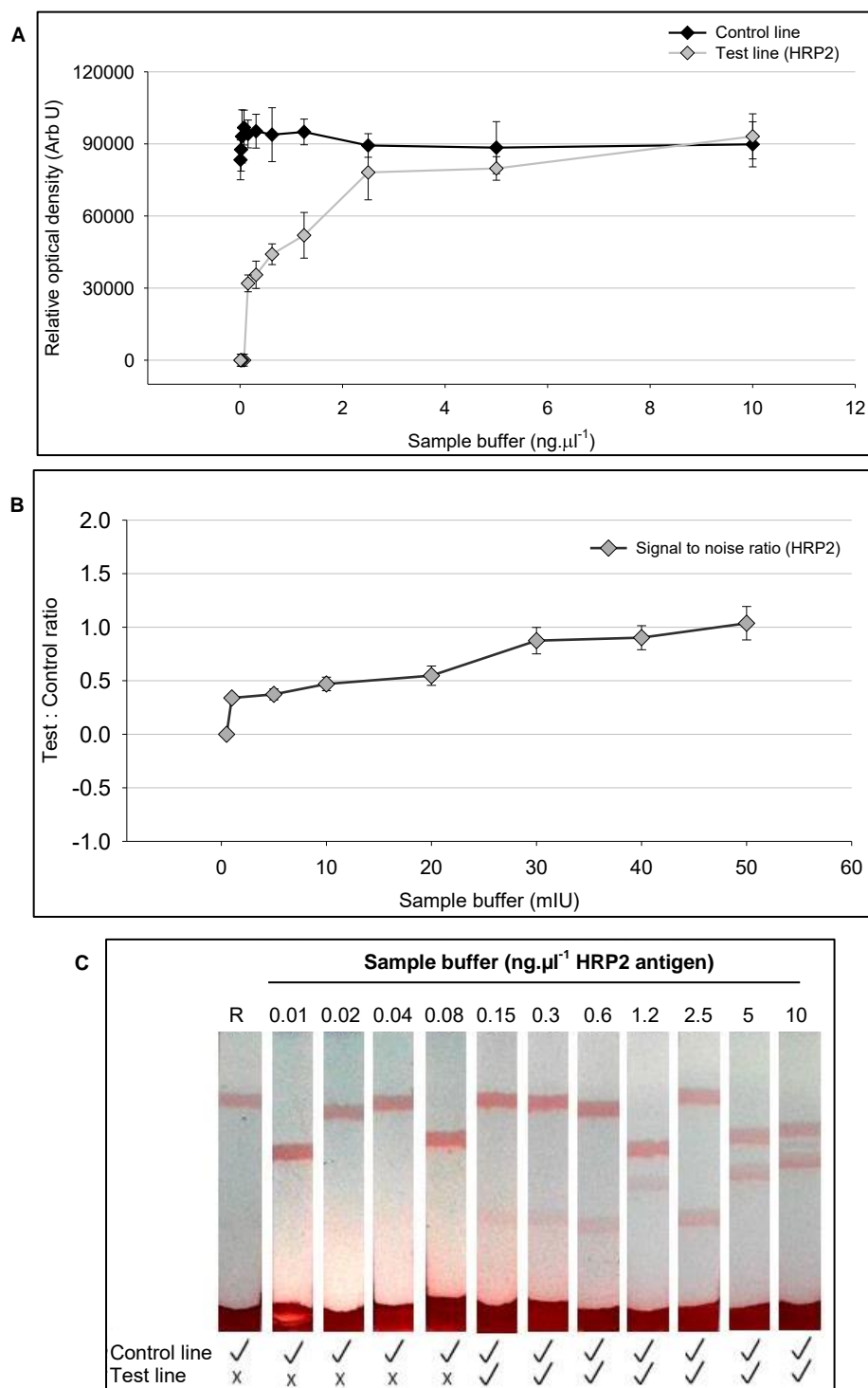


Figure 5.5: Lateral flow to determine the lowest limit of detection of HRP2 using a lateral flow assay in microwell format. **A:** Quantified results, **B:** signal to noise ratio depicting lower limit of detection, **C:** Representative lateral flow image with control line above the test line (HRP2). Error bars represent standard deviation of triplicate lateral flow experimental sets.

The nitrocellulose membranes were striped in several batches and although batch to batch variation in signal intensity was not observed, there was variability in the positioning of the control and test lines, as can be observed in Figure 5.5 and subsequent figures. According to densitometry and visual analysis, the control line intensities remained constant and clearly visually detectable across all sample dilutions while the test line intensity gradually decreased

below $2.5 \text{ ng.}\mu\text{l}^{-1}$ antigen present in the sample buffer with a distinct reduction in the test line intensity from $1.2 \text{ ng.}\mu\text{l}^{-1}$ (visual limit of detection) downwards. However, lower concentrations of antigen down to $0.15 \text{ ng.}\mu\text{l}^{-1}$ were still detectable by densitometry.

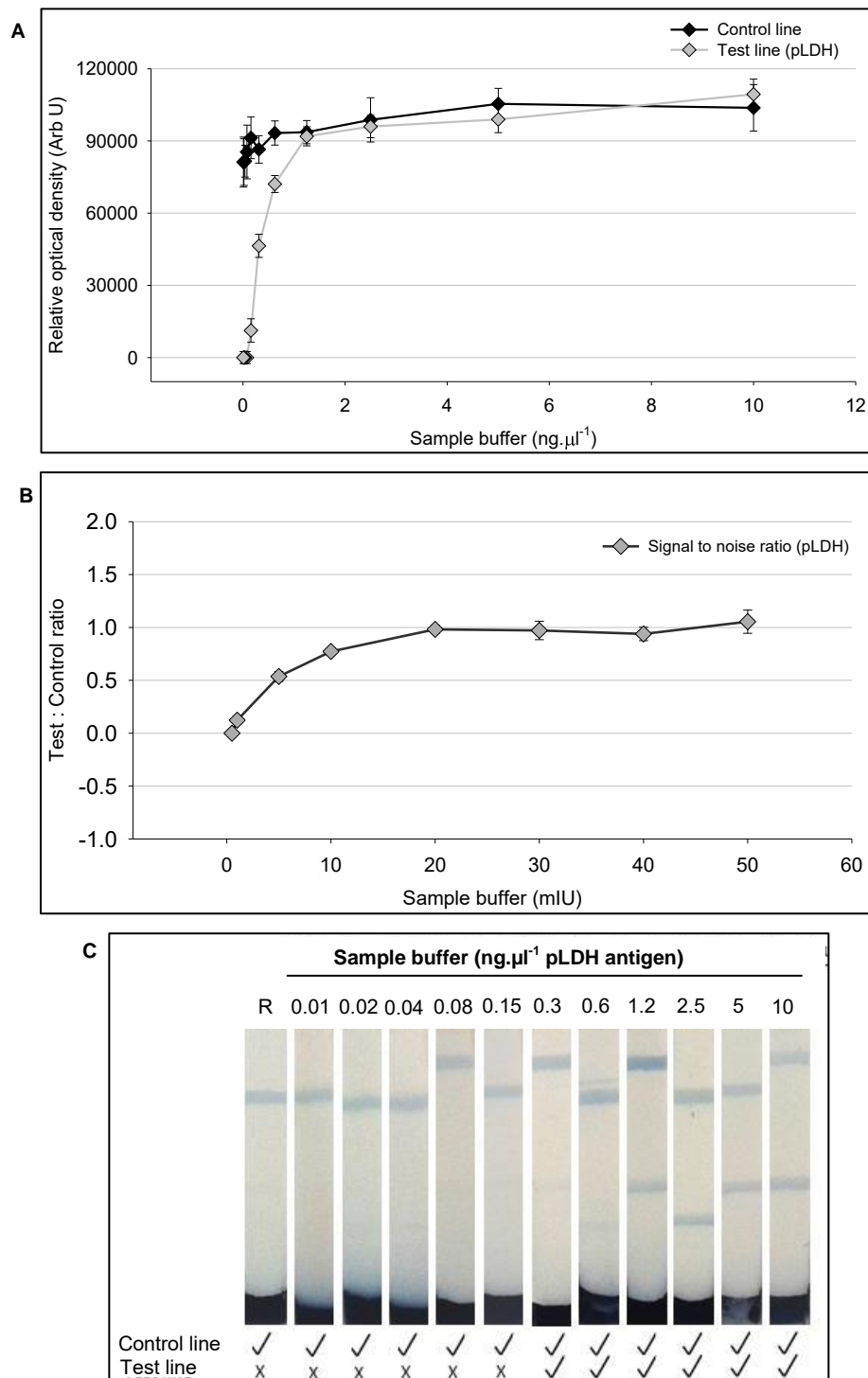


Figure 5.6: Lateral flow to determine the lowest limit of detection of pLDH using a lateral flow assay in microwell format. **A:** Quantified results, **B:** signal to noise ratio depicting lower limit of detection, **C:** Representative lateral flow image with control line above the test line (pLDH). Error bars represent standard deviation of triplicate lateral flow experimental sets.

The densitometry analysis and visual analysis reveal stable control line signals that remained relatively constant across all sample dilutions while the test line intensity gradually reduced with $1.2 \text{ ng.}\mu\text{l}^{-1}$ antigen concentration potentially being the lowest limit of visual detection. However, similar to that of HRP2, the lowest quantifiable concentration of antigen was considered to be $0.15 \text{ ng.}\mu\text{l}^{-1}$ antigen which was detectable by densitometry. The control line intensity remained consistent (90 000 – 100 000) across lateral flow strips, irrespective of the antigen being detected, which suggests good experimental reproducibility.

5.3.4. Antibody stability

The performance of anti-HRP2-conjugated-microspheres and anti-pLDH-conjugated-microspheres were evaluated after exposure to elevated temperatures. The accelerated denaturation results are presented in Figure 5.7 (HRP2 antigen) and Figure 5.8 (pLDH antigen)

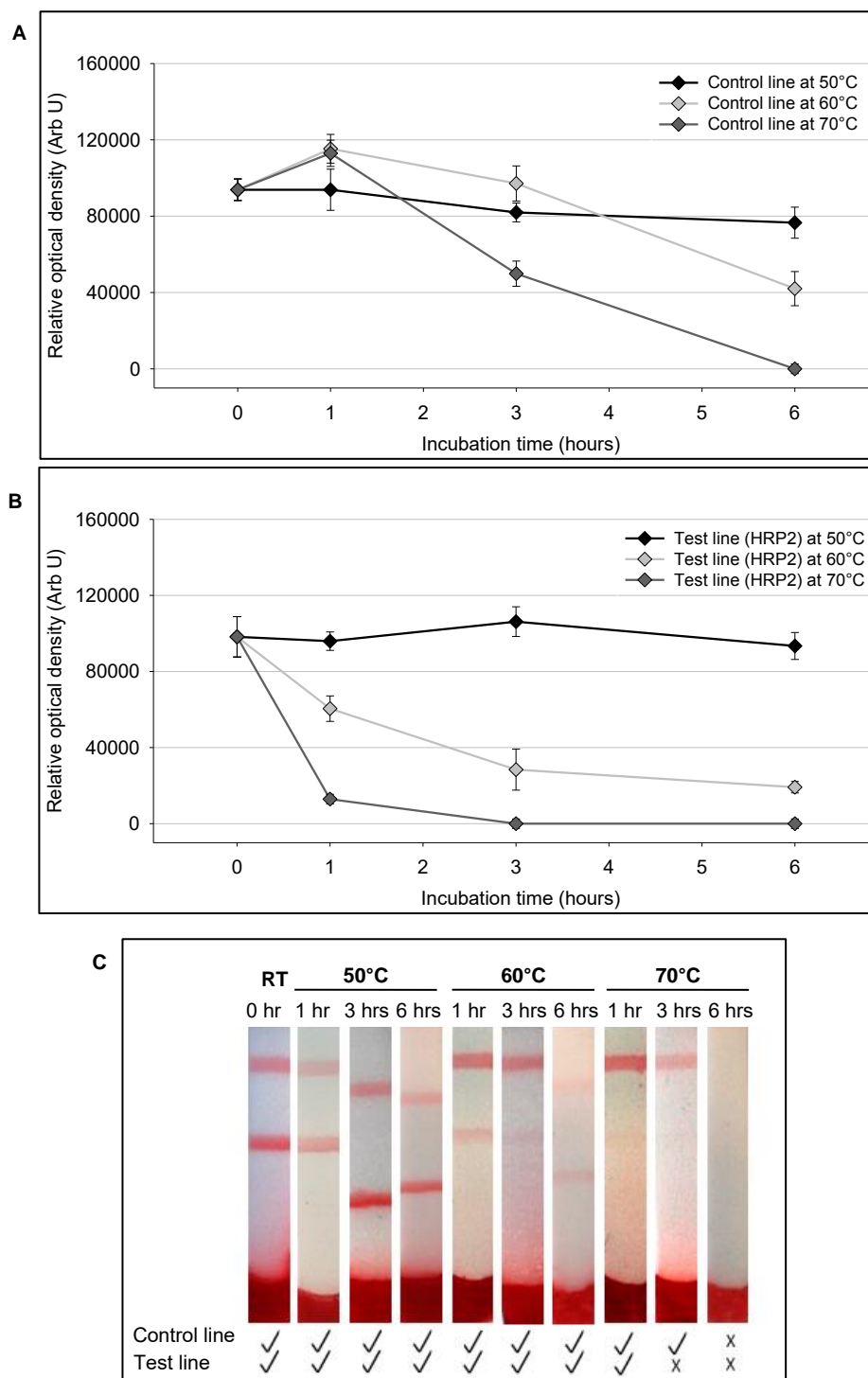


Figure 5.7: Stability of anti-HRP2-conjugated-microspheres incubated from 1 to 6 hours at 50°C, 60°C and 70°C. **A** and **B**: Quantified results, **C**: is the comparative lateral flow image with control line above the test line (HRP2). Error bars represent standard deviation of triplicate lateral flow experimental sets.

According to densitometry and visual analysis, the control line and test line intensities remained relatively constant at 50°C, 6 hour incubation. Incubation at 60°C resulted in stable control line signals for up to 3 hours incubation after which there was a distinct reduction in control line signal at 6 hours of incubation, while the test line signal gradually reduced with increasing incubation time (1, 3 and 6 hours). Incubation at 70°C for 1 hour resulted in visible

control and test lines, while 3 hours incubation was detrimental to test line development, resulting in a strong control line signal only. Similar to observations for hCG, longer incubation (6 hours) was detrimental to both control and test line development.

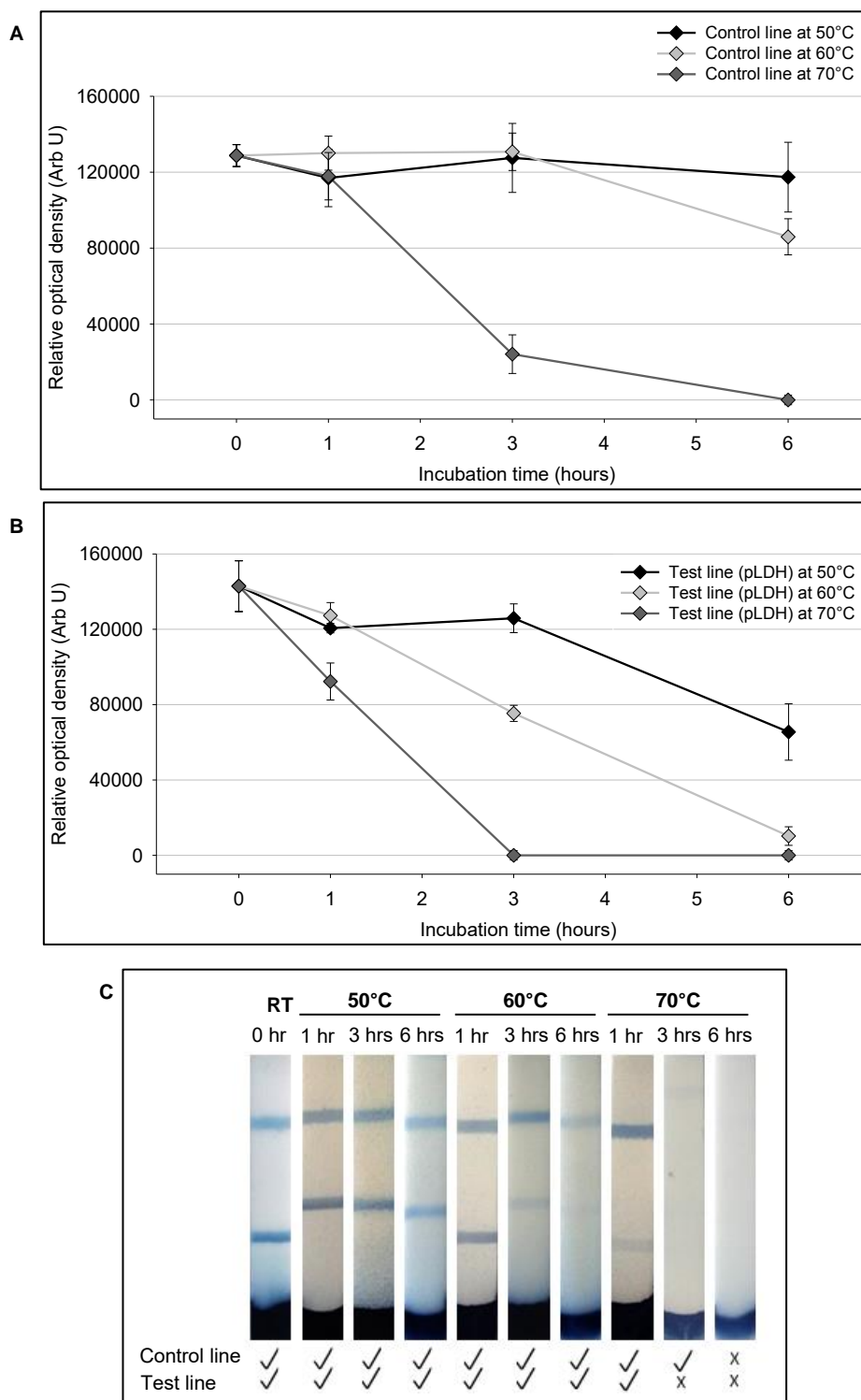


Figure 5.8: Stability of anti-pLDH-conjugated-microspheres incubated from 1 to 6 hours at 50°C, 60°C and 70°C. **A** and **B**: Quantified results, **C**: is the comparative lateral flow image with control line above the test line (pLDH). Error bars represent standard deviation of triplicate lateral flow experimental sets.

The densitometry and visual analysis of the anti-pLDH-conjugated-microspheres at 50°C reveal similar control and test line intensities for up to 3 hours incubation with a distinct

reduction in test line intensity at 6 hours incubation. Incubation at 60°C resulted in relatively similar control line signals for up to 3 hours incubation after which there was a distinct reduction with 6 hours incubation. Test line signal was strong with 1 hour incubation at 60°C but reduced with increasing incubation time (3 hours) to be visually undetectable after 6 hours incubation. Incubation at 70°C for 1 hour resulted in visible control and test lines (albeit faint), while longer incubation times (3 and 6 hours) were detrimental to both control and test line development. Comparative analysis of HRP2 and pLDH indicates that pLDH is slightly less stable than HRP2 and would be the limiting factor for the development of a stable multiplex lateral flow assay.

5.3.5. Multiplex lateral flow

A potential advantage of having a variety of coloured detection reagents for lateral flow is allowing for simple interpretation of multiplex lateral flow devices (Wong *et al.*, 2009). The advantage of using microspheres labelled with primary colours red and blue is the potential of creating a third discernible colour at the control line that indicates the test is working for both antibodies, and the possibility to discern what indeed is potentially wrong with the diagnostic assay.

The suitability for a multiplex lateral flow assay was evaluated using a combination of the microspheres on nitrocellulose striped with both test lines (and controls) in sample buffer containing both HRP2 and pLDH antigens. The results are presented in Figure 5.9.

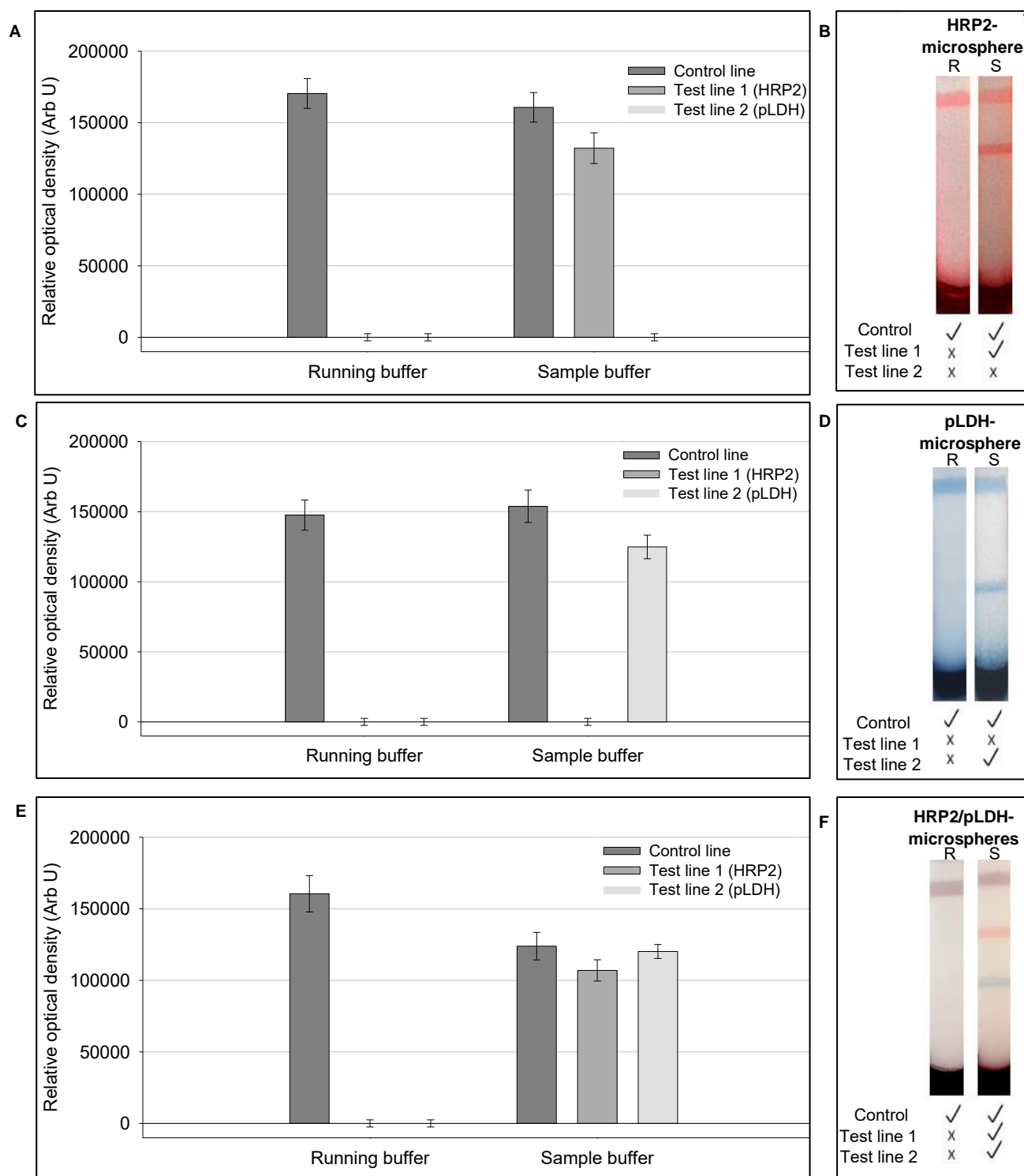


Figure 5.9: Multiplex lateral flow with both anti-HRP2-conjugated-microspheres and anti-pLDH-conjugated-microspheres in running (R) and sample (S) buffer on multiplex-striped nitrocellulose. **A:** Quantified results and **B**, representative lateral flow image of HRP2-microspheres with control line above test line 1 in the middle (HRP2) and test line 2 (pLDH) below test line 1, **C:** Quantified results and **D**, representative lateral flow image of pLDH-microspheres with control line above test line 1 (HRP2) in the middle and test line 2 (pLDH) below test line 1, **E:** Quantified results and representative lateral flow image **F**, of anti-HRP2-microspheres and anti-pLDH-microspheres with control line above test line 1 (HRP2) in middle and test line 2 (pLDH) below test line 1. Error bars represent standard deviation of triplicate lateral flow experimental sets.

Briefly, no non-specificity of the microspheres was observed across antigens, while the results at the test-lines corresponded to the presence of the antigens in the running buffer as expected. No cross reactivity of antibodies was observed for HRP2 or pLDH detection.

5.3.6. Colloidal gold comparison

The performance of the anti-HRP2-conjugated-microspheres was compared to the performance of the standard anti-HRP2-conjugated colloidal gold nanoparticles. A lateral flow assay with negative control colloidal gold (BSA finished) and anti-HRP2-conjugated-colloidal gold was set up in colloidal gold based running buffer (no antigen) and sample buffer (inclusive of antigen; Figure 5.10).

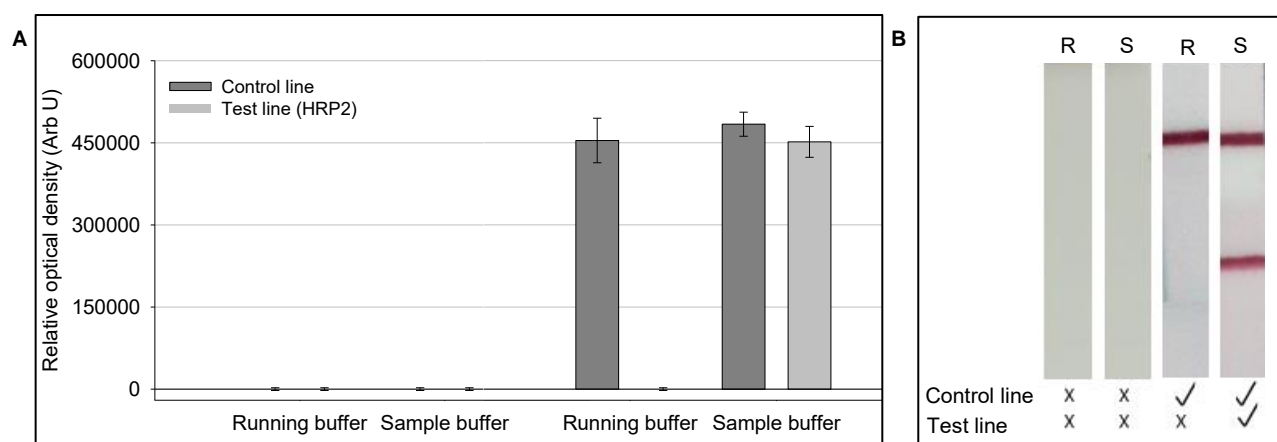


Figure 5.10: Lateral flow of negative control and positive (HRP2) colloidal gold nanoparticles in running (R) and sample (S) buffer. **A:** Quantified results, **B:** Representative lateral flow image with control line above the test line (HRP2). Error bars represent standard deviation of triplicate lateral flow experimental sets.

The densitometry and visual analysis resulted in no signal at either the test or control line for the negative control colloidal gold nanoparticles, in either buffer while the anti-HRP2-conjugated-colloidal gold nanoparticles resulted in a control line in the running buffer while sample buffer resulted in both control and test line development as expected.

The specificity of the lateral flow assay using anti-HRP2-conjugated-colloidal gold nanoparticles was determined individually for running buffer and sample buffer (containing the corresponding antigen on both the anti-HRP2-striped and anti-pLDH-striped membranes (Figure 5.11).

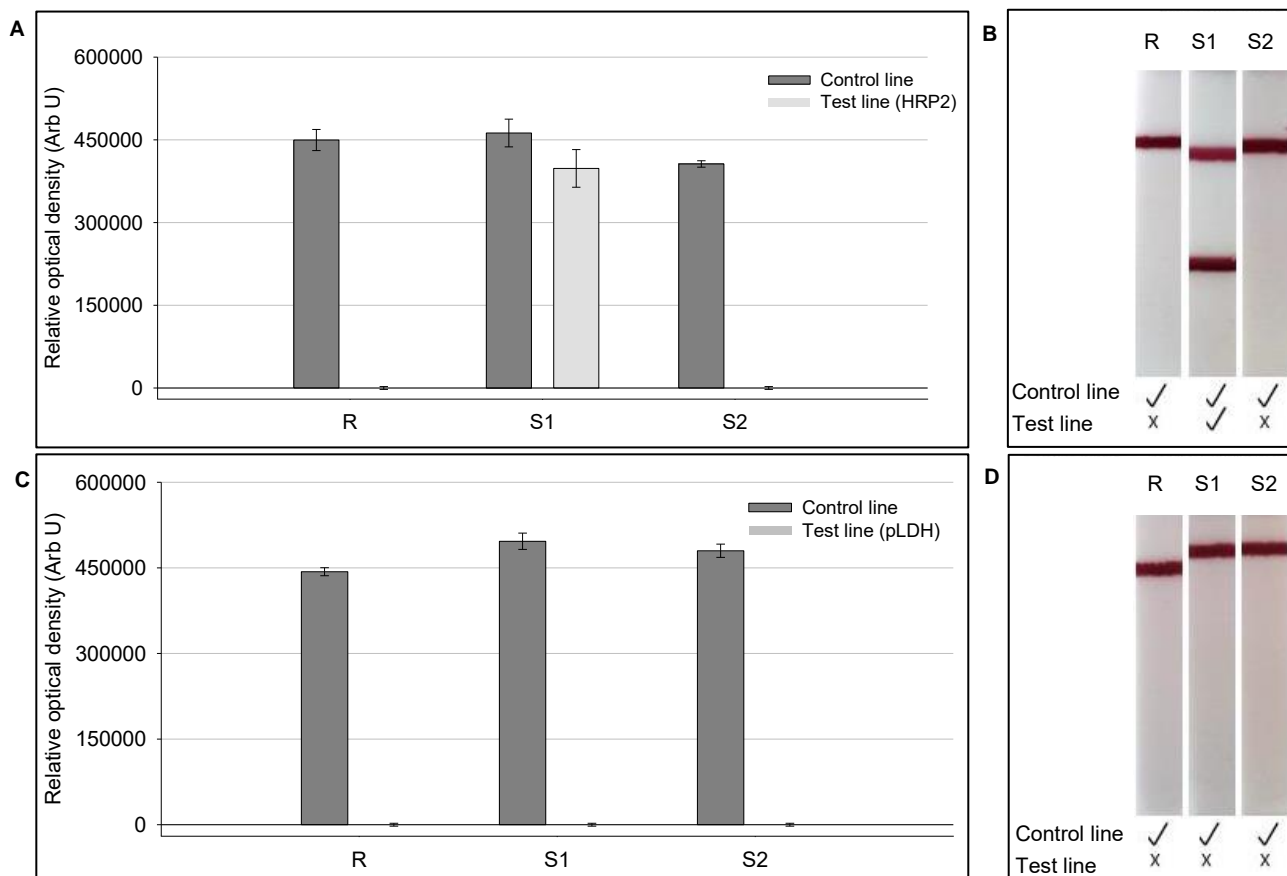


Figure 5.11: Specificity of anti-HRP2-conjugated-colloidal gold nanoparticles in running buffer (R) and running buffer supplemented with HRP2 antigen (S1) or pLDH antigen (S2). **A:** quantified results and **B,** representative lateral flow image on HRP2-stripped membrane with control line above test line, **C:** quantified results and **D,** representative lateral flow image on pLDH-stripped membrane with control line above test line. Error bars represent standard deviation of triplicate lateral flow experimental sets.

According to densitometry and visual results, no antibody cross-reactivity was observed. Briefly, for the anti-HRP2-stripped membranes a signal was observed at the control line with the antigen free running buffer with no non-specific binding at the test line; whereas in the sample buffer containing the HRP2 antigen (S1), a signal was observed at both the control and the test line indicating a positive result as anticipated. No antibody cross-reactivity was observed in controls with sample buffer containing pLDH as the antigen (S2) or on anti-pLDH-stripped membranes.

The lowest limit of antigen detection of the lateral flow assay using anti-HRP2-conjugated-colloidal gold nanoparticles was explored using sample buffer containing decreasing concentrations of HRP2 antigen for direct comparison to the sensitivity data for the polymer microspheres (Figure 5.12).

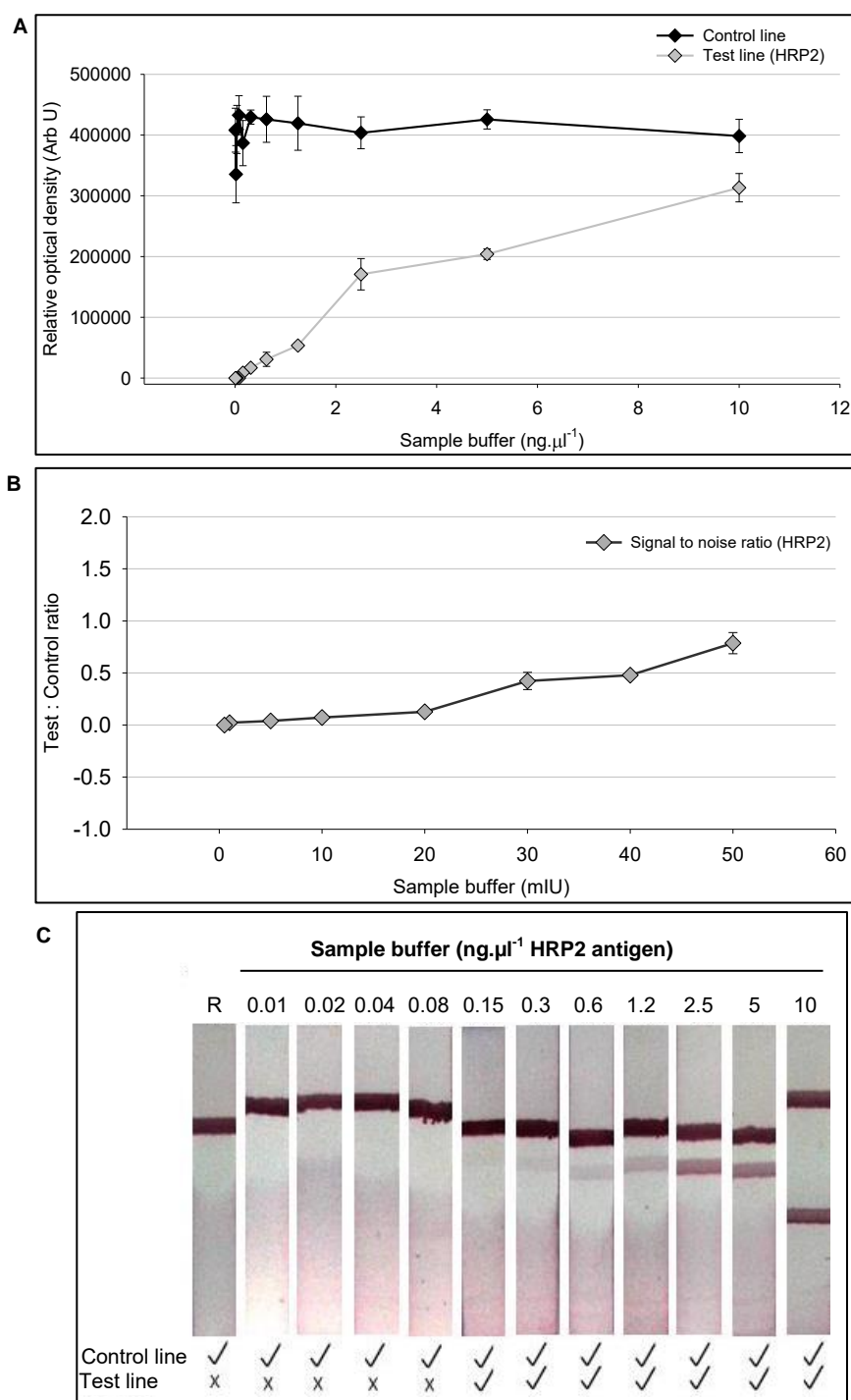


Figure 5.12: Lateral flow to determine the limit of antigen detection of HRP2-colloidal gold nanoparticles (standard). **A:** Quantified results, **B:** signal to noise ratio depicting lower limit of detection, **C:** Representative lateral flow image with control line above the test line (HRP2). Error bars represent standard deviation of triplicate lateral flow experimental sets.

The densitometry and visual analysis revealed that the control line signal intensity remained relatively constant irrespective of the amount of antigen in the sample buffer while there was a gradual reduction in test line intensity with increased sample dilution up to 2.5 ng.μl⁻¹, with a distinct reduction from 1.2 ng.μl⁻¹ antigen downwards, suggesting this as lower limit of detection. However, similar to densitometry analysis using the polymer microspheres, the signal was detectable down to 0.15 ng.μl⁻¹ antigen. The consistency of the control line intensity

(~450 000 arbitrary units) observed for colloidal gold, across the lateral flow strips, indicate good experimental reproducibility.

Accelerated decay at elevated temperatures was used to determine the stability of the anti-HRP2-conjugated-colloidal gold nanoparticles (Figure 5.13) for comparison to immobilised anti-HRP2 conjugated to the polymer microspheres.

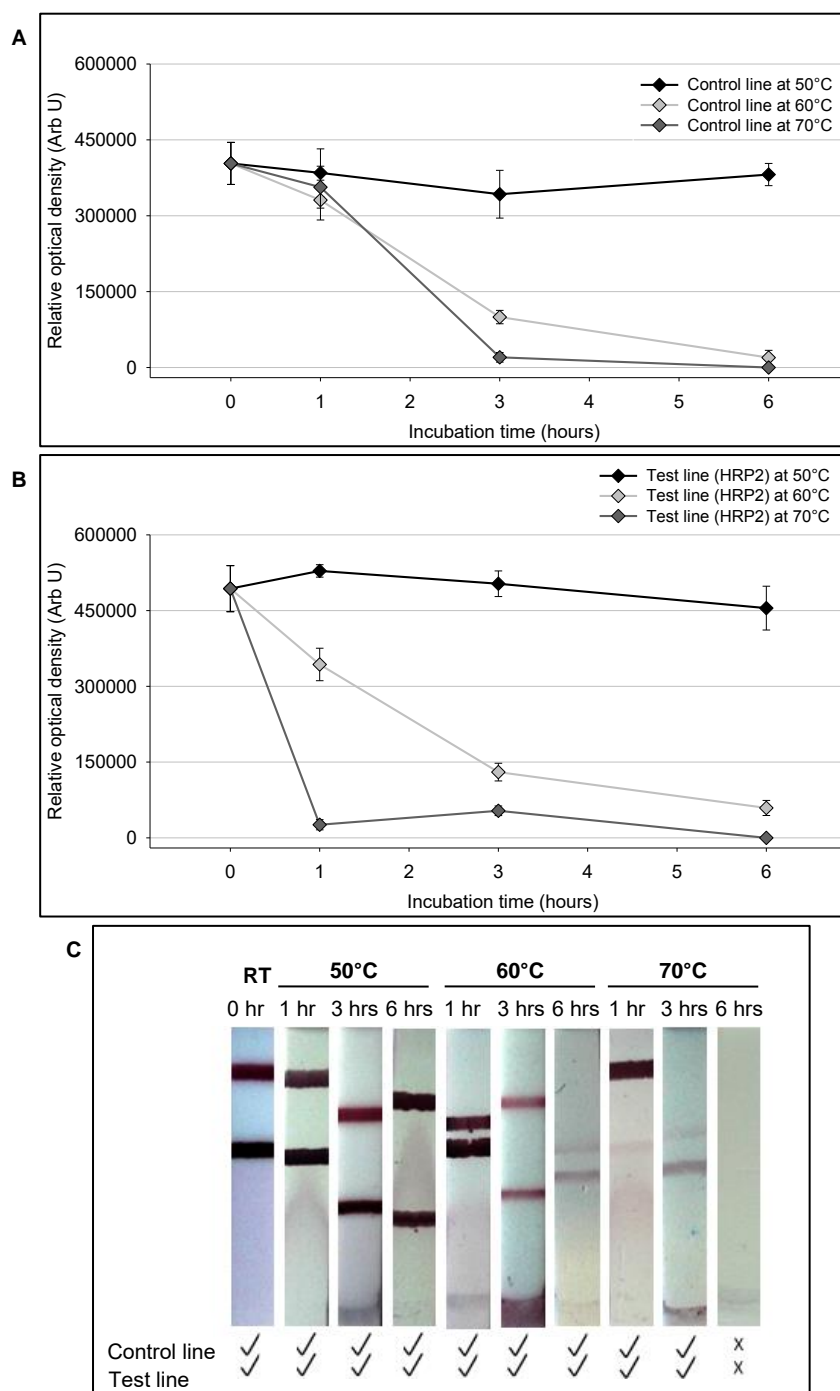


Figure 5.13: Stability of anti-HRP2-conjugated colloidal gold nanoparticles incubated from 1 to 6 hours at 50°C, 60°C and 70°C. **A** and **B**: quantified results, **C**: representative lateral flow images of experiment with control line above the test line (HRP2). Error bars represent standard deviation of triplicate lateral flow experimental sets.

According to the densitometry and lateral flow images, the control and test line signals remained stable and detectable for up to 6 hours incubation at 50°C, while incubation at 60°C resulted in detectable signals for both the control and test line for up to 1 hour incubation, after which there was a distinct reduction in both control and test line signal intensity (3 and 6 hours). Incubation at 70°C for 1 hour resulted in a detectable control line but barely visible test line. Interestingly 3 hours at 70°C resulted in increased binding at the test line (which is likely non-specific binding) while the control line was barely visible, while 6 hours of incubation resulted in no detectable signal at either line. Comparison of test and control lines at 60 and 70°C for the anti-HRP2 conjugated microspheres and colloidal gold suggest that the microsphere immobilised antibodies are more stable (control line at 70°C for 3 hours). It is worth mentioning the similarity in stability observed with different conjugated antibodies (hCG and HRP2 – refer Figure 4.16 and Figure 5.13), which may be indicative of instability in the colloidal gold or similar stabilities of the IgG (goat), and further investigation is required to identify the root cause of the instability. However, stability at elevated temperature is reduced for colloidal gold conjugated antibodies in both instances.

5.4. CONCLUSIONS

The performance of anti-HRP2-conjugated-microspheres and anti-pLDH-conjugated-microspheres were evaluated, and compared to a commercial preparation of anti-HRP2-conjugated colloidal gold as the standard detector particles for lateral flow assay in a microwell format. We have successfully demonstrated the suitability of the polymer microspheres for detection of a further two antigens, showing its suitability as a generic detection agent, and further sensitivity in the range of colloidal gold for lateral flow assay in a microwell format. The polymer microspheres have further been shown to be suitable for the development of multiplex assay formats, allowing for the easily discernible and simple interpretation of lateral flow results.

The lower limit of visual detection for all antigens was considered similar at 1.2 ng.µl⁻¹ while 0.15 ng.µl⁻¹ was the lower limit of detection using densitometry analysis. This lowest limit of detection may be as a direct result of the reported K_D of murine antibodies used in this study, where the K_D value gives a quantitative measurement of antibody affinity, where low affinity equals high K_D and vice versa (Scheinberg, 2010). For example, the K_D values of commercial therapeutic antibodies binding to their target antigen, is typically in the nanomolar range (Zhu *et al.*, 2009). By comparison, a concentration of 0.15 ng.µl⁻¹ equates to 4nM for the 37 kDa HRP2 antigen and it would be expected that the signal, in both the polymer microspheres and colloidal gold based assays, would drop rapidly once the antigen concentration in solution drops significantly below the K_D , due to fundamental thermodynamic considerations. To

potentially achieve lower sensitivities for lateral flow assays, alternate sources of antibodies with lower K_D values may therefore be of value. Sensitivity of the malaria assay is very important as patients with low parasitemia may go undetected and act as reservoirs for parasite transmission. The current limit of sensitivity for malaria lateral flow diagnostics using colloidal gold is 100 parasites. μl^{-1} blood (Tangpukdee *et al.*, 2009), and although the sensitivity results presented in this study are not directly comparable, the similar sensitivities of the anti-HRP2-conjugated-microspheres to the anti-HRP2-conjugated-colloidal gold nanoparticles suggests that the anti-HRP2-conjugated-microspheres could have a similar sensitivity as the market leader in a fully assembled diagnostic assay cassette. Literature advises that an average of 5.2 fg HRP2 is secreted per parasite per erythrocytic lifecycle, which suggests that 100 parasites would secrete ~ 0.0052 ng HRP2 per life cycle (Butterworth *et al.*, 2011). The claimed limit of detection for the commercial BinaxNOW malaria test is 1001 – 1500 parasites/ μl for *Plasmodium falciparum* and 5001 – 5500 parasites/ μl for *Plasmodium vivax* (www.alere.com, 2015). The visual and densitometric limit of detection for HRP2 is 1.2 ng and 0.15 ng respectively. Based on the above information, it can be calculated that 0.15 ng antigen is produced by ~ 2800 parasites/ μl and thus the assay is currently half as sensitive as commercial BinaxNOW assay. This is a rather preliminary comparison with literature values with the commercial test, and a direct comparison of the microsphere performance in a fully assembled device, to commercial devices, would allow for more valuable comparison.

In addition, the sensitivity of coloured latex beads are considered less than that of colloidal gold, due to the smaller size of colloidal gold (20 – 40 nm) compared to that of latex (100 – 300 μm) resulting in higher packing density of colloidal gold at the control and test line (O' Farrell, 2013). The high colour intensity of gold as compared to latex results in better visual discrimination at lower antigen concentration. The results presented here suggests that the coloured polymer microspheres may potentially be more sensitive than coloured latex, but this remains to be verified in further studies with direct comparison to latex. For the purpose of this study, and considering it is the standard detection agent for lateral flow assays, colloidal gold was considered the most suitable detection agent for direct comparison.

Comparative stability indicates that anti-pLDH antibody appears less stable than anti-HRP2 and would be the limiting factor in the stability of a lateral flow device for point-of-care.

A prerequisite for lateral flow assays is their stability at 35 – 45°C for 18 months (Bell *et al.*, 2006). It has been found that the lateral flow assays for use in the field often are exposed to temperatures above 50°C during transport while typical shelf storage temperature of the products in a village clinic is 30 – 45°C (Bell *et al.*, 2006). Preliminary results, indicating

improved stability of the microspheres, bode well for the development of point-of-care technologies utilising the microspheres as detection agents.

The antibody-conjugated-microspheres did not exhibit non-specific interaction with the test lines and were further applied in a multiplex format with three distinguishable colours, red (test line), blue (test line) and purple (control line – combination of red and blue). This allows for simple interpretation of tests, and possible troubleshooting of tests at the point-of-care. With a multiplex assay, as demonstrated here, all species of malaria are potentially detectable using a single assay and can further potentially allow for the monitoring of parasite clearance during treatment.

The high specificity of the polymer microspheres indicates that they may have application in alternate point-of-care diagnostic devices such as agglutination tests, where non-specific binding to latex beads results in non-specific agglutination, has been identified as a major problem for this type of test (Polpanich *et al.*, 2007), a problem the polymer microspheres described in this study could potentially overcome.

CHAPTER 6

CONCLUSIONS AND FUTURE PERSPECTIVES

The ReSyn microsphere technology was initially engineered for suitability to lateral flow technology (size) by optimising the emulsion parameters for preparation. Of interest were parameters including size and lack of aggregation. The optimisation studies resulted in multi-coloured (blue and red) polymer microspheres with a particle size distribution in the range from 0.1 – 4 μm in size, with a reasonable portion (just under 50%) of microspheres a suitable size ($\leq 1 \mu\text{m}$) for lateral flow on nitrocellulose membranes. Further microsphere engineering is however required to reduce the nominal size, to ensure that all microspheres are suitable for lateral flow and reduce possible collection of the microspheres at the point of application to the strip. The aim of this study was to achieve proof-of-concept for lateral flow detection reagents developed from a new polymer microsphere technology, with the potential benefit of increased dye binding capacity and improved stability of antibodies through covalent immobilisation.

Initial lateral flow development was performed on pregnancy biomarker hCG, and subsequently translated onto biomarkers for malaria detection (pLDH and HRP2). The parameters affecting sensitivity and specificity for lateral flow application were evaluated, resulting in sensitivity within the range of colloidal gold, the 'gold' standard for lateral flow RDT's. The antibodies on the microspheres displayed improved stability to heat over colloidal gold conjugated antibody, which was attributed to covalent immobilisation of the antibodies. The improvement in stability is potentially transferable to the capture line through immobilisation of microspheres at these capture lines, potentially providing for improved stability of diagnostic devices incorporating them as detection agents. For initial proof-of-concept in developing a lateral flow assay using the microspheres, covalent random immobilisation of the antibodies, (as opposed to the possibility of improved sensitivity that may be provided by antibody orientation) on the microspheres was selected, due to the simpler experimental design, reducing potential experimental variability. Partially oriented antibody immobilisation provided a 3 fold improvement in antibody availability and should be evaluated for application for lateral flow.

The potential for incorporation of a range of coloured reactive dyes within the microspheres enable multiplex detection in lateral flow format. The application of multiplex detection, with high specificity and sensitivity, was demonstrated using malaria biomarkers pLDH and HRP2. Multiplex detection not only allows for the detection of various analytes in a single sample but further potentially allows for simpler interpretation of lateral flow assay results.

This research demonstrates lateral flow detection with sensitivity in the range of the current detector reagents, but several areas for further optimisation and potential applications for the diagnostic microspheres were identified. The improved test line colour obtained with colloidal gold over polymer microspheres is considered as a result of their smaller size, which allows higher packing density of the nanoparticles at the capture lines (O' Farrell, 2013). We thus intend to further decrease the size of the polymer microspheres, as this may allow higher packing density of the microspheres at the capture lines, which could in turn translate to improved sensitivity, sharper control and test lines, enabling better quantification. Reduced aggregation may result in the requirement of fewer particles in the assay to obtain the same signal at the test and control line with reduced background and is an area for further investigation. In addition, different dyes, resulting in increased contrast against the white nitrocellulose membrane, could be evaluated as they may enhance visual detection of the assay. A degree of background staining of the nitrocellulose membrane was observed when using the microspheres, which may either be due to potential leaching of the dye during the assay, or the contrast of the microspheres against the membrane while flowing. This phenomenon needs further evaluation and alternate coupling chemistries can be evaluated to prevent leaching, if this is found to be the cause of the leaching. The polymer microspheres are currently suitable for integration in lateral flow and we intend evaluating them in a fully assembled diagnostic cassette with various sample matrices. The performance of the lateral flow assay in the presence of multiple proteins (spiked samples) and haemoglobin (real world blood samples) needs to be assessed. As per application of blood based samples on lateral flow, the red-blood cells should be filtered by the sample pad in a fully assembled assay, while hemolysis (rupturing of the erythrocyte membrane) could release free haemoglobin to the membrane which often results in background staining and may affect the sensitivity of the assay (Tan, 2008). Hemolysis is not commonly seen with fresh blood and can be avoided by using blood filter membranes, careful selection of the appropriate sample filter pad and blood volume added to the strip, (Tan, 2008; Wong *et al.*, 2009). It should also be noted that 100 μ l buffer was used in the development of the lateral flow assays, however clinical samples (field based) often supplement the volume of blood obtained from a finger-prick sample with additional buffer to enable efficient flow through the membrane. Literature states that 50 μ l sample fluid is not sufficient in lateral flow based assays as the liquid does not reach the absorbent pad, while sample volumes of 120 – 150 μ l resulted in overflow and therefore 80 – 100 μ l sample fluid appeared to be the most ideal volume (Leung *et al.*, 2003). For this reason, the sample volume applied to the lateral flow assays in these experiments was 100 μ l. The performance of the fully assembled assay remains to be evaluated.

Accelerated decay kinetics, increasing the rate of chemical and physical degradation, is frequently used to illustrate stability of biomolecules (Bajaj *et al.*, 2012). The amount of heat

input required to cause product failure is determined and used to predict shelf life or to compare performance early in development (Bajaj *et al.*, 2012). Accelerated decay studies were used to determine the stability of the microspheres and provided insight into how they compare to the market leader colloidal gold. The next phase will involve conditions that more stringently resemble/match the long term storage conditions (40 °C, 3 – 6 months) often found in point-of-care rural clinics. The performance of the microsphere lateral flow assay after high temperature exposure will also need to be evaluated using real world samples as previous stability studies, on commercially available RDT's using real world samples, revealed warped strips along with clear spots on the nitrocellulose membrane where the blood sample could not flow through (Chiodini *et al.*, 2007).

Several limitations have been identified for the use of latex beads in agglutination diagnostic assays (E.g. non-specific protein binding, false positives, inability to discriminate between *P. falciparum* and *P. vivax*) (Polpanich *et al.*, 2007). Although not currently evaluated for agglutination assay, this assay format may potentially utilise the polymer microspheres, due to the high specificity observed for the microspheres in the lateral flow assays. Furthermore, the use of microspheres as detection agents potentially provides for antibody orientation chemistries to be applied to RDT technologies such as lateral flow. Initial evaluation of oriented antibody immobilisation indicated a 3 fold increase in antibody presentation for antigen detection. The effect of antibody orientation on the sensitivity in lateral flow devices is a further aspect of research that requires investigation.

An advantage observed with the microspheres was the quantifiable detection of the control and test line signal, however the signal intensity requires improvement. The consistent intensity of the control line (~ 80 000 – 100 000 for microspheres and ~ 450 000 for colloidal gold) observed with each lateral flow test strip and the variance across experimental sets being below 10% (9.6% for ReSyn and 7.9% for colloidal gold), suggests good experimental consistency and reproducibility between strips (inter-strip), even with the batch to batch variation of antibody striping provided. The variation in antibody striping distance of the capture lines therefore did not appear to affect the quality of the data generated in the lateral flow assays, and this may be due to the presence of the absorbent pad “pulling” the liquid through the membrane. However, better care will be taken to ensure same distance of striping on future membranes.

The absorbent pad quantification of the signal using a reader has been noted to potentially reduce human error for interpretation of RDT's and could further improve the sensitivity of the assay. The application of microspheres allows for the incorporation of fluorescent labels, and the high capacity of the technology potentially allows for improved dynamic range and

sensitivity as compared to e.g. latex. Readers may therefore be advantageous to RDTs and may potentially reduce the lower limit of detection in the case of e.g. fluorescently labelled microspheres.

Malaria is considered to be a global epidemic and preventative measures such as the use of insecticide treated bed nets and indoor spraying, along with improved access to anti-malarial drugs, are inadequate to managing the disease in populations living in destitute, remote areas (Kokwaro, 2009; Sachs *et al.*, 2002). In these high transmission areas where adequate resources and healthcare infrastructure is limited, effective diagnosis, prevention and treatment of malaria are challenging and *P. falciparum* malaria could be life threatening if not managed properly (Pasvol, 2005). One of the major contributing factors for the high morbidity and mortality rate of malaria is the lack of accurate and sensitive diagnostics which can result in incorrect treatment, and further leads to the progression of drug resistance, which has severe implications for future treatment and increased healthcare expenditure (Amexo *et al.*, 2004; Kokwaro, 2009; Urdea *et al.*, 2006). Lateral flow diagnostic technology is preferred over alternate methods of diagnosis including microscopy and molecular techniques because of its rapidity, ease of use and reduced requirement for trained staff and specialised equipment (Makler *et al.*, 1998). Unfortunately, this is considered the least sensitive diagnostic technology (Humar *et al.*, 1997; Kilian *et al.*, 1997; Pieroni *et al.*, 1998). The potential impact of improved rapid diagnostic technologies for malaria point-of-care makes this an active field of research and was therefore used as model system to evaluate the microspheres in this study.

We proposed the development of a new polymer microsphere technology for application as diagnostic detection agents in lateral flow, which could potentially alleviate the drawbacks of existing technology. The incorporation of new detector particles in lateral flow diagnostic assays could potentially be applied to detection of a variety of diseases, resulting in RDT's with increased sensitivity and stability. The proof-of-concept has been achieved suggesting that these particles may be used for lateral flow assays (with potential advantage of increased stability) and that the option of various colours may be suitable for multiplexing. However, several problems identified in this study will need to be addressed before these particles may be used for lateral flow, including reducing the aggregation, background signal, and signal intensity. Although this study alludes to the potential benefit of the polymer microsphere technology as a detection reagent, further research is required to validate the findings, particularly evaluation in a working lateral flow device and real-world samples.

The goal of this research was achieved, the development of new polymeric detector reagents suitable for lateral flow diagnostic application. The preliminary results illustrate the use in a

lateral flow assay format, and suggest that the microspheres may offer a viable alternative to existing technologies, with potential enhancement to point-of-care application.

LIST OF REFERENCES:

- Ahmad, R., and Sardar, M. (2014). Immobilization of cellulase on TiO₂ nanoparticles by physical and covalent methods: A comparative study. *Indian Journal of Biochemistry and Biosphysics*. 51 314 - 320
- Amexo, M., Tolhurst, R., Barnish, G., and Bates, I. (2004). Malaria misdiagnosis: effects on the poor and vulnerable. *The Lancet*. 364 1896-1898
- Antia, M., Herricks, T., and Rathod, P.K. (2008). Microfluidic approaches to malaria pathogenesis. *Cellular Microbiology*. 10 (10): 1968-1974
- Arruebo, M., Valladares, M., and González-Fernández, A. (2009). Antibody-conjugated nanoparticles for biomedical applications. *Journal of Nanomaterials*. 439389 1 - 24
- Bahk, Y.Y., Na, B., Cho, S., Kim, J., Lim, K., and Kim, T. (2010). Proteomic analysis of haptoglobin and Amyloid A protein levels in patients with Vivax malaria. *Korean Journal of Parasitology*. 48 (3): 203-211
- Bailey, A., and Rasums, A. (1989). Patent title: Dye labelled antibodies as reagents for use in immunoassay systems. US 06/769,589.
- Bajaj, S., Singla, D., and Sakhuja, N. (2012). Stability Testing of Pharmaceutical Products. *Journal of Applied Pharmaceutical Science*. 2 (3): 129 - 138
- Baker, J., Ho, M., Pelecanos, A., Gatton, M., Chen, N., Abdullah, S., Albertini, A., Arie, F., Barnwell, J., Bell, D., Cunningham, J., Djalle, D., Echeverry, D.F., Gamboa, D., Hii, J., Kyaw, M.P., Luchavez, J., Membi, C., Menard, D., Murillo, C., Nhem, S., Ogutu, B., Onyor, P., Oyibo, W., Wang, S.Q., McCarthy, J., and Cheng, Q. (2010). Global sequence variation in the histidine-rich proteins 2 and 3 of *Plasmodium falciparum*: implications for the performance of malaria rapid diagnostic tests. *Malaria Journal*. 9 1-12
- Bandla, M., Thompson, R., and Shan, G. 2011. Lateral flow devices.91 - 114. Immunoassays in Agricultural Biotechnology. G. Shan, editor. John Wiley & Sons978-0-470-28952-5, eBook ISBN 978-0-470-90992-8
- Bates, R. 2005. Downstream processing.461. Cell culture technology for pharmaceutical and cell-based therapies. S.S. Ozturk and W. Hu, editors. Taylor & Francis Group CRC Press. 978-0-8493-5106
- Bell, D., and Winstanley, P. (2004). Current issues in the treatment of uncomplicated malaria in Africa. *British Medical Bulletin*. 71 29 - 43
- Bell, D., Wongsrichanalai, C., and Barnwell, J.W. (2006). Ensuring quality and access for malaria diagnosis: how can it be achieved? *Nature Reviews : Microbiology*. Supplementary Materials S7-S20

- Bissonnette, L., and Bergeron, M.G. (2012). Infectious disease management through point-of-care personalized medicine molecular diagnostic technologies. *Journal of Personalised Medicine*. 2 50 - 70
- Bonini, M.G., Siraki, A.G., Bhattacharjee, S., and Mason, R.P. (2007). Glutathione induced radical formation on lactoperoxidase does not correlate with the enzyme's peroxidase activity. *Free Radical Biology and Medicine*. 42 (7): 985 - 992
- Bosch, J., Buscaglia, C.A., Krumm, B., Ingason, B.P., Lucas, R., Roach, C., Cardozo, T., Nussenzweig, V., and Hol, W.G. (2007). Aldolase provides an unusual binding site for thrombospondin-related anonymous protein in the invasion machinery of the malaria parasite. *Proceedings of the National Academy of Science*. 104 (17): 7015-7020
- Bosman, A., ., Kassankogno, Y., and Kondrachine, A.V. (1999). Implementation of malaria control. *Parassitologia*. 41 (1-3): 391-393
- Bovaird, J.H., Ngo, T.T., and Lenhoff, H.M. (1982). Optimizing the o-Phenylenediamine assay for horseradish peroxidase: Effects of phosphate and pH, substrate and enzyme concentrations, and stopping reagents. *Clinical Chemistry*. 28 (12): 2423 - 2426
- Brady, D., and Jordaan, J. (2009). Advances in enzyme immobilisation. *Biotechnology Letters* 31 (11): 1639-1650
- Brown, W.M., Yowell, C.A., Hoard, A., Vander Jagt, T.A., Hunsaker, L.A., Deck, L.M., Royer, R.E., Piper, R.C., Dame, J.B., Makler, M.T., and Vander Jagt, D.L. (2004). Comparative structural analysis and kinetic properties of lactate dehydrogenases from the four species of human malarial parasites. *Biochemistry*. 43 (20): 6219-6229
- Bruchez, M., Moronne, M., Gin, P., Weiss, S., and Alivisatos, A.P. (1998). Semiconductor nanocrystals as fluorescent biological labels. *Science*. 281 (5385): 2013 - 2016
- Butterworth, A.S., Robertson, A.J., Ho, M., Gatton, M.L., McCarthy, J.S., and Trenholme, K.R. (2011). An improved method for undertaking limiting dilution assays for in vitro cloning of *Plasmodium falciparum* parasites. *Malaria Journal*. 10 (95): 1 - 5
- Butykai, A., Orbán, A., Kocsis, V., Szaller, D., Bordács, S., Tátrai-Szekeres, E., Kiss, L.F., Bóta, A., Vértessy, B.G., Zelles, T., and Kézsmárki, I. (2013). Malaria pigment crystals as magnetic micro-rotors: key for high-sensitivity diagnosis. *Scientific Reports*. 3 (1431): 1 - 10
- Chacko, J.T., and Subramaniam, K. (2011). Enzymatic Degradation of Azo Dyes – A Review. *International Journal of Environmental Sciences*. 1 (6): 1250-
- Chandler, C.I.R., Jones, C., Boniface, G., Juma, K., Reyburn, H., and Whitty, C.J.M. (2008). Guidelines and mindlines: why do clinical staff over-diagnose malaria in Tanzania? A qualitative study. *Malaria Journal*. 7 1-13
- Chaurasia, P.K., Singh, S.K., and Bharati, S.L. (2013). Study of peroxidase obtained from *Daucus carota* (carrot) juice extract. *Journal of Applied Chemistry*. 2 (5): 1123 - 1131

- Chenggang, S., Z., S., Kun, Z., Guobao, H., and Zhenyu, Z. (2008). Preparation of colloidal gold immunochromatography strip for detection of methamidophos residue. *Journal of Environmental Sciences*. 20 1392-1397
- Chiodini, P.L., Bowers, K., Jorgensen, P., Barnwell, J.W., Grady, K.K., Luchavez, J., Moody, A.H., Cenizal, A., and Bell, D. (2007). The heat stability of *Plasmodium* lactate dehydrogenase-based and histidine-rich protein 2-based malaria rapid diagnostic tests. *Transactions of the Royal Society of Tropical Medicine and Hygiene*. 101 331-337
- Choi, S., Choi, E.Y., Kim, D.J., Kim, J.H., Kim, T.S., and Oh, S.W. (2004). A rapid, simple measurement of human albumin in whole blood using a fluorescence immunoassay. *Clinica Chimica Acta*. 339 147 - 156
- Choi, S., Pradham, A., Hammond, N.L., Chittiboyina, A.G., Tekwani, B.L., and Avery, M.A. (2007). Design, synthesis and biological evaluation of *Plasmodium falciparum* lactate dehydrogenase inhibitors. *Journal of Medicinal Chemistry*. 50 (16): 3841-3850
- Choi, Y.H., Choi, B.K., Kim, H., Baek, S.J., Jung, J., and Makler, M.T. (2005). A supersensitive lateral-flow platform for the detection of *P. falciparum* malaria using the luminescent europium nanoparticle Abstract 61, Oak Ridge Conference 2005, Pushing the technology envelope II: An exploration of the Future of Clinical Laboratory Testing. https://www.aacc.org/meetings/oakridge/archive/2005/RC05_abs61.pdf
- Cobelens, F., van den Hof, S., Pai, M., Squire, S.B., Ramsay, A., and Kimerling, M.E. (2012). Which new diagnostics for tuberculosis, and when? *Journal of Infectious Diseases*. 15 (205): S191 - S198
- Correia, I.R. (2010). Stability of IgG isotypes in serum. *mAbs*. 2 (3): 221 - 232.1942-0862 (Print), 1942-0870 (Online). <http://www.ncbi.nlm.nih.gov/pmc/articles/PMC2881250/>
- Corstjens, P., Zuiderwijk, M., Brink, A., Li, S., Feindt, H., Niedbala, R.S., and Tanke, H. (2001). Use of Up-Converting Phosphor Reporters in lateral-flow assays to detect specific nucleic acid sequences: A rapid, sensitive DNA test to identify human papillomavirus type 16 infection. *Clinical Chemistry*. 47 (10): 1885 - 1893
- Cox, K.L., Devanarayan, V., Kriauciunas, A., Manetta, J., Montrose, C., and Sittampalam, S. (2012). Immunoassay Methods. Pub Med ID: 22553861. <http://www.ncbi.nlm.nih.gov/books/NBK92434/>
- David, P.H., Hommel, M., Miller, L.H., Udeinya, I.J., and Oligino, L.D. (1983). Parasite sequestration in *Plasmodium falciparum* malaria: spleen and antibody modulation of cytoadherence of infected erythrocytes. *Proceedings of the National Academy of Science of the USA*. 80 (16): 5075 - 5079
- del Prado, G.R.L., García, C.H., Cea, L.M., Espinilla, V.F., Moreno, F.M., Márquez, A.D., Polo, J.P., and García, I.A. (2014). Malaria in developing countries. *Journal of Infection in Developing Countries*. 8 (1): 1 - 4

- Denizli, A., and Pişkin, E. (2001). Dye-ligand affinity systems. *Journal of Biochemical and Biophysical Methods*. 49 (1-3): 391-416
- Desakorn, V., Dondorp, A.M., Silamut, K., Pongtavornpinyo, W., Sahassananda, D., Chotivanich, K., Pitisuttithum, P., Smithyman, A.M., Day, N.P.J., and White, N.J. (2005). Stage-dependent production and release of histidine-rich protein 2 by *Plasmodium falciparum*. *Transactions of the Royal Society of Tropical Medicine and Hygiene*. 99 517-524
- Di Marco, M., Shamsuddin, S., Razak, K.A., Aziz, A.A., Devaux, C., Borghi, E., Levy, L., and Sadun, C. (2010). Overview of the main methods used to combine proteins with nanosystems: absorption, bioconjugation and encapsulation. *International Journal of Nanomedicine*. 5 37-49
- Drakeley, C., and Reyburn, H. (2009). Out with the old, in with the new: the utility of rapid diagnostic tests for malaria diagnosis in Africa. *Transactions of the Royal Society of Tropical Medicine and Hygiene*. 103 333-337
- Dzakah, E.E., Kang, K., Ni, C., Wang, H., Wu, P., Tang, S., Wang, J., Wang, J., and Wang, X. (2013). Plasmodium vivax aldolase-specific monoclonal antibodies and its application in clinical diagnosis of malaria infections in China. *Malaria Journal*. 12 (199): 1 - 8
- Engstrand, C., Bergander, T., and Lacki, K. (2008). High-throughput screening for elution conditions on Capto MMC using PreDictor plates. GE Healthcare. https://www.gelifesciences.com/gehcls_images/GELS/Related%20Content/Files/1314787424814/litdoc28927790AA_20110831130403.pdf
- Esser, P. (2010). Blocking agent and detergent in ELISA. Thermo Fischer Scientific Inc. Technical Bulletin: 09. <http://www.thermoscientific.com/content/dam/tfs/LPG/LCD/LCD%20Documents/Product%20Support%20Bulletins/Cell%20Culture%20Vessels%20and%20Microplates/Microplates/Assay%20Microplates/D19564~.pdf>
- Fahmy, A.S., Salem, A.M.H., El-Hamid, M.M.S.A., El-Badry, M.O., and M., A.R.A. (2012). Role of calcium in enhancing the activity and thermal stability of a new cationic peroxidase purified from euphorbia tirucalli latex. *The Egyptian Journal of Biochemistry and Molecular Biology*. 30 (2): 245 - 268
- Fernández-Sánchez, C., McNeil, C.J., Rawson, K., Nilsson, O., Leung, H.Y., and Gnanapragasam, V. (2005). One-step immunostrip test for the simultaneous detection of free and total prostate specific antigen in serum. *Journal of Immunological Methods*. 307 1 - 12
- Fogg, C., Twesigye, R., Batwala, V., Piola, P., Nabasumba, C., Kiguli, J., Mutebi, F., Hook, C., Guillermin, M., Moody, A., and Guthmann, J.P. (2008). Assessment of three new parasite lactate dehydrogenase (pan-pLDH) tests for diagnosis of uncomplicated malaria.

- Transactions of the Royal Society of Tropical Medicine and Hygiene*. 102 (1): 25-31 <http://www.ncbi.nlm.nih.gov/pubmed/18031779>
- Fornera, S., and Walde, P. (2010). Spectrophotometric quantification of horseradish peroxidase with o-phenylenediamine. *Analytical Biochemistry*. 407 293–295
- Fribe, A., and Walther, M. (2009). A guide to diagnostic rapid test development. Whatman, <http://wenku.baidu.com/view/3416922ced630b1c59eeb5fa.html>
- Fu, E., Liang, T., Houghtaling, J., Ramachandran, S., Ramsey, S.A., Lutz, B., and Yager, P. (2011). Enhanced sensitivity of lateral flow tests using a two-dimensional paper network format. *Analytical Chemistry*. 83 (20): 7941 - 7946
- Gamboa, D., Ho, M., Bendezu, J., Torres, K., Chiodini, P.L., Barnwell, J.W., S., I., Perkins, M., Bell, D., McCarthy, J., and Cheng, Q. (2010). A large proportion of *P. falciparum* Isolates in the amazon region of Peru Lack *Pfhrp2* and *Pfhrp3*: implications for malaria rapid diagnostic tests. *PLOS ONE*. 5 (1): 1-8
- Gao, X., Xu, L., Zhou, Z., Liu, G., and Zhang, X. (2014). Recent Advances in Nanoparticles-based Lateral Flow Biosensors. *American Journal of Biomedical Sciences*. 6 (1): 41 - 57
- Garcia, M., Kirimoama, S., Marlborough, D., Leafasia, J., and Rieckman, K.H. (1996). Immunochromatographic test for malaria diagnosis. *The Lancet*. 347 1549
- Gascoyne, P., Satayavivad, J., and Ruchirawat, M. (2004). Microfluidic approaches to malaria detection. *Acta Tropica*. 89 (3): 357 - 369
- Gaye, O., Diouf, M., Dansokko, E.F., McLaughlin, G., and Diallo, S. (1998). Diagnosis of *Plasmodium falciparum* malaria using ParaSight-F, ICT malaria Pf and Malaria IgG Celisa assays. *Parasite*. 5 189-192
- Gella, F.J., Serra, J., and Gener, J. (1991). Latex agglutination procedures in immunodiagnosis. *Pure and Applied Chemistry*. 63 (8): 1131-1134
- Gerbase, A.C., Rowley, J.T., Heymann, D.H., Berkley, S.F., and Piot, P. (1998). Global prevalence and incidence estimates of selected curable STDs. *Sexually Transmitted Infections*. 74 S12 - S16
- Gething, P.W., Smith, D.L., Patil, A.P., Tatem, A.J., Snow, R.W., and Hay, S.I. (2010). Climate change and the global malaria recession. *Nature : Letters*. 465 342-345
- Gomez, M.S., Piper, R.C., Hunsaker, L.A., Royer, R.E., Deck, L.M., Makler, M.T., and Vander Jagt, D.L. (1997). Substrate and cofactor specificity and selective inhibition of lactate dehydrogenase from the malarial parasite *P. falciparum*. *Molecular and Biochemical Parasitology* 90 235-246
- Goryacheva, I.Y., Lenain, P., and De Saeger, S. (2013). Nanosized labels for rapid immunotests. *Trends in Analytical Chemistry*. 46 30 - 43
- Gubbins, P.O., Klepser, M.E., Dering-Anderson, A.M., Bauer, K.A., Darin, K.M., Klepser, S., Matthias, K.R., and Scarsi, K. (2014). Point-of-care testing for infectious diseases:

- Opportunities, barriers, and considerations in community pharmacy. *Journal of the American Pharmacist Association*. 52 (2): 163 - 171
- Gullan, P.J., and Cranston, P.S. (2010). The insects: An outline of entomology. Wiley Blackwell 393 pp
- Gunne, M., and Urlacher, V.B. (2012). Characterization of the Alkaline Laccase Ssl1 from *Streptomyces svaceus* with Unusual Properties Discovered by Genome Mining. *PLOS ONE*. 7 (12): 1 - 8
- Güven, E., Duus, K., Lydolph, M.C., Jørgensen, C.S., Laursen, I., and Houen, G. (2014). Non-specific binding in solid phase immunoassays for autoantibodies correlates with inflammation markers. *Journal of Immunological Methods*. 403 (1 - 2): 26 - 36
- Guzov, V.M., Rodionov, M.A., Golubovich, V.P., Butkova, L.S., Chashchin, V.L., and Usanov, S.A. (1988). Optimization of methods of immobilization of anti-immunoglobulins: Equilibrium parameters of the interaction of immobilized antibodies with antigen. *Biokhimiya*. 53 (2): 238 - 250
- Hamilton, T.M., Dobie-Galuska, A.A., and Wietstock, S.M. (1999). The o-phenylenediamine-horseradish peroxidase system: Enzyme kinetics in the general chemistry laboratory. *Journal of Chemical Education*. 76 (5): 642
- Hampl, J., Hall, M., Mufti, N.A., Yao, Y.M., MacQueen, D.B., Wright, W.H., and Cooper, D.E. (2001). Upconverting phosphor reporters in immunochromatographic assays. *Analytical Biochemistry*. 288 176 - 187
- Handali, S., Klarman, M., Gaspard, A.N., Dong, X.F., Laborde, R., Noh, J., Lee, Y.M., Rodriguez, S., Gonzalez, A.E., Garcia, H.H., Gilman, R.H., Tsang, V.C., and Wilkins, P.P. (2010). Development and evaluation of a magnetic immunochromatographic test to detect *Taenia solium*, which causes taeniasis and neurocysticercosis in humans. *Clinical and Vaccine Immunology*. 17 631 – 637
- Hassan, B.M., Mezher, I.A., and Mohammed, A.J. (2009). A comparative study among one step hCG test strip, direct agglutination test and elisa for detection hCG. *Iraqi Academic Scientific Journals*. 22 (4): 107 - 111
- Hatta, R.W., and Smits, H.L. (2008). Point-of-care testing for malaria outbreak management. *Transactions of the Royal Society of Tropical Medicine and Hygiene*. 102 699 - 704
- Henderson, K., and Stewart, J. (2002). Factors influencing the measurement of oestrone sulphate by dipstick particle capture immunoassay. *Journal of Immunological Methods*. 270 (1): 77 - 84
- Hermanson, G.T. (2008). Bioconjugate techniques. Elsevier inc. Page 67; page 125, page 512 - 514, page 726, page 903 - 905. 978-0-12-370501-3.
- Holmes, D., She, J.K., Roach, P.L., and Morgan, H. (2007). Bead-based immunoassays using a micro-chip flow cytometer. *Lab on a Chip*. 7 1048 - 1056

- Horton, J.K., Swinburne, S., and O'Sullivan, M.J. (1991). A novel, rapid, single-step immunochromatographic procedure for the detection of mouse immunoglobulin. *Journal of Immunological Methods*. 140 (1): 131 - 134
- Howard, R.J., Uni, S., Aikawa, M., Aley, S.B., Leech, J.H., Lew, A.M., Wellems, T.E., Renner, J., and Taylor, D.W. (1986). Secretion of a malarial histidine-rich protein (PfHRP II) from *Plasmodium falciparum*-infected erythrocytes. *The Journal of Cell Biology*. 103 1269-1277
- Hsiang, M.S., Greenhouse, B., and Rosenthal, P.J. (June 2014). Point of care testing for malaria using lamp, loop mediated isothermal amplification. *Journal of Infectious Diseases*. Editorial Commentary 1 - 3
- Hulden, L., and Hulden, L. (2011). Activation of the hypnozoite: a part of *Plasmodium vivax* life cycle and survival. *Malaria Journal*. 10 1 - 6
- Humar, A., Ohrt, C., Harrington, M.A., Pillai, D., and Kain, K.C. (1997). Parasight F-test compared with the polymerase chain reaction and microscopy for the diagnosis of *Plasmodium falciparum* malaria in travellers. *American Journal of Tropical Medicine and Hygiene*. 56 (1): 44-48
- Jelinek, T., Grobusch, M.P., and Nothdurft, H.D. (2000). Use of dipstick tests for the rapid diagnosis of malaria in nonimmune travelers. *Journal of Travel Medicine*. 7 (4): 175-179
- Jewett, T.J., and Sibley, L.D. (2003). Aldolase forms a bridge between cell surface adhesins and the actin cytoskeleton in apicomplexan parasites. *Molecular Cell*. 11 885-894
- Jeyachandran, Y.L., Mielczarski, J.A., Mielczarski, E., and Rai, B. (2010). Efficiency of blocking of non-specific interaction of different proteins by BSA adsorbed on hydrophobic and hydrophilic surfaces. *Journal of Colloid and Interface Science* 341 136–142
- Johannes, T.W., Woodyer, R.D., and Zhao, H. 2006. High-throughput screening methods developed for oxidoreductases. 77 - 93. Enzyme assays: high-throughput screening, genetic selection and fingerprinting. J.-L. Reymond, editor. WILEY-VCHPrint ISBN: 9783527310951, Online ISBN: 9783527607846
- Jordaan, J., Simpson, C., Brady, D., Gardiner, N.S., and Gerber, I.B. (2009). Patent title: Emulsion-derived particles. PCT/IB2008/054458. WO2009/057049.
- Jung, A.T., and Kropp, M.A. (2014). Color indicating acrylate resins and methods there of. EP20120783769. EP2771388 A1.
- Jung, Y., Jeong, J.Y., and Chung, B.H. (2008). Recent advances in immobilization methods of antibodies on solid supports. *The Royal Society of Chemistry - Analyst*. 133 697-701
- Kain, K.C., Harrington, M.A., Tennyson, S., and Keystone, J.S. (1998). Imported malaria: prospective analysis of problems in diagnosis and management. *Clinical Infectious Diseases*. 27 (1): 142-149
- Kakkilaya, B.S. (2003). Rapid diagnosis of malaria. *Laboratory Medicine*. 34 (8): 602-608

- Kang, J.H., Choi, H.J., Hwang, S.Y., Han, S.H., Jeon, J.Y., and Lee, E.K. (2007). Improving immunobinding using oriented immobilization of an oxidized antibody. *Journal of Chromatography A*. 1161 9 - 14
- Kausaite-Minkstiniene, A., Ramanaviciene, A., Kirlyte, J., and Ramanavicius, A. (2010). Comparative study of random and oriented antibody immobilization techniques on the binding capacity of immunosensor. *Analytical Chemistry*. 82 (15): 6401 - 6408
- Kelly-Hope, L.A., Hemingway, J., and McKenzie, F.E. (2009). Environmental factors associated with the malaria vectors *Anopheles gambiae* and *Anopheles funestus* in Kenya. *Malaria Journal*. 8 (1): 268
- Kersting, S., Rausch, V., Bier, F.F., and von Nickisch-Rosenegk, M. (2014). Rapid detection of *Plasmodium falciparum* with isothermal recombinase polymerase amplification and lateral flow analysis. *Malaria Journal*. 13 1 - 9
- Kestrel. 2013. Kestrel Biosciences Inc: Workshop on the development and manufacturing of lateral flow immunochromatographic assays, Bangkok, Thailand.
- Kifude, C.M., Rajasekariah, H.G., and Sullivan, D.J. (2008). Enzyme-Linked Immunosorbent Assay for detection of *Plasmodium falciparum* Histidine-Rich Protein 2 in blood, plasma, and serum. *Clinical and Vaccine Immunology*. 15 (6): 1012-1018
- Kilian, A.H.d., Mughusu, E.B., Kabagambe, G., and von Sonnenbur, F. (1997). Comparison of two rapid, HRP2-based diagnostic tests for *Plasmodium falciparum*. *Transactions of the Royal Society of Tropical Medicine and Hygiene*. 91 666-667
- Kiszewski, A., Mellinger, A., Spielman, A., Malaney, P., Sachs, S.E., and Sachs, J. (2004). A global index representing the stability of malaria transmission. *American Journal of Tropical Medicine and Hygiene*. 70 (5): 486-498
- Kokwaro, G. (2009). Ongoing challenges in the management of malaria. *Malaria Journal*. 8 (Supplementary Materials 1): S2
- Kommanaboyina, B., and Rhodes, C.T. (1999). Trends in stability testing, with emphasis on stability during distribution and storage. *Drug Development and Industrial Pharmacy*. 25 (7): 857 - 868
- Kuang, H., Wang, W., Xu, L., Ma, W., Liu, L., Wang, L., and Xu, C. (2013). Monoclonal antibody-based sandwich ELISA for the detection of Staphylococcal Enterotoxin A. *International Journal of Environmental Research and Public Health*. 10 1598-1608
- Lambourne, R., and Strivens, T.A. (1999). Paint and surface coatings. Woodhead Publishing Limited, William Andrew Publishing, .95, .1884207731, 9781884207730.
- Lee, N., Baker, J., Bell, D., J., M., and Cheng, Q. (2006). Assessing the genetic diversity of the Aldolase genes of *Plasmodium falciparum* and *Plasmodium vivax* and its potential effect on performance of Aldolase-detecting rapid diagnostic tests. *Journal of Clinical Microbiology*. 44 (12): 4547-4549

- Leech, J.H., Barnwell, J.W., Aikawa, M., Miller, L.H., and Howard, R.J. (1984). *Plasmodium falciparum* malaria : Association of knobs on the surface of infected erythrocytes with a histidine-rich protein and the erythrocyte skeleton. *The Journal of Cell Biology*. 98 1256 - 1264
- Leng, S.X., McElhaney, J., E., and Kuchel, G.A. (2008). ELISA and multiplex technologies for cytokine measurement in inflammation and aging research. *Journal of Gerontology Series A*. 63 (8): 879 - 884
- Lequin, R.M. (2005). Enzyme Immunoassay (EIA)/Enzyme-Linked Immunosorbent Assay (ELISA). *Clinical Chemistry*. 51 (12): 2415-2418
- Leung, W., Chan, P., Bosgoed, F., Lehmann, K., Renneberg, I., Lehmann, M., and Renneberg, R. (2003). One-step quantitative cortisol dipstick with proportional reading. *Journal of Immunological Methods*. 281 109 - 118
- Leuvering, J.H.W., Thal, P.J.H.M., Van der Waart, M., and Shuurs, A.H.W.M. (1981). A sol particle agglutination assay for human chorionic gonadotrophin. *Journal of Immunological Methods*. 45 183 - 194
- Li, A., Zhu, Y., Xu, L., Zhu, W., and Tian, X. (2008). Comparative study on the determination of assay for laccase of *Trametes sp.* *African Journal of Biochemistry Research*. 2 (8): 181-183
- Liao, J.Y., and Li, H. (2010). Lateral flow immunodipstick for visual detection of aflatoxin B1 in food using immuno-nanoparticles composed of a silver core and a gold shell. *Microchimica Acta*. 171 (3 - 4): 289 - 295
- Linares, E.M., Kubota, L.T., Michaelis, J., and Thalhammer, S. (2012). Enhancement of the detection limit for lateral flow immunoassays: Evaluation and comparison of bioconjugates. *Journal of Immunological Methods*. 375 (1-2): 264 - 270
- Loubiere, S., and Moatti, J.-P. (2010). Economic evaluation of point-of-care diagnostic technologies for infectious diseases. *Clinical Microbiology and Infection*. 16 (8): 1070-1076
- Lu, B., Smyth, M.R., and Kennedy, R.O. (1996). Oriented immobilization of antibodies and its applications in immunoassays and immunosensors. *Analyst*. 121 29R - 32R
- Ly, A.B., Tall, A., Perry, R., Baril, L., Badiane, A., Faye, J., Rogier, C., Touré, A., Sokhna, C., Trape, J., and Michel, R. (2010). Use of HRP-2-based rapid diagnostic test for *Plasmodium falciparum* malaria: assessing accuracy and cost-effectiveness in the villages of Dielmo and Ndiop, Senegal. *Malaria Journal*. 9 (153): 1-11
- Mabey, D., Peeling, R.W., Ustianowski, A., and Perkins, M.D. (2004). Diagnostics for the developing world. *Nature Reviews Microbiology*. 2 231 - 240
- Mak, W.C., Sin, K.K., Chan, C.P.Y., Wong, L.W., and Renneberg, R. (2011). Biofunctionalized indigo-nanoparticles as biolabels for generation of precipitated visible signal in immunodipsticks. *Biosensors and Bioelectronics*. 26 3148 - 3153

- Makler, M.T., Palmer, C.J., and Ager, A.L. (1998). A review of practical techniques for the diagnosis of malaria. *Annals of Tropical Medicine and Parasitology*. 92 (4): 419-433
- Malick, A., Feindt, H.H., and Hahn, G.D. (1996). Patent title: Stabilized microspheres and methods of preparation. US 08/343,305. 5580735.
- Mateo, C., Abian, O., Fernandez-Lorente, G., Pedroche, J., Fernandez-Lafuente, R., and Guisan, J.M. (2002). Epoxy sepabeads: A novel epoxy support for stabilization of industrial enzymes via very intense multipoint covalent attachment. *Biotechnology Progress*. 18 629-634
- Mateo, C., Grazu, V., Palomo, J.M., Lopez-Gallego, F., Fernandez-Lafuente, R., and Guisan, J.M. (2007). Immobilization of enzymes on heterofunctional epoxy supports. *Nature Protocols*. 2 (5): 1022 - 1033
- Matson, R.S. (2013). Applying genomic and proteomic microarray technology in drug discovery. Taylor & Francis Group. 274 - 276. 978-1-4398-5563-8.
- Mattia, A., Waldron, M.A., and Sierra, L.S. (1993). Use of the quantitative buffy coat system for detection of parasitemia in patients with babesiosis. *Journal of Clinical Microbiology*. 31 (10): 2816 - 2819
- Mens, P.F., de Bes, H.M., Sondo, P., Laochan, N., Keereecharoen, L., van Amerongen, A., Flint, J., Sak, J.R.S., Proux, S., Tinto, H., and Schallig, H.D.F.H. (2012). Direct blood PCR in combination with nucleic acid lateral flow immunoassay for detection of *Plasmodium* species in settings where malaria is endemic. *Journal of Clinical Microbiology*. 50 (11): 3520 - 3525
- Mens, P.F., Matelon, R.J., Nour, B.J.M., Newman, D.M., and Schallig, H.D.F.H. (2010). Laboratory evaluation on the sensitivity and specificity of a novel and rapid detection method for malaria diagnosis based on magneto-optical technology (MOT). *Malaria Journal*. 9 (207): 1-8
- Mens, P.F., van Amerongen, A., Sawa, P., Kager, P.A., and Schallig, H.D.F.H. (2008). Molecular diagnosis of malaria in the field: development of a novel 1-step nucleic acid lateral flow immunoassay for the detection of all 4 human *Plasmodium* spp. and its evaluation in Mbita, Kenya. *Diagnostic Microbiology and Infectious Disease*. 61 421 - 427
- Meza, M.B. (2000). Bead-based HTS applications in drug discovery. *Drug Discovery Today: HTS supplement*. 1 (1): 38 - 41
- Mika, A., and Lüthje, S. (2013). Properties of guaiacol peroxidase activities isolated from corn root plasma membranes. *Plant Physiology*. 132 1489 - 1498
- Mohamed, S.A., Abdel-Aty, A.M., Hamed, M.B., El-Badry, M.O., and Fahmy, A.S. (2011). *Ficus sycomorus* latex: A thermostable peroxidase. *African Journal of Biotechnology*. 10 (76): 17532 - 17543

- Moody, A. (2002). Rapid diagnostic tests for malaria parasites. *Clinical Microbiology Reviews*. 15 (1): 66-78
- Morawski, B., Quan, S., and Arnold, F.H. (2001). Functional expression and stabilization of horseradish peroxidase by directed evolution in *saccharomyces cerevisiae*. *Biotechnology and Bioengineering*. 76 (2): 99 - 107
- Murray, C.K., Gasser, R.A., Magill, A.J., and Miller, R.S. (2008). Update on rapid diagnostic testing for malaria. *Clinical Microbiology Reviews*. 21 (1): 97-110
- Nisnevitch, M., and Firer, M.A. (2001). The solid phase in affinity chromatography: strategies for antibody attachment. *Journal of Biochemical and Biophysical Methods*. 49 467 - 480
- Noedl, H., Yingyuen, K., Laoboonchai, A., Fukuda, M., Sirichaisinthop, J., and Miller, R.S. (2006). Sensitivity and specificity of an antigen detection elisa for malaria diagnosis. *The American Journal of Tropical Medicine and Hygiene*. 75 (6): 1205 - 1208
- Nooney, R.I., McCormack, E., and McDonagh, C. (2012). Optimization of size, morphology and colloidal stability of fluorescein dye-doped silica NPs for application in immunoassays. *Analytical and Bioanalytical Chemistry*. 404 (10): 2807 - 2818
- Nor, N.M., Razak, K.A., Tan, S.C., and Noordin, R. (2012). Properties of surface functionalized iron oxide nanoparticles (ferrofluid) conjugated antibody for lateral flow immunoassay application. *Journal of Alloys and Compounds*. 538 100 - 106
- Nosten, F., and Ashley, E. (2004). The detection and treatment of *Plasmodium falciparum* malaria: Time for change. *Journal of Postgraduate Medicine*. 50 (1): 35-39
- O' Farrell, B. 2013. Lateral Flow Immunoassay Systems: Evolution from the Current State of the Art to the Next Generation of Highly Sensitive, Quantitative Rapid Assays Brendan O'Farrell.89 - 107. *The Immunoassay Handbook: Theory and applications of ligand binding, ELISA and related techniques*. D. Wild, R. John, C. Sheehan, S. Binder, and J. He, editors. Elsevier, 978-0-08-097037-0
- Oh, S.W., Kim, Y.M., Kim, H.J., Kim, S.J., Chod, J.-S., and Choi, E.Y. (2009). Point-of-care fluorescence immunoassay for prostate specific antigen. *Clinica Chimica Acta*. 406 (1 - 2): 18 - 22
- Orbán, A., Butykai, A., Molnár, A., Pröhle, Z., Fülöp, G., Zelles, T., Forsyth, W., Hill, D., Müller, I., Schofield, L., Rebelo, M., Hänscheid, T., Karl, S., and Kézsmárki, I. (2014). Evaluation of a novel magneto-optical method for the detection of malaria parasites. *PLOS ONE*. 9 (5): 1 - 8
- Osmekhina, E., Neubauer, A., Klinzing, K., Myllyharju, J., and Neubauer, P. (2010). Sandwich ELISA for quantitative detection of human collagen prolyl 4-hydroxylase. *Microbial Cell Factories*. 9 (48): 1 - 11
- Pai, N.P., Vadnais, C., Denking, C., Engel, N., and Pai, M. (2012). Point-of-care testing for infectious diseases: Diversity, complexity, and barriers in low- and middle-income countries. *PLOS Medicine*. 9 (9): 1 - 7

- Parolo, C., de la Escosura-Muniz, A., and Merkoci, A. (2012). Enhanced lateral flow immunoassay using gold nanoparticles loaded with enzymes. *Biosensors and Bioelectronics*. 40 412 - 416
- Pasvol, G. (2005). The treatment of complicated and severe malaria. *British Medical Bulletin*. 75 and 76 29 - 47
- Peeling, R.W., and Mabey, D. (2010). Point-of-care tests for diagnosing infections in the developing world. *Clinical Microbiology and Infection*. 16 (8): 1062 - 1069
- Peluso, P., Wilson, D.S., Do, D., Tran, H., Venkatasubbaiah, M., Quincy, D., Heidecker, B., Poindexter, K., Tolani, N., Phelan, M., Witte, K., Jung, L.S., Wagner, P., and Nock, S. (2003). Optimizing antibody immobilization strategies for the construction of protein microarrays. *Analytical Biochemistry*. 312 113 - 124
- Piepenburg, O., Williams, C.H., Stemple, D.L., and Armes, N.A. (2006). DNA detection using recombination proteins. *PLOS Biology*. 4 (7): 1115 - 1121
- Pieroni, P., Mills, C.D., Ohrt, C., Harrington, M.A., and Kain, K.C. (1998). Comparison of the ParaSight- F test and the ICT Malaria Pf test with the polymerase chain reaction for the diagnosis of *Plasmodium falciparum* malaria in travellers. *Transactions of the Royal Society of Tropical Medicine and Hygiene*. 92 166-169
- Piper, R., Lebras, J., Wentworth, L., Hunt-Cooke, L., Houze', S., Chiodini, P., and Makler, M. (1999). Immunocapture diagnostic assays for malaria using *Plasmodium falciparum* lactate dehydrogenase (pLDH). *American Journal of Tropical Medicine and Hygiene*. 60 (1): 109-118
- Polpanich, D., Tangboriboonrat, P., Elaissari, A., and Udomsangpetch, R. (2007). Detection of malaria infection via latex agglutination assay. *Analytical Chemistry*. 79 (12): 4690-4695
- Pöschl, B., Waneesorn, J., and Panagiotis, K. (2010). Comparative Diagnosis of Malaria Infections by Microscopy, Nested PCR, and LAMP in Northern Thailand. *The American Journal of Tropical Medicine and Hygiene*. 83 (3): 56 - 60
- Posthuma-Trumpie, G.A., Korf, J., and van Amerongen, A. (2009). Lateral flow (immuno)assay: its strengths, weaknesses, opportunities and threats. A literature survey. *Analytical and Bioanalytical Chemistry*. 393 569-582
- Puertas, S., Moros, M., Fernandez-Pacheco, R., Ibarra, M.R., Grazu, V., and de la Fuente, J.M. (2010). Designing novel nano-immunoassays: antibody orientation versus sensitivity. *Journal of Physics D: Applied Physics*. 43 1-8
- Ramos-Vara, J.A. (2005). Technical Aspects of Immunohistochemistry. *Veterinary Pathology*. 42 405 - 426
- Rejeb, S.B., Tatouljian, M., Khonsari, F.A., Durand, N.F., Martel, A., Lawrence, J.F., Amouroux, J., and Le Goffic, F. (1998). Functionalization of nitrocellulose membranes using

- ammonia plasma for the covalent attachment of antibodies for use in membrane-based immunoassays. *Analytica Chimica Acta*. 376 133 - 138
- Riley, R.S., and Anderson, F.P. 2002. Basic Principles of Immunodiagnosis. 1357 - 1361. Clinical Laboratory Medicine. K.D. McClatchey, editor. Lippincott Williams and Wilkins, 0-683-30751-7
- Riuttamaki, T., and Soukka, T. 2014. Upconverting Phosphor labels for bioanalytical assays. 157 - 193. Advances in Chemical Bioanalysis. F.M. Matysik, editor. Springer 978-3-319-00181-4, eBook ISBN: 973-3-319-00182-1
- Rock, E.P., Marsh, K., Saul, A.J., Wellems, T.E., Taylor, D.W., Maloy, W.L., and Howard, R.J. (1987). Comparative analysis of the *Plasmodium falciparum* histidine-rich proteins HRP-I, HRP-II and HRP-III in malaria parasites of diverse origin. *Parasitology*. 95 (2): 209 - 227
- Rogers, D.J., and Randolph, S.E. (2000). The global spread of malaria in a future, warmer world. *Science*. 289 1763
- Sachs, J., and Malaney, P. (2002). The economic and social burden of malaria. *Nature*. 415 680-985
- Saha, B., Evers, T.H., and Prins, M.W.J. (2014). How antibody surface coverage on nanoparticles determines the activity and kinetics of antigen capturing for biosensing. *Analytical Chemistry*. 86 8158 - 8166
- Sajid, M., Kawde, A., and Daud, M. (2014). Designs, formats and applications of lateral flow assay: A literature review. *Journal of Saudi Chemical Society*. 1 - 17
- Scheinberg, D. 2010. Monoclonal Antibodies: Discovery & Development. 469 - 470. Cancer Chemotherapy and Biotherapy: Principles and Practice. B.A. Chabner and D.L. Longo, editors 978-1-6054-7431-1
- Setty, M.K.H.G., and Hewlett, I.K. (2014). Point of Care Technologies for HIV. *AIDS Research and Treatment*. 2014 1 - 20
- Shyu, R.H., Shyu, H.F., Liu, H.W., and Tang, S.S. (2002). Colloidal gold-based immunochromatographic assay for detection of ricin. *Toxicon*. 40 255 - 258
- Sinka, M.E., Bangs, M.J., Manguin, S., Rubio-Palis, Y., Chareonviriyaphap, T., Coetzee, M., Mbogo, C.M., Hemingway, J., Patil, A.P., Temperley, W.H., Gething, P.W., Kabaria, C.W., Burkot, T.R., Harbach, R.E., and Hay, S.I. (2012). A global map of dominant malaria vectors. *Parasite Vectors*. 5 (69): 2 - 11
- Siraj, A.S., Santos-Vega, M., Bouma, M.J., Yadeta, D., Carrascal, D.R., and Pascual, M. (2014). Altitudinal changes in malaria incidence in highlands of Ethiopia and Colombia. *Science*. 343 1154 - 1158
- Sirichaisinthop, J., Buates, S., and Jetsumon Sattabongkot, J. (2011). Evaluation of loop-mediated isothermal amplification (lamp) for malaria diagnosis in a field setting. *The American Journal of Tropical Medicine and Hygiene*. 85 (4): 594 - 596

- Sondhi, S., Sharma, P., Saini, S., Puri, N., and Gupta, N. (2014). Purification and characterization of an extracellular, thermo-alkali-stable, metal tolerant laccase from *Bacillus tequilensis* SN4. *PLOS One*. 9 (5): 1 - 10
- Steinitz, M. (2000). Quantitation of the blocking effect of Tween 20 and Bovine Serum Albumin in ELISA microwells. *Analytical Biochemistry*. 282 232 - 238
- Subramanian, A., and Velandar, W.H. (1996). Effect of antibody orientation on immunosorbent performance. *Journal of Molecular Recognition*. 9 528-535
- Sutherland, C.J., and Hallett, R. (2009). Detecting malaria parasites outside the blood. *The Journal of Infectious Disease*. 199 1561-1563
- Tajima, N., Takai, M., and Ishihara, K. (2011). Significance of antibody orientation unraveled: Well-oriented antibodies recorded high binding affinity. *Analytical Chemistry*. 83 1969–1976
- Talman, A.M., Duval, L., Legrand, E., Hubert, V., Yen, S., Bell, D., Le Bras, J., Arie, F., and Houze, S. (2007). Evaluation of the intra- and inter-specific genetic variability of *Plasmodium lactate dehydrogenase*. *Malaria Journal*. 6 (140): 1-6
- Tan, J.J. 2008. Analysis of whole blood samples: Optimization of sample preparation for rapid assays. Vol. Master of Engineering. Cornell university.
- Tan, Y.H., Pandey, B., Sharma, A., Bhattarai, J., and Stine, J.J. (2012). Bioconjugation reactions for covalent coupling of proteins to gold surfaces. *Global Journal of Biochemistry*. 3 (6):
- Tangpukdee, N., Duangdee, C., Wilairatana, P., and Krudsood, S. (2009). Malaria diagnosis: A brief review. *Korean Journal of Parasitology*. 47 (2): 93-102
- Tarcha, P.J., Chu, V.P., and Whittern, D. (1987). 2,3-diaminophenazine is the product from the horseradish peroxidase-catalyzed oxidation of o-phenylenediamine. *Analytical Biochemistry*. 165 (1): 230–233
- Thiramanas, R., Jangpatrapongsa, K., Asawapirom, U., Tangboriboonrat, P., and Polpanich, D. (2013). Sensitivity and specificity of PS/AA-modified nanoparticles used in malaria detection. *Microbial Biotechnology*. 6 (44): 406 - 413
- Tjitra, E., Suprianto, S., Dyer, M., Currie, B.J., and Anstey, N.M. (1999). Field evaluation of the ICT Malaria P.f/P.v immunochromatographic test for detection of *Plasmodium falciparum* and *Plasmodium vivax* in patients with a presumptive clinical diagnosis of malaria in eastern Indonesia *Journal of Clinical Microbiology*. 37 (8): 2412-2417
- Tonnang, H.E.Z., Kangalawe, R.Y.M., and Yanda, P.Z. (2010). Predicting and mapping malaria under climate change scenarios: the potential redistribution of malaria vectors in Africa. *Malaria Journal*. 9 1-10
- Tozzoli, R. (2007). Recent advances in diagnostic technologies and their impact in autoimmune disease. *Autoimmunity Reviews*. 6 334 - 340

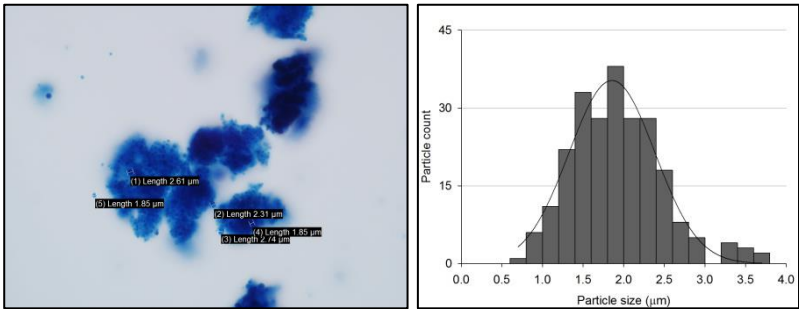
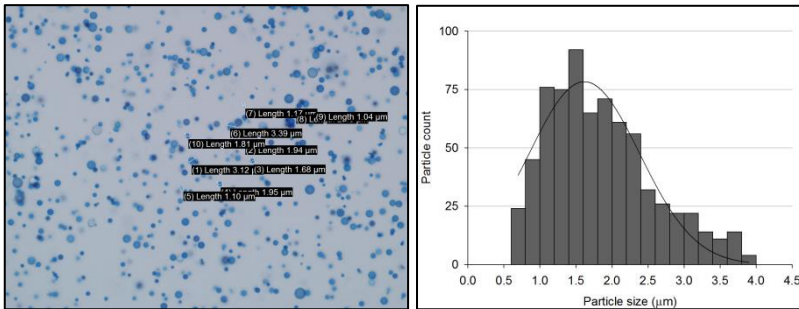
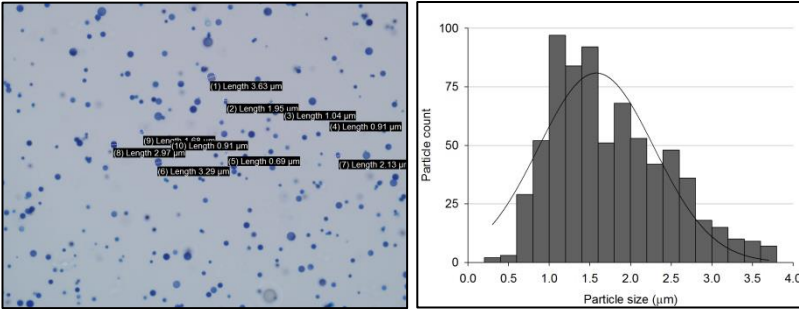
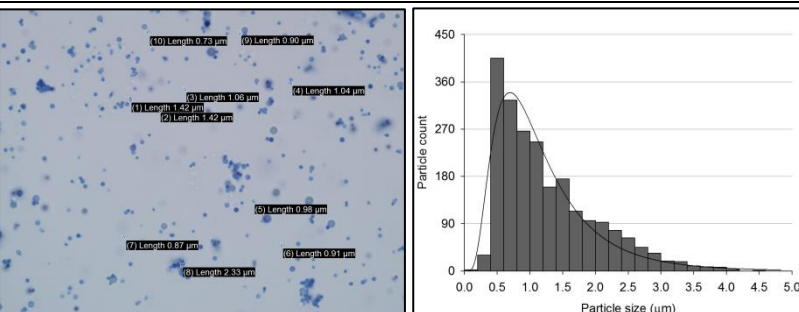
- Tritten, L., Matile, H., Brun, R., and Wittlin, S. (2009). A new double-antibody sandwich ELISA targeting *Plasmodium falciparum* aldolase to evaluate anti-malarial drug sensitivity. *Malaria Journal*. 8
- Turkova, J. (1999). Oriented immobilization of biologically active proteins as a tool for revealing protein interactions and function. *Journal of Chromatography B*. 722 11-31
- Twala, B.V., Sewell, B.T., and Jordaan, J. (2012). Immobilisation and characterisation of biocatalytic co-factor recycling enzymes, glucose dehydrogenase and NADH oxidase, on aldehyde functional ReSynTM polymer microspheres. *Enzyme and Microbial Technology*. 50 331 - 336
- Urdea, M., Penny, L.A., Olmsted, S.S., Giovanni, M.Y., Kaspar, P., Shepherd, A., Wilson, P., Dahl, C.A., Buchsbaum, S., Moeller, G., and Burgess, D.C.H. (2006). Requirements for high impact diagnostics in the developing world. *Nature*. 444 (Supplementary Material 1): 73-79
- Van Amerongen, A., Wichers, J.H., Berendsen, L.B., Timmermans, A.J., Keizer, G.D., van Doorn, A.W., Bantjes, A., and van Gelder, W.M. (1993). Colloidal carbon particles as a new label for rapid immunochemical test methods: quantitative computer image analysis of results. *Journal of Biotechnology*. 30 (2): 185 - 195
- Veitch, N.C. (2004). Horseradish peroxidase: a modern view of a classic enzyme. *Phytochemistry*. 65 249–259
- Verheijen, R., Stouten, P., Cazemier, G., and Haasnoot, W. (1998). Development of a one step strip test for the detection of sulfadimidine residues. *Analyst*. 123 2437 - 2441
- Vigário, A.M., Belnoue, E., Cumano, A., Marussig, M., Miltgen, F., Landau, I., Mazier, D., Gresser, I., and Rénia, L. (2001). Inhibition of *Plasmodium yoelii* blood-stage malaria by interferon {alpha} through the inhibition of the production of its target cell, the reticulocyte. *Blood*. 97 (12): 3966-3971
- Vogt, R.F., Phillips, D.L., Henderson, L.O., Whitfield, W., and Spierto, F.W. (1987). Quantitative differences among various proteins as blocking agents for ELISA microtiter plates. *Journal of Immunological Methods*. 101 43 - 50
- Voller, A., Bidwell, D.E., and Bartlett, A. (1976). Enzyme immunoassays in diagnostic medicine. *Bulletin of the World Health Organization* 53 (1): 55-65
- Wang, F., Tan, W.B., Zhang, Y., Fan, X., and Wang, M. (2006). Luminescent nanomaterials for biological labelling. *Nanotechnology*. 17 (1): R1
- Wang, S., Zhang, C., and Zhang, Y. 2009a. Lateral Flow Colloidal Gold-Based Immunoassay for Pesticide. 237-252. *Methods in Molecular Biology: : Biosensors and Biodetection*. A. Rasooly and K.E. Herold, editors. Humana Press, 978-1-60327-568-2 (Print) 978-1-60327-569-9 (Online)

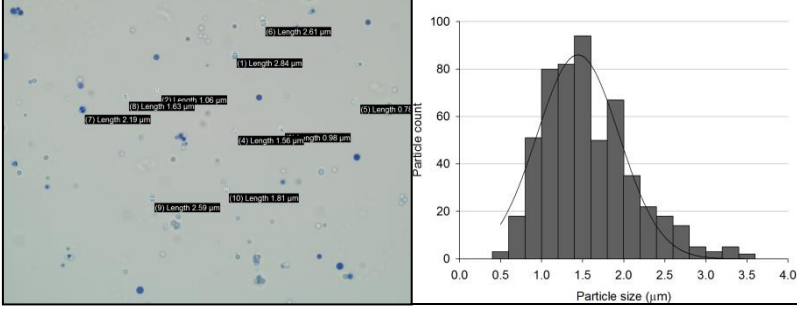
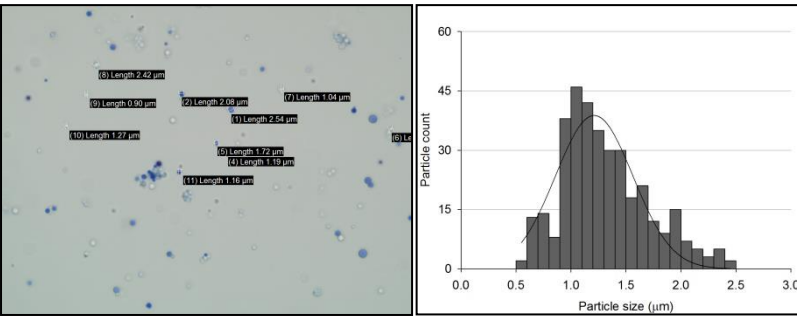
- Wang, Y., Xu, H., Wei, M., Gu, H., Xu, Q., and Zhu, W. (2009b). Study of superparamagnetic nanoparticles as labels in the quantitative lateral flow immunoassay *Materials Science and Engineering*. C 29 714 - 718
- White, N.J. 2014. Malaria.553 - 563. Manson's Tropical Diseases. J. Farrar, P.J. Hotez, T. Junghanss, G. Kang, D. Lalloo, and N. White, editors. Elsevier Saunders 9780702051012, Ebook ISBN 9780702053061
- White, N.J., Pukrittayakamee, S., Hien, T.T., Faiz, M.A., Mokuolu, O.A., and Dondorp, A.M. (2014). Malaria. *The Lancet*. 383 723 - 735
- WHO (2000). New perspectives in malaria diagnostics. <http://www.who.int/tdr/publications/documents/malaria-diagnosis.pdf>
- WHO (2004). HIV Assays: Operational Characteristics. Report 14. http://www.who.int/diagnostics_laboratory/publications/hiv_assays_rep_14.pdf
- WHO (2007). Tuberculosis fact sheet number 104. <http://www.who.int/mediacentre/factsheets/fs104/en/print.html44>
- WHO (2009). World Malaria Report. http://www.who.int/malaria/world_malaria_report_2009/en/
- WHO/UNAIDS (2006). IDS epidemic update: December 2006. http://data.unaids.org/pub/EpiReport/2006/2006_EpiUpdate_en.pdf
- Wilson, N.O., Adjei, A.A., Anderson, W., Baidoo, S., and Stiles, J.K. (2008). Short Report: Detection of *Plasmodium falciparum* Histidine-rich protein II in saliva of malaria patients. *American Journal of Tropical Medicine and Hygiene*. 78 (5): 733-735
- Winzeler, E.A. (2006). Applied systems biology and malaria. *Nature Reviews Microbiology*. 4 145-151
- Wiwanitkit, V. (2007). *Plasmodium* and host lactate dehydrogenase molecular function and biological pathways: implication for antimalarial drug discovery. *Chemical Biology and Drug Design*. 69 280-283
- Wong, R.C., and Tse, H. (2009). Lateral flow immunoassay. Humana Press. Print 978-1-58829-908-6, Online: 978-1-59745-240-3.
- Wongsrichanalai, C., Barcus, M.J., Muth, S., Sutamihardja, A., and Wernsdorfer, W.H. (2007). A Review of malaria diagnostic tools: Microscopy and rapid diagnostic Test (RDT). *American Journal of Tropical Medicine and Hygiene*. 77 (Supplementary Material 6): 119-127
- www.alere.com. 2015. BinaxNOW Malaria Test Kit product insert.
- Yager, P., Domingo, G.J., and Gerdes, J. (2008). Point-of-care diagnostics for global health. *Annual Review of Biomedical Engineering*. 10 107-144
- Yang, H., Li, D., He, R., Guo, Q., Wang, K., Zhang, X., Huang, P., and Cui, D. (2010). A Novel Quantum Dots–Based Point of Care Test for Syphilis. *Nanoscale Research Letters*. 5 (5): 875-881

- Yuan, Y., He, H., and Lee, L.J. (2008). Protein A-based antibody immobilization onto polymeric microdevices for enhanced sensitivity of Enzyme-Linked Immunosorbent Assay. *Biotechnology and Bioengineering*. 102 (3): 891 - 901
- Zhang, K., Mao, L., and Cai, R. (2000). Stopped-flow spectrophotometric determination of hydrogen peroxide with hemoglobin as catalyst. *Talanta*. 51 179–186
- Zhu, W., and Yu, G. 2009. Rabbit hybridomaTherapeutic monoclonal antibodies: From bench to clinic
- Z. An, editor. Wiley978-0-470-11791-0

APPENDIX

Table A1: Effect of detergent concentration (volume NP4 per 10 ml batch of microspheres) on microsphere synthesis and particle size distribution (PSD).

Detergent (NP4) volume	Picture with measurements (left) Particle Size Distribution (PSD) (right)	Comment
50 µl		<p>PSD ≤ 1 µm: 2.97%</p> <ul style="list-style-type: none"> - Aggregation of microspheres - Microspheres readily take up dye
100 µl		<p>PSD ≤ 1 µm: 9.7%</p> <ul style="list-style-type: none"> - Minimal aggregation of microspheres - Microspheres readily take up dye
150 µl		<p>PSD ≤ 1 µm: 12.1%</p> <ul style="list-style-type: none"> - Minimal aggregation of microspheres - Microspheres readily take up dye
200 µl		<p>PSD ≤ 1 µm: 46.9%</p> <ul style="list-style-type: none"> - Minimal aggregation of microspheres - Microspheres readily take up dye however appears to take up slightly less than 150 µl NP4. - Greatest fraction of microspheres below 1 µm

300 μ l		<p>PSD $\leq 1 \mu\text{m}$: 19.3%</p> <ul style="list-style-type: none"> - Minimal aggregation of microspheres - Microspheres do not take up dye readily.
600 μ l		<p>PSD $\leq 1 \mu\text{m}$: 21.1%</p> <ul style="list-style-type: none"> - Minimal aggregation of microspheres - Microspheres do not take up dye readily.

Discussion:

During microspheres synthesis, the size of the microspheres was manipulated by introducing varying concentrations of detergent during the synthesis step. Increasing concentrations of detergent allowed for smaller microspheres to be formed, with 200 μ l NP4 (per 10 ml batch) having the greatest effect in reducing the size of the microspheres, resulting in PSD $\leq 1 \mu\text{m}$ of 46.9%. Above this concentration of detergent (300 μ l and 600 μ l per 10 ml batch), the particle size remained relatively constant with fewer large ($\geq 3.0 \mu\text{m}$) microspheres. However, the microspheres absorbed less dye with higher concentrations of detergent ($\geq 300 \mu\text{l}$), resulting in semi-transparent light blue microspheres.